Evaluation of the therapeutic potential of GDF5 mutants to treat osteoarthritis

TECHNISCHE UNIVERSITÄT DARMSTADT

Vom Fachbereich Chemie
der Technischen Universität Darmstadt

zur Erlangung des Grades
Doctor rerum naturalium
(Dr. rer. nat.)

Dissertation
von Tanja Mang

Erstgutachter: Prof. Dr. Harald Kolmar
Zweitgutachter: Prof. Dr. Martin Michaelis

Darmstadt 2018

Mang, Tanja : Evaluation of the therapeutic potential of GDF5 mutants to treat osteoarthritis.
Darmstadt, Technische Universität Darmstadt,
Jahr der Veröffentlichung der Dissertation auf TUprints: 2019
URN: urn:nbn:de:tuda-tuprints-82062
Tag der mündlichen Prüfung: 13.07.2018

Veröffentlicht unter CC BY-SA 4.0 International
https://creativecommons.org/licenses/

Tag der Einreichung: 30. Mai 2018

Tag der mündlichen Prüfung: 13. Juli 2018

Danksagung

An dieser Stelle bedanke ich mich bei allen, die mich während meiner Dissertation unterstützt haben und dazu beigetragen haben diese Zeit zu einer Unvergesslichen zu machen!

Mein besonderer Dank gilt Prof. Dr. Martin Michaelis, der mir nicht nur die Möglichkeit gab meine Dissertation in seiner Abteilung über ein extrem spannendes Thema anzufertigen, sondern mir auch die Teilnahme an zahlreichen Konferenzen und Face-2-Face Meetings ermöglichte und mich dadurch enorm förderte. Darüber hinaus möchte ich mich für die Übernahme des Korreferats, die Korrektur der Arbeit, die stete Unterstützung und die exzellenten Denkanstöße bedanken.

Weiterhin bedanke ich mich bei Prof. Dr. Harald Kolmar für die Betreuung meiner Dissertation seitens der TU Darmstadt und zusätzlich für die Unterstützung in etlichen organisatorischen Belangen. Vielen Dank auch an Prof. Dr. Bertl und Prof. Dr. Schmitz für die Übernahme des Fachprüfers meiner Promotionsprüfung sowie an Prof. Dr. Schäfer für die Übernahme des Prüfungsvorsitzes.

Insbesondere bedanke ich mich bei meiner Betreuerin Dr. Anne Gigout. Anne, thank you very much for the excellent supervision, the permanent willingness to discuss, which has contributed significantly to the success of this work, the effective help in various matters and of course for the continuous support and proofreading of the work.

Vielen Dank auch an Dr. Sven Lindemann, Dr. Kerstin Kleinschmidt-Dörr, Dr. Daniela Werkmann und Dr. Christian Brenneis für den fachlichen Input, der es ermöglichte neue Ideen zu entwickeln und zu realisieren.

Meinen Laborkolleginnen Claudia und Yvonne danke ich herzlich für die permanente Hilfsbereitschaft bei allen praktischen Tätigkeiten, die vielen experimentellen Tipps, für das freundliche Arbeitsklima, das Motivieren und für die vielen netten Gespräche und Belustigungen.

Thomas möchte ich ganz herzlich danken für die Durchführung histologischer Arbeiten sowie für seine Sorgfältigkeit und Bemühungen.
Stephi dir auch ein großes Dankeschön! Nicht nur für die zahlreichen tollen Trips, die wirklich ein unfassbarer schöner Teil dieser Zeit waren, sondern auch dafür, dass du immer ein offenes Ohr für mich hast und mich, so gut es dir möglich war, unterstützt hast.
Zudem danke ich allen übrigen Mitarbeitern der Osteoarthrose-Abteilung für die tolle Zeit! Ein großes Dankeschön für die super tolle „Rund-um-die-Welt“ Schritt-Challenge, aber auch dafür, dass ihr einfach

seid wie ihr seid – danke, dass es immer Spaß mit euch macht! Vielen Dank an das ex-vivo lab Gudrun, Ralf und Matthias. Vielen Dank auch an die restliche Histo Donata, Nicole und Simone. Und natürlich auch vielen Dank an die in-vivos Andi, Herbert, Jenni, Juliane und Liselotte. Danke, dass ihr mich so freundlich in eure Gruppe aufgenommen habt - ich werde euch wirklich alle sehr vermissen!

Ein großes Dankeschön natürlich auch an alle, die mich außerhalb der Abteilung unterstützt haben.
Andreas vielen Dank für die Durchführung der Biacore Messungen und dafür, dass du mir immer alle meine Frage sehr geduldig und verständlich beantwortet und mit mir zusammen Brainstorming gemacht hast. Auch dir Daniel, vielen Dank, dass du die Messungen ermöglicht und mich unterstützt hast.
Melanie vielen Dank für die zahlreichen Tipps für „Zellkultur im Großmaßstab“ und auch für die Unterstützung bei den U2OS Messungen.
Jörg bei dir bedanke ich mich ganz herzlich für die Einarbeitung in die SimpleWes Technologie und allen Input dahingehend.
Auch ein großes Dankeschön an alle Mitglieder und Alumnis des AK Kolmars für die vielen netten Gespräche aller Art und die schönen Feiern.
Außerdem bedanke ich mich natürlich von ganzem Herzen auch bei unseren „guten Feen“ Margrit und Barbara für die Hilfestellungen in allen organisatorischen Angelegenheiten. Danke, dass ihr es immer wieder schafft, dass alles funktioniert und sich zum Guten wendet!

Zu guter Letzt danke ich allen meinen Freunden und meiner Familie, die mich über die gesamte Studienzeit nach allen Kräften unterstützt haben – ganz besonders danke ich meinen Eltern Mario und Ursula Mang. Danke, dass ihr jederzeit bedingungslos und liebevoll hinter mir steht und immer an mich geglaubt habt! Ohne euch hätte ich diesen gesamten Weg nicht annähernd so reibungslos gehen können – danke für all das, was man gar nicht in Worte fassen kann.
Fabian auch dir ein großes Dankeschön für die aufbauenden Worte und dafür, dass du mich immer wieder ermutigt, mir den Rücken gestärkt und dich sogar zu meiner Entlastung zu einem echten Kochprofi entwickelt hast.

Table of contents

I List of figures and tables

II Abbreviations

°C	degree Celsius
μg	microgram
μl	microliter
aa	amino acid
Ab	antibody
ADAMTS	a disintegrin and metalloproteinase with thrombospondin motifs
bFGF	basic fibroblast growth factor
BM	bone marrow
BMP	bone morphogenetic protein
BMPR	bone morphogenetic protein receptor
BSA	bovine serum albumin
$CaCl_2$	calcium chloride
cDNA	complementary deoxyribonucleic acid
CO_2	carbon dioxide
COMP	cartilage oligomeric matrix protein
CS	chondroitin sulfate
Ct	cycle threshold
C/T	cytosine/thymine
CTA	cartilage tissue analogue
DEPC	diethyl pyrocarbonate
DMEM	Dulbecco's Modified Eagle's Medium
DMMB	dimethylmethylene blue
DMOADs	disease modifying osteoarthritis drugs
DNA	deoxyribonucleic acid
dNTPs	deoxynucleotide triphosphate
dsDNA	double-stranded deoxyribonucleic acid
DTT	Dithiothreitol
EC50	half maximal effective concentration
ECM	extracellular matrix
EDC	1-Ethyl-3-(3-dimethylaminopropyl) carbodiimid
EDTA	ethylenediaminetetraacetic acid
EF1α	elongation factor 1α
em	emission
EtOH	ethanol

ex	excitation
FACIT	fibril-associated collagen with interrupted triple helices
FACS	fluorescence-activated cell sorting
FBS	fetal bovine serum
FCD	fixed-charge density
FIC	freshly isolated chondrocytes
GAG	glycosaminoglycan
GDF5	growth and differentiation factor 5
h	hour
HA	hyaluronic acid
HCl	hydrochloride acid
HEPES	4-(2-hydroxyethyl)-1-piperazineethanesulfonic acid
hOAC	human osteoarthritic chondrocytes
HPro	hydroxyproline
HS	heparan sulfate
ia.dial FBS	heat inactivated, dialyzed fetal bovine serum
IFP	infrapatellar fat pad
IHC	immunohistochemistry
Il1α	interleukin1 alpha
Il1β	interleukin1 beta
Il6	interleukin6
ITS	insulin, transferrin, sodium selenite
KD	dissociation constant
kDa	kilo Dalton
KS	keratan sulfate
l	liter
LDS	lithium dodecyl sulfate
Mab	Monoclonal antibody
MAPK	mitogen-activated protein kinase
MES	2-(N-morpholino) ethane sulfonic acid
min	minutes
ml	milliliter
mM	millimolar
MMP	matrix metalloproteinases
mOsm	milliosmoles
MS	mass spectrometry

MSCs	mesenchymal stem cells
MW	molecular weight
Na^+	sodium
Na_2HPO_4	disodium hydrogen phosphate
NaCl	sodium chloride
NaOH	sodium hydroxide
ng	nanogram
NHS	N-hydroxysuccinimide
NSAIDs	nonsteroidal anti-inflammatory drugs
O_2	oxygen
OA	Osteoarthritis
OARSI	Osteoarthritis Research Society International
Pab	Polyclonal antibody
PAGE	polyacrylamide gel electrophoresis
PBS	phosphate buffered saline
Pen/strep	penicillin/streptomycin
PFA	paraformaldehyde
pg	picogram
PGs	proteoglycans
$ProC_2$	pro-peptide of collagen 2
PVDF	polyvinylidene fluoride
qRT-PCR	quantitative real-time polymerase chain reaction
R^2	goodness-of-fit of linear regression
RFU	relative fluorescence units
RPL13a	ribosomal protein L13a
RT	room temperature
RU	resonance units
SDS	sodium dodecyl sulfate
SF	synovial fluid
SM	synovial membrane
SMAD	small mothers against decapentaplegic
TGFβ	transforming growth factor beta
TNFα	tumor necrosis factor alpha
TonEBP	tonicity responsive enhancer binding protein
WB	western blot

III Abstract

Osteoarthritis (OA) is characterized by a progressive destruction of articular cartilage. Current treatment options do not enable to heal or stop the disease progression. Consequently, there is a strong need for disease-modifying OA drugs (DMOADs). The growth and differentiation factor 5 (GDF5) is a promising DMOAD candidate. It is a key regulator of cartilage development and is involved in cartilage maintenance during adulthood. GDF5 was shown to stimulate matrix production in chondrocytes, to promote chondrogenesis in mesenchymal stem cells (MSCs) and to induce cartilage formation in an OA model [1-3]. Moreover, it was shown to exhibit anti-catabolic properties [4]. Thus, GDF5 could enable to regenerate damaged OA cartilage and to prevent further cartilage worsening in vivo. However, GDF5 was also shown to have hypertrophic and osteogenic activities [3, 5], which could result in the formation of inferior cartilage and unwanted bone formation. To reduce the hypertrophic/osteogenic properties of GDF5, different GDF5 mutants were produced and three of them (M1673, W417F, W417R) were selected. The aim of the present work was to evaluate these GDF5 mutants for their therapeutic potential in the two cells types, which can produce cartilage: chondrocytes and MSCs.

Among the GDF5 mutants, M1673 was previously shown to have the strongest anabolic effect in chondrocytes from different non-human species. The first aim of this work was to confirm the anabolic effect of M1673 in human OA chondrocytes (hOAC). This was achieved with the use of a 3D culture system and modified culture conditions (slightly increased medium osmolarity). Increasing the medium osmolarity was shown to favor the chondrocytes phenotype and its matrix production. In addition, the OA characteristics (cytokine and protease production) were reduced and the expression of BMPR1a, BMPR1b and BMPR2 enhanced. With these culture conditions, M1673 was shown to exhibit anabolic and anti-catabolic effects on hOAC. Moreover, the results also suggested M1673 to be less hypertrophic in hOAC compared to GDF5.

In addition, the GDF5 mutants were tested in the present work for their chondrogenic and osteogenic properties in MSCs. First, it was shown that the GDF5 mutants display a lower BMPR1a affinity compared to GDF5 but a similar BMPR1b affinity. Among the GDF5 mutants, M1673 was shown to induce the strongest chondrogenic differentiation while preventing hypertrophy. In addition, the osteogenic differentiation was delayed with M1673 compared to GDF5. Originally, it was hypothesized that chondrogenesis is mediated through BMPR1b, while osteogenesis is mediated through BMPR1a. However, in the light of the results presented here, this had to be refined: it now appears that the activation of BMPR1a is necessary for chondrogenesis as well as for osteogenesis. In addition, BMPs with a higher BMPR1a/BMPR1b ratio appear to prevent hypertrophy and delay osteogenesis.

Taken together, the results of this work show that M1673 can stimulate cartilage production in both hOAC and MSCs, while having a reduced hypertrophic and osteogenic potential in comparison to GDF5. Therefore, it could be demonstrated that M1673 bear potential as a DMOAD.

IV Zusammenfassung

Osteoarthrose (OA) ist durch eine zunehmende Zerstörung des Gelenkknorpels charakterisiert. Zurzeit steht keine Behandlung zur Verfügung, die eine Heilung herbeiführt oder ein Fortschreiten der OA verhindert. Daher besteht ein Bedarf an krankheits-modifizierenden OA Medikamenten. In diesem Zusammenhang ist der Wachstums- und Differenzierungsfaktor 5 (GDF5) ein vielversprechender Kandidat. GDF5 spielt während der Knorpelentwicklung und bei der Knorpelerhaltung im erwachsenen Menschen eine Schlüsselrolle. Es wurde bereits gezeigt, dass GDF5 sowohl die Matrixproduktion im Chondrozyten, als auch die Chondrogenese von mesenchymalen Stammzellen (MSCs) und die Knorpelneubildung in einem OA Modell induziert [1-3]. Zusätzlich werden GDF5 anti-katabole Fähigkeiten zugeschrieben [4]. Somit könnte GDF5 in vivo die Regenerierung von OA Knorpel ermöglichen, wie auch ein Fortschreiten des Knorpelabbaus verhindern. Es wurde jedoch auch gezeigt, dass GDF5 hypertrophe/osteogene Fähigkeiten besitzt [3, 5], die den Aufbau minderwertigen Knorpels und eine unerwünschte Knochenbildung zur Folge haben. Zur Verringerung der Osteogenizität von GDF5 wurden verschiedene GDF5 Mutanten generiert, von denen M1673, W417F und W417R selektiert wurden. Ziel der vorliegenden Arbeit war es, diese Mutanten in Bezug auf ihr therapeutisches Potential hin in zwei Knorpel-produzierenden Zelltypen, den Chondrozyten und den MSCs, zu untersuchen.

In früheren Studien zeigte die Mutante M1673 den größten anabolen Effekt in nicht-humanen Chondrozyten. Das erste Ziel dieser Arbeit war es, den anabolen Effekt von M1673 in humanen OA Chondrozyten (hOAC) zu bestätigen. Dies konnte in einem 3D Kultursystem unter modifizierten Bedingungen (leicht erhöhte Osmolarität) nachgewiesen werden. Dabei zeigte sich, dass eine erhöhte Medium-Osmolarität den Phänotyp von Chondrozyten sowie deren Matrixproduktion begünstigt. Zusätzlich wurden Charakteristika der OA (Zytokin und Protease Produktion) reduziert und die Expression von BMPR1a, BMPR1b und BMPR2 erhöht. Unter diesen Kulturbedingungen zeigte M1673 anabole und anti-katabole Effekte in hOAC. Zudem wurde gezeigt, dass M1673 im Vergleich zu GDF5 in hOAC weniger hypertroph sein könnte.

Weiterhin wurden die GDF5 Mutanten auf ihr chondrogenes und osteogenes Potential in MSCs getestet. Zunächst wurde gezeigt, dass alle drei Mutanten im Vergleich zu GDF5 eine reduzierte BMPR1a und eine vergleichbare BMPR1b Affinität besitzen. Die GDF5 Mutante M1673 wies das stärkste chondrogene Potential auf und verhinderte gleichzeitig Hypertrophie. Zusätzlich zeigte M1673 im Vergleich zu GDF5 eine reduzierte Osteogenizität. Die initiale Hypothese war, dass Chondrogenese über BMPR1b und Osteogenese über BMPR1a vermittelt wird. Versuche im Rahmen dieser Arbeit konnten allerdings nachweisen, dass BMPR1a sowohl für Chondrogenese als auch für Osteogenese benötigt wird und dass BMPs mit erhöhtem BMPR1a/BMPR1b Ratio Hypertrophie verhindern und Osteogenese verzögern.

Zusammenfassend stimulierte M1673 die Knorpelproduktion sowohl in hOAC als auch in MSCs. M1673 zeigte im Vergleich zu GDF5 reduzierte hypertrophe und osteogene Eigenschaften. Somit konnte gezeigt werden, dass M1673 Potential für ein krankheits-modifizierendes OA Medikament besitzt.

1 Introduction

Osteoarthritis (OA) is the most common joint disease. It was estimated that 250 million people worldwide are affected by symptomatic knee and hip OA with an increasing tendency [6]. This disease is characterized by a slow, progressive degradation of articular cartilage, which occurs non-linearly with periods of fast progression which alternate with periods of joint stability [7-8]. OA can affect any joint, but particularly the weight-bearing knee and hip joints. It is also recognized that OA is a multifactorial disease involving not only articular cartilage, but also subchondral bone, synovial membrane, infrapatellar fat pad, menisci, tendons, muscles and ligaments [9].

Several risk factors for OA have been described, like age [6, 10-11], gender [12-13], race [13], obesity [12, 14], genetic predisposition [14], cartilage injuries [12, 14] or joint malalignments [15], which interact in complex ways [10]. Due to the aging society and the increased life span, there is a growing tendency for age-related OA [6]. The real mechanism of the correlation between an increased age and the clinical incidence of OA remains unclear, but it probably depends on a combination of changes in the joint structure resulting in a decreased capacity to adapt to mechanical loading [10].

The predominant symptom of OA is pain, which occurs during movement and normally decline at rest. However, patients with advanced stages of OA even awake from sleep because of OA-related pain at rest. Further symptoms are stiffness, swelling or muscle spasm [16]. All the symptoms result in a significant reduction of life quality because of forced inactivity and decreased mobility, which can result in social isolation, depression and dependency [17]. Moreover, it can result in several comorbidities like cardiovascular diseases or the loss for self-management in chronic diseases like diabetes or hypertension [6], which in turn increase the risk of premature mortality of about 23% in OA patients. Additionally to the burden carried by the patients, OA is combined with very high costs burdening the global health care systems [10].

Presently, available medications for OA solely focus on pain relief but do not heal or stop further progression of the disease so that many patients are advancing towards a need for total joint replacement. Consequently, there exists an unmet medical need for disease-modifying OA drugs (DMOADs).

All in all, OA is an important cause of disability for millions of patients, it is challenging the health system, and missing DMOADs define a clear unmet need. Based on this, the Osteoarthritis Research Society International (OARSI) has submitted a white paper in December 2016 to the Food and Drug Administration (FDA) for OA to become recognized as a serious disease.

1.1 Cartilage physiology

Cartilage is a connective tissue localized in different areas in the body and can be classified into three different types, namely elastic cartilage, fibrocartilage and hyaline cartilage [18]. These three cartilage types differ in their composition and function. Elastic cartilage is localized in the larynx and the ears and is composed of randomly oriented elastic fibers making it elastic and flexible. Fibrocartilage is localized in intervertebral discs and menisci, and contains large amounts of type 1 collagen, which interact with type 2 collagen and together form dense collagen fibers making it very tough and strong. Finally, hyaline cartilage is the most predominant cartilage type and is localized in the articulations [18]. Articular cartilage is a typical hyaline cartilage, which covers the ends of the subchondral bones and provides a smooth, gliding, visco-elastic surface of 2 to 4 mm [19] to minimize friction and distribute mechanical stress in the joint.

1.1.1 Chondrocytes

Healthy articular cartilage is composed of one single cell type, the chondrocytes, which occupy only 1-3% of the total tissue volume. Nevertheless, they produce, organize and maintain the extracellular matrix (ECM) of the cartilage [6] and are therefore responsible for cartilage metabolism. Unfortunately, chondrocytes have a limited cell division potential leading to a low metabolic activity which contributes to the limited self-healing capability of cartilage even after a minor injury [17]. Articular cartilage is an avascular, alymphic and aneural tissue, which forces the chondrocytes to an anaerobic metabolism [16]. The nutrition of articular cartilage occurs mainly by diffusion from synovial fluid (SF) nutrients, but also to a lesser extent from the bone marrow (BM) [20].

1.1.2 Extracellular matrix of articular cartilage

The extracellular matrix (ECM) of articular cartilage is composed of a fluid water phase, which represents up to 80% of the total cartilage weight, and a solid organic phase of approximately two-thirds of collagens, one-third of proteoglycans and of a minor amount of non-collagenous proteins like cartilage oligomeric matrix proteins (COMPs), fibronectin or link proteins [19].

Type 2 collagen is the main collagen type in healthy articular cartilage and represents 90 to 95% of the total collagen amount. It consists of three polypeptide chains, which are mainly composed of glycine and proline. The chains are wound into a triple helix via hydrogen bonds which are formed with the help of hydroxyproline amino acids [19]. Moreover, the type 2 collagen triple helices are associated to type 9 and 11 collagens to form large collagen fibrils. Type 11 collagen is located inside the fibril and regulates the fibril size. On the contrary, type 9 collagen is located at the surface of the collagen fibril, induce the type 2 collagen formation and enables the interaction with other ECM molecules (Figure 1). This fibril

network constitutes a dense network which stabilize the ECM and contribute to the cartilage rigidity [18, 21-22].

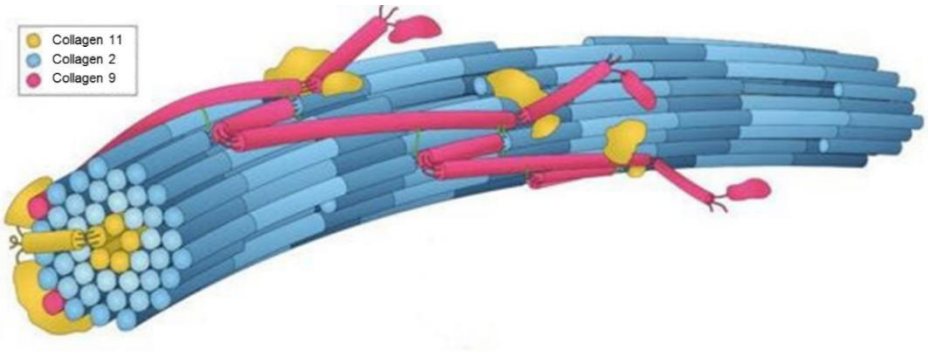

Figure 1 **Structure of type 2 collagen fibrils.** Type 2 collagen fibrils are formed by several type 2 collagen triple helices (blue) which are associated to type 9 (pink) and 11 collagens (yellow) with type 9 collagen being at the surface and type 11 collagen being inside the fibril. Adapted from [22] with permission from Elsevier.

Many other collagen subtypes are present in lower quantities in articular cartilage. Nevertheless, they play an important role as stabilizers of the cartilage ECM and also exhibit specific biological functions. For instance, type 6 collagen have a high affinity to other ECM molecules and to the cell membrane and therefore mediates cell-matrix interactions and plays an important role as signal transducer from the ECM to the cartilage [21]. Type 9, 12, 14, 16 and 22 collagen are members of the fibril-associated collagens with interrupted triple helix (FACITs) and participate to the cartilage organization [21]. Type 4 collagen may be responsible for maintenance of the cartilage phenotype and viability, whereas type 10 collagen maintains the tissue stiffness and facilitates calcification processes. Type 10 collagen is not available in healthy articular cartilage and is mostly used as a hypertrophic marker [21].

Proteoglycans (PGs) can be divided into large PGs like aggrecan or versican, small leucine-rich PGs like decorin, biglycan, fibromodulin or lumican, basement membrane PGs like perlecan, cell surface associated PGs like syndecan and intracellular PGs like serglycin [23]. They are responsible for the lubrication function and mediate the resistance of the articular cartilage to compressive load [24]. All PGs consist of several core proteins, which are connected non-covalently to a hyaluronic acid (HA) molecule. The core protein is attached covalently to glycosaminoglycan (GAG) chains, which are long hetero polysaccharide chains consists of repetitive disaccharide units connected to sulfate or carboxyl residues [24]. According to their disaccharide units and the linkage type between the sugars, the GAGs are divided into hyaluronic acid (HA), keratin sulfate (KS), chondroitin sulfate (CS), dermatan sulfate (DS) and heparan sulfate (HS) [23]. The most dominant PG in articular cartilage is the large, 250 kDa aggrecan, which is composed of several core proteins comprising approximately 30 KS and 100 CS molecules (Figure 2). The core proteins are attached to one single HA molecule through link proteins and consisting three globular domains (G1, G2 and G3) and an interglobular domain, which is localized between G1 and G2. The N-terminal G1 domain is responsible for the connection of the PG to the HA molecule via link proteins and is followed by the G2 domain, which is unique for aggrecan. Proximal to the G2 domain

is the KS binding site and distal the CS binding site, followed by the C-terminal G3 domain, which promotes post-translational processing and secretion of aggrecan [25].

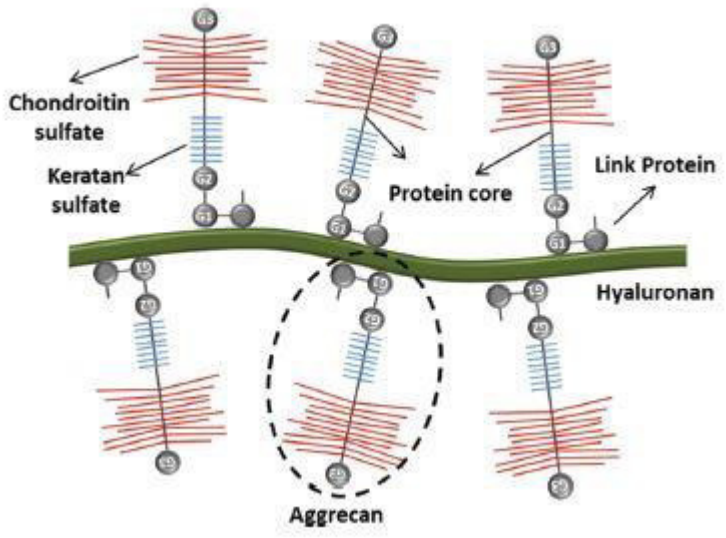

Figure 2 **Structure of aggrecan aggregates.** The aggrecan core protein is composed of three globular domains (G1, G2 and G3). G2 and G3 are separated by a large GAG attachment site. Proximal to G2 are ~ 30 keratin sulfates and distal ~ 100 chondroitin sulfates covalently attached. Several core proteins are connected non-covalently through link proteins to one single hyaluronic acid molecule and build a large aggrecan aggregate. Reproduced from [18] with permission of The Royal Society of Chemistry.

Other proteins are available in smaller amounts than collagens or proteoglycans. Nevertheless, they exhibit specific functions and many of these contribute to the strengthening of the complex structural ECM network. The glycoprotein fibronectin supports the cartilage ECM formation by interacting with other ECM molecules like collagens [26]. Another important glycoprotein is COMP, which strengthen the ECM network by binding to aggrecan, type 2 and 9 collagen and fibronectin. Moreover COMP was shown to contribute to lubrication properties of articular cartilage [26]. Furthermore there are many other functional proteins like proteases, inhibitors, degradation products, growth factors, chemokines and cytokines [27].

The articular cartilage ECM can be divided according to the distance of the matrix from chondrocytes into three regions: the pericellular, territorial and interterritorial matrix. The pericellular matrix (PCM) is a thin layer, which surrounds each chondrocyte and is together referred as the chondron. This matrix region may transduce load signals from the cartilage ECM to the chondrocytes [28]. The territorial matrix (TM) is located above the PCM and is thicker than the PCM. It contributes to both, the response to mechanical stress and to the elasticity of articular cartilage [19]. Thus, the PCM and TM mostly exhibit protective functions. On the contrary, the interterritorial matrix (ITM) is the largest matrix region and provides the mechanical properties of articular cartilage [19].

1.1.3 Zonal architecture of articular cartilage

The structure and composition of articular cartilage differ according to the distance from the articular surface. The articular cartilage can be divided in 4 different zones, which differ in their composition, cell density, cell shape, the cell arrangement, and exhibit different functions (Figure 3). The superficial or tangential zone (STZ) is the thinnest, and corresponds to 10 to 20% of the articular cartilage thickness and directly faces the joint cavity. It contains a high number of flattened chondrocytes that are oriented parallel to the articular cartilage surface. They produce lubricin, which supports the frictionless movement of the joint and simultaneously protect the deeper cartilage layers from shear stress. The STZ contains densely packed collagen fibers, mainly type 2 and 9 collagens, which are also oriented parallel to the articular cartilage surface. Only a low proteoglycan content is available in this zone making it more permeable for water flow than the other cartilage layers [18].

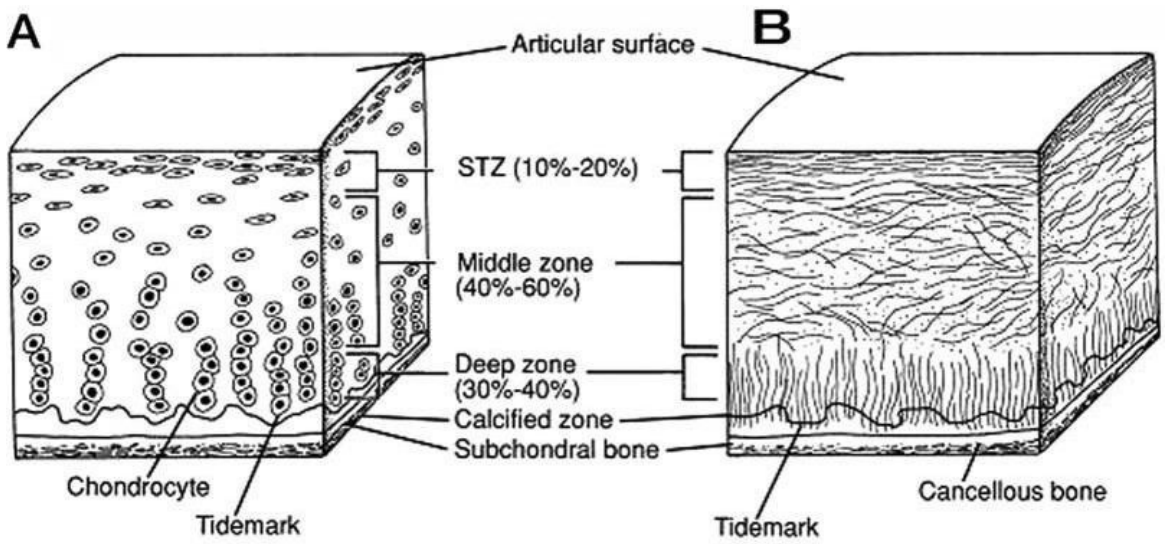

Figure 3 **Zonal architecture of healthy articular cartilage.** Healthy articular cartilage can be divided into different zones which vary in its cellular (A) and collagen organization (B). Reproduced with permission from SAGE Publications: [19], Copyright 2009 SAGE Publications.

The middle or transitional zone corresponds to 40 to 60% of the articular cartilage thickness and is composed of a lower density of round shaped chondrocytes embedded in a loose-packed network of high amounts of proteoglycans and lower amounts of collagens, mainly type 2 collagen. The collagen fibers are thicker than those of the STZ and start to change their orientation from parallel to columnar [29]. This zone is the first responder to mechanical loading [19]. The deep zone corresponds to 30% of the total articular cartilage volume, contains a low chondrocyte number, the highest proteoglycan content and the thickest collagen fibers. The chondrocytes are still round, but they are arranged in a columnar fashion. The collagen fibers are located parallel to the chondrocytes and therefore perpendicular to the subchondral bone. Altogether, this arrangement is responsible for the resistance of articular cartilage to compressive forces [19]. Finally, the calcified zone contains a low number of hypertrophic chondrocytes and is separated from the other zones by the tide mark. The tide mark serves as an interface between

the soft articular cartilage and the hard subchondral bone to further reduce the mechanical shear stress [18].

1.1.4 Cellular microenvironment in articular cartilage

Due to their localization in articular cartilage, chondrocytes are exposed to a specific microenvironment. Two specific aspects of this microenvironment are described below.

1.1.4.1 Oxygen

Chondrocytes are exposed to a hypoxic environment and adapted to it, because articular cartilage is an avascular tissue [30]. The calcified zone containing the tide mark represents a calcified barrier for the oxygen supply from blood vessels of the subchondral bone to the articular cartilage. Therefore, the main oxygen supply of articular cartilage occurs by diffusion from the synovial fluid, which is in contact with the superficial zone of the articular cartilage [20]. Therefore, the oxygen nutrition from synovial fluid results in an oxygen gradient from 10% oxygen in the superficial zone to 1% oxygen the deep zone [31-32]. Hypoxia-induced factors (HIFs) are the key transcription factors to regulate cellular response to hypoxia. Up to now the existence of three different HIF members are described. HIF1α possesses protective cell effects and drives the synthesis of cartilage ECM genes and is therefore described as a survival factor. On the contrary, HIF2α exhibits deleterious effects by upregulating catabolic genes leading to ECM destruction. Next to HIF1α and HIF2α, a third member exists, HIF3α, which is a negative regulator of HIF1α and HIF2α [31]. It was shown that the culture of chondrocytes in vitro at hypoxia has a positive influence on the chondrocytes phenotype and the chondrocytes ECM production compared to the culture at normoxia. This positive influence was shown to be mediated by HIF1α [33-34]. Culturing human OA chondrocytes at hypoxia even was shown to reduce their OA characteristics compared to normoxia [35].

1.1.4.2 Osmolarity

The strength of the articular cartilage and the ability to resist compressive loads is mainly determined by its local proteoglycan content, particularly of the GAG sidechains, which carry negative charges resulting in a high negative fixed-charge density (FCD) and give rise to osmolarity.

The osmolarity of healthy articular cartilage ranges between 350 and 480 mOsm depending on the local proteoglycan concentration within the different cartilage zones. As the proteoglycan content increases with the depth of articular cartilage, the osmolarity in the superficial zone is lower (350 to 370 mOsm) than in the deep zone (370 to 480 mOsm) [36]. Chondrocytes are osmo-sensitive and adjust to osmolarity changes during short times [37]. Osmolarity changes can occur under physiological conditions for example during mechanical loading or under pathophysiological conditions like OA. During mechanical loading water efflux from articular cartilage results in a higher fixed charge density and an increased osmolarity.

After relaxation from mechanical loading, water moves back into the articular cartilage resulting in an osmolarity decrease within the cartilage which is mediated by cations (mainly sodium, but also potassium and calcium) neutralizing the negative charge of the GAGs [38-39]. On the other hand, under pathological conditions like OA, the loss of proteoglycans, particularly of the negatively charged GAG sidechains, is accompanied by an irreversible decrease of osmolarity down to 270 mOsm [37, 39-40]. In conclusion, the osmolarity within articular cartilage is very variable depending not only on the different proteoglycan content in respective cartilage zones, but also on mechanical loading as well as the severity of OA [41].

The osmolarity of in vitro culture media is with a range of 260 to 320 mOsm [42] too low to represent the specific microenvironment within healthy articular cartilage in vivo [39, 43-44]. The osmolarity of culture media can be varied by the addition of salts like NaCl or sucrose. It was shown that culturing chondrocytes at medium osmolarities which rather correspond to the microenvironment within healthy articular cartilage in vivo is beneficial compared to the culture at lower osmolarities of standard culture media. Increasing the medium osmolarity was shown to enhance the cartilage ECM production of chondrocytes and improved their phenotype. The expression of aggrecan, type 2 collagen and sox9, as a key chondrogenic transcription factor, was enhanced while the expression of type 1 collagen was reduced [37, 39, 41, 45-46]. The molecular mechanism behind the effect of osmolarity is only partially understood until now. However, the tonicity enhancer binding protein (TonEBP) is recognized as a key transcription factor, which is activated by hyperosmotic stress [47] and is also involved in the expression of cartilage ECM production markers. In combination with the observation that TonEBP knockdown in chondrocytes lead to a decreased expression of cartilage ECM production markers, there is evidence for an osmo-induced expression of ECM molecules through a TonEBP pathway [45, 48].

1.2 Pathophysiology of OA

Osteoarthritis (OA) is a multifactorial disease of the whole joint resulting in structural and functional failures of all connective joint tissues. Consequently, the hallmark of OA is not only the destruction of articular cartilage, but also bone sclerosis, osteophyte formation, synovial membrane inflammation (synovitis), meniscal tear and extrusion or weakening and fraying of ligaments, muscles and tendons (Figure 4) [9, 49].

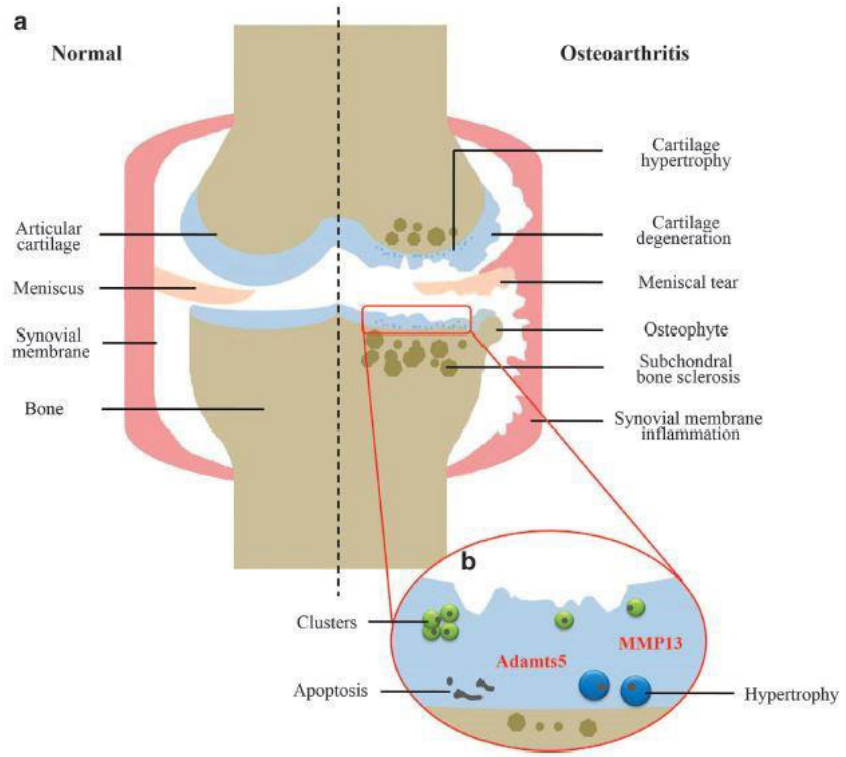

Figure 4 **Joint tissues involved in OA pathogenesis.** In contrast to the healthy joint (a), the OA joint is characterized by changes in the joint structures like cartilage degradation, subchondral bone remodeling, synovial membrane inflammation or meniscal tear and extrusion. Chondrocytes respond to this changes with production of proteolytic enzymes like MMP13 and ADAMTS5 (b). Reprinted with permission from Creative Commons Attribution 4.0 International License: [16], Copyright 2016 Sichuan University.

All these changes interact in a complex way and contribute to OA development and progression. The interplay of multiple paracrine factors coming from several joint tissues lead to a very complex molecular pathomechanism of OA initiation and progression, which is not fully understood until now [14, 50].

1.2.1 Shift in articular cartilage homeostasis

The homeostasis of articular cartilage is maintained by a defined content of collagens and proteoglycans within the ECM to provide optimal conditions to ensure tensile strength and resist compressive stress during mobility. The articular cartilage itself is continuously remodeled as chondrocytes remove the existing ECM components by releasing proteolytic enzymes and replace them by synthesizing new ECM components. This is an exceptionally slow progress. The turnover rate of aggrecan is relatively rapid with an approximately lifetime of 3.5 years, whereas the collagen turnover is extremely slow with an

approximately lifetime of 100 years [16-17]. These extremely slow turnover rates are conditioned by the low metabolic activity of chondrocytes which is in turn responsible for the poor healing capacity of cartilage. Therefore, the cartilage is very susceptible to injuries, which can be generated by abnormal joint stress like excessive load bearing, orthopedic malposition's or cartilage traumata, and is therefore very sensitive to degenerative processes. The abnormal joint stress first affects the chondrocytes localized in the superficial zone. In an early stage, the chondrocytes attempt to protect the articular cartilage by initiating compensatory mechanism like the increased proliferation of chondrocytes inter alia to ensure an increased ECM synthesis to maintain the healthy articular cartilage structure [9]. In addition, mesenchymal stem cell (MSC)-like progenitor cells are present in the superficial zone which could contribute to the replenishment of chondrocytes [29, 51]. Unfortunately, the chondrocytes cannot maintain the cartilage integrity for a long time and at some point, the chondrocyte death exceed the chondrocyte proliferation. The homeostasis in the articular cartilage is disrupted and shifted towards an elevated catabolism. The degradation of aggrecan is regarded as an early event during OA and is followed by the degradation of collagens [52-53].

1.2.1.1 Cartilage-degrading enzymes

The degradation of aggrecan during OA is mainly mediated by members of the 'a disintegrin and metalloproteinase with thrombospondin motifs' (ADAMTS) family. The most important members are ADAMTS4 and ADAMTS5, which are produced by chondrocytes and known to play a predominant role in OA. ADAMTS5 is 100-fold more active than ADAMTS4 in vitro and knockout of ADAMTS5, but not of ADAMTS4, in mice protect them for developing severe OA. However, there is some evidence that ADAMTS4 is involved in aggrecan degradation of human articular cartilage [53-55]. Additionally, several other ADAMTS members as well as 'a disintegrin and metalloproteinases' (ADAMs) are available, but their function within healthy and OA cartilage is largely unknown. Nevertheless, they contribute to the homeostasis of articular cartilage and exhibit specific functions. ADAMTS2, ADAMTS3 and ADAMTS14 for example promote anabolism of the cartilage ECM and ADAMs are actors in several signaling pathways to regulate articular cartilage homeostasis. Changes of expression- or protein levels may contribute to catabolic events during OA and should be further investigated [56].

The degradation of collagens during OA is mediated by matrix metalloproteinases (MMPs). MMP13 is the most important collagenase during OA, because of its cleavage prevalence for type 2 collagen [44]. Moreover, it is also able to degrade aggrecan [53]. MMP13 is hardly detectable in healthy articular cartilage, but significantly over-expressed in chondrocytes within osteoarthritic cartilage [52-53, 57]. Additionally, it was found that the MMP13 levels within the synovial fluid correlate with the severity of OA [52]. Examinations with mice, which continually express MMP13, showed OA development with aging, whereas MMP13 knockout mice were protected from collagen and aggrecan degradation indicating a significant impact of MMP13 during OA [53, 57]. Next to MMP13, MMP1 and MMP8 are also

able to degrade type 2 collagen, but less efficient than MMP13. In contrast, MMP2 and MMP9 further degrade collagen fragments generated by the other MMPs [44]. Another important MMP is MMP3 which is able to degrade cartilage ECM components, but also upregulates the expression and activation of MMPs like MMP13 [58-59].

All in all, the most dominant proteolytic enzymes during OA are the aggrecan degrading ADAMTS5 and the collagen as well as aggrecan degrading MMP13.

1.2.1.2 Cytokines

Cytokines are hormone-like proteins, which are released not only by chondrocytes, but also by the connective tissues synovial membrane (SM), infrapatellar fat pad (IFP) and subchondral bone [60-63]. They regulate the intensity and duration of inflammation processes and interactions between different cells [64]. The articular cartilage homeostasis of modeling and remodeling in response to mechanical forces during joint loading is maintained by chondrocytes, which produce inter alia cytokines for remodeling processes. Overload and enhanced biomechanical stress increase the synthesis of pro-inflammatory cytokines [64-65]. During OA, the balance between anti- and pro-inflammatory cytokines is shifted towards pro-inflammatory ones, which in turn shift the articular cartilage homeostasis towards catabolism by upregulating inter alia proteolytical enzymes like MMPs and ADAMTS. Simultaneously pro-inflammatory cytokines decrease the synthesis of articular cartilage ECM molecules [66]. Osteoarthritic chondrocytes produce cytokines like Il1β, TNFα and Il6 [65]. Il1β and TNFα are the most important and well-studied pro-inflammatory cytokines as they decrease the production of the main ECM molecules aggrecan and type 2 collagen. Additionally they stimulate their own production and the production of Il6, which contribute to the inflammatory status of the joint during OA [64-65, 67]. The production of Il1β and TNFα was correlated with OA severity and pain. Pain was assessed in this study after intra-articular injection of hyaluronic acid in OA patients and its decrease was correlated to reduced synovial fluid levels of Il1β and TNFα [66]. In addition, Il6 levels were also shown to be enhanced in the serum and the synovial fluid of OA patients [67].

Taken together, the key pathophysiological mediators of articular cartilage catabolism are pro-inflammatory cytokines like Il1β, TNFα and Il6 and proteolytic enzymes like ADAMTS5 and MMP13, which interact in a complex way and disrupt the cartilage homeostasis leading to OA progression.

1.2.2 Other tissues involved in OA

To understand the complex pathomechanism of OA, it is important to pay attention not only to changes within the articular cartilage, but also on changes within the other connective tissues, which contribute to the disease in different ways.

The connective tissues synovial membrane (SM) and the infrapatellar fat pads (IFP) are prone to changes during OA. The tissue alterations enhance the joint inflammation processes by shifting the balance between anti- and pro-inflammatory mediators towards the latter, which finally contributes to articular cartilage degradation and leading to symptomatic OA [62, 68]. The SM contains two main cell types, macrophage-like and fibroblast-like synoviocytes. Macrophage-like synoviocytes produce and secrete cytokines, chemokines and other enzymes involved in tissue alterations and stimulate fibroblast-like synoviocytes to produce and secrete proteolytical enzymes [62]. The primary histological change of SM during OA is hyperplasia, which is accompanied by an increased vascularity and infiltration of immune cells. Both the increased vascularity and infiltration correlates with SM inflammation, which is called 'synovitis', and with OA severity [9, 68]. Synovitis is an active component of OA progression and is mediated by complex mechanisms, which are in the following shortened and simplified. Articular cartilage fragments as well as any kind of tissue debris are released into the synovial fluid, which is in contact with the SM. Macrophage-like synoviocytes phagocytose these fragments what provokes the production of pro-inflammatory mediators within the SM followed by the secretion of those into the synovial fluid. This is the start of a vicious cycle, as the chondrocytes located in the superficial zone are activated leading to a production and secretion of cytokines and proteolytic enzymes by the chondrocytes resulting in the progression of articular cartilage destruction [9, 62]. In this way, more cartilage fragments are released into the synovial fluid, which in turn stimulate the SM inflammation. The IFP also produces inflammatory cytokines like Il6 and TNFα [63] and exerts its effects primarily on the SM contributing to an enhanced synovitis [69]. All in all, the SM and the IFP are both tissues contributing to an elevated pro-inflammatory level within the synovial fluid of OA patients and are together with chondrocytes the main sources of cytokines. Besides this inflammation features, both tissues mediate OA pain, probably through the release of the pain neurotransmitters substance P and nerve growth factor (NGF) [62].

The subchondral bone is also prone to changes during OA. Already during early OA, sclerotic bone changes, bone cysts, bone marrow lesions (BML) and hypomineralization of the bone can appear. Characteristics of advanced OA are bone thickening and the formation of bony outgrowths at joint edges, called osteophytes, which compensate the reduced strength of the subchondral bone [70-72]. Advanced bone remodeling and BML are associated with increased articular cartilage damage and pain [9, 71-72] . A viscous circle starts as the loss of articular cartilage increases the loading and remodeling of the subchondral bone, which in turn progress articular cartilage damage [73]. In addition, during OA the articular cartilage becomes vascularized by blood vessels from the subchondral bone resulting in an

increased oxygen concentration within the OA cartilage as well as the presence of additional cytokines coming from the subchondral bone.

1.2.3 Conclusion pathophysiology of OA

Taken together, OA is a multifractional disease affecting not only the articular cartilage, but also connective tissues. OA leads to a disbalance of several homeostatic mediators like chemokines, inhibitors, growth factors, proteolytic enzymes or cytokines produced and secreted by the different joint tissues. It remains unknown which tissue changes are initial for OA and which are responsible for further OA progression. Both the trigger as well as the course of OA can vary among the different OA patients resulting in different OA phenotypes. Consequently, it is necessary to further evaluate the complex pathomechanism of OA. This knowledge will accelerate the development of new OA therapeutics.

1.3 Current treatment options for OA

At present OA is an incurable disease. Many treatment options are available, but they are mainly focusing on symptomatic relief. In a last resort a surgical intervention consisting in a total joint replacement is performed. There is currently no efficacious structure-modifying drug approved, which can prevent OA initiation, reduce or stop OA progression or even rebuilt articular cartilage. Therefore, there exist an unmet medical and clinical need for disease-modifying OA drugs (DMOADs).

1.3.1 Existing OA medications

Pain is increased dramatically during the course of OA what is the main reason for patients to seek for treatments [74]. The common OA medications mainly target the symptomatic relief of pain (Figure 5). The oral analgesic acetaminophen is prescribed first for mild to moderate OA. For moderate to severe OA, nonsteroidal anti-inflammatory drugs (NSAIDs) are prescribed as a second choice to address not only the pain, but also the inflammatory relief during OA. NSAIDs are more efficient but less well tolerated than acetaminophen [16], because adverse gastrointestinal or cardiovascular side effects are observed [75-76]. Consequently, the balance between efficacy and safety is questionable and it is recommended by the OARSI to use the minimal effective dose and only for a limited time [16]. An alternative medication to NSAIDs are opioid analgesics like tramadol. The use of tramadol shows comparable efficacy than NSAIDs but may be even more harmful combined with the risk of opioid dependence and abusive use. There is also no recommendation for routinely use of tramadol [16]. Besides the oral application of analgesics, the intra-articular injection of corticosteroids and hyaluronic acid is commonly used as a fourth choice to manage pain and improve joint function of moderate to serve OA [77]. However, the efficacy of these injections is highly controversial and varies among the patients [16, 78-79]. As a last choice, total joint replacements (TJR) are performed, but they should not be regarded as a

real cure. Many people still have mobility/certain sport limitations resulting in a modification of life style post-surgery, there is a high infection risk, some people reported a kind of 'phantom pain' in the replaced joint [80] and the protheses have a limited lifetime of up to 15 years [16, 81]. Patients suffering from OA are often treated with a combination of these existing OA medications and non-pharmacological treatments or food supplements. Non-pharmacological treatments are for example physiotherapy to strengthening muscles, thermal therapy or diet [16]. Food supplements like glucosamine or chondroitin, which are both components of the cartilage ECM, are safe and commonly used. However, there is only limited clinical evidence for their efficacy, also because of quality and validity doubts of the performed clinical studies [81-82]. Furthermore, some surgical interventions like chondral shaving and debridement are applied, but mainly gaining time of less symptoms. Microfracture and drilling techniques are applied for younger and very active patients and aim to stimulate tissue repair, but they failed as the repaired tissue is inferior, less durable fibrocartilage [16, 77].

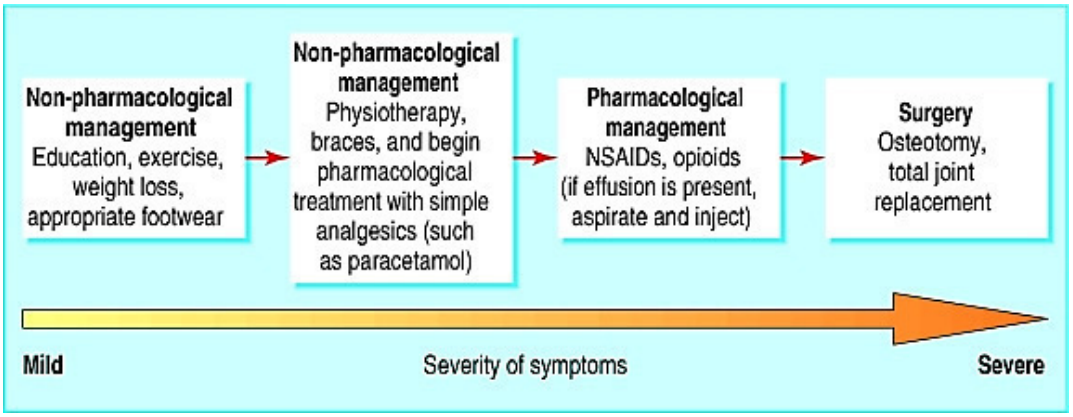

Figure 5 **Existing medications to treat mild to serve OA.** As a first step, mild non-pharmacological treatments are applied like exercise or diet. Secondly stronger non-pharmacological treatments are applied like physiotherapy and mild pharmacological treatments like analgesics. Thirdly NSAIDs and opioids are applied to treat moderate to serve OA and as a last choice the joint is replaced orthopedically. Reproduced from [83] with permission from BMJ Publishing Group Ltd.

All these applications have strong limitations and mainly targeting symptomatic alleviations, which reflects and points up the unmet medical need for disease-modifying OA drugs (DMOADs).

1.3.2 Disease-modifying OA drugs

Disease-modifying OA drugs (DMOADs) should prevent OA initiation, reduce or even stop the course of joint destruction or promote tissue regeneration by influencing specific molecular mechanism during OA, leading to a reduced catabolism and/or restored anabolism. DMOADs ideally address both structural joint improvement combined with pain relief [77, 84-85]. In general, there exist two different approaches, the anti-catabolic and the anabolic approach, to reach this requirement [84-85].

Anti-catabolic DMOADs directly or indirectly address the inhibition of cartilage-degrading proteolytic enzymes to prevent articular cartilage destruction during OA while anabolic DMOADs promote tissue

repair. Growth factors (GFs) involved in tissue development and maintenance of tissue homeostasis are ideal anabolic candidates.

There is and was a great number of possible DMOADs under investigation (Figure 6), but many of these attempts failed in the clinic due to different reasons like sub-optimal selection of patient groups, wrong drug dosage, sub-optimal set of the end-point measurement or a lack of efficacy [86].

Promising, but failed therapeutic approaches belonging to the field of anti-catabolic DMOADs are the unselective inhibition of MMPs, the selective inhibition of MMP13, the inhibition of inducible NO synthase (iNOS) which indirect inhibits the MMP activity as well as antiresorptive approaches like the administration of bisphosphates, calcitonin or strontium [86-87]. Anti-catabolic DMOADs which are currently under clinical investigation target the selective inhibition of the proteolytic enzyme cathepsin K [86, 88], the selective inhibition of ADAMTS5 [89], the selective inhibition of Il1α/β [90-92] or the inhibition of the Wnt pathway which induce the production of proteolytic enzymes and cytokines during OA [93-95].

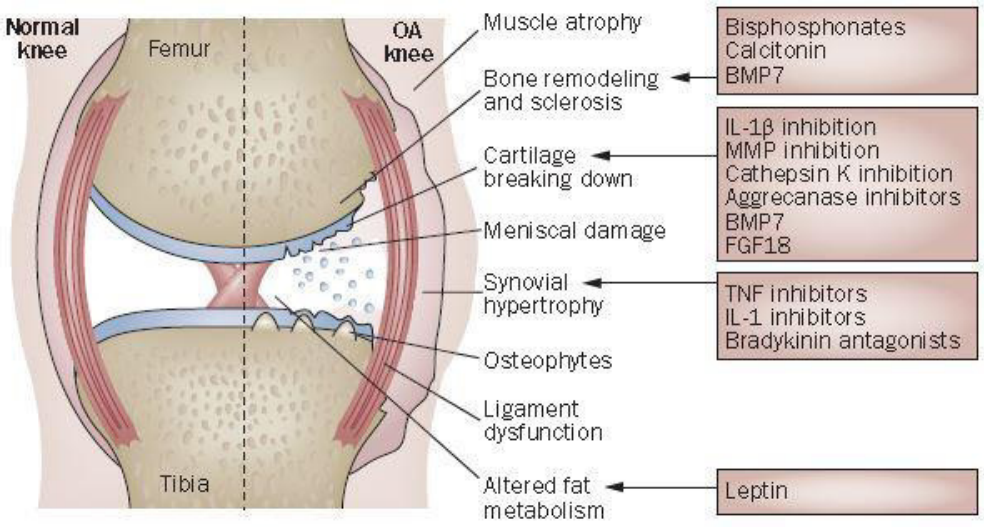

Figure 6 **Different joint tissues involved in OA are targets for possible DMOAD candidates.** Some of the DMOAD candidates that targeting bone (e.g. bisphosphonates), cartilage (e.g. proteolytical inhibitors or growth factors like BMP7 and FGF18) or synovial membrane (cytokine inhibitors) are listed. Reprinted by permission from Springer Nature Terms and Conditions for RightsLink Permissions Springer Customer Service Centre GmbH: [96], Copyright 2010.

In the following, anabolic DMOADs are listed which are currently under clinical investigation.

A potential anabolic DMOAD is TPX-100, a peptide derived from matrix extracellular phosphor-glycoprotein, which occurs naturally in humans and is involved in the formation of cartilage and bone [86, 97]. In a recently published phase II study in patients with knee OA, the intra-articular application of TPX-100 resulted in a significant pain reduction. However, no significant improvement of articular cartilage thickness or volume was measurable. Further clinical studies of longer duration have been announced [97-98]. Platelet rich plasma (PRP), which contains a mixture of different growth factors is under investigation but the efficacy is still questionable. Several clinical studies demonstrated the potential of intra-articular injected PRP to improve joint structure and reduce pain. However, the patient

size was small and the clinical trial duration short. Additionally, the preparation and application is not standardized among the clinical studies [99-100]. Furthermore, a cell-mediated gene therapy is under clinical investigation (TissueGene-C/Invossa), which originally aimed to relief pain. TissueGene-C (TG-C) is a 3:1 mixture of normal allogenic human chondrocytes and TGFβ1-expressing allogenic human chondrocytes. The growth factor TGFβ1 is important during articular cartilage formation and possess anti-inflammatory properties. A clinical phase II and III study demonstrated pain alleviation after one single intra-articular injection of TG-C lasting up to 1 year. Additionally, the phase III trial lead to the suggestion of structural tissue improvements [101]. TG-C was approved in 2017 for South Korea as gene therapy to relief pain in OA patients and is currently under investigation in a phase III trial over a longer duration to see possible structural changes delivered by intra-articular injections of TG-C. Another anabolic DMOAD candidate is the growth factor BMP7 which is involved in cartilage modeling and whose levels were shown to be decreased in OA cartilage explants compared to healthy explants [96, 102]. A clinical phase I study led to the suggestion of a possible symptomatic pain relief after intra-articular injection of BMP7 compared to placebo [103]. As stated on the company's website, the clinical phase IIa led to promising results in an initial result analysis. The data of 78 out of 320 patients were analyzed and as a conclusion it was formulated that even one single intra-articular injection of BMP7 resulted in anabolic effects and prevented the further degradation of articular cartilage. As a conclusion, a pivotal phase III trial should be conducted (see company´s webpage, http://www.embertx.com/news.html). As a last anabolic DMOAD candidate, a recombinant and shortened version of the growth factor FGF18 (Sprifermin/AS902330) is currently under clinical investigation. Preclinically Sprifermin was shown to induce the proliferation of chondrocyte resulting in an enhanced cartilage ECM production [84, 86, 104]. Sprifermin is injected intra-articularly and showed a dose-dependent structural cartilage improvement in a clinical phase I studies with OA patients [16, 104]. Two-year data out of a currently running five-year clinical phase II study confirmed the dose-dependent increase in total cartilage thickness. In addition, a 50% pain alleviation was observable in all patient groups but also in the placebo group [105].

Up to now, there is no DMOAD approved, but some of the DMOAD candidates have shown promising results. Nevertheless, there is still an unmet medical need for DMOADs. Members of the bone morphogenetic proteins (BMPs) could bear DMOAD potential as they are involved in the formation of cartilage and bone.

1.4 Bone morphogenetic protein (BMP) family

Bone morphogenetic proteins (BMPs) were first discovered in 1965 by Marshall Urist. He implanted demineralized bone matrix (DBM) under the skin or within the muscle of animals and observed the formation of ectopic bone within the non-skeletal tissues [106]. This finding predicts the availability of bioactive factors within the DBM, which initiate bone formation, leading to the search for these factors [107-108]. These factors were named 'bone morphogenetic proteins' based on the observed bone development. Only 20 years later, a key step was done when the first BMPs, named BMP1, 2, 3 and 4, were characterized and cloned [109]. This enabled the biochemical investigation of individual BMPs and their classification to the transforming growth factor β (TGFβ) superfamily [110].

Bone can be formed directly by intramembranous ossification, which is characterized by the differentiation of mesenchymal stem cells (MSC) into osteoid matrix producing osteoblasts [111], but most of the skeletal volume (~80%) is formed by endochondral ossification [112]. During the endochondral ossification process, the MSCs differentiate first to chondroblasts (= condensation), which begin to proliferate and form chondrocytes. The central chondrocytes can be further differentiated and become hypertrophic resulting in their apoptosis. The apoptotic chondrocyte matrix is eroded by osteoclasts leading to the invasion of blood vessels and osteoblasts, which ultimately initiate the bone formation. Thus, the chondrocytes forming a template for the formation of bone [111-113]. Based on this, the function of BMPs was focused on cartilage and bone formation. Later it was shown that BMPs play important roles during many processes of embryogenic development or during tissue homeostasis and also during tissue regeneration in adulthood [110, 114-115]. Not all BMPs exhibit the same osteogenicity and some BMPs even exhibit non-osteogenic properties depending on the expressing tissue, the molecule structure and the signaling events [107]. They are suggested to be attractive targets to treat different diseases, like organ fibrosis or skeletal disorders including OA [114].

1.4.1 BMP subgroups and synthesis

Over 30 BMP family members were identified, of which about 15 BMP members appear in mammals [116]. They can be divided into four subgroups according to their structural similarity and function. The first group includes BMP2 and 4, the second group includes BMP5, 6, 7 and 8, the third group includes BMP9 and 10 and the fourth group includes BMP12, 13 and 14 [107, 110, 117]. Some BMPs are described with additional names. For example BMP7 and 8 are also known as osteogenic protein (OP) 1 and 2 or BMP12, 13 and 14 are also known as growth and differentiation factor (GDF) 7, 6 and 5 or cartilage-derived morphogenetic protein (CDMP) 3, 2 and 1 [107, 116].

BMPs are synthesized intracellularly as large inactive precursor molecules [118]. In contrast to other members of the TGFβ superfamily, the BMPs are usually activated inside the cell before secretion [117] (Figure 7). The activation takes place by proteolytic cleavage through proprotein convertases at a

consensus RXXR region within the pro-domain to frees the mature BMP from the pro-domain. The mature protein consists of approximately 100 to 140 amino acids [118] and contains six highly conserved cysteine residues that are characteristic for members of the TGFβ family. These cysteine residues form three intramolecular disulfide bonds, named cysteine knots. BMPs contain a seventh cysteine residue, which is located outside the cysteine knots and form intermolecular disulfide bonds allowing the covalent dimerization with another BMP monomer.

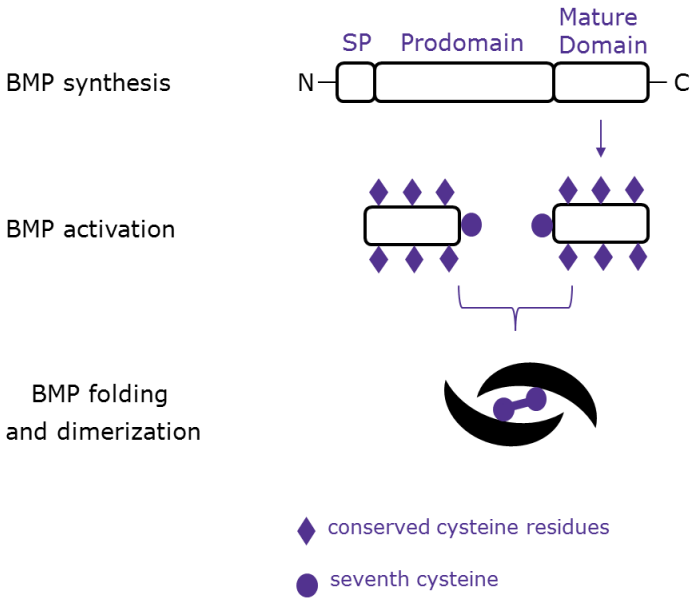

Figure 7 **BMPs are synthesized as precursor molecules and are activated inside the cell.** Inactive BMP precursor molecules are made up of a n-terminal signal sequence/peptide (SP), followed by a prodomain and the mature domain. The BMP activation occurs by secession of the signal sequence and prodomain through proprotein convertases. The mature BMP contain seven cysteine residues from which six form intramolecular disulfide bonds, whereas the seventh form an intermolecular disulfide bond to connect two BMP monomers to a biological active BMP dimer.

Usually homodimers are formed with its characteristic wrist and knuckle or banana shape structure (Figure 7). The biological active BMP dimers are secreted and mediate their effects by binding to BMP receptors to initiate intracellular signaling events [107, 110, 114, 117, 119].

1.4.2 BMP signaling

The dimeric BMPs within the extracellular space elicit intracellular signaling by binding to two classes of serine/threonine kinase transmembrane receptors known as type 1 and type 2 BMP receptors (BMPRs). There are altogether seven type 1 and four type 2 receptors for the TGFβ superfamily. BMPs can interact with three type 1 receptors, namely activin receptor-like kinase (ALK) 2, ALK3 (also known as BMPR1a) and ALK6 (also known as BMPR1b), and with three type 2 receptors, namely activin A receptor (ActR) type 2 and type 2b and BMPR2 [110, 117-118]. BMPs preferentially bind to the BMP-specific receptors BMPR1a, BMPR1b and BMPR2 [110]. All BMPRs consist of three parts, a short extracellular domain, followed by a single transmembrane domain and an intracellular domain responsible for

serine/threonine kinase activity [119]. For signal transmission, a heteromeric complex of two type 1 and two type 2 receptors is required (Figure 8).

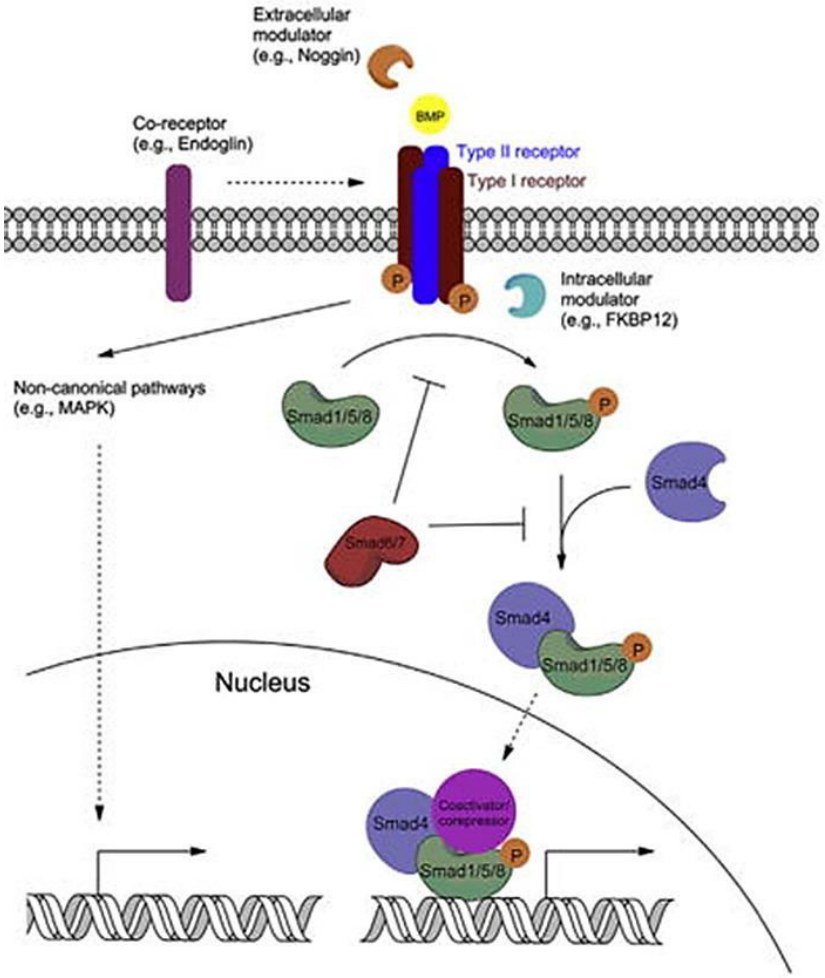

Figure 8 **BMP signaling activates the canonical SMAD-dependent and the non-canonical MAPK pathway**. Dimeric BMPs bind to a heteromeric receptor complex of two type 1 and type 2 receptors. The type 2 receptors transphosphorylate the type 1 receptors, which in turn phosphorylate the receptor regulated SMAD (R-SMAD), SMAD1/5/8. Phosphorylated SMAD1/5/8 complexes the common mediator SMAD (co-SMAD), SMAD4. The complex translocates into the nucleus and initiate gene transcription. This signaling cascade is regulated at several checkpoints from the extracellular space (e.g. antagonist like noggin) over the transmembrane region (e.g. agonistic co-receptors) to the intracellular space (e.g. inhibitory SMADs like SMAD6 and 7) and the nucleus (transcriptional regulation through coactivators/-repressors). Reprinted with permission from Creative Commons Attribution 3.0 International License: [110].

The binding of dimeric BMPs leads to the transphosphorylation of the type 1 receptor through the constitutively active type 2 receptor (Figure 8). The transphosphorylation occurs at the TTSGSGSG motif within the conserved GS-domain, which is located between the transmembrane domain and the kinase domain of the type 1 receptor [118]. The type 1 receptor transduce the signal by phosphorylation of the receptor regulated SMAD (R-SMAD), namely SMAD1/5/8, which change its conformation to enable the binding of the common mediator SMAD (co-SMAD), known as SMAD4. This complex is built usually by a trimer of two R-SMADs and one co-SMAD and translocates to the nucleus to regulate gene expression [114, 118].

1.4.2.1 Regulation of BMP signaling

This signaling cascade is strictly regulated by agonists and antagonists at several checkpoints from the extracellular space over the transmembrane region to the intracellular space and the nucleus. Extracellular modulators can be divided into antagonists and agonists. Extracellular antagonists bind to the dimeric BMPs and regulate the extracellular BMP concentration and -bioavailability. The binding results in a blockade of the BMPs preventing the interaction with their receptors and leading to limited intracellular signaling [114, 117]. Extracellular BMP antagonists include on the one hand proteins like noggin, chordin, gremlin or follistatin [114]. On the other hand, ECM components like collagens or fibronectin can compete for BMP binding [117]. In contrast cartilage ECM components like heparan sulfates (HS) can act as extracellular agonists. BMPs contain a HS binding site and the binding of the BMP dimer to HS is thought to potentiate the BMP effects by prolonging the bioavailability/activity of the BMPs [120]. Furthermore, at the transmembrane region, several co-receptors and pseudo-receptors, which are lacking an intracellular signal domain, modify the signal transduction. Intracellular modulators of BMP signaling are SMAD ubiquitination regulatory factors (Smurf), inhibitory SMADs (I-SMAD), proteins regulating phosphorylation and dephosphorylation as well as different binding proteins. Smurf1 and Smurf2 mark R-SMADs with ubiquitin residues at their proline, serine, threonine enriched domain leading to a selective proteosomal degradation of R-SMADs. SMAD6 and 7 belonging to the I-SMADs and prevent the interaction of R-SMADs with co-SMADs directly or indirectly [114]. Another kind of intracellular modulation is mediated by phosphatases, which inactivate R-SMADs by dephosphorylation [114, 117]. Transcriptional regulation is mediated through several co-activators and co-repressors. BMP signaling itself also initiates the expression of several antagonists and agonists, which act as feedback loops. Negative feedback loops occur by expression of the extracellular antagonists, pseudo-receptors or I-SMADs. Positive feedback loops are induced by enhanced expression of the R-SMADs [107].

Another kind of BMP signaling regulation is the crosstalk with other signaling pathways such as TGFβ, Wnt, Notch or hedgehog. The crosstalk is either mediated directly through protein interactions or indirectly through transcriptional feedback loops [117, 121].

1.4.2.2 Diversity of BMP signaling

It is surprising that the limited number of receptors for BMP ligands can mediate such a diverse spectrum of cellular responses and functions. On the one hand, the crosstalk between several non-SMAD pathways mentioned above expands significantly the diversity of cellular responses. On the other hand, next to the well-described SMAD pathway, BMPs can initiate the SMAD-independent mitogen-activated protein kinase (MAPK) pathway including p38 MAPK, extracellular signal-regulated kinases (ERK) and c-Jun amino-terminal kinases (JNK) [122]. This additional SMAD-independent pathway differs from crosstalk pathways, because it is induced directly by BMP-receptor binding. The SMAD and MAPK pathways are

both crucial not only for MSC migration, proliferation and differentiation during cartilage and bone development, but also for the maintenance of joint integrity (including modeling and remodeling processes) and possible cartilage repair mechanisms during adulthood [123-124]. A differentiation factor for the activation of the SMAD or the MAPK pathway, is the distinct mode of receptor oligomerization [125]. Receptor oligomerization to build a heteromeric complex of two type 1 and type 2 receptors respectively, can occur in the absence of BMP ligands. Thus, the BMPs can directly bind to the preformed receptor complex (PFC) inducing the SMAD pathway (Figure 9). Upon BMP binding to the PFC, the receptor complex is internalized by clathrin-dependent endocytosis, followed by dissociation of the phosphorylated SMAD1/5/8 [126].

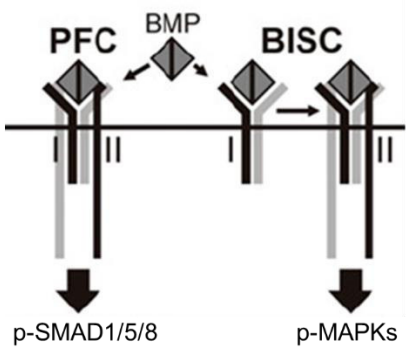

Figure 9 **The mode of receptor oligomerization determines intracellular signaling pathways.** Receptors can oligomerize to preformed tetrameric receptor complexes (PFC) or to tetrameric BMP-induced signaling complexes (BISC) lead to the phosphorylation of SMAD1/5/8 or MAPKs respectively. Adapted with permission from Creative Commons Attribution 4.0 International License from [125], Copyright 2017 The Authors.

As a second way of receptor oligomerization, the BMPs can bind to their high affine type 1 receptor dimer complex leading to the recruitment of the type 2 receptor dimer complex (Figure 9). Thus, the formation of the required heteromeric receptor complex is activated after BMP binding and results in a BMP induced signaling complex (BISC). The BISC induces mainly the MAPK pathway resulting in the phosphorylation of p38, ERK and JNK, but activates also the SMAD pathway and is internalized in caveolae [122, 126]. The induction of the SMAD-independent pathway via BISC requires a greater stability of the heteromeric complex compared to the PFC, because the type 2 receptor needs a high mobility required for recruitment. Thus, not only the mode of oligomerization, but also the location and mobility of the BMPRs within the membrane contribute to broadening of cellular responses of BMPs [122]. Furthermore, phosphorylated MAPKs (pMAPK) can regulate the SMAD pathway and can be viewed as a kind of fine-tuning for the SMAD pathway. However, the specific role of the SMAD-independent pathway remains unclear, especially within chondrocytes. In addition to the different ways of receptor oligomerization, different binding affinities of the BMPs to their receptors resulting in specific functions which varies among the BMP ligands.

1.4.2.3 Distinct roles of BMPR1a and BMPR1b in cartilage and bone formation

The respective roles of the BMPRs in the formation of cartilage and bone is not fully understood and remains controversial. However, most of the literature consider that BMPR1a and BMPR1b are the important receptors trigger the formation of cartilage and bone. Consequently, different binding affinities of the BMPs to BMPR1a or BMPR1b can determine the cell fate. As mentioned above, most of the skeletal volume is formed by endochondral ossification. The initial step of this developmental process is the chondrogenesis of stem cells resulting in the formation of articular cartilage. This step is clearly mediated through activation of BMPR1b [113, 115, 124, 127-128], but it remains unclear if the activation of BMPR1a is additionally required [129-131] or if BMPR1a and BMPR1b even have overlapping functions [113, 115]. As a second step of endochondral ossification, the chondrocytes become hypertrophic and the cartilage is finally substituted by bone. This bone formation process is described as hypertrophy and osteogenesis and BMPR1a is the main trigger of these processes [112, 115, 124, 127, 130-131]. This is in accordance with expression analysis of BMPR1a and BMPR1b. BMPR1a is mainly expressed in osteolineage cells, bone marrow cells and pre-hypertrophic chondrocytes, whereas BMPR1b is mainly expressed in pre-cartilaginous condensation and limb prefigures [113, 115, 124]. Amongst others, two members of the BMP family are considered as indispensable during bone and cartilage formation. BMP2 has a high binding affinity for BMPR1a and is best known for its great osteoinductive properties, is expressed in hypertrophic chondrocytes to trigger osteogenesis and is consequently a key regulator for endochondral ossification [110, 132]. In contrast GDF5 is one of the earliest markers during joint formation and is expressed at the sites of cartilage development as well as in adult articular cartilage making it a key regulator for cartilage development and cartilage maintenance [3, 131, 133]. Therefore, GDF5 could bear DMOAD potential.

1.4.3 GDF5 as a possible DMOAD candidate

GDF5 plays a key role during embryonic cartilage development and cartilage maintenance during adulthood and combines anabolic and anti-catabolic capacities. The anabolic potential of GDF5 to induce articular cartilage production was demonstrated in vitro and in vivo. The addition of exogenous GDF5 promotes chondrogenesis of human mesenchymal stem cells [128, 134], induces cartilage ECM synthesis in human, mature healthy and OA chondrocytes cultured in alginate beads [135], aggregate cultures [134] or pellet cultures [1, 4] and was also shown to induce cartilage formation in a rat model of OA [3]. Recently, different MSC niches within the joint including the superficial zone of articular cartilage itself, the synovial membrane, the fat pads, the synovial fluid as well as subchondral bone were discovered. Probably these MSCs migrate toward the damaged OA cartilage and adhere to it to initiate tissue regeneration [51]. Based on the in vitro and in vivo observations mentioned above, it would be possible that GDF5 stimulates not only the chondrocytes itself to regenerate articular cartilage, but also to support the chondrogenic differentiation of MSCs. Consequently, GDF5 could enable to regenerate articular

cartilage. Additionally, anti-catabolic features of GDF5 were demonstrated on human OA chondrocytes (hOAC) by inhibition of the Wnt signaling pathway resulting in a downregulation of MMP13 and ADAMTS4 [4]. Based on that, GDF5 could additionally prevent further cartilage worsening/OA progression. Finally, single nucleotide polymorphisms (SNPs) were identified within the promotor sequence of the human GDF5 gene, namely rs143383 and rs143384. Both SNP variants lead to a substitution of the cytosine to a thymine allele which significantly reduce the expression of GDF5 within the whole joint [136-137]. These SNPs were associated with OA in a genome-wide association study. In addition, mutations within the GDF5 gene causes several joint malformations like brachydactyly type C (heterozygous GDF5 mutation) and chondrodysplasias like Hunter-Thompson dysplasia (homozygous GDF5 mutation) [3, 110, 131, 138] which are also associated with an enhanced OA risk.

In summary, GDF5 may have therapeutic potential to treat OA. However, GDF5 was also shown to induce hypertrophic differentiation in MSCs [5] resulting in the production of cartilage with inferior properties and was shown to induce the formation of osteophytes in an OA rat model [3]. The BMPR1a affinity of GDF5 is believed to promote hypertrophy and osteogenesis. To reduce these hypertrophic and osteogenic capacities of GDF5, which are unwanted when considering GDF5 as treatment option for OA, different GDF5 mutants were produced and those having a lower BMPR1a affinity selected. It has been shown in prior investigations that these GDF5 mutants stimulate the cartilage ECM production in bovine and porcine chondrocytes. The goal of the work presented here was to evaluate the therapeutic potential of these GDF5 mutants to treat OA and to show a possible superiority over GDF5.

2 Objectives of the work

Current treatment options for OA are limited and mainly focusing on symptomatic relief. These medications do not provide a real cure for OA and consequently, there is an unmet medical need for disease-modifying OA drugs (DMOADs), which reduce/stop OA progression or even regenerate the articular cartilage. Ideally, a DMOAD should provide an improvement of the articular cartilage structure combined with symptomatic alleviation.

The growth and differentiation factor 5 (GDF5) could be a promising DMOAD candidate. GDF5 is a key-regulator during embryonic cartilage development and for its maintenance during adulthood. Furthermore, single nucleotide polymorphisms within the GDF5 gene were associated with OA [3]. Previous studies demonstrated that GDF5 can induce cartilage production in chondrocytes, promote chondrogenesis in mesenchymal stem cells (MSCs) and induce cartilage repair in a rat model of OA [1-3]. Furthermore, it was shown that GDF5 downregulates the production of proteases in chondrocytes [4]. Therefore, GDF5 could combine anabolic and anti-catabolic features resulting in the ability to induce cartilage repair and simultaneously inhibit disease progression in vivo. Unfortunately, GDF5 was also shown to exhibit undesired hypertrophic and osteogenic features in vitro and in vivo [3, 5].

To reduce the hypertrophic and osteogenic properties of GDF5, different GDF5 mutants were produced. Three of these GDF5 mutants (M1673, W417F, W417R) were selected. They display a lower BMPR1a affinity in comparison to GDF5 which was thought to be involved in hypertrophic differentiation and osteogenesis but a similar BMPR1b affinity, which was thought to be relevant for chondrogenesis. The present work aimed to evaluate these GDF5 mutants for their therapeutic potential in chondrocytes and MSCs, as both cell types can contribute to cartilage repair.

Among the GDF5 mutants, M1673 previously showed the strongest effect on cartilage ECM molecule production in porcine and bovine chondrocytes. The first objective of this work was to confirm the anabolic effect of M1673 in human OA chondrocytes (hOAC). However, in order to do so, the culture conditions for the hOAC needed to be optimized.

MSCs can differentiate into chondrocytes and participate to cartilage repair but can also differentiate into bone-producing cells [110]. Another objective of this work was to evaluate the GDF5 mutants for their abilities to stimulate chondrogenesis and osteogenesis in MSCs. It was aimed to identify the GDF5 mutant, which combines the highest chondrogenic capacity and, in comparison to GDF5, a lower hypertrophic/osteogenic capacity. BMP2 was used as a positive control for hypertrophy and osteogenesis of MSCs. In addition, it was aimed to better understand the respective roles of BMPR1a and BMPR1b in chondrogenesis and osteogenesis.

3 Materials

3.1 Consumable Material

Product	Supplier	Cat. No.
Adhesive Clear Seal Sheets	Biozym	600208
Biopsy cassettes	VWR	87002586
Cell sample cup	Beckman-Coulter	7091168
Cell sieve 100 μm	BD Falcon	352-340
Cell sieve 40 μm	BD Falcon	352-360
Combi TIPS	Eppendorf	613-3532 613-3533
ep TIPS	VWR	613-3554 613-3555 613-3557
ep TIPS, dualfilter	VWR	613-3562 613-3563 613-3565
Falcon tubes, 15 mL	BD Bioscience	734-0451
Falcon Tubes, 50 mL	BD Bioscience	734-0448
Falcon Tubes light sensitive, 50 ml	VWR	7320438
Flat 8-Cap Stripes	Bio-Rad	TCS0803
iBlot Transfer Stacks, PVDF	Thermo Scientific	IB401001
Microscope slides	VWR	6302131
Mx3000 96-well plates	Agilent Technologies	401333
NuPage 4-12% Bis-Tris Gels, 1.5mm, 10 well	Thermo Scientific	NP0335BOX
Osmomat measuring vessels	Gonotec	30.9.0010
PCR clean dualfilter tips 1000 μl	Eppendorf	0030 077.652
PCR clean dualfilter tips 200 μl	Eppendorf	0030 077.555
PCR clean dualfilter tips 20 μl	Eppendorf	0030 077.628
Petri dish, 10 cm	VWR	7341709
Petri dish, 15 cm	VWR	7341710

Petri dish, 6 cm	VWR	7341708
Safe Lock tubes PCR clean 1.5 ml	Eppendorf	0030 123.328
Safe Lock tubes PCR clean 2.0 ml	Eppendorf	0030 123.344
Safe-Lock tubes 1.5 ml	VWR	700-5239
Sample cups ViCell	Beckman-Coulter	383198
Scalpel blade holder	VWR	233-5202
Scalpel blades, Size 22	Braun	BB522
Series S Sensor Chip CM5	GE Healtcare	BR100668
single use serological pipette 10 ml	VWR	734-0352
single use serological pipette 25 ml	VWR	734-0347
single use serological pipette 50 ml	VWR	734-0351
Syringe, 10 ml	VWR	10753946
Syringe filter, 0.2 μm	VWR	5140073
T-Flask, 75 cm²	VWR	734-0050
T-Flask, primaria 75 cm²	Corning	353810
T-Flask, 175 cm²	Corning	356780
24 well plates	Falcon	353226
24 well plates, primaria	Corning	353847
24 well plates, low binding	VWR	7341584
48 multiwell plates	VWR	734-0956
48 multiwell PCR plates	Bio-Rad	MLL4801
96 multiwell plates	Falcon	353226
96 multiwell plates, low binding	VWR	7341585
96 multiwell plates, black	Nunc	7342018
96 multiwell plates, white	Greiner Bio-One	655083

3.2 Chemicals and reagents

Product	Supplier	Cat. No.	Application
Alginic acid sodium salt	Fluka	71238	Alginate beads
Calcium chloride	Alfa Aesar	L13191	
HEPES	AppliChem	A3268	
Hydrochloric acid, 1 M	Merck	109057	
Sodium chloride	Merck	106404	
Sodium citrate	Merck	1064480	
Sodium hydroxide, 0.2 M	Merck	109140	
Glycine	Merck	104201	ALP analysis
Magnesium chloride hexahydrate	Merck	105833	
Nonidet-P40	Calbiochem	492616	
Sodium hydroxide	Merck	109141	
Phosphatase substrate	Sigma	N7660	
Zinc chloride	Merck	108815	
4-Nitrophenol Solution, 10 mM	Sigma	P5869	
Concentration control	Beckman-Coulter	175478	Cell concentration
Reagent quad pak	Beckman-Coulter	383198	
Alcian blue (1% in acetic acid; pH 2.0)	Morphisto	10126.01000	Cell staining
Alizarin red (0.5% in distilled water)	Sigma	A5533	
Paraformaldehyde	Merck	818715	
Chondroitin sulfate	Sigma	C4384	GAG analysis
Dimethylmethylen blue	AppliChem	A1279	
Ethanol p.a	Merck	1.00983	
Formic acid	VWR	20318	
Sodium chloride	Merck	106404	

Sodium citrate	Merck	106448	
Sodium formate	Merck	106443	
Acetic acid	VWR	818755	Histology
Alizarin red	Morphisto	13154	
Dewax Solution	Leica	AR9222	
EtOH	VWR	1009843	
Fast Green FCF	Sigma	F7258	
Isopropanol	VWR	818766	
NeoClear	VWR	109843	
NeoMount	VWR	109016	
Paraffin	Merck	111609	
PFA	VWR	818715	
Safranin O	Sigma	S2255	
Wash buffer (Bond-III)	Leica	AR9590	
Weise Buffer	Merck	109468	
Acetonitrile	Merck	100030	HPro analysis
Formic acid	Merck	251364	
Hydrochloric acid	Merck	100316	
4-Hydroxyproline	Merck	816007	
Tween-20	Calbiochem	655204	Multispot immunoassays (Mesoscale)
EDTA	Merck	106346	Papain digestion
L-cystein	Merck	102838	
Na_2HPO_4	Merck	106346	
Papain	Merck	107144	
Benchmark Prestained Protein Ladder	Thermo Scientific	10748010	SDS-PAGE
Magic Mark XP	Thermo Scientific	LC5602	

NuPage Antioxidant	Thermo Scientific	NP0005	
NuPage Sample Reducing Agent	Thermo Scientific	NP0009	
Acetate			SPR affinity analysis
HEPES	Merck	1101101	
Hydrochloric acid 1 M	Merck	1090571	
Protein-A	Sigma	P7837	
Sodium chloride	Merck	106404	
Sodium hydroxide	Merck	109141	
Tween20, 10% solution	Calbiochem	655206	
β-glycerolphosphate	Sigma	50020	Stem cells
Dexamethasone	Sigma	D2915	
Hydrochloric acid 1 M	Merck	1090571	
Calibration standard 300 mOsm/kg	Gonotec	30.9.0020	To adjust the medium osmolarity
Calibration standard 850 mOsm/kg	Gonotec	30.9.0850	
Sodium chloride	Merck	1.064.04	
Sucrose	Calbiochem	573113	
M-Per mammalian protein extraction reagent	Thermo Scientific	78503	Western blot
PMSF	Thermo Scientific	36978	

3.3 Buffers

Product	Supplier	Cat. No.
MES SDS Running Buffer (20x)	Thermo Scientific	NP0002
NuPage LDS Sample Buffer (4x)	Thermo Scientific	NP0007

3.4 Kits

Product	Supplier	Cat. No.
Amine coupling kit	GE Healthcare	BR100633
Biocore maintenance kit, type 2	GE Healthcare	BR100651
Bond Polymer Refine Detection kit	Leica	DS9800
EnVision+ anti-rabbit HRP kit	Dako	K4011
Human MMP3 Plex Ultra-Sensitive Kit	Mesoscale	K150034C
Human proinflammatory-4 tissue culture Kit	Mesoscale	K15025B
Micro BCA Protein Assay Kit	Thermo Scientific	23235
Path Hunter Bioassay Detection Kit	DiscoverX	93-0933
ProC2 kit	kindly provided by Nordic Bioscience	-
Proinflammatory Panel 1 (human)	Mesoscale	K15049D
Protease Inhibitor Cocktail Kit	Thermo Scientific	78410
RNA 6000 Nano Series II Lab Chip Kit	Agilent Technologies	5067-1511
RNeasy Mini Kit	Qiagen	74106
SuperScript III First-Strand Synthesis SuperMix for RT-PCR	Invitrogen	11752050
SYBR Green JumpStart Taq Ready Mix	Sigma	S5193
Quant-iT Picogreen dsDNA Assay Kit	Invitrogen	P7589
WesternBreeze Chemiluminescence Kit, anti-mouse	Thermo Scientific	WB7104
WesternBreeze Chemiluminescence Kit, anti-rabbit	Thermo Scientific	WB7106

3.5 Enzymes & Cytokines

Product	Supplier	Cat. No.
Chondroitinase ABC	Sigma	C2905
Collagenase NB4G	Serva	17465
DNaseI Set	Qiagen/Omega	79254/E1091
Il1β	Sigma	I9401
Il6	R&D	206-IL/CF
Proteinase K	Qiagen	19131
Proteinase K for IHC	Leica	AR9551
TNFα	R&D	210-TA/CF

3.6 Antibodies

3.6.1 Antibodies for WB

Primary antibody	Protein, MW, source	Dilution	Supplier	Cat. No
Anti-BMPR1A	BMPR1A, 60 kDa, rabbit	WB:1/1000	Sigma	SAB2701963
Anti-BMPR1B	BMPR1B, 57 kDa, rabbit	WB:1/1000	LSBio	LSB12897

3.6.2 Antibodies for IHC

Primary antibody	Dilution	Supplier	Cat. No
Mouse anti-collagen I mab	0.55 or 5.5 μg/ml	Abcam	ab6308
Rabbit anti-collgen II pab	2 μg/ml	Abcam	ab34712

3.7 Compounds

Product	Supplier	Cat. No.
bFGF	Merck	GF003AF
BMP2	R&D	355-BM-500/CF
BMP6	Peprotech	120-06
TGFβ1	R&D	7754-BH/CF
TGFβ3	R&D	243-B3-010/CF

GDF5 was kindly provided by Biopharm GmbH, while M1673, W417F and W417R were produced at Merck KGaA. All of them were dissolved in 10 mM HCl. Accordingly, BMP2 was also dissolved in 10 mM HCl. The remaining compounds were dissolved as stated by the manufacturer.

3.8 BMP receptors

Product	Supplier	Cat. No.
rhBMPR-IA/Fc Chimera	R&D	315BR/CF
rhBMPR-IB/Fc Chimera	R&D	505PR
rhmBMPR-II/Fc Chimera	R&D	811BR

3.9 Cell culture

Product	Supplier	Cat. No.
Accutase	PAN	P10-21100
Amphotericin B	PAN	P06-01005
Beaker, 100 ml	VWR	2131105
Beaker, 150 ml	VWR	2131106
BSA	Merck	1120180100
DEPC-treated water	Ambion	AM9922

FBS	Biochrom	S0615
Gelatin solution, 0.1%	Merck	ES006B
Geneticin	Gibco	10131027
HEPES	Gibco	15630080
Hygromycin	Invitrogen	10687010
ITS premix	Sigma	I2521
L-Ascorbic acid-2-phosphate	Sigma	A8960
L-Glutamine Solution, 200mM	Merck	TMS002C
L-Proline	Sigma	P5607
Magnetic stirring bars, micro	VWR	4420359 - 4420368
PBS	Gibco	14190
Pen/Strep	PAN	P06-07100
RNase Away	Molecular Bio Products	7002/7000
Sodium pyruvate	Gibco	11360

3.10 Culture medium

Product	Supplier	Cat. No.
McCoy´s	Invitrogen	26600
MEMalpha+	Gibco	A1049001
DMEM high glucose	Gibco	41966029
DMEM low glucose	Gibco	12320032

3.11 Cell lines

Name	Supplier	Cat. No.	Description
C3H10T1/2	ATCC	ATCC® CCL-226™	Isolated from a line of C3H embryo cells
U2OS BMPR1A/BMPR2	DiscoverX	93-1006C3	Human osteosarcoma transfected with BMPR1a/BMPR2
U2OS BMPR1B/BMPR2	DiscoverX	93-1053C3	Human osteosarcoma transfected with BMPR1b/BMPR2

3.12 Devices

Instrument	Supplier
Analog vortex mixer	VWR
Analytical balance "Cubis"	Satorius
AxioCam MRc	Zeiss
Biacore 4000	GE Healtcare
Centrifuge	VWR
Chip priming station	Agilent Technologies
CoolClamp RM	Leica
Embedding Station EG1160	Leica
Fusion SoloS	Vilber
Glass Coverslipper CV5030	Leica
HandyStep electronic	Brand
iBlot Dry Blotting System	Invitrogen
IHC stainer BOND-III	Leica
Incubator Forma Serie II	Thermo Scientific
Labor-pH-Meter 766	Knick
Laminarflow KS-12	Hera-safe
LC-MS/MS System API 4000	Sciex

Magnetic stirrer variomag multipoint	VWR
Meso Sector S600, model 1201	Mesoscale
Microplate Washer	BioTek
Microscope Axio Observer.A1	Zeiss
Multistainer ST5020	Leica
Osmomat 030-3P	Gonotec
Paradigm detection platform	Beckmann-Coulter
PowerPac 300	Bio-Rad
Qiavac24 Plus Manifold	Qiagen
Rotary microtome RM2255	Leica
SallyA plate sealer	Biozym
Slide Scanner SCN400	Leica
SpeedVac SPD131DDA	Thermo Scientific
Standard Analog Shaker	VWR
Stratagene Mx3000P	Agilent Technologies
Tabletop centrifuge CT15RE	Hitachi/VWR
Thermal Cycler C1000	Biorad
Thermomixer comfort	Eppendorf
ThermoStat plus	Eppendorf
Tissue Processor ASP300S	Leica
Vicell XR cell and viability analyzer	Beckmann-Coulter
Vortex mixer MS 3 basic S36 Agilent	IKA
Water bath HI1210	Leica
XCell Sure Lock Mini Cell	Thermo Scientific
2100 Bioanalyzer	Agilent Technologies

3.13 Software's

Software Name	Supplier
Analyst 1.62	Sciex
Axio Vision 4.7	Zeiss
Discovery Workbench, 4.0	Mesoscale
GraphPad Prism 5.0.4	GraphPad Software
ImageJ 1.49v	Wayne Rasband
MxPro qPCR Software	Stratagene
SildePath Gateway	Leica
SoftMax Pro 5.4.2	Molecular Devices
ViCell XR Version 2.04.02	Beckmann-Coulter
Vision Capt	Vilber
2100 Expert, B.02.08	Agilent Technologies

4 Methods

4.1 Chondrocyte culture

4.1.1 Isolation of primary chondrocytes

Porcine chondrocytes were isolated from the cartilage of pig hips and bovine chondrocytes from metacarpophalangeal or knee joint cartilage of cows. The porcine and bovine joints were obtained from a local slaughterhouse (Odenwald Schlachthaus GmbH in Brensbach, Germany). The animals were slaughtered either the day of the isolation (porcine material) or the day before (bovine material) and were approximately one year old.

The isolation of human OA chondrocytes was performed from human knee or hip joints of OA patients who underwent a total joint replacement surgery (Figure 10). These joints were provided by the clinic for orthopedics, traumatology and sports medicine in Agaplesion Elisabethenstift (Darmstadt, Germany) or by the university clinic Mannheim (Mannheim, Germany) with full, ethical, written consent (ethical approval No. FF24/2015 or 2013-576N-MA).

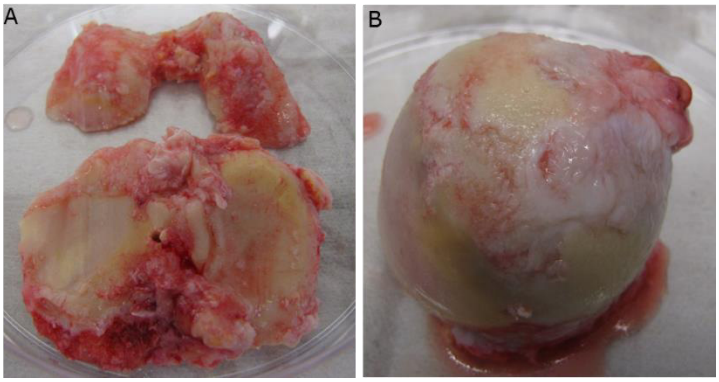

Figure 10 Human OA material from knee (A) or hip (B) joints.

Prior to the isolation of porcine and bovine chondrocytes, the whole joint was incubated in DMEM high glucose (DMEM-hg) + 4% Pen/Strep at least for one hour at 4°C. This step is not necessary for human OA chondrocyte isolation, because the joint replacement surgery is performed under sterile conditions.

The cartilage was peeled off the bone and finely chopped with a scalpel. The small pieces were transferred into a pre-weighted 50 ml reaction tube filled with 20 ml DMEM-hg. The amount of cartilage was determined by weighing the reaction tube again. The cartilage was washed three times with 20 ml DMEM-hg in the 50 ml reaction tube. Afterwards remaining fat- and epithelial cells were removed by adding 18 ml DMEM-hg containing 0.25% collagenase solution (1/10 dilution of collagenase 2.5% NBG4 in DMEM-hg) for 30 min at room temperature (RT) under agitation. The cartilage was washed again with 20 ml DMEM-hg and transferred into a beaker with 50 ml medium containing 0.1% collagenase solution (1/25 dilution of collagenase 2.5% NBG4 in DMEM-hg) and 1% Pen/Strep. The incubation was

conducted overnight (24 h +/- 5 h) at 37°C in a 5% CO_2 humified incubator under agitation. On the following day, the resulting cell suspension was sterile filtered through a 100 μm and 40 μm cell strainer. Afterwards, the cell suspension was centrifuged at 1400 x g for 5 min at RT, the medium was removed and the cell pellet resuspended in 20 ml DMEM-hg. This step was repeated three times. Finally, the cell pellet was resuspended in DMEM-hg containing 10% FBS. The cell concentration was determined by a Vi-CELL® cell counter (see chapter 4.4.6). 5 up to 10 million chondrocytes can be extracted out of 1 g cartilage.

For most of the cell cultures, the cells were first cultured one week in monolayer. $1.5x10^6$ porcine and bovine chondrocytes and $8\text{-}10x10^6$ human OA chondrocytes were seeded into PRIMARIA™ tissue culture flasks (75 cm^2) with 20 ml DMEM-hg containing 10% FBS, 50 μg/ml ascorbic acid-2-phosphate, 400 μM proline and 1% Pen/Strep for 5 to 7 days at 37°C in a 5% CO_2 humified incubator. Afterwards, the primary chondrocytes were harvested by removing the medium from the culture flasks, washing the cells with 10 ml PBS per culture flask and incubating the cells with 3 ml accutase per culture flask at 37°C until the cells were detached from the bottom of the flask. To stop the reaction 7 ml DMEM-hg + 10% FBS was added per culture flask, the cell suspension was transferred into a 50 ml reaction tube and centrifuged at 1000 rpm for 5 min. The supernatant was removed and the cell pellet resuspended in DMEM-hg + 10% FBS. 500 μl of the cell suspension was filled in Vi-CELL® cups to determine the cell concentration (see chapter 4.4.6).

4.1.2 Culture medium preparation and adjustment of the osmolarity

The osmolarity in healthy articular cartilage ranges between 350 and 480 mOsm while in end-stage OA cartilage it decreases down to 270 mOsm [40]. The DMEM medium has an osmolarity of 340 mOsm what rather corresponds to conditions within OA cartilage. To reproduce the healthy cartilage condition, the medium osmolarity was increased by adding NaCl to the medium. In addition, the medium osmolarity was increased by addition of sucrose to exclude sodium and chloride specific effects.

The culture medium used was DMEM-hg containing 10% FBS, 50 μg/ml ascorbic acid-2-phosphate and 400 μM proline (DMEM-hg complete). In a first instance, the osmolarity was increased by adding different amounts of NaCl or sucrose to the medium according to the following formula: $\frac{MW}{1000} \times \Delta$ mOsm / n= $\frac{\text{g NaCl or sucrose}}{\text{l medium}}$. With 'MW' the molecular weight (g/mol) of NaCl or sucrose, 'Δ mOsm' the difference between the desired osmolarity and the osmolarity of the medium and 'n' the number of particles in solution (n=2 for NaCl and n=1 for sucrose). After addition of the calculated quantities of NaCl or sucrose, the osmolarity was verified and further adjusted if needed. Osmolarity measurements were performed with a cryoscopic osmometer as specified by the manufacturer.

In a second instance to simplify this procedure, NaCl was dissolved in MilliQ-water (250 mg/ml) and sterile filtered through a 0.2 μm strainer. Afterwards a standard curve was created by osmolarity measurements after adding different volumes of the 250 mg/ml NaCl solution to the DMEM-hg (Figure

11). The standard curve can be used to calculate the required volume of NaCl solution to adjust defined medium osmolarities. This approach was used instead of calculating the required volume (with the help of the formula above) of NaCl. This enable to take in account the non-ideality of the solution.

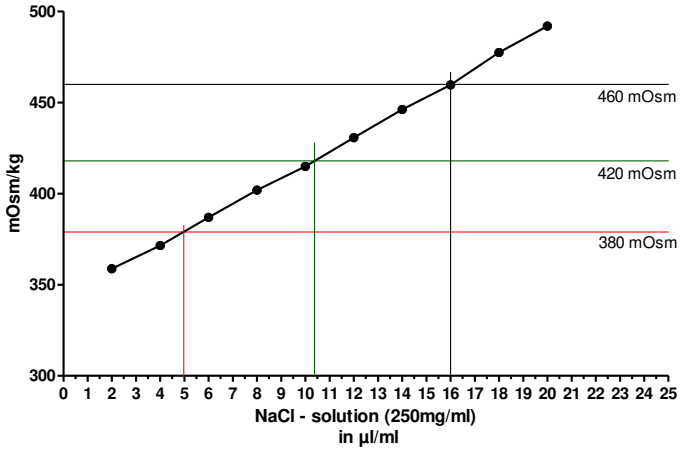

Figure 11 **Standard curve to adjust medium osmolarity with a NaCl-solution.** To obtain an osmolarity of 380, 420 and 460 mOsm (red, green and black lines), a volume of 5 µl, 10.4 µl and 16 µl need to be added to 1 ml DMEM-hg.

A volume of 5 μl NaCl solution need to be added to 1 ml DMEM-hg to create a medium osmolarity of 380 mOsm. 10.4 μl and 16 μl need to be added to 1 ml DMEM-hg respectively to obtain a medium osmolarity of 420 and 460 mOsm.

The osmolarity was systematically verified before and after addition of the medium supplements (10% FBS, 50 μg/ml ascorbic acid-2- phosphate and 400 μM proline) for the five first batches of medium prepared. Afterwards, the osmolarity was only verified when a new NaCl solution was prepared and used for the first time.

4.1.3 Monolayer experiments with passaged hOAC

After a first passage (see chapter 4.1.1), the hOAC were seeded in a volume of 0.5 ml DMEM-hg complete (usual osmolarity of 340 or adjusted with NaCl to 380 mOsm, see chapter 4.1.2) into 24 well plates at a concentration of $0.4x10^6$ cells per well. The cells were cultured at least for 2 hours at 37°C in a 5% CO_2 humified incubator to enable them to adhere to the bottom of the well plate. Afterwards, the cells were stimulated with 0.5 ml DMEM-hg complete containing 600 ng/ml GDF5 or M1673 or 25 μM HCl (control) and were cultured at 37°C in a 5% CO_2 humified incubator at 21% or 1% oxygen. Every 3 to 4 days of culture, the medium was renewed. After a total culture time of 7, 14, 21 or 28 days, morphological analysis was performed and medium samples were analyzed for its GAG concentration (see chapter 4.4.1). In addition, cell samples were analyzed for the cell concentration, viability and gene expression (see chapter 4.4.6 and 4.5).

4.1.4 Monolayer experiments with passaged hOAC in the presence of cytokines

After a first passage (see chapter 4.1.1), the hOAC were seeded in a volume of 1 ml DMEM-hg complete (adjusted with NaCl to 380 mOsm, see chapter 4.1.2) into 24 well plates at a concentration of $0.4x10^6$ cells per well. The cells were cultured for 1 day at 37°C in a 5% CO_2 humified incubator to enable them to adhere to the bottom of the well plate. Afterwards, the medium was removed and the cells were either cultured in 1 ml of serum-free DMEM-hg complete (adjusted with NaCl to 380 mOsm, see chapter 4.1.2) or stimulated with 10 ng/ml Il1β and TNFα or 100 ng/ml Il6 in 1 ml of serum-free DMEM complete (adjusted with NaCl to 380 mOsm, see chapter 4.1.2). After 2 days of culture, cell samples were harvested for gene expression (see chapter 4.5).

4.1.5 Monolayer experiments with freshly isolated hOAC

Freshly isolated hOAC (FIC) were used directly after collagenase digestion (see chapter 4.1.1) and without expansion of the cells. A part of these cells was used for total RNA extraction for gene expression (see chapter 4.5.1). These cells were designated 'day 0'. The remaining cells were divided into different tubes and resuspended in DMEM-hg complete with different osmolarities (340, 380, 420 and 460 mOsm). The osmolarity was adjusted either with NaCl or sucrose (see chapter 4.1.2). FIC were seeded in a volume of 1 ml into PRIMARIA™ 24 well plates at a concentration of $0.24x10^6$ cells per well and were cultured at 37°C in a 5% CO_2 humified incubator. After 3 days of culture, the medium was renewed. After a total culture time of 6 days, morphological analysis was performed and medium samples were analyzed for the GAG concentration (see chapter 4.4.1) and for the presence of cytokines and MMPs (see chapter 4.4.5). Additionally, cell samples were analyzed for the cell concentration, viability and gene expression (see chapter 4.4.6 and 4.5).

4.1.6 3-D culture experiments

4.1.6.1 Cartilage tissue analogs (CTAs)

CTAs were generated by seeding the cells in a high density of $5x10^6$ cells per ml. One million cells/well were inoculated in a 96 well ultra-low attachment plate with 200 μL of DMEM-hg complete + 1% Pen/Strep and cultivated for one week at 37°C and 5% CO2 in a humified incubator to enable them to aggregate and form CTAs. Every second day a medium change was carefully performed.

Afterwards the CTAs were transferred in a 24 well plate (1 CTA/well) containing 1 mL of DMEM-hg complete (usual osmolarity of 340 or adjusted with NaCl to 380 mOsm, see chapter 4.12) in the absence or presence of 300 ng/mL of GDF5, M1673, W417F or W417R or 12.5 μM HCl (control). The CTAs were cultured at 37°C in a 5% CO_2 humified incubator at 21% or 1% oxygen. The medium was changed twice a week. On a weekly basis, medium samples were taken and analyzed for the GAG content (see chapter 4.4.1). After 4 weeks of culture, the CTAs were collected and either lysed to analyze gene expression (see chapter 4.5) or fixed for histology (see chapter 4.7) or digested with papain to analyze the DNA,

GAG and HPro content (see chapter 4.4.7, 4.4.1 and 4.4.3). To do so, the CTAs were washed with PBS and incubated in 250 μL of the papain solution at 60°C overnight. The papain solution consists of 0.125 mg/mL papain in 5 mM L-cystein, 0.1 M Na_2HPO_4 and 0.01 M ETDA at pH 6 with papain and L-cystein being freshly added to the solution. The dsDNA was measured directly to analyse cell content (see chapter 4.4.6). For GAG and HPro measurement (see chapter 4.4.1 and 4.4.3) the samples were stored at -20°C until use.

4.1.6.2 Alginate beads

After the expansion of hOAC at 340 mOsm, the cells were harvested (see chapter 4.1.1) and a cell suspension with $2x10^6$ cells/ml was prepared in alginate gel. The alginate gel consists of 0.2 M HEPES, 1.5 M NaCl and 1.25% alginate, adjusted to pH 7.4 and was autoclaved before use. With the help of a 10 mL syringe and a 22 g needle, the cell suspension in alginate was poured drop by drop in the polymerization solution (120 mM $CaCl_2$ and 10 mM HEPES, sterile) which was kept under agitation. It is important that the space between the needle and the polymerization solution is lesser then 10 cm to generate round shaped beads. During this step, the total bead number as well as the cells per bead were calculated. Once the complete cell suspension was poured in the polymerization solution, the beads were enabled to polymerize for 15 min under agitation. The formed alginate beads contained between 40.000 to 60.000 cells. The beads were washed with a 150 mM NaCl solution 3 times and placed in petri dishes with 20 ml DMEM-hg complete adjusted with NaCl to 340, 380, 420 or 460 mOsm (see chapter 4.1.2) and cultured at 37°C and 5% CO_2 in a humified incubator for 7 days. After 1 day of culture, a medium change was performed and after 7 days, the beads were transferred in 24 well ultra-low attachment plates with 5 beads /well (≈$0.2\text{-}0.3x10^6$ cells/well) in 1 mL of DMEM-hg complete (340, 380, 420 or 460 mOsm) in the presence of 300 ng/ml GDF5 and M1673 or 12,5 μM HCl (control) with or without 4 μg/ml heparin. Twice a week, the medium was renewed and medium samples were taken to analyze the GAG content in medium (see chapter 4.4.1). After 14 days, the alginate beads were dissolved and analyzed for their GAG content (see chapter 4.4.1), cell concentration and viability (see chapter 4.4.6) or cytokine concentration (see chapter 4.4.5). In addition, the cells were harvested for gene expression analysis (see chapter 4.5). To do so, the alginate beads were washed with PBS and incubated in 460 μL dissolution solution mixed with 40 μl of 2.5% collagenase (in DMEM-hg + 0.2 mM $CaCl_2$) for a maximum of 1 hour at 37°C and 800 rpm. This enables the beads to depolymerize and dissolves cell clumps. The dissolution solution consists of 55 mM Na-citrate and 150 mM NaCl at pH 8. After dissolution of the beads, 500 μl PBS or DMEM-hg were added, the solution was centrifuged at 500 g for 10 min and the supernatant was collected. The cell concentration was measured directly to analyse cell content (see chapter 4.4.6). For GAG and cytokine measurement (see chapter 4.4.1 and 4.4.5) the samples were stored at -20°C until use.

4.2 Stem cell culture and differentiation

The murine mesenchymal stem cell line C3H10T1/2 as well as human mesenchymal stem cells (human MSCs) were cultured and either differentiated into chondrocytes and osteoblasts or further cultured in an undifferentiated state. To enhance the compound effect on chondrogenesis of the stem cells, TGFβ3 was added to the cells additionally to the compounds.

4.2.1 Culture of the C3H10T1/2 cell line

C3H10T1/2 cells were obtained from the American Type Culture Collection (ATCC). The cells were seeded from a cryoconserved aliquot with $1x10^6$ cells in BME basal medium + 10% FBS + 2 mM glutamine with 8% DMSO. To do so, the cell aliquot was thawed at 37°C in a water bath and quickly transferred in a tissue culture flask (75 cm^2) containing 20 ml DMEM-hg + 10% FBS. The cells were cultured at 37°C in a 5% CO_2 humified incubator. For expansion of the cells, they were routinely plated at a density of $4\text{-}5x10^6$ cells in tissue culture flasks (175 cm^2), maintained in DMEM-hg supplemented with 10% FBS and grown at 37°C in a 5% CO_2 humified incubator. After reaching approximately 80% confluence (4-5 days), the cells were harvested: the medium was removed from the culture flasks, the cells were washed with 10 ml PBS per culture flask and subsequently incubated with 10 ml accutase per culture flask at 37°C until the cells were detached from the bottom of the flask. To stop the reaction 10 ml DMEM-hg + 10% FBS was added, the cell suspension transferred into a 50 ml reaction tube and centrifuged at 1000 rpm for 5 min. The supernatant was removed and the cell pellet resuspended in DMEM-hg + 10% FBS. 500 μl of the cell suspension was filled in Vi-CELL® cups to determine the cell concentration (see chapter 4.4.6).

4.2.2 Isolation, characterization and cultivation of human MSCs

The human MSCs were provided from MilliPore Sigma (located in the United states of America). Detailed information concerning the origin and the processing of the human bone marrow can be found in the supplementary section (see supplementary, S1).

After shipping of the cryoconserved human MSCs on dry ice to Merck KGaA Darmstadt, the cells were immediately kept in liquid nitrogen until use. Before cell recovery, tissue culture flasks (175 cm^2) were coated with 15 ml gelatin for 15 min at RT. Afterwards the gelatin was removed from the flask and 40 ml DMEM low glucose + 10% FBS + 2 mM glutamine + 8 ng/ml bFGF (DMEM-lg complete) was added to each flask. The gelatin-coated culture flasks with the medium were stored at 37°C and 5% CO_2 in a humified incubator until cell seeding. For cell recovery, the cell aliquots were thawed in a water bath at 37°C and the cells quickly transferred in a 50 ml reaction tube containing an appropriated volume of DMEM-lg complete. Thereafter, the cell suspension was centrifuged at 500 g for 5 min, the supernatant containing the remaining DMSO was removed and the cell pellet resuspended in DMEM-lg complete to

obtain a cell concentration of $1x10^6$ cells per ml medium. $1x10^6$ human MSCs were seeded per tissue culture flask (175 cm^2) and incubated at 37°C in a 5% CO2 humified incubator. After 3 days, the medium was renewed with freshly added bFGF (8 ng/ml). After another 4 days, the cells normally reached approximately 80% confluence. They were harvested and the cell concentration was determined as described for C3H10T1/2 cells (see chapter 4.2.1), except that DMEM-lg complete was used.

4.2.3 Osteogenic induction

For osteogenic induction of murine and human MSCs, the cells were seeded into 24 well plates.

For the human MSCs, the 24 well plates were coated with 400 μl gelatin for 15 min at RT. Afterwards, the gelatin solution was removed and 500 μl DMEM-lg complete (culture medium for human MSCs) was added to each well. Next, $0.2x10^6$ human MSCs were seeded per well and cultured at 37°C in a 5% CO_2 humified incubator.

C3H10T1/2 cells were seeded directly, without gelatin-coating, into 24 well plates at a density of $0.1x10^6$ cells per well in DMEM-hg + 10% FBS + 1% Pen/Strep (culture medium for C3H10T1/2 cells) and cultured at 37°C in a 5% CO_2 humified incubator.

Both stem cell types reached approximately 90% confluence after 2 days of culture, which was designated ‘day 0’. Some of the cells were lysed to harvest total RNA (see chapter 4.5.1). The medium of the remaining wells was changed into DMEM-hg supplemented with 10% FBS, 50 μg/ml ascorbate-2-phosphate, 10 mM β-glycerolphosphate, 10^{-8} M dexamethasone and 1% Pen/Strep (osteogenic medium) or only renewed with the respective standard culture media without osteogenic inductors to determine the effect of the osteogenic medium.

The cells were cultured in either osteogenic medium or standard culture medium in the presence of 300 ng/ml GDF5, M1673, W417F, W417R and BMP2 or in the presence of 12.5 μM HCl (control) for 28 days at 37°C in a 5% CO_2 humified incubator. The medium was renewed twice a week with freshly added compounds. Medium and cell samples were harvested on a weekly basis and analyzed for ALP activity (see chapter 4.4.2), alizarin red staining (see chapter 4.4.8) and gene expression (see chapter 4.5). In addition, pictures were taken with an invert microscope (10X objective) on a weekly basis.

4.2.4 Chondrogenic induction

For chondrogenic induction, murine as well as human MSC suspensions were divided into 6 different 50 ml reaction tubes, spun down at 500 g for 5 min and the respective pellets were resuspended in DMEM-hg supplemented with 50 μg/ml ascorbate-2-phosphate, 400 μM proline, 10 mM β-glycerolphosphate, 10^{-7} M dexamethasone, 1% ITS premix and 1% Pen/Strep (chondrogenic medium) to obtain a cell concentration of $1x10^6$ cells per ml medium. Afterwards, 300 ng/ml GDF5, M1673, W417F, W417R or BMP2 were added per cell suspension individually or in combination with 10 ng/ml TGFβ3. As negative controls, 12.5 μM HCl was added individually or in combination with 10 ng/ml

TGFβ3 per cell suspension. Next 1 ml of each cell suspension supplemented with the different compounds were aliquoted in sterile 1.5 ml eppendorf tubes and spun down at 500 g for 10 min. Afterwards, a hole was made in each eppendorf tube with a sterile needle and the cells cultured at 37°C in a 5% CO_2 humified incubator. The medium was renewed twice a week with freshly added compounds. Medium and cell samples were harvested on a weekly basis and analyzed for ALP activity (see chapter 4.4.2), GAG concentration (see chapter 4.4.1) and gene expression (see chapter 4.5). Additionally, histology was performed of the 28 days old cell pellets as described in chapter 4.7.

4.3 Compound analysis

4.3.1 Bioactivity measurement with U2OS Assays

The potency and efficacy of different GDF5 mutants, GDF5 and BMP2 was evaluated with U2OS BMPR1a/BMPR2 or BMPR1b/BMPR2 cells, obtained from DiscoverX. The U2OS cells were engineered by the supplier to co-express the BMPR1a or BMPR1b and the dimer partner BMPR2. The dimerization of BMPR1a or BMPR1b with BMPR2 induced by the binding of the ligand was analyzed via enzyme fragment complementation technology. The enzyme β-galactosidase (β-Gal) is split into a small peptide fragment, which acts as an enzyme donor and is fused to BMPR1a or BMPR1b, and a large protein fragment, which acts as an enzyme acceptor and is fused to BMPR2. These enzyme fragments have no β-Gal activity itself. The binding of a ligand, as GDF5, to one receptor subunit induce the dimerization of both receptor subunits resulting in the forced complementation of the two enzyme fragments. The combined enzyme fragments form an active β-Gal enzyme, which hydrolyses a substrate resulting in a chemiluminescence signal [139-140].

The cells were seeded from a cryoconserved aliquot with 1-2x10^6 cells (in McCoys medium + 10% FCS ia.dial. + 0.2 mg/ml geneticin + 0.1 mg/ml hygromycin with 8% DMSO). To do so, the cell aliquot was thawed at 37°C in a water bath and quickly transferred in a tissue culture flask (75 cm^2) containing 20 ml culture medium (McCoys + 10% FBS ia.dial. + 0.2 mg/ml geneticin + 0.1 mg/ml hygromycin). After 7 days of culture, the cells were harvested as described for primary chondrocytes (see chapter 4.1.1). The cell pellet was resuspended and the cell suspension adjusted to a concentration of 0.2x10^6 cells per ml in seeding medium (MEMalpha + 2% ia.dial. FBS + 10 mM HEPES + 0.5% Pen/Strep). Afterwards 20.000 cells were seeded in a volume of 100 μl into 96 well microtiter plates (white) and incubated for 30 min at 37°C and 5% CO_2 in a humified incubator. During the incubation step, the protein dilutions for 10-point dose response curves were prepared. As a first step, stock solutions of GDF5, GDF5 mutants and BMP2 (0.48 mg/ml) as well as of the reference control BMP6 (100 μg/ml) were 3-fold serial diluted with 10 mM HCl + 0.1% BSA to obtain concentrations ranking from 24.4 to 480000 ng/ml or from 5.1 to 100000 ng/ml respectively. These concentrations are 400-fold higher than the final dose response curve concentrations. Afterwards, the prepared serial dilutions were 66.67-fold diluted in seeding

medium to obtain concentrations from 0.37 to 7200 ng/ml or 0.08 to 1500 ng/ml respectively, which are 6-fold higher than the final dose response curve concentrations. As a last step, the final concentrations were achieved by adding 20 µl of the prepared dilutions to the assay plate containing 100 µl of cell suspension. The resulting concentrations ranking from 0.06 to 1200 ng/ml for the GDF5 mutants, GDF5 and BMP2 or from 0.01 to 250 ng/ml for the reference control BMP6. In all samples the final concentration of HCl was 0.025 mM. Consequently, a negative control of 0.025 mM HCl was carried on the assay plate. The treated cells were incubated for 20-24 hours at 37°C and 5% CO_2 in a humified incubator.

The next day, the assay plates were analyzed by using the path hunter bioassay detection kit. Initially, reagent 1 + 2 were thawed and equilibrated to RT for around 1 hour. Afterwards, 12 µl of the ready to use reagent 1 was added to each well, the plate was shaken for 10 sec at 500 rpm and incubated for 15 min at RT in the dark. After that incubation step, 48 µl of the ready to use reagent 2 was added to each well, the plate was shaken for 10 sec at 500 rpm and incubated for 1 hour at RT in the dark. Chemiluminescence was measured using a Paradigm MTP reader.

The EC50 values were calculated with the GraphPad prism software 5.0.4. The concentration of the compounds (ng/ml) was transformed into Log(ng/ml). The data were fitted with the least squares fitting method by using the *log(agonist) vs response – variable slope (four parameters)* equation. To fit the data of the BMPR1b/BMPR2 dimerization assay, no constrain was used. In contrast, the upper plateau was not reached in the BMPR1a/BMPR2 assay and consequently a top strain was used being the EC50 value detected with the highest BMP2 concentration.

4.3.2 Affinity measurements

Surface plasmon resonance (SPR) is a powerful tool to investigate the functional nature of protein-protein interactions and binding events. The SPR technique was used for affinity measurements of GDF5, GDF5 mutants and BMP2 to their receptors BMPR1a, BMPR1b and BMPR2. A glass sensor chip coated with a thin metal surface, typically a thin layer of gold was used. The metal layer consists of several positive charges and mobile, negative charged electrons. Incident light hits the metal layer in a defined angle and the electrons oscillate due to excitation of the light energy. The electron oscillation is called plasmon wave, propagates on the metal layer and the intensity is detected for every point on the surface in a defined angle by a detector. Binding events, like the interaction of a potential DMOAD to their receptors changes the molecule complex size, which is immobilized on the metal layer and consequently changes the plasmon wave and the angle of the reflected light. This signal change is described with resonance units (RU), where an angle shift of 10^{-4} degree results in a change of 1 RU [141-142].

The affinity measurements with the SPR technology was performed in the molecular interaction laboratory by Andreas Schoenemann. For SPR analysis, a Biacore4000 was used, which contains 4 independent flow cells with 5 detection spots each, which enable to analyze 20 binding events

simultaneously. The detection spots 1+5 were immobilized with two different concentrations of protein A and an equal concentration of the BMP receptor or Erbitux as negative control (1 μg/ml for BMPR1a, BMPR2 and Erbitux or 1.75 μg/ml for BMPR1b). The detection spot 2+4 were immobilized only with the two different concentrations of protein A and were used as reference surfaces. Detection spot 3 was activated and deactivated but neither immobilized with protein A nor with a BMP receptor or Erbitux to exclude unspecific sensor chip binding events. The flow cells 1, 2, 3 and 4 were used to detect binding affinities to BMPR1a, BMPR1b, BMPR2 or Erbitux respectively.

In general, a Biacore Maintenance Kit was used for cleaning, normalization of RU signals and performance testing of the Biacore4000. At the start of the SPR experiments, the immobilization buffer (10 mM Acetate, pH 4.0), the running buffer for immobilization (10 mM HEPES + 150 mM NaCl, pH 7.4) and the running buffer for kinetic evaluation (10 mM HEPES + 500 mM NaCl + 0.05% Tween20, pH 7.4) were prepared. In addition, all reagents, solutions and remaining buffers were prepared, added in 96 well plates and placed into the Biacore4000. The BMPR were solved in PBS to reach a concentration of 1 μg/ml for BMPR1a, BMPR2 and Erbitux (negative control to exclude unspecific binding) and of 1.75 μg/ml for BMPR1b. Ligand samples (GDF5, M1673, W417F, W417R and BMP2) were adjusted to a start concentration of 200 nM in running buffer for kinetic evaluation and 2-fold serial diluted to reach concentrations of 100, 50, 25, 12.5, 6.25, 3.13, 1.56, 0.78, 0.39 nM. Additionally, two non-ligand control samples were prepared (= running buffer for kinetic evaluation) which were injected before and after the different ligand concentrations respectively.

The CM5 sensor chip was first activated, protein A was coupled and remaining activated groups deactivated. Therefore, 0.4 M EDC and 0.1 M NHS were mixed by the device and were injected (10 min @ 10 μl/min) to ensure the amine coupling of protein A on the sensor chip surface. Protein A (52 mg/ml) was diluted 2000-fold in immobilization buffer and injected for 90 sec for detection spot 1+2 and 180 sec for detection spot 4+5 at a flow rate of 10 μl/min in running buffer for immobilization. Deactivation of remaining active groups on the surface was performed using 1 M ethanolamine-HCl (7min @ 10μl/min). The receptor capture was performed at the beginning of each cycle at a flow rate of 10 μl/min for 60 sec in running buffer for kinetic evaluation. Protein A interacts specifically with the Fc portion of antibodies (Ab) and therefore mediates the correct aligned immobilization of the different Fc-tagged BMP receptors on the sensor chip surface [143]. Before the binding studies were performed, the CM5 sensor chip immobilized with the BMP receptors was equilibrated with running buffer for kinetic evaluation. One ligand or non-ligand control was injected per cycle at a flow rate of 30 μl/min for 300 sec followed by a dissociation phase of 900 sec in running buffer for kinetic evaluation respectively. Between the different ligand concentrations, an 'extra wash' was performed with 50 mM NaOH to clean the flow system and the injection needle followed by a stabilization time of 60 sec. At the end of each cycle, the running buffer for kinetic evaluation was injected, the sensor chip surface was regenerated with 50 mM HCl for 30 sec and the running buffer for kinetic evaluation was injected again before

starting a new cycle. The regeneration step removes all molecules bound to the protein A surface but without affecting the protein A surface. Data were collected with 10 Hz corresponding to 10 points/sec and fitted to a 1:1 Langmuir binding model.

4.4 Cell and medium analysis

4.4.1 Glycosaminoglycan analysis

Glycosaminoglycan (GAG) concentration was quantified in medium or in alginate beads and CTAs. A spectrophotometric assay based on metachromasia was used. In the presence of sulfated GAGs, which are negatively charged and located in the cartilage ECM, the absorption maximum of the cationic dimethylmethylene blue (DMMB) shifts and the blue dye changes his color to purple [144].

The DMMB solution was prepared by solving 8 mg DMMB in 2.5 ml ethanol. After the dissolution of DMMB, 1 g sodium formate and 1 ml formic acid was added. The solution was completed to 500 ml with MilliQ-water.

To generate a standard curve, a chondroitin stock solution (1 mg/ml) was prepared in appropriate medium or buffer. The stock solution was diluted 1/20 to obtain a concentration of 50 μg/ml. To generate the subsequent concentrations, serial 1/2 dilutions were performed down to 0.78 μg/ml. As a blank control only medium or buffer was used. 50 μl of the respective standard solutions were transferred in a 96 well microtiter plate in a 3-fold determination.

GAG concentration in medium

To determine the GAG concentration in medium, the supernatant was collected, 50 μl of the undiluted samples were transferred in the 96 well microtiter plate containing the standards. Samples and standards were mixed with 200 μl DMMB solution. The absorbance at 540/595 nm was read using a Paradigm MTP reader and compared to that of chondroitin sulfate standards.

GAG concentration in alginate beads and CTAs

For GAG quantification in alginate beads and CTAs, they were firstly dissolved (see chapter 4.1.6.1 and 4.1.6.2). To quantify the GAG concentration, the alginate bead samples were diluted at least 1/10 to avoid interference from remaining alginate. 50 μl of the samples were transferred in the 96 well microtiter plate containing the standards. Samples and standards were mixed with 200 μl DMMB solution. The absorbance at 540/595 nm was read using a Paradigm MTP reader and compared to that of chondroitin sulfate standards.

4.4.2 Alkaline phosphatase (ALP) activity

Alkaline phosphatase (ALP) is considered as a marker of hypertrophic chondrocytes and osteogenesis [145-146]. ALP catalyzes the hydrolysis of p-nitrophenylphosphatase to p-nitrophenol and phosphatase. P-nitrophenol has a strong yellow color and an absorbance at 405 nm, which directly correlates with the enzyme activity.

First, the ALP-buffer was prepared by solving 3.754 g glycine, 101.65 mg $MgCl_2x6H_2O$ and 68.15 mg $ZnCl_2$ in 500 ml MilliQ-water. Afterwards, the pH value was set to 9.6, the solution was sterile filtered and stored at 4°C.

To generate a standard curve, p-nitrophenol solution (10 mM) was diluted in ALP-buffer to obtain a concentration of 200 μg/ml. Afterwards, 100 μl of the p-nitrophenol solution was diluted in 100 μl of corresponding medium and was 2-fold serial diluted directly in the 96 well microtiter plate to obtain concentrations ranking from 1.56 to 100 μg/ml. Additionally, a blank value of the used medium was carried on the assay plate. The standard curve was performed in a 3-fold determination.

The ALP substrate solution was prepared freshly by dissolving one capsule containing 100 mg p-nitrophenylphosphatase in 10 ml ALP buffer at 37°C in the water bath. For ALP activity analysis, 100 μl of the samples were transferred in the 96 well microtiter plate with the prepared standard samples. 100 μl of the ALP substrate solution was added to each well and incubated for 1 hour at RT. Afterwards the absorption was measured at 405/490 nm using a Paradigm MTP reader and compared to that of p-nitrophenol standards.

4.4.3 Hydroxyproline measurement

The quantitative determination of 4-Hydroxyproline was realized in the quantitative bioanalytics laboratory and was performed by using an HPLC-MS/MS assay. 4-Hydroxyproline [$^2H_3$] was used as an internal standard. A stock solution of 4-Hydroxyproline was prepared with a concentration of 30 mg/mL in MilliQ-water. The working solution of the internal standard was prepared by diluting the stock solution to a concentration of 1.2 μg/mL in MilliQ-water. Calibration standards from 0.1 to 200 μg/mL of 4-Hydroxyproline were prepared in the cell culture medium.

5 μL of the samples were mixed with 10 μL of internal standard solution and 200 μL of 25% HCl and hydrolysed overnight at 110°C. After centrifugation for 1 min at RT and 1200 rpm the samples were evaporated to dryness at 55°C/10 Torr. Samples were then resuspended in 1 ml MilliQ-water and an aliquot of 100 μl was mixed 1/5 in acetonitrile for injection in a HPLC-MS/MS system. HPLC separation was achieved on a HILIC column (Sequant ZIC-HILIC, 50-2.1mm, 3.5μm, 200Å column, Merck KGaA) using a mobile phase gradient (eluent A: 0.1% formic acid, eluent B: acetonitrile). Detection was performed on a Tandem MS with a turbo ion spray interface operating in the positive ion mode. Selectivity of the method was achieved using multiple reaction monitoring (MRM) for MS/MS detection of the compounds. The concentrations of 4-Hydroxyproline in unknown samples and calibration

standards were calculated by interpolation of the peak area ratio of analytes/internal standard versus the ratio of their nominal concentrations into the regression line obtained from the calibration standards using the program Analyst 1.62.

4.4.4 ProC2 measurement

ProC2 is a marker for type 2 collagen production developed by Nordic Bioscience [147] and was measured in the dissolved alginate beads (see chapter 4.1.6.2). All incubations were performed at RT with shaking. A standard curve was obtained by a 2-fold serial dilution of the provided standard in the provided assay buffer and was carried on the plate in a double determination. The provided streptavidin-coated 96 well plates were additionally coated with 100 μl biotin-peptide per well (diluted 1/100 in provided assay buffer) for 30 min and were washed 5 times with the provided washing buffer (diluted 1/50 in ddH_2O). 20 μL of the standards, samples or controls were added together with 100 μL of the primary antibody (1/100 in provided assay buffer). After an incubation time of 3 hours the wells were washed 5 times with the provided washing buffer (diluted 1/50 in ddH_2O) and 100 μL of the secondary antibody (1/100 in provided assay buffer) was added per well. After 1 hour of incubation, the wells were washed 5 times with the provided washing buffer (diluted 1/50 in ddH_2O) and 100 μL of the ready to use TMB was added and incubated 15 min in the dark. The reaction was stopped with 100 μL of the ready to use stopping solution. Absorbance was read at 450 nm and the absorbance at 650 nm was used as reference. Absorbance of the samples were compared to the absorbance of the standard curve. The two controls provided should give a concentration of 6.75 ng/mL (±20%) for the low control and 18.2 ng/mL for the high control (±20%).

4.4.5 Cytokine and matrix metalloproteinase (MMP) measurements

Cytokine and matrix metalloproteinase (MMP) measurements from cell supernatants were performed using sandwich multi-spot immunoassays from Mesoscale Discovery. For this purpose, a specific microtiter plate was used with a working electrode surface pre-coated with capture antibodies. After adding the sample, the capture antibodies bind specific cytokines present in the sample. Detection of the captured cytokines is achieved by subsequent binding of the detection antibodies which are labeled with a sulfo-tag™ and able to emit light after applying voltage on the plate [148].

For cytokine measurements, two different multi-spot arrays were used. The 4-spot proinflammatory tissue culture array and the 10-spot proinflammatory panel. Both arrays are designed for the detection of human cytokines and were used to detect Il1β, Il6 and TNFα. The 10-spot arrays were used additionally because of a higher sensitivity compared to the 4-spot assay. For MMP measurements, the human MMP3 Plex Ultra-Sensitive Kit were used.

As an initial step, all reagents were equilibrated to RT before starting the multisport arrays. Afterwards the calibrator solutions were prepared.

In the case of the 4-spot array a ready to use calibrator solution (10000 pg/ml) was diluted 4-fold in the corresponding sample medium to obtain concentrations of 2500, 625, 156.25, 39.06, 9.77 and 2.44 pg/ml. In addition, a medium blank was used (0 pg/ml). Afterwards, 25 μl of the calibrator or blank solutions were added in a double determination and 25 μl of the undiluted samples were added to the pre-coated plate and incubated with vigorous shaking for 2 hours at RT. During the incubation time, the detection antibody was prepared by gently mixing 2.94 ml of diluent 100 with 60 μl of the antibody, which has been previously diluted 1/50. Next, 25 μl of the prepared detection antibody was added on the plate containing the pre-coated antibody and the calibrator/sample and incubated with vigorous shaking for another 2 hours at RT. During this incubation time, the washing buffer was prepared by diluting the 10-fold concentrate down to a 1-fold solution in MilliQ-water. Afterwards the plate was washed 3 times with the washing buffer consists of PBS + 0.05% Tween-20 by using a microplate washer. An appropriate chemical environment for the detection of electrochemiluminescence was created by diluting the 4-fold concentrated read buffer down to a 2-fold dilution and dispensing 150 μl to each well.

In the case of the 10-spot array the lyophilized calibrator was reconstituted by adding 1000 μl of the sample medium. This solution was inverted 3 times, equilibrated to RT for 30 min and vortexed with short impulses. Afterwards the calibrator solution was diluted 4-fold in the same medium to generate seven calibrators. The medium was used as a zero control. Il1β has a starting concentration of 599, Il6 of 799 and TNFα of 371 pg/ml. The plates were washed 3 times with the washing buffer (preparation see above) using a microplate washer. Next, 50 μl of calibrator solutions/samples were added to the pre-coated plate and incubated with vigorous shaking over night at 4°C. This step was performed overnight at 4°C to further improve the sensitivity of the array. The next day, the detection antibody was prepared by diluting the 50-fold stock solutions of Il1β, Il6 and TNFα down to a 1-fold working solution in diluent 3. The plates were washed 3 times with the washing buffer using a microplate washer and 25 μl of the detection antibody was added to each well and incubated with vigorous shaking for 2 hours at RT. Afterwards the plates were washed 3 times again and 150 μl reading buffer (preparation see above) was added to each well.

In the case of the MMP3 plex array, the ready to use calibrator solution was diluted 10-fold in the corresponding sample medium to prepare the highest calibrator solution of the 8-point standard curve (MMP1 and MMP3 $1x10^6$, MMP9 $5x10^6$ pg/ml). Afterwards the calibrator solution was diluted 4-fold in the same medium to generate the required calibrators. The medium was used as a zero control. As a first step, 25 μl diluent 2 were added to the pre-coated plate and incubated with vigorous shaking for 30 min at RT. All the next steps were performed as described for the 4-spot proinflammatory tissue culture array. The plates were read on the SECTOR instrument and analyzed with the Software Discovery Workbench according to the manufacturer protocol.

4.4.6 Cell counting

Cell suspensions were analyzed for their cell concentration and viability by using the automated trypan blue dye exclusion method with a Vi-CELL® Counter. A minimum of 500 μl cell suspension had to be transferred into Vi-CELL® sample cups and placed into the Vi-CELL® Counter. The cell suspension is mixed with a trypan blue solution (provided by the manufacturer), aspirated in a capillary and is delivered to a flow cell system containing a camera. For imaging up to 100 images per sample are captured and analyzed with digital image analysis. During analysis, the dead cells were differentiated from the viable cells. Dead cells have a higher permeability for trypan blue and consequently appear darker than viable cells, which are not penetrable by this dye. Therefore, the concentration of viable cells per ml cell suspension as well as the viability of the cell suspension can be determined.

4.4.7 dsDNA measurement

Papain digestion of the CTAs disrupt the cells making it impossible to assess the cell content. Alternatively, the dsDNA content was measured in the lysed CTAs to estimate their primary cell content. An ultrasensitive dye, named Quant-iT PicroGreen-dsDNA reagent, was used for dsDNA quantification. Before usage, the Quant-iT PicroGreen-dsDNA reagent was equilibrated at RT without light exposure. Afterwards a 1xTE buffer was prepared by diluting the 20xTE (200 mM Tris-HCl, 20 mM ETDA, pH 7.5) buffer in MilliQ-water. The Quant-iT PicroGreen-dsDNA reagent was diluted 200-fold in 1xTE buffer to obtain the working picogreen solution. The lambda DNA standard (100 μg/ml) provided in the kit was diluted with 1xTE buffer to obtain concentrations of 1000, 750, 500, 250, 125, 62.5 and 31.25 ng/ml. As a last calibrator to complete the 8-point calibration curve, a 1xTE buffer blank was used (0 pg/ml). The papain digested samples were centrifuged at 3000 g for 5 min to remove any particles and subsequently diluted 100-fold in 1xTE buffer. 80 μl of the 1xTE buffer was pipetted into a 96 well microtiter plate (black) and 20 μl of the samples, standards and blanks were added respectively. Afterwards 100 μl of the picogreen solution was added to each well and incubated for 5 min at RT in the dark. The fluorescence at 485/535 nm was measured using a Paradigm MTP reader and compared to that of lambda DNA standards.

4.4.8 Alizarin red staining

To determine the cell type in vitro or test the capability of cells to differentiate into osteoblasts, the Alizarin red staining can be used to identify calcium depositions. Alizarin Red is a small hydrophilic anionic dye, which chelates several cationic metals such as calcium and form a dye-metal covalent bond. As 99% of the calcium in the body is localized in the bone, Alizarin red selectively interacts with bone or calcium deposits in mineralized extracellular matrix.

To stain cells, which were grown in monolayer cultures, as a first step the medium was carefully aspirated. Afterwards, the cells were washed with PBS and fixed with 0.5 ml PFA (4% in PBS) for 1 hour.

After fixation, the cells were washed with 1 ml MilliQ-water for 2 times. For cell staining, 400 μl of the staining solution was added to the fixed cells and incubated for 20 min at RT. Subsequently the cells were washed with 1 ml MilliQ-water for 4 to 5 times. For documentation and storage, the cells were covered with 1 ml PBS.

4.5 Gene expression analysis

Gene expression analysis is an important tool to analyze different properties of potential DMOADs. As a first step, RNA was extracted, analyzed and transformed into cDNA by reverse transcription. Afterwards the gene expression was analyzed by quantitative real time PCR (qRT-PCR) to investigate, which genes were up- or downregulated at different conditions or after compound treatments. Therefore, the cDNA is first denatured, followed by primer annealing and elongation to create a double-stranded DNA (dsDNA). A fluorescence dye, which incorporates in dsDNA, is used to determine the amount of the amplified product in real-time.
The extraction of RNA is a crucial step, which works very well for chondrocyte monolayer cultures, while the extraction from 3D cultures, like CTAs or human MSC pellets, is very difficult because of the ECM which surrounds the chondrocytes. Therefore, different methods, like the extraction by using several freeze-thaw cycles, pestles or ultra-turrax as well as combined methods were evaluated for their ability to extract RNA. The method with the most robust results was the lysis of the samples with the RLT buffer provided in the RNeasy Mini Kit from Qiagen, followed by proteinase K treatment, homogenization with absolute ethanol and purification using RNeasy spin columns.
All steps were performed by using PCR clean dual filter tips.

4.5.1 RNA extraction

Total RNA was extracted from all samples by using the Qiagen RNeasy Mini Kit as specified by the manufacturer. As a first step, the biological samples were lysed with a highly denaturing guanidine-thiocyanate-containing buffer (RLT Buffer) and were subsequently homogenized.
For monolayer cultures of primary chondrocytes, cell disruption was performed by adding 350 μl RLT buffer to each well and scraping the cell layer with the pipette tip. The lysate was collected in a QIAshredder spine column placed in a 2 ml collection tube and spun down at full speed for 2 min to remove insoluble materials and reduce lysate viscosity. The lysate can be stored at -20°C or directly processed. In both cases 1 volume of 70% EtOH was added and gently mixed to homogenize the mixture and to provide conditions which facilitate the specific binding of RNA to the column.
3D cultures as well as monolayer cultures of stem cells were lysed with 300 μl RLT buffer. After cell lysis, an additional step of proteinase K treatment was performed to remove the ECM as well as endogenous proteases such as RNases. To do so, the lysate was mixed with 590 μl DEPC-water and 10 μl proteinase

K, incubated for 10 min at 55°C and centrifuged at 10000 g for 5 min. The supernatant was collected in a 2 ml collection tube and either stored at -20°C or directly processed. In both cases RNA isolation started by gently homogenizing the lysate with 0.5 volumes of absolute EtOH.

For the RNA extraction, RNeasy spin columns (up to 24) were inserted in the VacConnector manifold, which was connected to the house vacuum. Homogenized lysates were transferred to the columns containing a silica-membrane, which binds RNA. Subsequently the house vacuum was turned on to draw the lysates efficiently through the columns. Afterwards 350 μl RW1 buffer was added to each column to remove contaminants and was vacuumed. A DNA digestion was performed directly on the column by adding 80 μl of the DNase I incubation mix on the silica-membrane. The incubation was performed at least for 15 min. 350 μl RW1 buffer was added on top and was vacuumed. After this wash step 500 μl of the EtOH containing RPE Buffer (4 volumes of absolute EtOH were added to the concentrate to obtain a working solution) was added to the columns and was vacuumed. This step was repeated once. Next the empty RNeasy spin columns were removed from the manifold and placed in the provided collection tubes and centrifuged for 1 min at full speed to remove the residual RPE buffer from the silica-membrane. Elution of the total RNA was performed by carefully placing the spin columns in 1.5 ml collection tubes respectively, adding 30 μl DEPC-water directly to the silica-membrane and spun down in a centrifuge for 1 min at 8000 g. The final RNA concentration was increased by adding the obtained eluate on the silica-membrane again and spun it down as described previously.

The collection tubes were labelled and the samples were either immediately analyzed for their RNA concentration and purity or stored at -20°C.

4.5.2 RNA Analysis

RNA concentration and purity of samples were analyzed by capillary gel electrophoresis using the “lab-on-a-chip” technology with an Agilent 2100 Bioanalyzer. The chip contains several interconnected microchannels. Once the chip is filled with a sieving polymer, a fluorescence dye and the RNA sample, an electrical voltage is applied. The RNA, as a charged molecule, is size separated by the sieving polymer. The intercalation of the fluorescence dye enables the detection of the RNA molecules by laser-induced fluorescence which enables for instance to determine the RNA concentration and integrity.

As an initial step, the RNA ladder was prepared. The ladder was thawed, spun down, heat denatured for 2 min at 70°C and immediately cooled down on ice. Afterwards, the denatured ladder was aliquoted at 1.2 μl in 0.5 ml RNase-free collection tubes and stored at -80°C.

All reagents were equilibrated to RT for approximately 30 min before preparing the assay. Afterwards 550 μl of the RNA nano gel matrix (sieving polymer) was transferred into a spin filter and centrifuged for 10 min at 1500 g. The gel matrix was stored at 4°C and can be used within 1 month. In order to prepare the gel-dye mix, 65 μl of the filtered gel was transferred into a 1.5 ml RNAse-free collection tube and the RNA dye concentrate was mixed and spun down for 10 sec. Afterwards 1 μl of the dye was added

to the gel aliquot, mixed by vortexing and centrifuged for 10 min at 13000 g. The gel-dye mix can be used for two chips within 1 day.

Before starting the experiment, one cleaning electrode was filled with 350 μl of RNeasy away solution and another one with 350 μl of RNase-free water. The electrode cleaner with RNeasy away solution was placed in the Bioanalyzer. A new RNA nano chip was inserted in the chip priming station and 9 μl of the gel-dye mix was pipetted into the appropriately marked well. It is very important to pipette all substances on the bottom of the RNA chip to avoid bubbles. Once it was verified that the plunger is positioned at 1 ml, it was pushed down until it was hold by the chip priming station. After waiting for exactly 30 sec, the plunger was released with the chip release mechanism, it was waited about 5 sec and subsequently the plunger was slowly and carefully pulled back at the 1 ml position to finish the 'pressurize procedure'. The chip priming station was opened and another 9 μl of the gel-dye mix was pipetted into the remaining appropriately marked two wells, respectively. As a next step, 5 μl of the nano marker was loaded into the well which is marked with the ladder symbol as well as in each of the sample wells. Further 1 μl of the nano ladder and of each sample, which were thawed and kept on ice, were loaded into the ladder and sample wells respectively. Unused wells were filled with a total of 6 μl of the nano marker to guarantee the same volume in all wells of the chip.

The chip was vortexed for exactly 1 min at 2200 rpm by the IKA vortex mixer. At the same time, the electrode cleaner filled with RNase-free water was inserted into the bioanalyzer. Once the 1 min shacking was finished, the chip was inserted into the Bioanalyzer and the software was started within 5 min. After starting the analyzing procedure, the sample and chip information were entered. The analyzed data are translated into a gel-like image or an electropherogram by the bioanalyzer. In addition, the RNA concentration and integrity number (RIN) are displayed.

4.5.3 cDNA synthesis

Complementary DNA (cDNA) was generated by reverse transcription of RNA samples using the SuperScript III First-Strand Synthesis Supermix Kit. The kit contains a 2xRT reaction mix, which includes oligo $(dT)_{20}$, random hexamers, $MgCl_2$ and dNTPs, and an enzyme reaction mix. The enzyme reaction mix includes the reverse transcriptase and RNase OUT which inhibit RNases.

First the 2xRT reaction mix was thawed and 12 μl were pipetted in each well of the 48 well PCR plate. Afterwards 2 μl of the enzyme reaction mix was added. The RNA samples were thawed on ice to inhibit degradation processes. The same RNA concentration in the range of 20 ng up to 1 μg was used for all RNA samples of 1 experiment to synthesize cDNA. A maximum of 8 μl RNA sample was added to each well. RNA samples with a higher RNA concentration were diluted in DEPC-treated water to reach a volume of 8 μl. Afterwards the 48 well PCR plate was sealed, centrifuged and placed in the thermal cycler. The samples were first incubated at 25°C for 10 min to enable primer annealing, followed by a 30 min incubation at 50°C for cDNA synthesis and terminated by a 5 min incubation at 85°C. Afterwards,

the samples were cooled down to 4°C and 1 μl RNase H was added to each well and incubated at 37°C for 20 min to remove the RNA template from the synthesized cDNA. The plate was stored at -20°C.

4.5.4 Quantitative real time PCR

Quantitative real time PCR (qRT-PCR) was performed using SYBR Green as a fluorescence dye, which exhibits only a little fluorescence signal in unbound state, but emits a strong fluorescence signal upon incorporation in double-stranded DNA (dsDNA). The fluorescence signal was measured in the exponential phase of the qRT-PCR after each cycle and is directly proportional to the amplified DNA. This allows the detection of product accumulation in real-time. Additionally, the reference dye ROX was used to compensate non-PCR related fluorescence changes and to stabilize the baseline, which is used for sample normalization [149-150].

As a first step, sequence specific primers were designed, ordered (from Eurofins MWG Operon, see Table 1) and the delivered lyophilizates were solved with DEPC-water to a 100 pmol/μl stock solution. Primer working solutions of 10 pmol/μl were prepared by diluting the stock solution with DEPC-water. For primer validation, cDNA (containing the target gene) was serial diluted and a standard curve was created by qRT-PCR. The standard curve should have a coefficient of correlation (R^2) over 0.985 indicating a good data point fit and an efficiency of 90-110% [151].

Table 1 **Primers used for qRT-PCR reactions.**

Gene	Primers
Bovine EF1α	Forward: 5'- AGCTGAAGGAGAAGATTGATC -3' Reverse: 5'- GGCAGACTTGGTGACCTTG -3'
Bovine Aggrecan	Forward: 5'- GAAACCTCTGGACTCTTTGGTGTC -3' Reverse: 5'- GCCAGATATTTCTCCATAAAACCCTGA -3'
Bovine Collagen 2	Forward: 5'- GAACCCAGAACCAACACAATCC -3' Reverse: 5'- TCTGCCCAGTTCAGGTCTCTTAGAGA -3'
Human EF1α	Forward: 5'- CCTTGTGGAAATTTGAGACC -3' Reverse: 5'- CCATTTTGTTAACACCGACA -3'
Human ADAMTS5	Forward: 5'- TCAAAGCCAAAGACCAGACT -3' Reverse: 5'- ATTTCCTTCGTGGCAGAGTA -3'
Human Aggrecan	Forward: 5'- GAAAGGCATCGTGTTCCATT -3' Reverse: 5'- ACGTCCTCACACCAGGAAAC -3'
Human BMPR1a	Forward: 5'- CAGGTTCCTGGACTCAGCTC -3' Reverse: 5'- CTTTCCTTGGGTGCCATAAA -3'
Human BMPR1b	Forward: 5'- AAAGGTCGCTATGGGGAAGT -3' Reverse: 5'- GCAGCAATGAAACCCAAAAT -3'
Human BMPR2	Forward: 5'- GCTAAAATTTGGCAGCAAGC -3' Reverse: 5'- CTTGGGCCCTATGTGTCACT -3'
Human Collagen2	Forward: 5'- TCCATAGCTGAAATGGAAGC -3' Reverse: 5'- CCTGAGTGGAAGAGTGGAGA -3'

Human Collagen 10	Forward: 5'- AGGGTTACCAGGTCCAAAAG -3' Reverse: 5'- TGAGGCCCTTAGTTGCTATG -3'
Human MMP13	Forward: 5'- CCAACCCTAAACATCCAAAAAC -3' Reverse: 5'- AAAAACAGCTCCGCATCAAC -3'
Human Osteocalcin	Forward: 5'- GTGCAGAGTCCAGCAAAGGT -3' Reverse: 5'- TCAGCCAACTCGTCACAGTC -3'
Human Osteopontin	Forward: 5'- TGAAACGAGTCAGCTGGATG -3' Reverse: 5'- TGAAATTCATGGCTGTGGAA -3'
Murine EF1α	Forward: 5'- ACAGGCGCAGAGGTAAAAAT -3' Reverse: 5'- TATATGGCACAGCCTCCTCA -3'
Murine Aggrecan	Forward: 5'- TGGCTTCTGGAGACAGGACT -3' Reverse: 5'- GGGACATGGTTGTTTCTGCT -3'
Murine BMPR1a	Forward: 5'- CTTCTCCAGCTGCTTTTGCT -3' Reverse: 5'- ATAGCGGCCTTTACCAACCT -3'
Murine BMPR1b	Forward: 5'- AGCTGGTTCCGAGAGACTGA -3' Reverse: 5'- CAGCATGGACTTTGCGTCTA -3'
Murine BMPR2	Forward: 5'- TGGCAGTGAGGTCACTCAAG -3' Reverse: 5'- TTGCGTTCATTCTGCATAGC -3'
Murine Collagen 2	Forward: 5'- AGGTGTTCGAGGAGACAGTG -3' Reverse: 5'- CAACAATGCCCCTTTGACCA -3'
Murine Collagen 10	Forward: 5'- TTCTCCTACCACGTGCATGT -3' Reverse: 5'- GAGGCCGTTTGATTCTGCAT -3'
Murine Osteocalcin	Forward: 5'- ATGAGGACCATCTTTCTGCTCA -3' Reverse: 5'- GTAGCGCCGGAGTCTGTT -3'
Porcine RPL13A	Forward: 5'- TCAAGGTGGTGCGTCTGAAG -3' Reverse: 5'- TACGTTCTTTTCCGCCTGCT -3'
Porcine Aggrecan	Forward: 5'- GCTTATGCCTTCCCAGCTAC -3' Reverse: 5'- GATGCTGCTCAGGTGTGACT -3'
Porcine Collagen 2	Forward: 5'- GGATGGGCAGAGGTATAATG -3' Reverse: 5'- TCTCCAGGTTCTCCTTTCTG -3'

During qRT-PCR each cDNA sample was analyzed in duplicates against the selected gene of interest and against EF1α or RPL13A as housekeeping genes. Additionally, a non-template control (NTC) was run for each primer-pair used in the qRT-PCR to evaluate the absence of contamination of the master mix.

The components listed in Table 2 were mixed to generate a master mix. One master mix per primer pair was prepared. The reference dye was diluted 1/10 in DEPC-water before mixing it with the other components.

Table 2 **Master mix preparation per cDNA sample and analyzed gene for qRT-PCR reaction.**

Component	Volume (μl) per sample
SYBR Green	12.5
diluted reference dye	0.25
Forward primer	0.5
Reverse primer	0.5
$MgCl_2$	3.0
DEPC-H_2O	3.25

20 μl of the master mix was transferred into each well of a Mx3000 96 well plate. Afterwards 5 μl of the cDNA sample (1/5 diluted with DEPC-water) or 5 μl of DEPC-water (NTC) was pipetted into the appropriate wells. The plate was sealed, centrifuged and checked for disturbing air bubbles. Immediately the plate was run in the thermocycler Mx3000P using the thermal profile of Table 3.

Table 3 **Thermal profile used for qRT-PCR reactions.**

Temperature [°C]	Time	Reason	
94	4 min	Initial denaturation of DNA	
94	30 sec	Denaturation of DNA	] cycle repetition 40x
60	30 sec	Annealing of primer	
72	1 min	Elongation	
95	1 min	Melt curve analysis (fluorescence is read at each degree)	
55	30 sec		
95	30 sec		

For each sample and each gene, the cycle threshold (Ct) was determined in the amplification plot, which reflects the fluorescence change during cycling. This change is inversely proportional to the product. The more product, the lower is the Ct value, because lesser cycles are necessary to reach a fluorescence signal above the background. The relative abundance of target mRNA is calculated according to the following formula [152]:

$$relative\_abundance = 2^{(ctHKG-ctGOI)} = \frac{2^{ctHKG}}{2^{ctGOI}}$$

The dsDNA of the PCR product has a higher melting point compared to unspecific dsDNA fragments or primer dimers. Thus, a melt curve analysis was performed following qRT-PCR to determine the specificity of the qRT-PCR.

4.6 Western blot analysis

The Western blot (WB) is an important tool for the identification and characterization of specific proteins from cell samples. The cell samples were lysed, separated by a discontinuously SDS-PAGE and transferred to a PVDF membrane. Afterwards the immobilized proteins were incubated with specific antibodies against the protein of interest and the antibody signal was developed with chemiluminescence.

4.6.1 Sample preparation

First, the lysis buffer was freshly prepared by mixing 5 ml M-PER extraction reagent with 1 mM PMSF (1/100 dilution of 100 mM PMSF solved in isopropanol) as well as with 5 mM EDTA and 1% protease inhibitor (provided in the Protease Inhibitor Cocktail Kit).

To evaluate the presence of BMP receptors by western blot analysis, a cell concentration of $0.2x10^6$ C3H10T1/2 cells and human MSCs were transferred in a 1.5 ml eppendorf tube and centrifuged for 10 min at 500 g. The cell pellets were lysed with 100 μl of the freshly prepared lysis buffer and stored at -80°C until further processing.

4.6.2 SDS PAGE

The lysed samples were thawed and prepared for SDS PAGE by mixing 39 μl of each sample with 6 μl NuPage Sample Reducing agent (10x), 15 μl NuPage LDS Sample Buffer (4x) to reach a total volume of 60 μl. One sample were used for the detection of both BMPR1a and BMPR1b, to allow their comparison. Afterwards, the prepared samples were mixed, briefly centrifuged and heated for 10 min at 70°C. During this step, the 1x running buffer was prepared by mixing 40 ml of MES SDS Running Buffer (20x) with 760 ml MilliQ-water. Additionally, 200 ml of the 1x running buffer was mixed with 0.5 ml NuPage antioxidant. The XCell Sure Lock Mini cell was constructed according to the manufacturers manual and the required number of NuPage 4-12% Bis-Tris Protein Gels were unpacked and rinsed with water. The tapes covering the slot on the back on the pre-cast gels and the combs were carefully removed and the lanes were rinsed with 1x running buffer several times. Afterwards the gels were placed in the electrophoresis apparatus, the 1x running buffer containing antioxidant was filled in the upper buffer chamber to completely cover the sample lanes and the 1x running buffer was filled in the lower buffer chamber to dissipate heat during the run. Afterwards 5 μl of the Bench Mark Prestained Protein Ladder as well as 5 μl of the Magic Mark were loaded together in 1 lane, the remaining lanes were loaded with 25 μl of the prepared samples respectively. The gels were run at 150 volts for approximately 1-1.5 hours with the PowerPac 300 until the pre-stained ladder was separated and the dye of the sample buffer was run out the separation gel. Afterwards, the gel cassettes were opened, the stacking gel were cut off the

gels, the gels were removed from the cassette plates and put in a petri dish containing 20 ml MilliQ-water respectively.

4.6.3 Immunoblotting & detection

The protein transfer from the gels to a PVDF membrane was performed using a dry blotting system with the iBlot Gel Transfer device. For the transfer the iBlot Transfer Stacks kit was used, it contains the PVDF membrane and the filters and sponge, ready to use. First the anode stack, then the gels and finally the cathode stack were placed in the transfer devise according to the manufacturer instructions. Two gels, out of 1 XCell Sure Lock Mini cell, could be transferred simultaneously. The transfer ran for 7 min at 20 volts. For immunodetection of the transferred proteins, the WesternBreeze Chemiluminescent Kit was used. During the protein transfer, the blocking solution was prepared by mixing 5 ml MilliQ-water, 2 ml Diluent A (concentrated buffered saline solution with detergent) and 3 ml Diluent B (concentrated hammarsten casein solution) per membrane. All incubation steps were performed under agitation on a shaker. As a first step, the PVDF membrane with the immobilized proteins was incubated in 10 ml of blocking solution for 1 hour. Afterwards the membranes were washed with 20 ml MilliQ-water for 5 min. This washing step was repeated once and during the incubation time the primary antibody solution was prepared by mixing 7 ml MilliQ-water, 2 ml Diluent A, 1 ml Diluent B and the necessary volume of primary antibody (dilutions see chapter 3.6.1). The primary antibody solution was incubated overnight at 4°C. The next day, a sufficient volume of 16x antibody wash solution was diluted to 1x antibody solution with MilliQ-water. The membranes were washed three times with 20 ml of 1x antibody wash solution for 5 min. Next the membranes were incubated with secondary antibody solution (ready to use, anti-rabbit or anti-mouse) for 1 hour. The membranes were washed three time with the 1x antibody wash solution and rinsed twice with 20 ml MilliQ-water for 2 min. Afterwards they were placed on a clean, transparent plastic sheet and incubated with 2 ml chemiluminescence substrate (ready to use) for 5 min. Next, the membranes were covered with another clean, transparent plastic sheet to prepare a membrane sandwich for imaging with the Fusion SoloS using the Vision Capt Software.

4.7 Histology

Histology was realized in the exploratory osteoarthritis laboratory by Thomas Schnellbaecher and was performed for bovine and porcine CTAs as well as for human MSC pellets at the end of the culture (cultivation conditions see chapter 4.1.6.1 and 4.2.4). CTAs and pellets were prepared for histology by fixing the cell samples with a 4% phosphate buffered PFA solution for 30 min at RT. Afterwards the cell samples were washed with PBS for 15 min. This washing step was repeated 3 times and the cell samples were transferred in biopsy cassettes and handed over in PBS to the histology laboratory. As a first step, the cell samples were dehydrated with an increasing alcohol series and infiltrated with paraffin. To do

so, the cell samples were incubated with 30% EtOH for 2 hours and followed by 50% EtOH for 2 hours. Afterwards the cell samples were transferred into a fully enclosed tissue processor, which further dehydrated the cell samples with 70, 80, 90 and 96% EtOH as well as with isopropanol and NeoClear (Xylol derivate) and infiltrated them with paraffin as described in Table 4.

Table 4 Process for cell dehydration and paraffin infiltration using a tissue processor.

Station	Reagent	Time
1	70% EtOH	15 min
2	80% EtOH	15 min
3	90% EtOH	1 h
4	96% EtOH	1 h
5	96% EtOH	1 h
6	Isopropanol	1 h
7	Isopropanol	1:15 h
8	Neoclear	1:30 h
9	Neoclear	1:30 h
10	Neoclear	1:30 h
11	Paraffin	2 h
12	Paraffin	12 h

Cell samples were subsequently embedded with paraffin (60°C) in paraffin blocks on an embedding station and were cooled down on a cold plate (-4°C) until paraffin solidification. The paraffin embedded samples can be stored at RT until further processing.

As a next step, the cell preparations were cut with a rotary microtome (5 μm) under the use of a CoolClamp to ensure a continuous cooling. The slices were applied on microscope slides and transferred into a water bath (40°C) for straightening. Afterwards the slices were dried on a heat plate overnight.

The slices could be analysed for different extracellular matrix components via histochemical or immunohistochemical stainings.

For histochemistry a combined auto- and multistrainer was used. The slices were de-paraffinized in NeoClear and rehydrated in decreasing concentrations of EtOH. Next, the slices were stained with Fastgreen (counterstaining) and Safranin O (stains proteoglycans) or Alizarin Red (stains calcium deposit indicating mineralization) and finally dehydrated in absolute EtOH and NeoClear as described in Table 5. At the end of the process, slides were mounted with Neomount with a Glass Coverslipper.

Table 5 **Process for Safranin O staining (left) and Alizarin Red staining (right) with an auto- and multistainer.**

Step	Reagent	Time [min]		Step	Reagent	Time [min]
1	NeoClear	5		1	NeoClear	5
2	NeoClear	7		2	NeoClear	7
3	96% EtOH	5		3	96% EtOH	5
4	80% EtOH	5		4	80% EtOH	5
5	70% EtOH	5		5	70% EtOH	5
6	60% EtOH	5		6	60% EtOH	5
7	Water	3		7	Water	3
8	Fastgreen	5		8	0.5% Alizarin Red	5
9	1% acetic acid	0.75		9	Weise Buffer	0.5
10	0.01% Safranin O	10		10	0.04% Fastgreen	0.25
11	100% EtOH	1		11	Glacial acetic acid	0.33
12	100% EtOH	2		12	96% EtOH	2
13	100% EtOH	5		13	100% EtOH	5
14	NeoClear	5		14	NeoClear	5
15	NeoClear			15	NeoClear	

The immunohistochemical detection of type 2 and type 10 collagen was performed using a fully automated immunohistochemistry stainer (Leica Bond III). First the samples were baked on the slides for 30 min at 60°C and de-paraffinized with dewax solution for 30 sec followed by 2 washing steps with dewax solution at 72°C. Afterwards, the slices were cooled down to RT, rehydrated with 96% EtOH for 3 times and washed with a washing buffer. The washing step was repeated 3 times and next an antigen retrieval step was performed. This step was performed with chondroitinase for 15 min (type 2 collagen: 0.5 U/ml) or with proteinase K for 10 min (type 10 collagen: 97.1 μg/ml) at 37 °C. Following antigen retrieval, the sections were rinsed 3 times using the bond wash solution. The following steps were performed by using different detection kits (type 2 collagen: EnVision+ anti-rabbit HRP kit K4011 from DAKO; type 10 collagen: Polymer refine detection kit DS9800 from Leica). Endogenous peroxidase activity was quenched for type 2 and 10 collagen using a peroxidase block (provided in the kits) for 10 min at RT, followed by 3 bond wash solution steps. A saturation of binding sites was performed for type 2 collagen using the antibody dilution buffer for 10 min at RT. Afterwards primary antibodies diluted in the antibody diluent were applied to all sections for 30 min at RT, followed by 4 wash steps. To detect type 2 collagen, a rabbit anti-Collagen 2 antibody was used at 2 μg/ml. Type 10 collagen was detected by using a mouse anti-Collagen 10 antibody diluted 1/20. The secondary antibody was incubated for 20 min (type 2 collagen: goat anti-rabbit HRP labeled, Kit K4011 from DAKO) or 15 min (type 10 collagen:

rabbit anti-mouse HRP labelled, Kit DS9800 from Leica) at RT. Next 3 washing steps were performed with the bond washing solution. For the detection of type 10 collagen, the polymer solutions provided in the kits were added to the slices to enhance the signal and incubated for 10 min followed by 3 washing steps with bond washing solution. An additional washing step with MilliQ-water was performed for both collagens. Next the slices were treated with the substrate solutions of the kits. A DAB solution was added for 12 min to detect type 2 collagen and for 10 min to detect type 10 collagen. Following 3 washing steps were performed with MilliQ-water and a counterstaining with hematoxylin was performed for 30 sec (type 2 collagen) or 15 sec (type 10 collagen). The slices were digitalized by scanning them using the Leica Scanner SCN400 (40x magnification), the recordings were imported and examined with the software Leica Slidepath Gateway. Finally, the sections were dehydrated in increasing concentrations of EtOH and subsequently in NeoClear with the combined Auto- and Multistainer. At the end of the process slides were mounted with Neomount with a Glass Coverslipper.

4.8 Statistics

Statistical analysis was performed with the GraphPad Prism Software 5.0.4.
Stimulated samples were compared to the control or between each other using a 1-way ANOVA followed by a Bonferroni or Dunnett test to correct for multiple comparisons.
Correlations between the osmolarity and the effect size of the analyzed parameters were performed with a Pearson correlation test.
Regarding the MSC trials the samples were compared to each other using a 2-way ANOVA and a Bonferroni´s multiple comparison test. The compound was defined as the column factor and the time as the row factor.

5 Results

GDF5 was shown to induce matrix synthesis in chondrocytes, to stimulate chondrogenesis in mesenchymal stem cells and to promote cartilage repair in a rat model of osteoarthritis (OA). These results indicate that GDF5 might be a promising therapeutic agent for OA. However, GDF5 was also demonstrated to increase hypertrophy in mesenchymal stem cells and osteophyte formation in vivo. To design an improved GDF5 version, single point mutations were performed in the receptor binding site leading to different receptor binding profiles. For the present work three of these mutants (M1673, W417F and W417R) were selected, all having a reduced affinity for BMPR1a and a similar affinity for BMPR1b in comparison to GDF5. These GDF5 mutants were characterized for their ability to stimulate cartilage ECM production in the two only cell types which can produce cartilage: chondrocytes and mesenchymal stem cells (MSCs).

Of the three GDF5 mutants M1673 was previously shown to have the strongest anabolic effect in porcine and bovine chondrocytes. In a first instance, the present work aimed at confirming the anabolic effect of M1673 in human OA chondrocytes (hOAC). However, to be able to do so the hOAC culture needed to be optimized. In another part of this work, the chondrogenic/hypertrophic and osteogenic properties of the three GDF5 mutants were evaluated on MSCs and compared to GDF5 and BMP2. From these results, it could be determined which of the GDF5 mutants can promote chondrogenesis but simultaneously show a low ossification potential. In addition, the respective roles of the BMPR1a and BMPR1b in chondrogenesis and osteogenesis could be further elucidated.

5.1 Establishment of an in vitro model to analyze the anabolic effect of M1673 in hOAC

To evaluate the anabolic effect of M1673 on hOAC and compare it to GDF5, the monolayer culture was first used. Next, the culture conditions were optimized to develop a system that is better mimicking the physiology of articular cartilage and enabled a more robust response to M1673.

5.1.1 Effect of M1673 on hOAC in monolayer

As a first step, the anabolic effect of GDF5 and M1673 was investigated in hOAC monolayer cultures over 7 days. Previous experiments showed that with a compound concentration of 300 ng/ml a significant effect was achieved and that increasing the concentration did not result in an enhanced effect. Consequently, a compound concentration of 300 ng/ml was chosen for the present work. Ten cultures were realized with cells isolated from ten different donors. At the end of the cultures three cartilage ECM production markers, namely the GAG concentration in medium, type 2 collagen and aggrecan expression, were analyzed. In the presence of GDF5 or M1673 only four out of ten monolayer cultures

showed a significant upregulation of at least one of the three tested ECM production markers compared to untreated cells. Not a single monolayer experiment showed a significant upregulation of all three analyzed ECM production markers with GDF5 or M1673 compared to control cells (Table 6). Overall, the effect of GDF5 and M1673 in hOAC monolayer cultures was weak or inexistent.

Table 6 **Effect of GDF5 and M1673 on ECM production of hOAC in monolayer cultures over 7 days.** Monolayer cultures were performed with hOAC from ten different donors and were treated with 300 ng/ml GDF5 and M1673 or remained untreated over 7 days. At the end of the culture, medium samples were analyzed for the GAG concentration. Additionally, cell samples were analyzed for cell concentration or gene expression of type 2 collagen and aggrecan. For each donor and each readout, the mean value of three replicates was calculated. The results presented are x-fold differences of these mean values in comparison to untreated cells. Significant results are highlighted in blue.

	Cell content	GAG content	Collagen 2 expression	Aggrecan expression
Donor 1				
GDF5	1.06	1.03	1.50	1.14
M1673	0.77	0.97	0.50	0.43
Donor 2				
GDF5	0.92	1.00	**1.80**	**4.00**
M1673	0.94	0.82	1.00	3.80
Donor 3				
GDF5	0.92	1.00	1.20	1.50
M1673	0.87	0.95	0.67	1.75
Donor 4				
GDF5	0.98	0.96	1.50	**1.80**
M1673	0.98	0.92	0.83	1.00
Donor 5				
GDF5	1.08	0.96	1.30	1.67
M1673	0.97	0.94	1.70	2.33
Donor 6				
GDF5	1.05	1.05	1.32	1.00
M1673	0.92	1.03	1.18	1.20
Donor 7				
GDF5	0.90	0.92	2.00	**2.00**
M1673	0.88	0.83	1.50	**1.39**
Donor 8				
GDF5	0.97	1.00	0.74	1.00
M1673	0.91	1.00	0.63	0.98
Donor 9				
GDF5	0.98	1.17	**2.16**	1.08
M1673	0.97	1.00	1.00	1.04
Donor 10				
GDF5	1.14	1.07	1.79	1.17
M1673	1.00	1.21	0.79	1.25

It was first hypothesized that GDF5 and M1673 might need a longer time to exert their effects. Consequently, a 28-day long monolayer culture was realized. Two independent experiments were performed with cells from two different donors. On a weekly basis, medium samples were analyzed for the GAG concentration. The first experiment showed an enhanced GAG concentration in medium after GDF5 treatment, but not after M1673 treatment for all analyzed time points from 7 up to 28 days compared to untreated cells (Figure 12 A). Similarly, the second experiment showed an enhanced GAG concentration in medium after GDF5 treatment for all analyzed time points from 7 up to 28 days compared to untreated cells. However, M1673 treatment enhanced the GAG concentration in medium after 7 and 21 days, but not after 14 and 28 days compared to untreated cells (Figure 12 B). These results show that there is no advantage for a long-term monolayer culture. Indeed, when there was an effect of the compounds it was already visible after 7 days of culture.

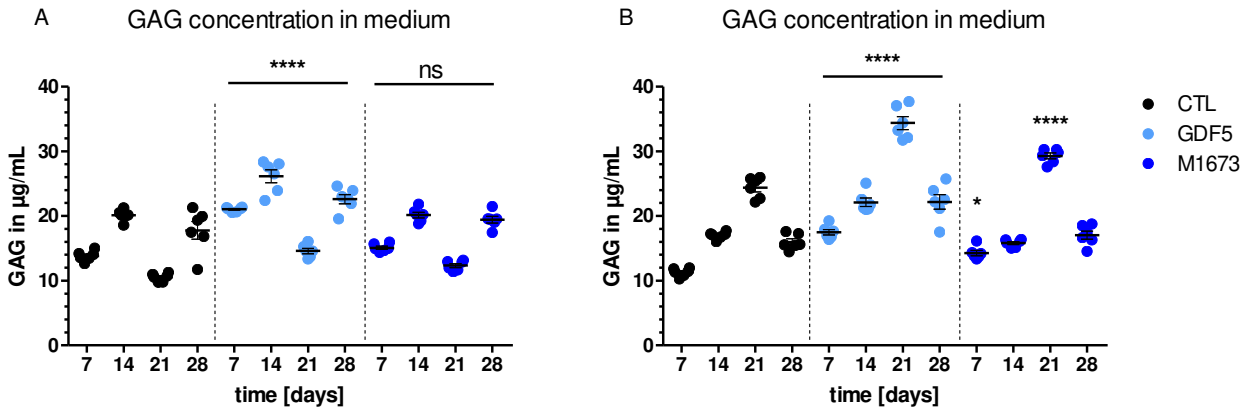

Figure 12 **Effect of GDF5 and M1673 on GAG concentration in hOAC monolayer cultures over 28 days.** hOAC of two different donors (A and B) were cultured in monolayer over 28 days and treated with 300 ng/ml GDF5 and M1673 or remained untreated (CTL). On a weekly basis, medium samples were analyzed for the GAG concentration. Stars indicate significance over control for the same day (Bonferroni comparison, * and **** means $p<0.05$ and $p<0.0001$ respectively). ns = not significant. Data represent mean ± SEM.

Overall, in hOAC cultured in monolayer GDF5 and M1673 showed only an inconsistent and weak anabolic effect.

5.1.2 Optimization of hOAC culture conditions

As a first instance to optimize the hOAC culture conditions, two different 3D culture systems were tested. Generally, 3D culture systems better mimic the physiological environment of chondrocytes and are known to better preserve their phenotype in comparison to monolayer cultures. The hOAC were either seeded into low attachment plates without scaffold and pre-cultured for one week to allow the cells to aggregate and form cartilage tissue analogs (CTAs) or encapsulated in alginate beads. For both 3D cultures, the hOAC were treated with 300 ng/ml GDF5 or M1673 or remained untreated. At the end of the culture the GAG concentration was analyzed within the CTAs or the alginate beads and compared to

untreated cells. No significant effect of GDF5 or M1673 on GAG concentration in neither CTAs nor alginate beads was detectable compared to untreated cells (Figure 13). These results were confirmed with two more CTA and alginate experiments respectively (data not shown).

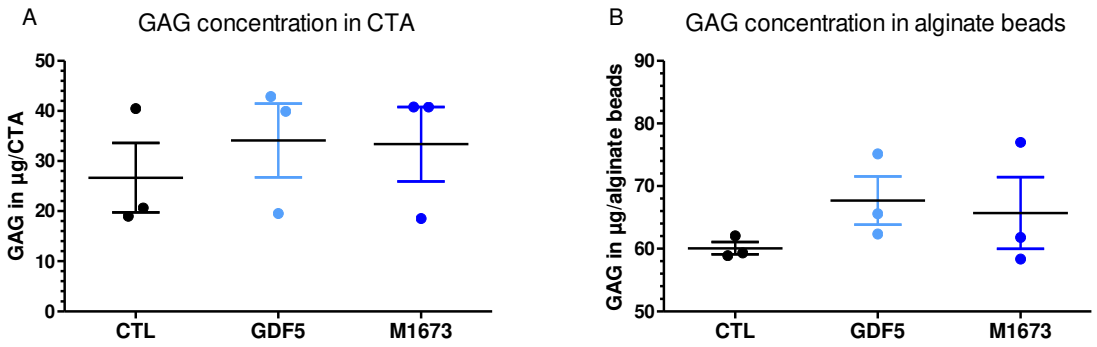

Figure 13 **Effect of GDF5 and M1673 on GAG concentration in hOAC cultured as CTAs or encapsulated in alginate beads.** hOAC were either cultured as CTAs over 28 days or encapsulated in alginate beads and cultured over 14 days. The hOAC in both culture systems were treated with 300 ng/ml GDF5 or M1673 or remained untreated (CTL). At the end of the cultures, cell samples were analyzed for the GAG concentration. Data represent mean ± SEM.

In summary, hOAC in monolayer as well as in 3D cultures (CTAs or alginate beads) showed only a weak, non-reproducible effect on ECM production after GDF5 or M1673 treatment.

These results are not in accordance with previous results showing a strong anabolic effect of M1673 in porcine and bovine chondrocytes cultured in 3D as CTAs. It was then hypothesized that the difference between the response observed with animal and human chondrocytes resides in the disease status of the cells. Animal chondrocytes were isolated from healthy cartilage while the human chondrocytes were extracted from late-stage OA cartilage. Indeed, in contrast to healthy chondrocytes, the environment of late-stage OA chondrocytes is profoundly altered. The joint is usually inflamed, the cartilage is degraded and shows altered physicochemical properties: for instance, it has a decreased osmolarity and increased oxygen tension in comparison to healthy cartilage. These parameters - among others - lead to an aberrant behavior of the cells and possibly unresponsiveness to anabolic factors that persists in culture after cell isolation. In the following experiments, the end-stage disease hOAC were cultured at conditions imitating a 'healthier' cartilage environment to possibly improve their responsiveness to GDF5 and M1673. The conditions chosen to mimic a 'healthier' cartilage environment were the cultivation of hOAC at low oxygen (1% instead of the usual 21%) and higher osmolarity (380 mOsm instead of 340 mOsm, the usual osmolarity of DMEM medium). In a first attempt, the culture of hOAC was performed in monolayer over 7 days with a hypoxic (1%) or normoxic (21%) oxygen tension combined with a medium osmolarity of 340 mOsm (osmolarity of the medium was unchanged) or 380 mOsm. 340 mOsm rather corresponds to conditions within OA cartilage and 380 mOsm to the osmolarity within healthy cartilage. The monolayer culture of hOAC at 1% or 21% oxygen combined with the standard medium osmolarity of 340 mOsm showed nearly the same GAG concentrations in medium. Consequently, a low oxygen tension

of 1% had no beneficial effect over a standard cultivation at 21% oxygen on the GAG concentration in hOAC at 340 mOsm. Moreover, it was shown that at 380 mOsm using 21% instead of 1% oxygen was beneficial regarding the GAG concentration (Figure 14). Additionally, it was observed that the monolayer culture of hOAC at 380 mOsm significantly enhanced the GAG concentration in medium at both oxygen tensions of 1% and 21% compared to the respective oxygen tensions at 340 mOsm (Figure 14).

To summarize, reducing the oxygen tension had no or even a negative influence while a moderate osmolarity increase had a positive influence on the GAG concentration of hOAC cultured in monolayer over 7 days.

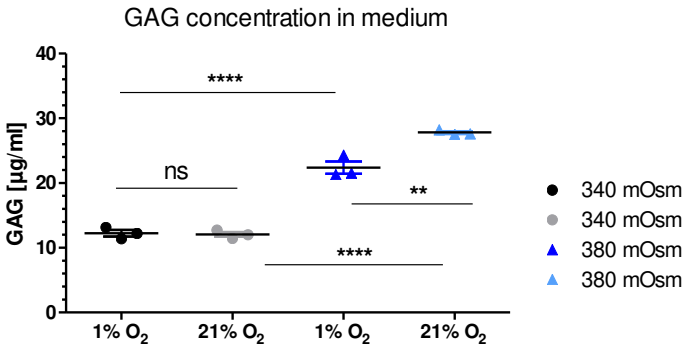

Figure 14 **Effect of oxygen and osmolarity on GAG concentration in hOAC cultured in monolayer over 7 days**. hOAC were cultured in monolayer at standard oxygen tension (21%) or low oxygen tension (1%) combined with a standard medium osmolarity (340 mOsm) or an increased medium osmolarity (380 mOsm). After 7 days of culture, the GAG concentration was analyzed in medium and compared between the different culture conditions. Stars indicate significance over the marked conditions (Bonferroni comparison, ** and **** means $p<0.01$ or $p<0.0001$ respectively). ns = not significant. Data represent mean ± SEM.

The negative effect of a reduced oxygen tension on the GAG concentration in hOAC was confirmed in a CTA culture system over 28 days (Figure 15). The GAG concentration in medium was significantly higher after 7, 14, 21 and 28 days at 21% oxygen compared to 1% oxygen (Figure 15 A). Similarly, the GAG concentration in CTAs was significantly increased after cultivation at 21% oxygen compared to 1% oxygen for 28 days (Figure 15 B). Additionally, the cell concentration per CTA was significantly higher after cultivation at 21% compared to 1% oxygen for 28 days (Figure 15 C). Thus, a low oxygen tension of 1% is accompanied with an increased cell loss and lesser ECM accumulation in the CTAs compared to 21% oxygen. These results were confirmed in one additional CTA experiment (data not shown). Taken together, these results indicate that the exposure of hOAC to an oxygen tension of 1% is not beneficial.

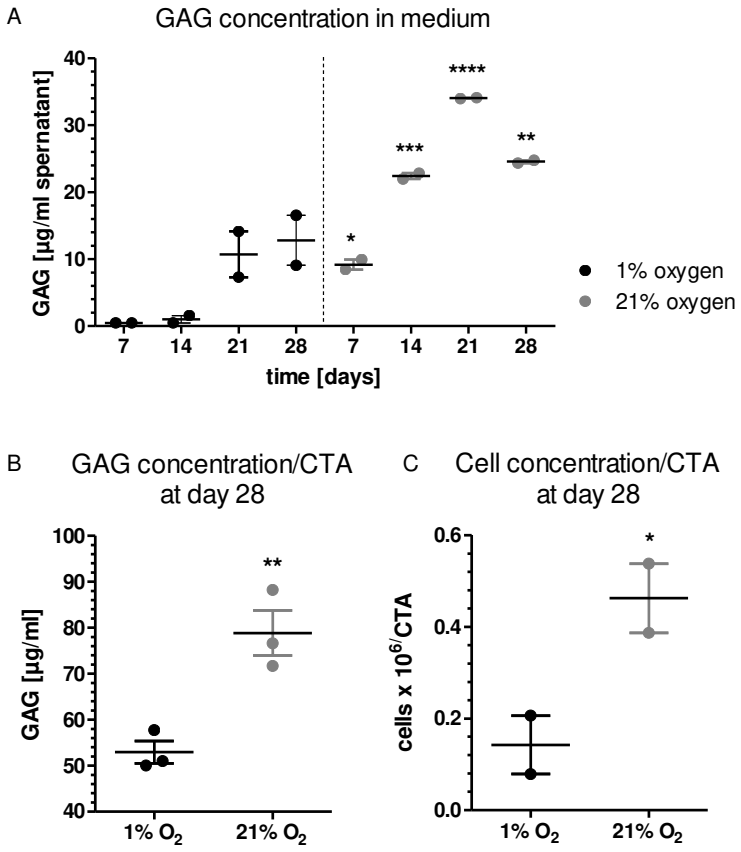

Figure 15 **Effect of oxygen in hOAC cultured as CTAs over 28 days**. hOAC were cultured as CTAs at standard oxygen tension (21%) or low oxygen tension (1%) over 28 days. Medium samples were analyzed on a weekly basis for the GAG concentration (A). Additionally, at the end of the culture the GAG (B) and cell (C) concentration per CTA was analyzed. Stars indicate significance at 21% over 1% oxygen for the same time points (Bonferroni comparison, *, **, *** and **** means $p<0.05$, $p<0.01$, $p<0.001$ or $p<0.0001$ respectively). Data represent mean ± SEM.

In contrast increasing the medium osmolarity to 380 mOsm already showed an increased GAG concentration in medium after culturing hOAC over 7 days in monolayer compared to the standard medium osmolarity of 340 mOsm (Figure 14). As a consequence, the effect of 380 mOsm osmolarity was next tested in hOAC cultured as CTAs or in alginate in the presence of 300 ng/ml GDF5 or M1673 over 28 days. Neither the GAG accumulation in medium over 28 days, nor the GAG concentration within the CTAs at day 28 were increased after GDF5 or M1673 treatment at 380 mOsm compared to untreated cells at the same osmolarity (Figure 16 A+B). In contrast, hOAC encapsulated in alginate beads showed a significant increase of GAG accumulation in medium over 14 days in the presence of GDF5 and M1673 at 380 mOsm compared to untreated cells at the same osmolarity. Similarly, the GAG concentration within the alginate beads at day 14 was significantly enhanced after GDF5 and M1673 treatment compared to untreated cells at 380 mOsm (Figure 16 C+D).

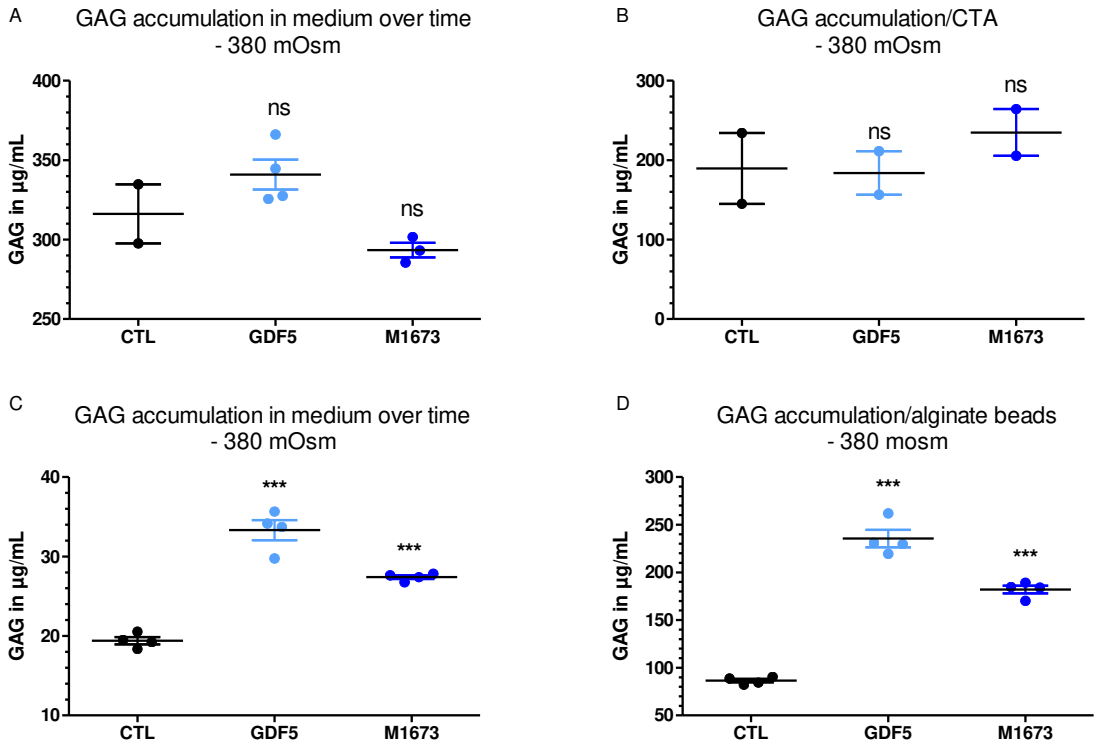

Figure 16 **Effect of GDF5 and M1673 on GAG accumulation in hOAC cultured as CTAs or in alginate beads at 380 mOsm.** hOAC were either cultured as CTAs over 28 days (A+B) or cultured in alginate beads over 14 days (C+D). Both cultures were treated with 300 ng/ml GDF5 or M1673 or remained untreated (CTL). Medium samples were taken on a weekly basis for the CTA culture and every three to four days for the alginate culture and analyzed for the GAG concentration, which was subsequently summed over time (A+C). At the end of the cultures, the GAG concentration within the 3D constructs was analyzed (B+D). Stars indicate significance over untreated cells (Dunnett comparison, *** means $p<0.001$). ns = not significant. Data represent mean ± SEM.

Based on these results it can be concluded that an increased medium osmolarity of 380 mOsm together with the 3D culture in alginate results in an improved responsiveness of hOAC to GDF5 and M1673. Therefore, this culture system seems to be more appropriate to investigate the effect of M1673 in hOAC. Besides the role of osmolarity and oxygen on the response of hOAC to GDF5 and M1673, the effect of heparin was also analyzed. BMPs like GDF5 and M1673 contain a heparin/heparan sulfate binding site, which is believed to potentiate the BMP effect upon binding of heparin/heparan sulfate. Healthy chondrocytes produce an abundant ECM containing inter alia heparan sulfates. However, hOAC have a reduced capacity to produce ECM molecules and the lack of heparan sulfate could also explain their low responsiveness to GDF5 or M1673. Therefore, the effect of heparin on the GDF5 and M1673 response was analyzed in the alginate system with hOAC over 14 days. In presence of GDF5 combined with heparin the GAG concentration was unchanged, whereas in presence of M1673 combined with heparin a small, not significant reduction of the GAG concentration was observed within the alginate beads at day 14 compared to the treatment with solely GDF5 or M1673 respectively (Figure 17). These results were confirmed in two additional experiments (data not shown). Overall, the addition of heparin did not increase the effect of neither GDF5 nor M1673 in hOAC cultured in alginate beads over 14 days.

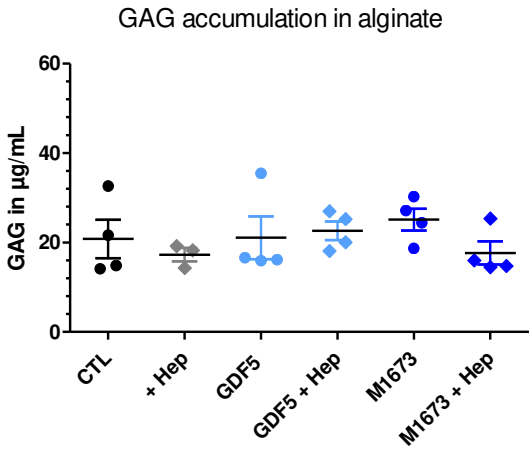

Figure 17 **Heparin effect on the GDF5 and M1673 response in hOAC cultured in alginate beads over 14 days**. hOAC were cultured in alginate beads over 14 days and treated with 300 ng/ml GDF5 or M1673, in the presence or absence of 4 µg/ml heparin (hep) or remained untreated (CTL). At the end of the culture, the GAG concentration was analyzed within the alginate beads. Data represent mean ± SEM.

Taken together these results show that hOAC are responsive to GDF5 and M1373 in alginate culture at 380 mOsm. Therefore, these culture conditions were selected to further investigate the effects of these two compounds on hOAC. However, before doing so, it was aimed at better characterizing the effect of osmolarity on hOAC and better understand the physiological relevance of this parameter.

5.1.3 Characterization of the osmolarity effect on hOAC

To evaluate the effect of osmolarity on hOAC, several monolayer and alginate cultures were realized with a triple objective: 1. Better understand the effect of osmolarity on hOAC phenotype and inflammatory status and 2. Evaluate if higher osmolarities than 380 mOsm could bring an additional benefit and 3. Understand how osmolarity influence the responsiveness of hOAC to M1673 and GDF5.

5.1.3.1 Effect of osmolarity adjusted with NaCl on hOAC in monolayer cultures

To investigate the effect of an increased medium osmolarity on hOAC, cells were used directly after cell isolation to preserve as much as possible their OA characteristics which tends to get lost in culture. These cells were cultured over 6 days at the standard medium osmolarity of 340 mOsm what rather corresponds to the osmolarity within OA cartilage and at increased medium osmolarities of 380, 420 and 460 mOsm what covers the range of osmolarities that have been reported for healthy cartilage. At the end of the culture the cell concentration and viability, ECM synthesis, cytokines and proteases production as well as BMPR expression were evaluated. In addition, freshly isolated chondrocytes (FIC) were sampled before starting the culture and analyzed for determining initial gene expression. For all parameters, the correlation between the osmolarity and the effect size was evaluated with a Pearson correlation test. In addition, the single osmolarities 380, 420 and 480 mOsm were compared to 340 mOsm for statistical difference.

The cell concentration increased at all medium osmolarities over 6 days of culture compared to the seeding concentration. However, the increase in cell concentration became lower with increasing osmolarities from 340 to 460 mOsm indicating a reduced cell proliferation at increased osmolarities. This effect reached statistical significance (Figure 18 A). In contrast, the viability of the cells remained unchanged and stayed between 90 and 95% at all osmolarities (Figure 18 B). The GAG production (μg/million cells) was increased and significantly correlated to increasing osmolarities. Furthermore, the GAG production at 380, 420 or 460 mOsm was also significantly higher than at 340 mOsm (Figure 18 C).

Regarding gene expression, the expression of type 2 collagen and aggrecan was increased from 340 to 460 mOsm and significantly correlated to increasing osmolarities. However, when looking at single osmolarities, a significant difference to 340 mOsm was only achieved at 460 mOsm (Figure 18 E+F). On the contrary, type 1 collagen expression negatively correlated with increasing osmolarities (Figure 18 D).

For the gene expression, the expression was also analyzed in cells sampled just after isolation (FIC, freshly isolated chondrocytes) and before starting the cell culture to evaluate how the phenotype evolves during the culture. An enhanced type 1 collagen and a decreased type 2 collagen expression was detectable after culturing hOAC for 6 days at 340 mOsm compared to the FIC (Figure 18 D+E). That indicates a dedifferentiation and therefore a phenotype loss of hOAC in monolayer cultures. Increasing the medium osmolarity from 380 to 460 mOsm prevented this phenomenon and resulted in type 1 and 2 collagen expressions approaching the values obtained with the FIC (Figure 18 D+E). That indicates a better phenotype maintenance of hOAC at increased medium osmolarities. These results were confirmed in four additional experiments (see supplementary, S2).

Overall, the medium osmolarity seems to play an important role for the cultivation of hOAC. Increasing the medium osmolarity in monolayer cultures improved the phenotype of hOAC and enhanced the ECM production but also resulted in a decreased proliferation of the cells.

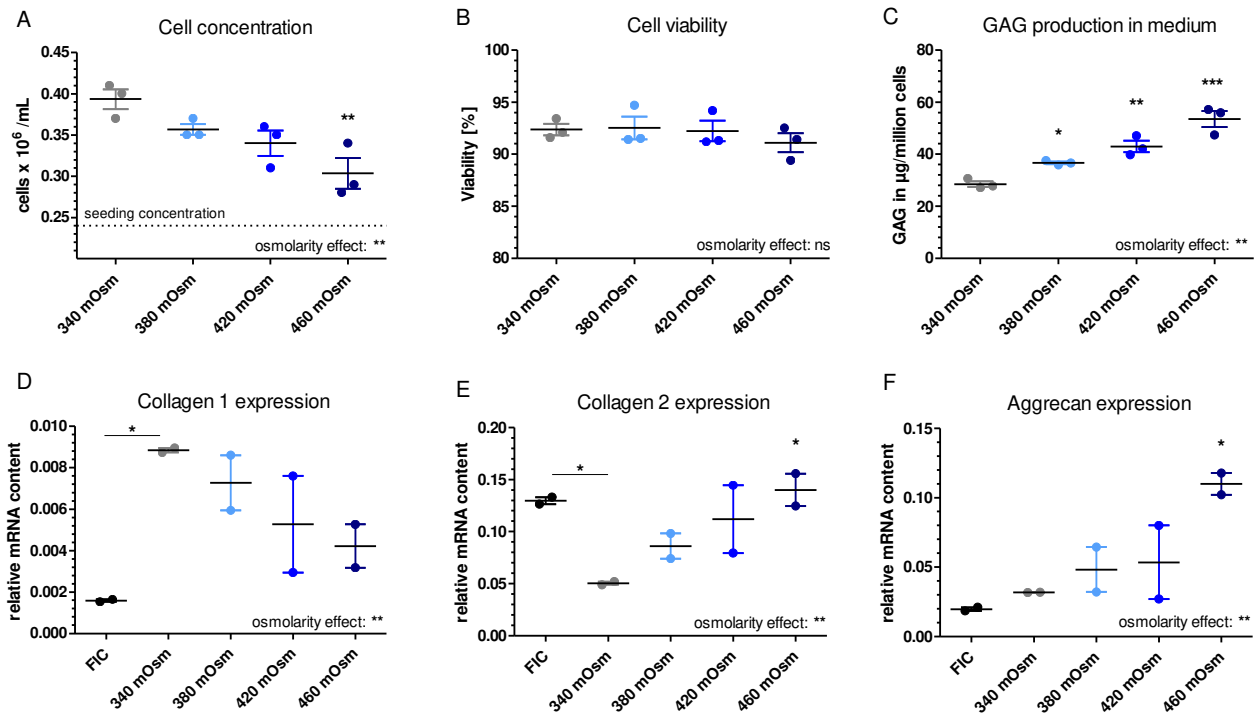

Figure 18 **ECM production and phenotype analysis of hOAC in monolayer culture at different osmolarities adjusted with NaCl.** Freshly isolated chondrocytes (FIC) were lysed at the start of the experiment and analyzed for the type 1 and type 2 collagen as well as aggrecan expression. Monolayer cultures were performed over 6 days at different osmolarities of 340, 380, 420 and 460 mOsm. Afterwards the cell concentration (A) and cell viability (B) as well as the GAG production (µg/million cells) (C) were determined. Additionally, the expression of type 1 collagen (D), type 2 collagen (E) and aggrecan (F) was analyzed. These data are representative for four more experiments. The osmolarity was increased by adding NaCl to the medium. Stars indicate significance over 340 mOsm or as marked (Bonferroni comparison, *, ** and *** means $p<0.05$, $p<0.01$ or $p<0.001$ respectively). Additionally, a correlation between the osmolarity and the effect size was performed and displayed directly on the graph (Pearson correlation, ** means $p<0.01$). ns = not significant. Data represent mean ± SEM.

To further characterize the osmolarity effect on hOAC, the production of ECM-degrading enzymes and inflammatory cytokines was analyzed in the same culture. The expression of the two major proteolytic enzymes, MMP13 and ADAMTS5, which are responsible for degradation of the two main cartilage ECM components, type 2 collagen and aggrecan, was significantly decreased after 6 days of monolayer culture at 340 mOsm in comparison to FIC. The expression of MMP13 was further significantly decreased at 380, 420 and 460 mOsm in comparison to 340 mOsm, whereas the ADAMTS5 expression was nearly the same at all osmolarities after 6 days of culture (Figure 19 A+B). Additionally, the production of MMP1, MMP3 and MMP9 (pg/million cells) were evaluated. A negative correlation between MMP1 production and osmolarity could be found. Although the MMP1 production decreased with increasing the medium osmolarity, it was only significant different at 460 mOsm compared to 340 mOsm (Figure 19 C). A negative correlation between MMP3 and osmolarity was also observed. Furthermore, the MMP3 production at 380, 420 or 460 mOsm was significantly reduced compared to that at 340 mOsm (Figure 19 D). On the contrary, a correlation between the MMP9 production and osmolarity was not observed. However, the MMP9 concentration was significantly decreased at 380 mOsm compared to 340 mOsm, but was not further reduced at higher osmolarities (Figure 19 E). Moreover, the production of the

inflammatory cytokines TNFα, Il1β and Il6 was measured. A negative correlation was only found between TNFα and osmolarity. However, when looking at single osmolarities, the production of all tested cytokines was significantly decreased with increasing medium osmolarities from 380 to 460 mOsm compared to 340 mOsm (Figure 19 F+G+H). The results of protease expression and cytokine production were confirmed in four additional experiments (see supplementary, S3).

Overall these results show that using osmolarities corresponding to healthy cartilage tends to decrease the OA phenotype of the hOAC: they produce less cytokines and less proteases. This effect was already significant at 380 mOsm.

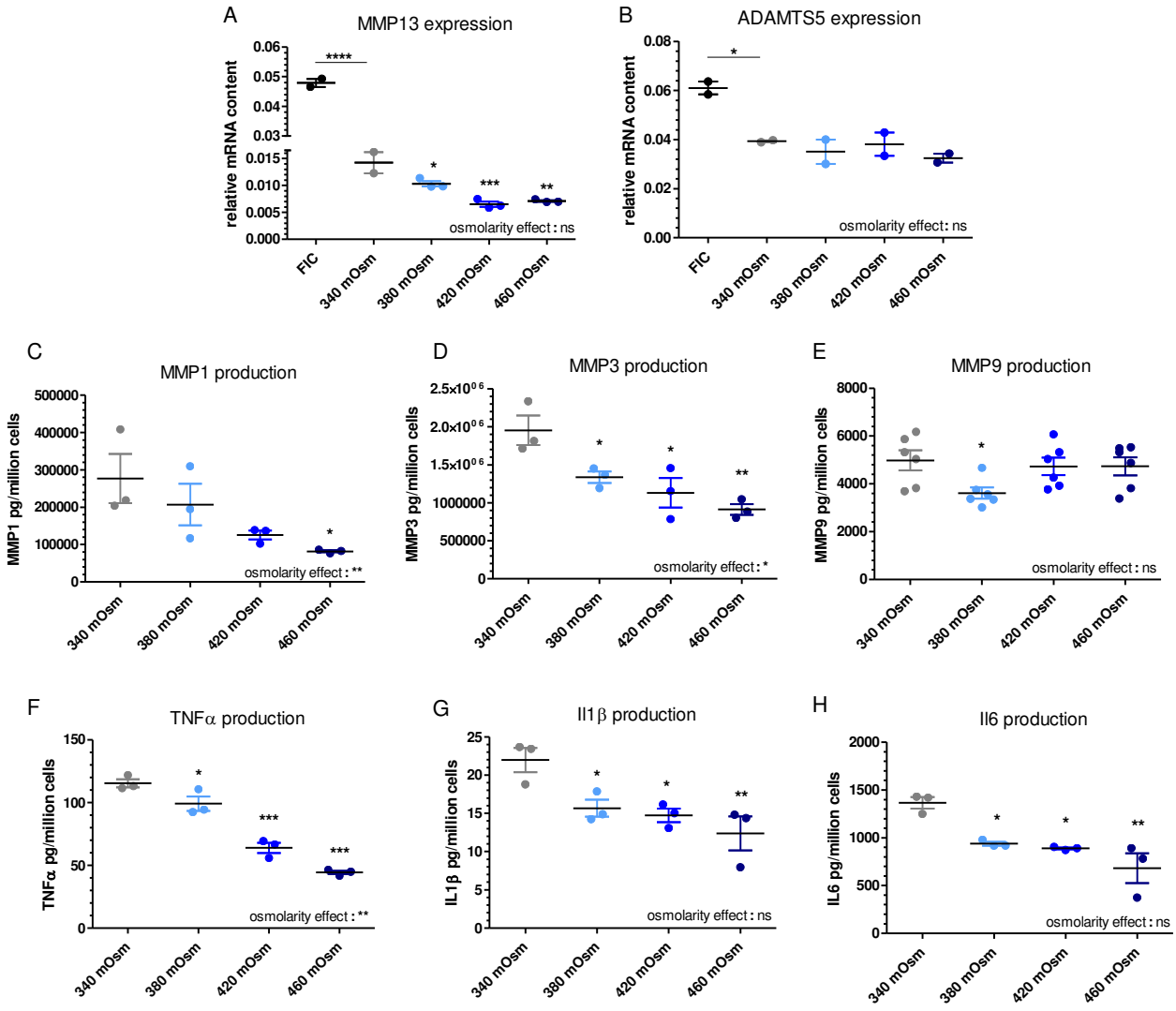

Figure 19 **Proteases and cytokines production of hOAC in monolayer culture at different osmolarities adjusted with NaCl.** Freshly isolated chondrocytes (FIC) were lysed at the start of the experiment and analyzed for the MMP13 and ADAMTS5 expression. Monolayer cultures were performed over 6 days at different osmolarities of 340, 380, 420 and 460 mOsm. Afterwards the expression of MMP13 (A) and ADAMTS5 (B) were analyzed. Additionally, the production of the proteases MMP1 (C), MMP3 (D) and MMP9 (E) and of the cytokines TNFα (F), Il1β (G) and Il6 (H) were determined. These data are representative for four more experiments. The osmolarity was increased by adding NaCl to the medium. Stars indicate significance over 340 mOsm or as marked (Bonferroni comparison, *, **, *** and **** means p<0.05, p<0.01, p<0.001 or p<0.0001 respectively). Additionally, a correlation between the osmolarity and the effect size was performed and displayed directly on the graph (Pearson correlation, * and ** means p<0.05 or p<0.01 respectively). ns= not significant. Data represent mean ± SEM.

Finally, to understand why hOAC are unresponsive to M1673 and GDF5 at 340 mOsm but become responsive at 380 mOsm, the influence of the osmolarity on BMPR expression was investigated. The BMPR expression of hOAC was analyzed in freshly isolated chondrocytes (FIC) or after 6 days of monolayer culture at different osmolarities of 340, 380, 420 and 460 mOsm. The expression of BMPR1a, BMPR1b and BMPR2 was significantly decreased after 6 days of culture at 340 mOsm compared to the initial BMPR expression profile in FIC (Figure 20) but were increased with increasing osmolarities. A positive correlation was only observed between BMPR1a and BMPR1b expression and osmolarity (Figure 20 A+B). Although, the BMPR2 expression seems to increase with increasing osmolarities, it showed neither a correlation to the osmolarity nor a significant difference by comparing the single osmolarities (Figure 20 C). These results were confirmed in four additional experiments for BMPR1a and BMPR2 and in three additional experiments for BMPR1b (see supplementary, S4).

Thus, culturing hOAC at higher osmolarities than 340 mOsm seems to enhance the expression of BMPR1a and BMPR1b, which are necessary for signal transmission of M1673.

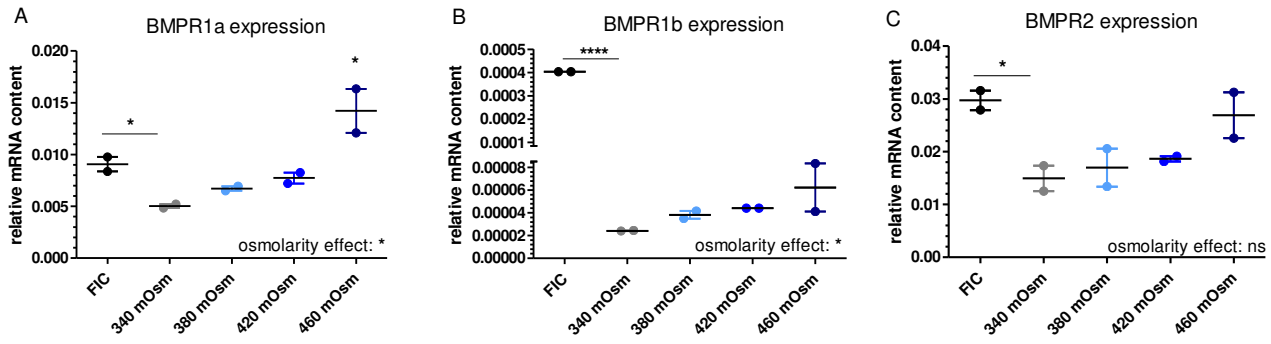

Figure 20 **BMPR expression of hOAC in monolayer culture at different osmolarities adjusted with NaCl.** Freshly isolated chondrocytes (FIC) were lysed at the start of the experiment and analyzed for the BMPR1a, BMPR1b and BMPR2 expression. Monolayer cultures were performed over 6 days at different osmolarities of 340, 380, 420 and 460 mOsm. Afterwards the expression of BMPR1a (A), BMPR1b (B) and BMPR2 (C) was analyzed. These data are representative for three (BMPR1b) or four (BMPR1a+BMPR2) more experiments. The osmolarity was increased by adding NaCl to the medium. Stars indicate significance over 340 mOsm or as marked (Bonferroni comparison, * and **** means $p<0.05$ or $p<0.0001$ respectively). Additionally, a correlation between the osmolarity and the effect size was performed and displayed directly on the graph (Pearson correlation, * means $p<0.05$). ns= not significant. Data represent mean ± SEM.

In summary, increasing the medium osmolarity positively influenced hOAC in monolayer cultures. The cartilage ECM production was enhanced and the chondrocytes phenotype was improved at 380, 420 and 460 mOsm compared to 340 mOsm. Moreover, the production of inflammatory cytokines and proteases (OA phenotype) was reduced with increasing osmolarities. The OA phenotype was already significantly attenuated at 380 compared to 340 mOsm. In addition, the BMPR expression tended to increase at 380, 420 and 460 mOsm in comparison to 340 mOsm.

5.1.3.2 Effect of osmolarity adjusted with sucrose on hOAC in monolayer cultures

To confirm that the observed results are 'real' osmolarity effects and not a NaCl effect, the experiment was repeated by using sucrose to increase the medium osmolarity. After 6 days of hOAC monolayer culture at 340, 380, 420 and 460 mOsm, cell concentration and viability, ECM synthesis, cytokines and proteases production as well as BMPR expression were evaluated. In addition, freshly isolated chondrocytes (FIC) were sampled before starting the culture and analyzed for determining initial gene expression levels. For all parameters, the correlation between the osmolarity and the effect size was evaluated with a Pearson correlation test. In addition, the single osmolarities 380, 420 and 460 mOsm were compared to 340 mOsm for statistical difference.

As seen before, the cell concentration increased at all medium osmolarities over 6 days of cultivation compared to the seeding concentration. The cell concentration was significantly reduced at 460 mOsm compared to 340 mOsm, but a statistically significant negative correlation between the cell concentration and an increased osmolarity was not observed (Figure 21 A). Similarly to the NaCl experiment, the viability of the cells remained nearly unchanged and stayed around 80% at the different medium osmolarities (Figure 21 B). As seen before with NaCl, the GAG production (μg/million cells) was increased and significantly correlated to increasing osmolarities. Furthermore, the GAG production at 380, 420 and 460 mOsm was also significantly enhanced in comparison to 340 mOsm (Figure 21 C).

Gene expression analysis was also in accordance to the data obtained with NaCl. The type 2 collagen and aggrecan expressions were both positively correlated to increasing osmolarities. However, when looking at the single osmolarities, a significant difference between 380, 420 and 460 mOsm compared to 340 mOsm was only achieved for the expression of aggrecan, but not for the expression of type 2 collagen (Figure 21 E+F). In contrast, type 1 collagen expression negatively correlated to increasing osmolarities. In addition, the type 1 collagen expression was significantly reduced at 380, 420 and 460 mOsm compared to 340 mOsm (Figure 21 D).

For the gene expression, freshly isolated chondrocytes (FIC) were also sampled before starting the cell culture to evaluate the chondrocytes phenotype development during cell culture. The type 1 collagen expression was enhanced while the type 2 collagen expression was reduced after culturing hOAC for 6 days at 340 mOsm compared to FIC (Figure 21 D+E). That confirmed the dedifferentiation and phenotype loss of hOAC during monolayer cultures observed previously in the NaCl experiment. Increasing the medium osmolarity from 380 to 460 mOsm also prevented this phenomenon and resulted in type 1 and 2 collagen expressions approaching the values obtained with the FIC (Figure 21 D+E). These results were confirmed in one additional experiment (data not shown).

Overall, increasing the medium osmolarity with sucrose instead of NaCl resulted in comparable observations on the hOAC phenotype. Increasing the medium osmolarity enhanced the ECM synthesis, improved the hOAC phenotype and led in trend to lower proliferation of the cells.

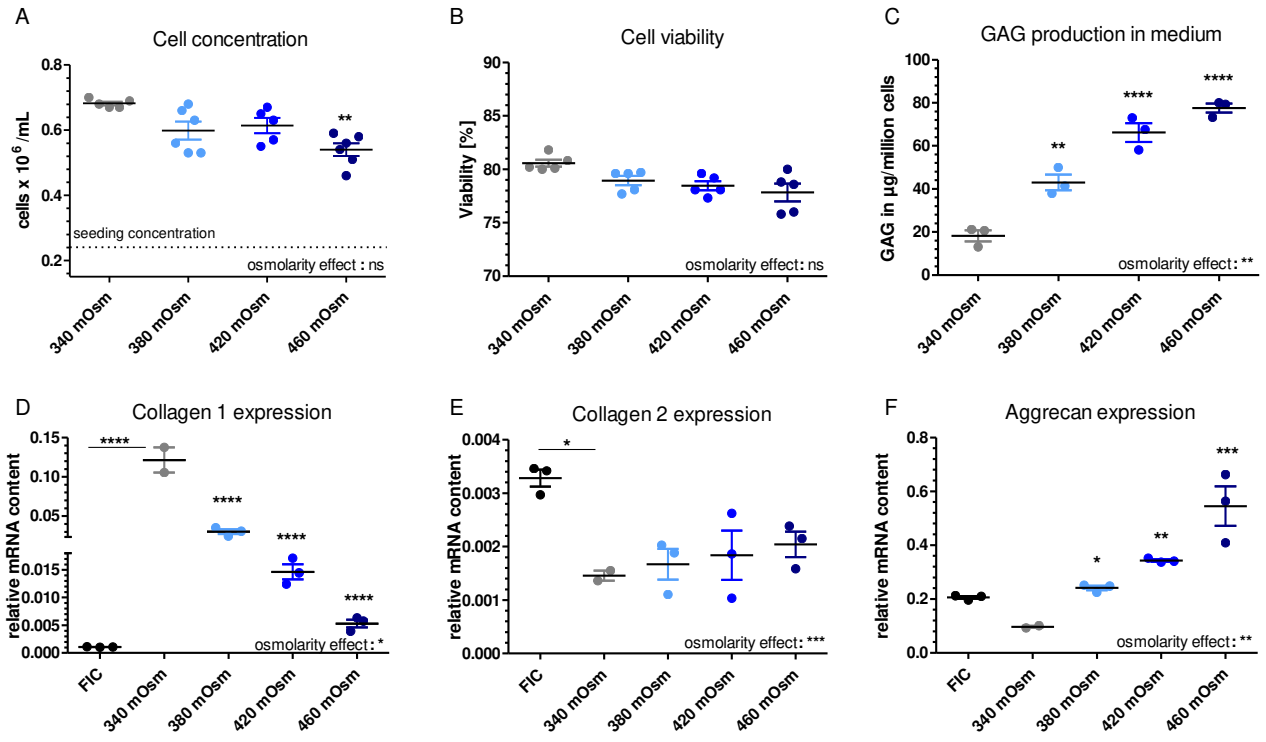

Figure 21 **ECM production and phenotype analysis of hOAC in monolayer culture at different osmolarities adjusted with sucrose.** Freshly isolated chondrocytes (FIC) were lysed at the start of the experiment and analyzed for the type 1 and type 2 collagen as well as aggrecan expression. Monolayer cultures were performed over 6 days at different osmolarities of 340, 380, 420 and 460 mOsm. Afterwards the cell concentration (A) and cell viability (B) as well as the GAG production (µg/million cells) (C) were determined. Additionally, the expression of type 1 collagen (D), type 2 collagen (E) and aggrecan (F) was analyzed. These data are representative for one more experiment. The osmolarity was increased by adding sucrose to the medium. Stars indicate significance over 340 mOsm or as marked (Bonferroni comparison, *, **, *** and **** means $p<0.05$, $p<0.01$, $p<0.001$ or $p<0.0001$ respectively). Additionally, a correlation between the osmolarity and effect size was performed and displayed directly on the graph (Pearson correlation, *, ** and *** means $p<0.05$, $p<0.01$ or $p<0.001$ respectively). ns = not significant. Data represent mean ± SEM.

The influences of increasing the medium osmolarity with sucrose was further evaluated by analyzing the production of proteolytic enzymes and inflammatory cytokines in the same culture.

As seen before with NaCl, the expression of MMP13 decreased significantly after 6 days of monolayer culture at 340 mOsm in comparison to FIC. Furthermore, a negative correlation between the MMP13 expression and increasing osmolarities was found (Figure 22 A). In contrast, the expression of ADAMTS5 was not correlated with increasing osmolarities while its expression was significantly reduced after 6 days of culture at 380 or 420 mOsm compared to 340 mOsm (Figure 22 B). Additionally, the production of MMP1, MMP3 and MMP9 (pg/million cells) was analyzed. In contrast to the NaCl experiment, a negative correlation was only observed for the MMP3 production, but not for the MMP1 production, and increasing osmolarities (Figure 22 C+D). Although, the MMP3 production decreased with increasing osmolarities, it was only significantly reduced at 460 mOsm compared to 340 mOsm (Figure 22 D). The MMP1 and MMP9 production was nearly the same at all osmolarities (Figure 22 C+E). Moreover, the production of the inflammatory cytokines TNFα, Il1β and Il6 was evaluated. A negative correlation was not only found for TNFα, but also for Il1β and increasing osmolarities. However, when looking at single osmolarities, the production of all analyzed inflammatory cytokines was significantly decreased with

increasing medium osmolarities from 380 to 460 mOsm compared to 340 mOsm as seen before with NaCl (Figure 22 F+G+H). By comparing the NaCl and the sucrose monolayer cultures with each other, some differences can be noticed. Contrary to the NaCl experiment, the MMP13 concentration in the sucrose experiment showed a negative correlation, but did only decrease in trend, but not statistically significant from 380 to 460 mOsm compared to 340 mOsm (Figure 19+22 A). The other way around, a significantly decreased ADAMTS5 expression was detectable at 380 and 420 mOsm compared to 340 mOsm in the sucrose experiment, whereas the ADAMTS5 expression of the NaCl experiment was comparable at all osmolarities (Figure 19+22 B). Furthermore, the decrease of MMP concentrations in medium was more pronounced in the NaCl compared to the sucrose experiment (Figure 19+22 C,D,E). These results were confirmed in one additional experiment (data not shown).

Overall, using NaCl or sucrose to increase the medium osmolarity resulted nearly in the same effects on the production of proteolytic enzymes and inflammatory cytokines; observed differences were small. Increasing the medium osmolarity to match the osmolarity of healthy articular cartilage led to a reduced production of proteases and cytokines and consequently decreased the OA phenotype of the cells. This effect was already significant at 380 mOsm.

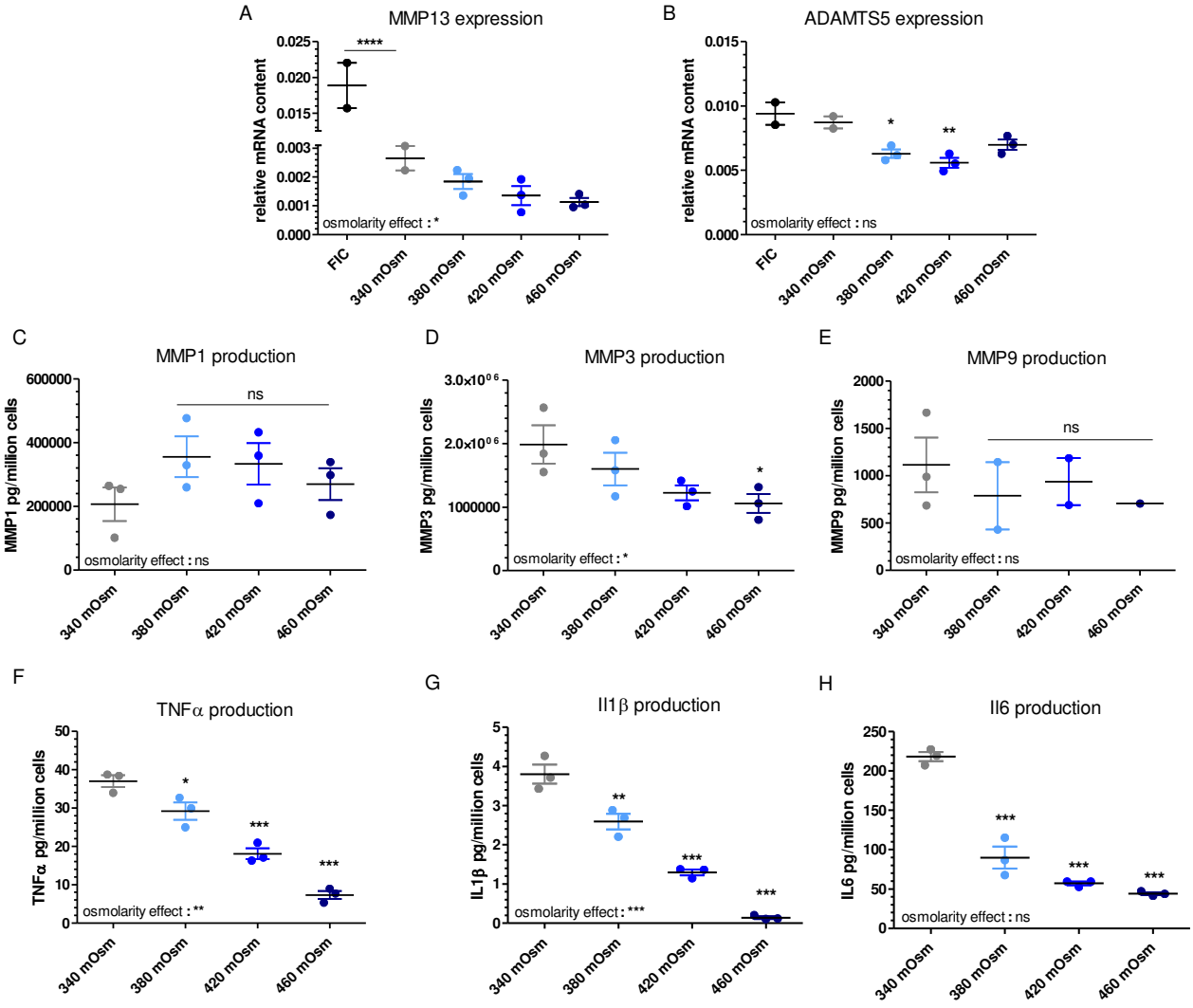

Figure 22 **Proteases and cytokines production of hOAC in monolayer culture at different osmolarities adjusted with sucrose.** Freshly isolated chondrocytes (FIC) were lysed at the start of the experiment and analyzed for the MMP13 and ADAMTS5 expression. Monolayer cultures were performed over 6 days at different osmolarities of 340, 380, 420 and 460 mOsm. Afterwards the expression of MMP13 (A) and ADAMTS5 (B) were analyzed. Additionally, the production of the proteases MMP1 (C), MMP3 (D) and MMP9 (E) and of the cytokines TNFα (F), Il1β (G) and Il6 (H) were determined. These data are representative for one more experiment. The osmolarity was increased by adding sucrose to the medium. Stars indicate significance over 340 mOsm or as marked (Bonferroni comparison, *, **, *** and **** means p<0.05, p<0.01, p<0.001 or p<0.0001 respectively). Additionally, a correlation between the osmolarity and effect size was performed and displayed directly on the graph (Pearson correlation, *, ** and *** means p<0.05, p<0.01 or p< 0.001 respectively). ns= not significant. Data represent mean ± SEM.

Lastly, the expression profile of the different BMPRs, BMPR1a, BMPR1b and BMPR2, was measured in hOAC cultured for 6 days in monolayer at the different osmolarities of 340, 380, 420 and 460 mOsm adjusted with sucrose. The expression of BMPR1a and BMPR1b was significantly decreased after 6 days of culture compared to that of FIC (Figure 23 A+B), whereas the BMPR2 expression was not altered (Figure 23 C). A positive correlation between the expression of BMPR1a and increasing osmolarities was observed. Similarly, a significant difference of BMPR1a expression with increasing medium osmolarities from 380 to 460 mOsm compared to 340 mOsm was detectable (Figure 23 A). Although, the BMPR1b expression was not correlated with increasing osmolarities, it was significant different at 380 and 460 mOsm in comparison to 340 mOsm (Figure 23 B). The expression of BMPR2 positively correlated with

increasing osmolarities, but was only significant different at 420 and 460 mOsm compared to 340 mOsm (Figure 23 C). These results were confirmed in one additional experiment (data not shown).

As seen before with NaCl, increasing the medium osmolarity from 380 to 460 mOsm increased the expression of BMPRs. This effect was even more pronounced when the osmolarity was adjusted with sucrose instead of NaCl (Figure 20+23).

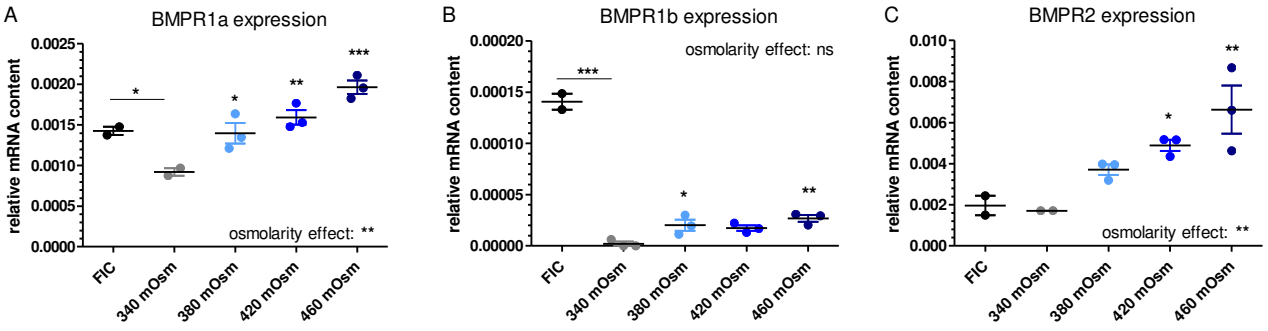

Figure 23 **BMPR expression of hOAC in monolayer culture at different osmolarities adjusted with sucrose.** Freshly isolated chondrocytes (FIC) were lysed at the start of the experiment and analyzed for the BMPR1a, BMPR1b and BMPR2 expression. Monolayer cultures were performed over 6 days at different osmolarities of 340, 380, 420 and 460 mOsm. Afterwards the expression of BMPR1a (A), BMPR1b (B) and BMPR2 (C) was analyzed. These data are representative for one more experiment. The osmolarity was increased by adding sucrose to the medium. Stars indicate significance over 340 mOsm or as marked (Bonferroni comparison, *, ** and *** means $p<0.05$, $p<0.01$ or $p<0.001$ respectively). Additionally, a correlation between the osmolarity and effect size was performed and displayed directly on the graph (Pearson correlation, ** means $p<0.01$). ns= not significant. Data represent mean ± SEM.

From these results, it can be concluded that the observed effects can be really attributed to osmolarity changes and not to an effect of NaCl or sucrose itself. Consequently, for further experiments it was decided to use NaCl to increase the medium osmolarity.

In summary, the monolayer experiments with hOAC at different osmolarities indicate that increasing the medium osmolarity has a positive impact on hOAC in monolayer cultures. The ECM production was enhanced and the chondrocytes phenotype was improved at 380, 420 and 460 mOsm in comparison to 340 mOsm. Furthermore, the production of proteolytic enzymes and inflammatory cytokines was significantly reduced – already at 380 compared to 340 mOsm - indicating a decreased OA phenotype of the cells at increased medium osmolarities. The expression of BMPRs increased with increasing osmolarities from 340 to 460 mOsm. It was, however, unclear if the osmolarity has a direct effect on the BMPR expression or if this effect is indirectly driven by other factors as for instance the inflammatory status of the chondrocytes.

5.1.3.3 Influence of inflammatory cytokines on BMP receptor expression

To analyze the impact of an inflammatory environment on BMPR expressions, the effect of various cytokines known to be produced by hOAC was evaluated on the expression of BMPR1a, BMPR1b and BMPR2. The hOAC were cultured in monolayer, treated with 10 ng/ml TNFα and Il1β or 100 ng/ml Il6

over two days and analyzed for the BMPR expression. The presence of TNFα and Il6 resulted in a significant downregulation of BMPR1a and BMPR1b compared to unstimulated cells. In addition, the presence of Il6 also reduced significantly the BMPR2 expression compared to unstimulated cells. On the contrary, the addition of Il1β enhanced significantly the expressions of BMPR1a, BMPR1b and BMPR2 compared to unstimulated cells (Figure 24) These results are representative of three experiments (see supplementary, S5).

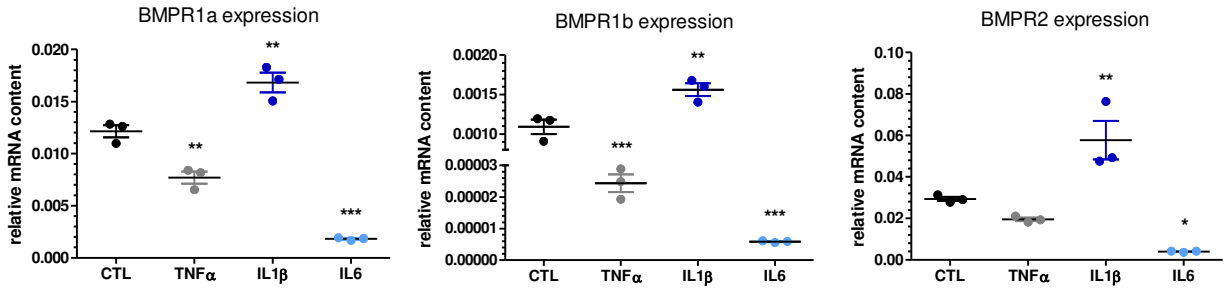

Figure 24 **Expression of BMP receptors in hOAC cultured in monolayer after stimulation with TNFα, Il1β or Il6.** hOAC were cultured in monolayer and stimulated with 10 ng/ml TNFαand Il1β or 100 ng/ml Il6 for 2 days. Afterwards cell samples were analyzed for the expression of BMPR1a, BMPR1b and BMPR2. These data are representative for three more experiments. Significance over unstimulated cells (CTL) is indicated as stars (Dunnett comparison, *, ** and *** means p<0.05, p<0.01 or p<0.001 respectively). Data represent mean ± SEM.

From these results, it can be hypothesized that the enhanced BMPR expression of hOAC cultured at higher osmolarities indirectly could be driven by the reduced inflammatory status of hOAC. Here a clear link was established between the presence of specific cytokines and BMPR expression. However, it cannot be excluded that osmolarity could also influence directly BMPR expression, or that other indirect effects are at play.

5.1.3.4 Effect of osmolarity on hOAC in 3D culture

As a next step, the osmolarity effect observed in monolayer cultures was evaluated in the alginate system, which was found to be a favorable 3D culture system to investigate the anabolic effects of M1673 (Chapter 5.1). The hOAC were encapsulated in alginate and cultured over 14 days at the usual medium osmolarity of 340 mOsm or at higher medium osmolarities of 380, 420 and 460 mOsm which were adjusted with NaCl. At the end of the culture cell concentration and viability, ECM synthesis, cytokines and protease production as well as BMPR expression were evaluated. In addition, freshly isolated chondrocytes (FIC) were sampled before starting the culture to analyze the initial gene expression levels. For all parameters, the correlation between the osmolarity and the effect size was evaluated with a Pearson correlation test. In addition, the difference between the single osmolarities 380, 420 and 460 mOsm were compared to 340 mOsm for statistical analysis.

As seen before in the monolayer system, the cell concentration negatively correlated with increasing osmolarities from 340 to 460 mOsm indicating a reduced cell proliferation at higher osmolarities. The

cell concentration was significantly reduced with 420 and 460 mOsm, but not with 380 mOsm, compared to 340 mOsm (Figure 25 A). On the contrary, the cell viability remained unchanged and stayed between 90 and 95% at all osmolarities (Figure 25 B). The GAG production (μg/million cells) in alginate beads did not correlate to increasing osmolarities. However, when looking at the single osmolarities, the GAG production at 380, 420 and 460 mOsm was significantly higher in comparison to 340 mOsm (Figure 25 C).

Regarding gene expression, the expression of type 2 collagen and aggrecan was increased from 340 to 460 mOsm and significantly correlated to increasing osmolarities (Figure 25 E+F). Similarly, the type 2 collagen expression increased at 380, 420 and 460 mOsm compared to 340 mOsm osmolarities, whereas the expression of aggrecan was only significantly enhanced at 420 and 460 mOsm in comparison to 340 mOsm (Figure 25 E+F). Although, no statistically significant negative correlation between type 1 collagen expression and increasing osmolarities was detectable, it was significantly reduced at 380, 420 and 460 mOsm compared to 340 mOsm (Figure 25 D).

In addition, freshly isolated chondrocytes (FIC) were sampled before starting the cell culture and analyzed for gene expression to evaluate the chondrocytes phenotype change during cell culture. In contrast to the monolayer experiments, the type 2 collagen expression increased significantly while type 1 collagen expression decreased significantly after 14 days of alginate culture at 340 mOsm in comparison to FIC. That indicates a preserved chondrocytes phenotype in 3D culture (Figure 25 D+E).

Overall, the positive impact of increasing osmolarities on hOAC was confirmed in the 3D culture system using alginate beads. Increasing the medium osmolarity further improved the hOAC phenotype, enhanced the ECM production but also resulted in a reduced proliferation of the cells.

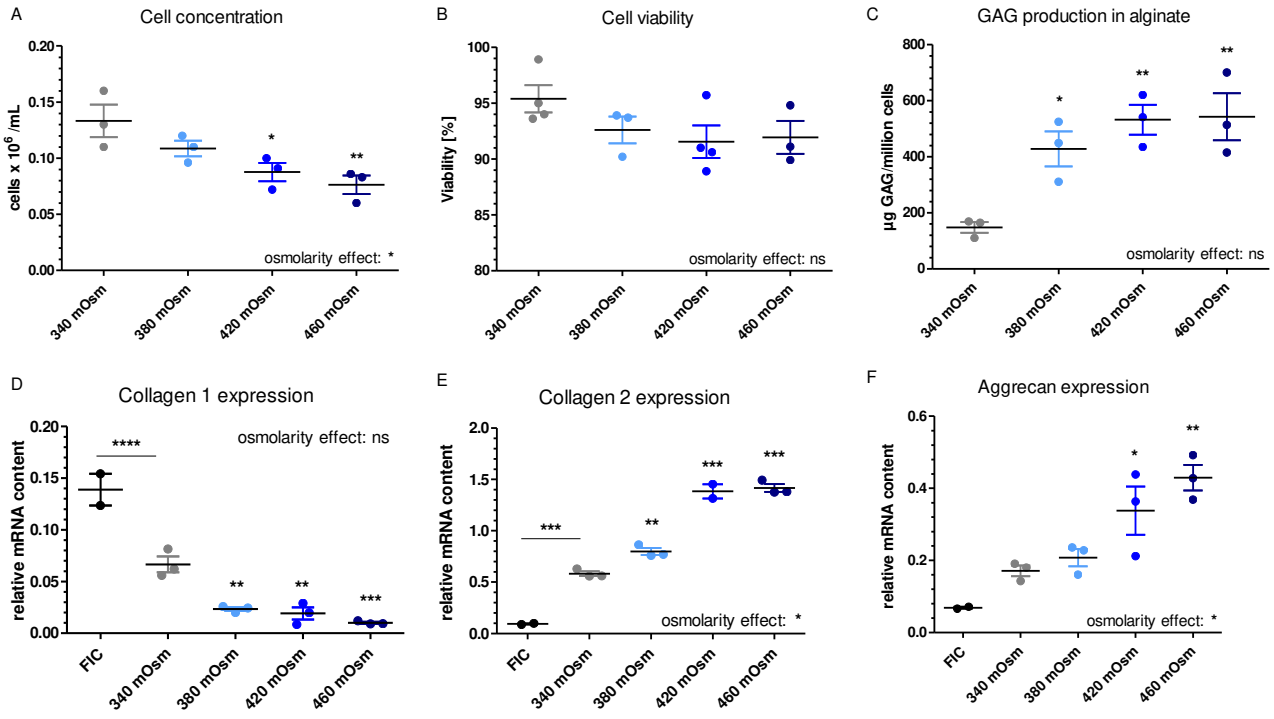

Figure 25 **ECM production and phenotype analysis of hOAC in alginate beads at different medium osmolarities.** Freshly isolated chondrocytes (FIC) were lysed at the start of the experiment and analyzed for the type 1 and type 2 collagen as well as aggrecan expression. Alginate bead cultures were performed over 14 days at different osmolarities of 340, 380, 420 and 460 mOsm. Afterwards the cell concentration (A) and cell viability (B) as well as the GAG production (µg/million cells) (C) were determined. Additionally, the expression of type 1 collagen (D), type 2 collagen (E) and aggrecan (F) was analyzed. The osmolarity was increased by adding NaCl to the medium. Stars indicate significance over 340 mOsm or as marked (Bonferroni comparison, *, ** and *** means $p<0.05$, $p<0.01$ or $p<0.001$ respectively). Additionally, a correlation between the osmolarity and effect size was performed and displayed directly on the graph (Pearson correlation, * means $p<0.05$). ns = not significant. Data represent mean ± SEM.

As done in the previous section, the osmolarity effect was further characterized on hOAC in alginate culture by analyzing the expression of proteolytic enzymes and the production of inflammatory cytokines in the same culture. The expressions of MMP13 and ADAMTS5, two key proteolytic enzymes able to degrade collagens and aggrecans, were significantly decreased after 14 days of alginate culture at 340 mOsm in comparison to FIC (Figure 26 A+B). The expression of MMP13 was further significantly decreased at 380, 420 and 460 mOsm in comparison to 340 mOsm. In contrast, the ADAMTS5 expression was only significantly decreased at 460 mOsm compared to 340 mOsm (Figure 26 A+B). Regarding cytokine production, the production of TNFα, Il1β and Il6 was decreased with increasing osmolarities, but a significant negative correlation between the effect size and osmolarity was only found for TNFα and Il1β. However, when looking at the single osmolarities, the production of all of them was significantly decreased with increasing medium osmolarities from 380 to 460 mOsm compared to 340 mOsm (Figure 26 C+D+E).

Overall, it was confirmed that increasing the medium osmolarity in alginate culture reduced the OA phenotype of the cells by decreasing cytokines production and the expression of proteolytic enzymes. This effect of higher osmolarities was already significant at 380 mOsm.

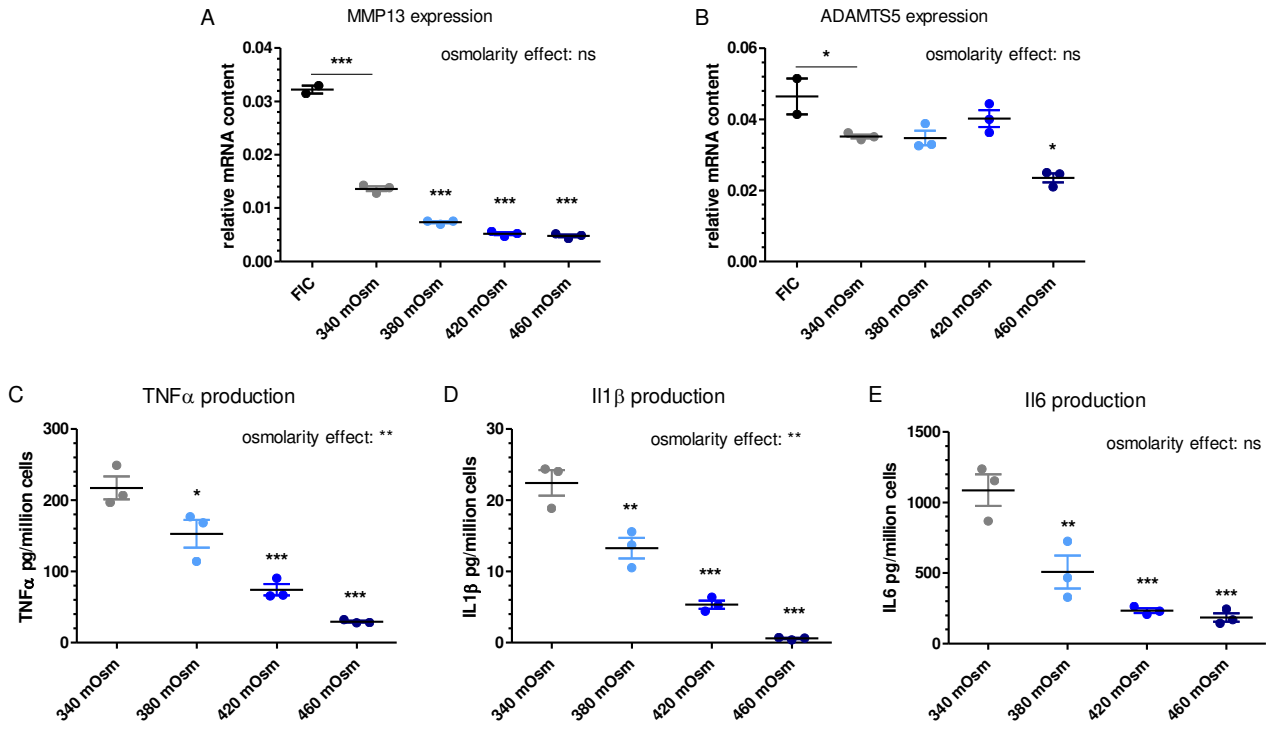

Figure 26 **Proteases and cytokines production of hOAC in alginate beads at different osmolarities.** Freshly isolated chondrocytes (FIC) were lysed at the start of the experiment and analyzed for the MMP13 and ADAMTS5 expression. Alginate bead cultures were performed over 14 days at different osmolarities of 340, 380, 420 and 460 mOsm. Afterwards the expression of MMP13 (A) and ADAMTS5 (B) were analyzed. Additionally, the production of the cytokines TNFα (C), Il1β (D) and Il6 (E) were determined. The osmolarity was increased by adding NaCl to the medium. Stars indicate significance over 340 mOsm or as marked (Bonferroni comparison, *, ** and *** means $p<0.05$, $p<0.01$ or $p<0.001$ respectively). Additionally, a correlation between the osmolarity and effect size was performed and displayed directly on the graph (Pearson correlation, ** means $p<0.01$). ns = not significant. Data represent mean ± SEM.

Finally, the influence of osmolarity on BMPR expression in alginate culture was evaluated. The BMPR expression was analyzed in freshly isolated chondrocytes (FIC) as well as after 14 days of alginate culture at the different osmolarities of 340, 380, 420 and 460 mOsm. The expression of BMPR1a and BMPR2 was significantly increased, whereas the BMPR1b expression was significantly decreased after 14 days of culture at 340 mOsm compared to FIC (Figure 27). A positive correlation was detectable between BMPR1a and BMPR2 expression and increasing osmolarities. In addition, a significant difference to 340 mOsm was achieved at 420 and 460 mOsm (Figure 27 A+C). In contrast, the expression of BMPR1b could not be correlated to increasing osmolarities, but was significantly enhanced at 460 mOsm compared to 340 mOsm (Figure 27 B).

Overall, it was confirmed in alginate culture that increasing the medium osmolarity enhances the expression of BMPRs.

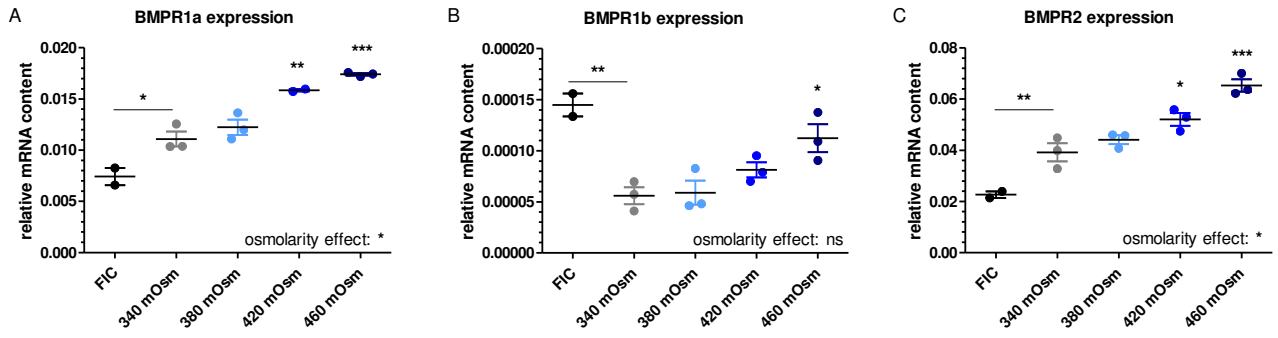

Figure 27 **BMPR expression of hOAC in alginate beads at different osmolarities.** Freshly isolated chondrocytes (FIC) were lysed at the start of the experiment and analyzed for the BMPR1a, BMPR1b and BMPR2 expression. Alginate bead cultures were performed over 14 days at different osmolarities of 340, 380, 420 and 460 mOsm. Afterwards the expression of BMPR1a (A), BMPR1b (B) and BMPR2 (C) were analyzed. The osmolarity was increased by adding NaCl to the standard medium. Stars indicate significance over 340 mOsm or as marked (Bonferroni comparison, *, ** and *** means $p<0.05$, $p<0.01$ or $p<0.001$ respectively). Additionally, a correlation between the osmolarity and effect size was performed and displayed directly on the graph (Pearson correlation, * means $p<0.05$). ns = not significant. Data represent mean ± SEM.

Taken together, increasing the osmolarity positively influenced hOAC in monolayer and in alginate cultures. The ECM production was enhanced and the phenotype of chondrocytes improved at 380, 420 and 460 mOsm in comparison to 340 mOsm in both cultures. In addition, increasing the medium osmolarity reduced the OA phenotype by decreasing inflammatory cytokines and proteolytic enzymes. This effect was already significant at 380 mOsm. Moreover, the expression of BMPRs were enhanced by increasing the medium osmolarity in both culture systems.

5.1.3.5 Conclusion: Effect of osmolarity on hOAC

To summarize, increasing the osmolarity of the culture medium towards the osmolarity of healthy articular cartilage favors the chondrocytes phenotype and ECM production as well as reduced the inflammatory status of the cells. In addition, it also resulted in an increased BMPR expression what could possibly restore the responsiveness of the hOAC to M1673 (Figure 28).

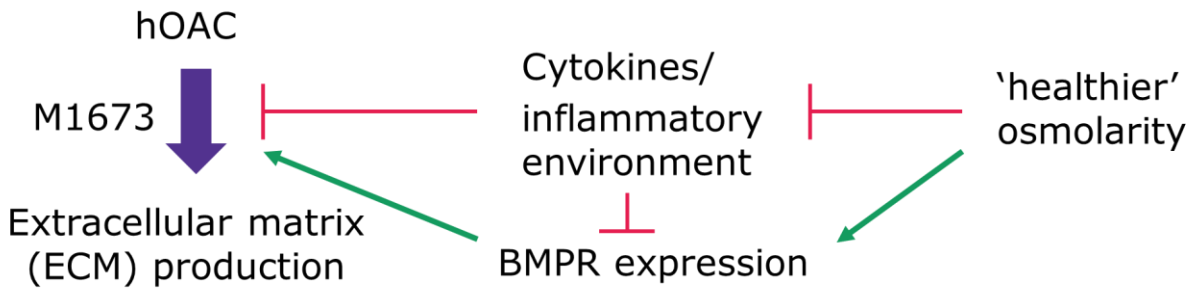

Figure 28 **A new paradigm for culturing hOAC and analyzing effects of anabolic factors in hOAC.** The hOAC are issued from end-stage OA cartilage and therefore exhibit a late-OA phenotype. They produce cytokines, proteases and are poorly responsive to anabolic factors like M1673. The present work showed that adjusting the osmolarity of the culture medium to mimic the osmolarity of more healthy cartilage reduces cytokines production what in turn could lead to an increased expression of BMPRs and an improved responsiveness to M1673. hOAC = human osteoarthritic chondrocytes, BMPR = bone morphogenetic protein receptors.

This hypothesis was investigated in the next section.

5.1.3.6 Responsiveness of hOAC to M1673 at 380 mOsm

From the previous results it was hypothesized that a reduction of cytokine production, which already occurred at 380 mOsm can decrease the cellular stress, enhance the BMPR expression and enable hOAC to respond to M1673. This hypothesis was first tested with only one ECM production marker; the GAG production. Therefore, seven different hOAC donors were investigated for their responsiveness to GDF5 and M1673 by analyzing the GAG production in alginate beads after 14 days at 380 mOsm compared to 340 mOsm (Figure 29). GDF5 and M1673 showed no significant effect on GAG accumulation at 340 mOsm (Figure 29 A). In contrast, GDF5 and M1673 enhanced significantly the GAG concentration within the alginate beads in these hOAC when culturing them at 380 mOsm (Figure 29 B). Thus, a medium osmolarity of 380 mOsm enabled to obtain a more robust and an enhanced effect of GDF5 and M1673 on GAG accumulation of hOAC cultured in alginate beads.

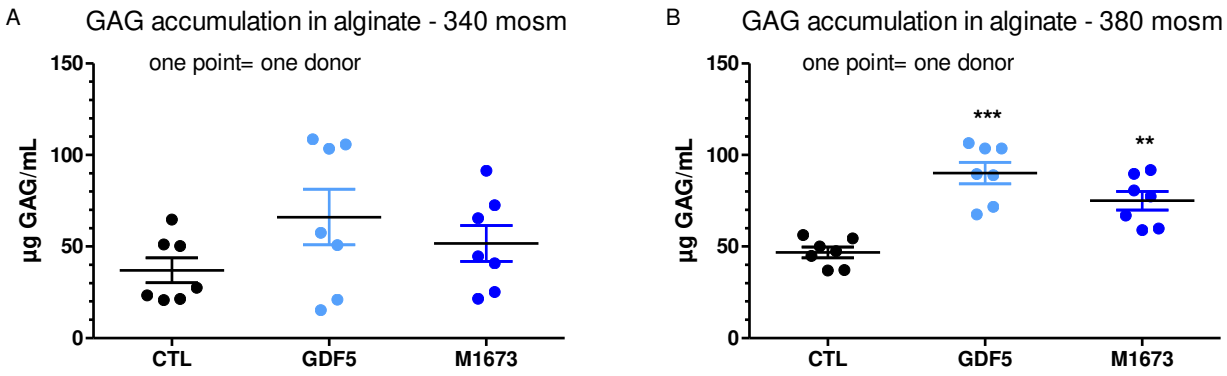

Figure 29 Effect of GDF5 and M1673 on GAG accumulation in hOAC from seven donors at 380 mOsm compared to 340 mOsm. The hOAC were encapsulated in alginate beads and treated over 14 days with 300 ng/ml GDF5 or M1673 or remained untreated (CTL) at 340 mOsm or 380 mOsm. At the end of the culture the GAG concentration in the beads were analyzed. The osmolarity was increased by adding NaCl to the medium. Stars indicate significance over untreated cells (Dunnett comparison, ** and *** means $p<0.01$ or $p<0.001$ respectively). Data represent mean ± SEM.

To characterize the effect of M1673 on hOAC, it was chosen to culture the cells at 380 mOsm.

Indeed, the target cells of a DMOAD like M1673 are OA chondrocytes located in middle-stage OA cartilage. However, the chondrocytes used in the present work were isolated mostly from end-stage cartilage. These end-stage chondrocytes cultured at 380 mOsm instead of 340 mOsm showed reduced OA characteristics corresponding possibly to a shift from end-stage chondrocytes toward middle-stage chondrocytes. On the other hand, using higher osmolarities exacerbate this shift and leads possibly to almost healthy chondrocytes exhibiting low protease and cytokine production. Consequently, it was estimated that 380 mOsm would be the condition enabling to obtain chondrocytes that are the closest to the target cells in comparison to the other tested osmolarities.

5.2 Effect of M1673 on hOAC

Previously, the anabolic effect of the GDF5 mutants M1673, W417F and W417R had been investigated in healthy porcine and bovine chondrocytes. The highest cartilage ECM production was observable after addition of 300 ng/ml M1673, whereas the addition of 300 ng/ml W417F and W417R only led to a weak effect on cartilage production (see supplementary, S6+7). Therefore, only the effect of M1673 was evaluated in hOAC. It was also compared to GDF5. The anabolic effect of 300 ng/ml GDF5 and M1673 on hOAC was analyzed in alginate culture at 380 mOsm as previously defined (Chapter 5.1). After 14 days of culture the proteoglycan synthesis (GAG production and aggrecan expression) and collagen synthesis (hydroxyproline and pro-peptid of collagen 2 content as well as type 2 collagen expression) were evaluated respectively as the two main protein components of the cartilage ECM.

Both, GDF5 and M1673, exerted a strong increase on proteoglycan synthesis in hOAC. On the one hand, the GAG accumulation in alginate beads was enhanced significantly after treatment with GDF5 or M1673 compared to untreated cells. GDF5 treatment led to a 3.8-fold increase, whereas M1673 led to a 2.0-fold increase in GAG concentration over untreated cells (Figure 30 A). On the other hand, the aggrecan expression in alginate beads was significantly increased after treatment with GDF5 by 4.4-fold or M1673 by 2.7-fold over untreated cells (Figure 30 B). The GAG results were confirmed with fourteen other hOAC donors and the results of aggrecan expression with six other hOAC donors (see supplementary, S8).

Moreover, GDF5 and M1673 exerted a strong beneficial effect on collagen synthesis in hOAC. First, the hydroxyproline (HPro) accumulation in alginate beads was significantly increased after GDF5 and M1673 treatment compared to untreated cells, although the fold-increase over control cells was only about 1.2 for both compounds (Figure 30 C). Second, the accumulation of the pro-peptide of collagen 2 (ProC2) was enhanced significantly after treatment with GDF5 or M1673 compared to untreated cells. Similarly, to HPro, the fold-increase over control was only about 1.1 to 1.2 (Figure 30 D). The same trend was confirmed for HPro and ProC2 production with two additional hOAC donors (see supplementary, S9). Third, the type 2 collagen expression in alginate beads increased significantly with GDF5 or M1673 compared to untreated cells. The increase of type 2 collagen expression after GDF5 and M1673 treatment was the strongest of all analyzed cartilage production markers. GDF5 treatment led to a 9.8-fold increase and M1673 treatment to a 4.7-fold increase of type 2 collagen expression over untreated cells (Figure 30 E). Similar results regarding type 2 collagen expression were confirmed with six other hOAC donors (see supplementary, S9).

In summary, the anabolic effect of M1673 was confirmed in hOAC and was similar to the effect observed in bovine and porcine chondrocytes. M1673 showed a strong and significant effect on cartilage ECM production in hOAC, which was similar or slightly lesser than that of GDF5.

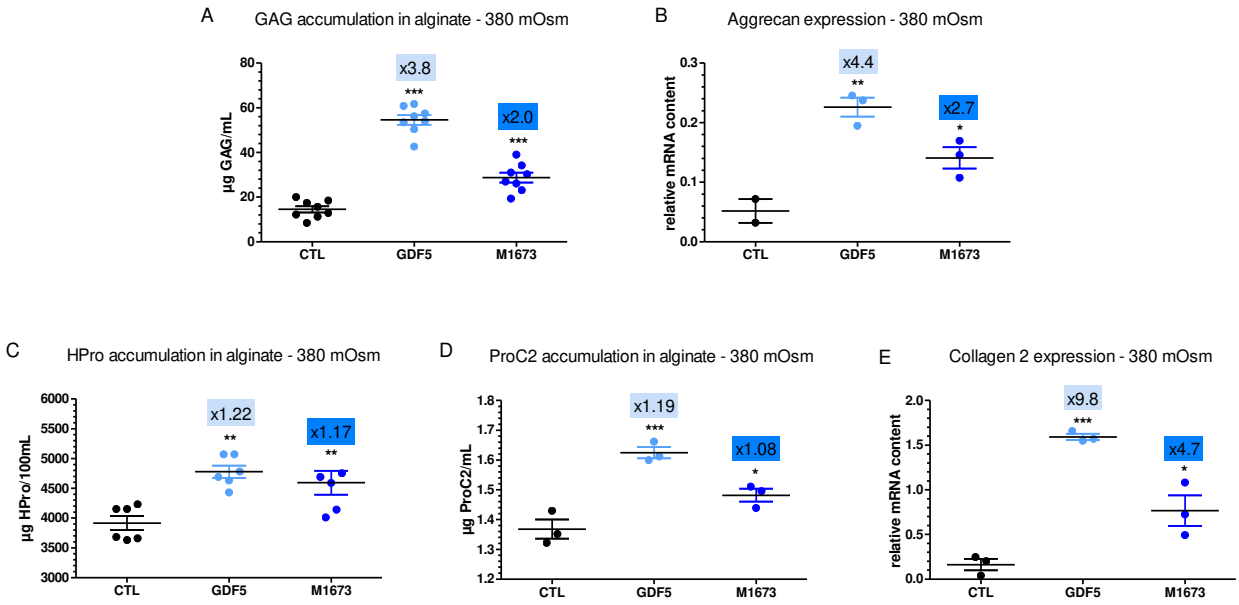

Figure 30 **Anabolic effect of GDF5 and M1673 on ECM synthesis in hOAC at 380 mOsm.** hOAC were encapsulated in alginate beads and treated over 14 days with 300 ng/ml GDF5 or M1673 or left untreated (CTL). At the end of the culture the glycosaminoglycan (GAG) accumulation in the beads (A) and the expression of aggrecan (B) were measured. Additionally, the collagen production was analyzed by measuring hydroxyproline (HPro) accumulation (C) and pro-peptide of collagen 2 (ProC2) accumulation (D) or gene expression of type 2 collagen (E) in the beads. The osmolarity was increased by adding NaCl to the medium. Stars indicate significance over untreated cells (Dunnett comparison, *, ** and *** means $p<0.05$, $p<0.01$ or $p<0.001$ respectively). The x-fold increase of the mean values over untreated cells is described directly on the graph. Data represent mean ± SEM.

There are some indications in the literature that GDF5 also exhibit anti-catabolic characteristics. To investigate if M1673 shows a similar effect, MMP13 and ADAMTS5 expressions were evaluated. The expression of MMP13 and ADAMTS5 was significantly reduced in hOAC after treatment with 300 ng/ml GDF5 and M1673 compared to untreated hOAC. However, M1673 showed a less pronounced reduction of MMP13 and ADAMTS5 expression in comparison to GDF5 (Figure 31 A+B). The results for MMP13 were confirmed with 5 other hOAC donors (see supplementary, S10). Additionally, the expression of the hypertrophic marker type 10 collagen and the dedifferentiation marker type 1 collagen were analyzed, but only in one donor. The expression of type 10 collagen was significantly enhanced with GDF5, but not with M1673 compared to untreated cells. In addition, a significantly reduced type 10 collagen expression was observable with M1673 compared to GDF5 indicating a reduced hypertrophic capacity of M1673 compared to GDF5 in this donor (Figure 31 C). Similarly, the expression of type 1 collagen was significantly enhanced after GDF5 and to a lesser extent after M1673 treatment compared to untreated cells. In addition, a significantly reduced type 1 collagen expression was detected with M1673 compared to GDF5 indicating a reduced dedifferentiation capacity of M1673 compared to GDF5 in this donor (Figure 31 D).

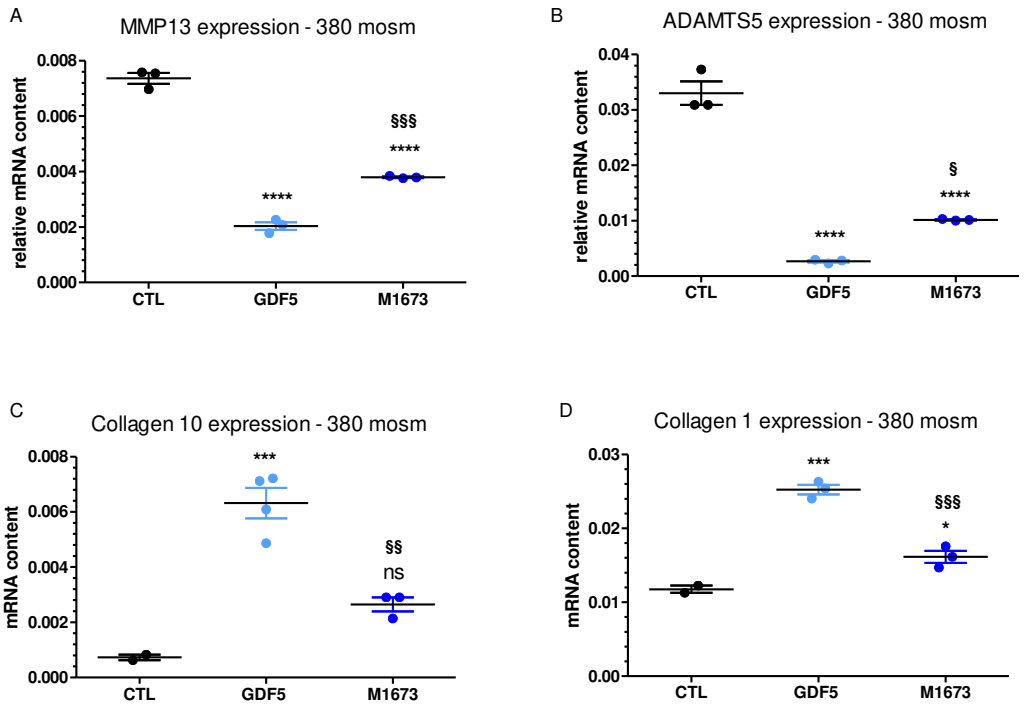

Figure 31 **Effect of GDF5 and M1673 on catabolic, hypertrophic and dedifferentiation markers in hOAC at 380 mOsm.** hOAC were encapsulated in alginate beads and treated over 14 days with 300 ng/ml GDF5 or M1673 or left untreated (CTL). At the end of the culture the gene expression of MMP13 (A), ADAMTS5 (B), type 10 collagen (C) and type 1 collagen (D) was analyzed in the beads. The osmolarity was increased by adding NaCl to the medium. Stars indicate significant differences compared to untreated cells (Dunnett comparison, *, *** and **** means $p<0.05$, $p<0.001$ or $p<0.0001$ respectively). Section signs indicate significant differences compared to GDF5 (Dunnett comparison, §, §§ and §§§ means $p<0.05$, $p<0.01$ or $p<0.001$ respectively). ns = not significant. Data represent mean ± SEM.

In conclusion, it was shown that M1673 exerts an anabolic as well as an anti-catabolic effect on hOAC cultured in alginate beads at 380 mOsm. In addition, it can be suggested that M1673 might have a less hypertrophic capacity than GDF5 in hOAC. These results confirm the therapeutic potential of M1673 as a DMOAD.

5.3 Differentiation capacities of GDF5 mutants in mesenchymal stem cells

Bone morphogenetic proteins (BMPs) induce the formation of cartilage and bone during embryonic development by binding to the BMP receptors BMPR1a or BMPR1b (both type 1 receptors) which dimerize with BMPR2. After binding of BMPs to the BMPR complex, the type 1 receptors initiate the intracellular signal transmission. It is believed that the affinities of the different BMPs towards BMPR1a and BMPR1b influence the differentiation of mesenchymal stem cells (MSCs) into bone or cartilage during skeletal development. However, the distinct roles of BMPR1a and BMPR1b are not completely understood. It is known that BMPR1a is mainly expressed in osteolineage cells and pre-hypertrophic chondrocytes while BMPR1b is mainly expressed at sites were cartilage will be developed. In addition, GDF5 which exhibits a higher affinity for BMPR1b compared to BMPR1a is known to be involved in cartilage formation while BMP2 which exhibit similar affinities for BMPR1b and BMPR1a is involved in bone formation. Thus, the initial hypothesis of this work was that BMPs with a higher binding selectivity to BMPR1b induce chondrogenesis resulting in cartilage formation, while BMPs with a higher binding selectivity to BMPR1a induce chondrocytes hypertrophy and osteogenesis resulting in bone formation. GDF5 mutants were designed by single point mutations in the type 1 receptor binding site of GDF5 to modify the binding affinities to BMPR1a and BMPR1b. Three GDF5 mutants (M1673, W417F, W417R) with a similar affinity to BMPR1b and a lower affinity to BMPR1a were selected for further evaluations. It was hypothesized that these mutants will have a maintained chondrogenic but a reduced hypertrophic and osteogenic capacities in comparison to GDF5. The aim of the following experiments was to verify this hypothesis. BMP2 was used as control for osteogenesis and chondrocyte hypertrophy. In addition, it was aimed to better understand the respective roles of BMPR1a and BMPR1b.

5.3.1 Receptor affinity and bioactivity of GDF5 mutants

As a first step, all GDF5 mutants as well as GDF5 and BMP2 were characterized regarding their receptor affinities and their bioactivity in vitro. The aim of the receptor affinity measurement was to confirm former measurements showing the impact of the mutations on BMPR1a and BMPR1b affinities. In addition, it was evaluated if the binding to BMPR2 was also affected.

The affinity measurements were performed in the molecular interaction laboratory by Andreas Schoenemann. The smaller the KD value, the greater is the binding affinity of the analyzed BMPs for its target receptor. For BMPR2 the lowest binding affinity was detected for BMP2 with a KD of 104 nM. GDF5, M1673 and W417F exhibit similar BMPR2 affinities with KD values of 26.5 nM, 23 nM and 15 nM. For W417R no binding was observed to BMPR2 (Table 7). The highest binding affinity to BMPR1a was obtained for BMP2 with a KD of 119 pM, followed by GDF5 with a KD of 2.1 nM. Among the GDF5 mutants, M1673 showed the highest BMPR1a affinity with a KD value of 12.4 nM followed by W417F with a KD value of 85.9 nM. For W417R no binding was observed to BMPR1a. These results confirm that

the BMPR1a binding affinity was reduced in the GDF5 mutants compared to GDF5 (Table 7). Regarding BMPR1b, the highest binding affinity was obtained for GDF5 (42 pM), followed by BMP2 (72 pM) and the GDF5 mutants. Among the GDF5 mutants, M1673 and W417F exhibit similar affinities for BMPR1b with KD values of 110 and 115 pM, whereas W417R with a KD of 273 pM has a slightly lower BMPR1b affinity (Table 7). By comparing the affinities of the tested compounds for BMPR1a and BMPR1b, it can be noticed that there are large differences among KDs for BMPR1a, whereas the BMPR1b affinities showed smaller variations. To compare the binding affinities of the respective compounds towards BMPR1a compared to BMPR1b, the KD ratio of BMPR1a/BMPR1b was calculated. A high ratio indicates a higher ability of the compound to bind BMPR1b compared to BMPR1a. The GDF5 mutants obtained a higher KD ratio of BMPR1a/BMPR1b compared to GDF5 and showed therefore a higher binding selectivity towards BMPR1b than towards BMPR1a. In detail, W417F has the highest ratio (747), followed by M1673 (113) and GDF5 (50). The $KD_{BMPR1a/BMPR1b}$ ratio for W417R could not be determined, because of the absence of binding to BMPR1a in our experimental setting but this ratio can virtually be considered as being $+\infty$. With 1.7, BMP2 showed the lowest $KD_{BMPR1a/BMPR1b}$ ratio of all tested compounds (Table 7). The calculated KD ratio of BMPR1a/BMPR1b results in a ranking of (W417R)>W417F>M1673>GDF5>BMP2.

Table 7 **Affinity measurements of BMP2, GDF5 and GDF5 mutants for BMPR2, BMPR1a and BMPR1b.** The affinities of BMP2, GDF5 and GDF5 mutants were measured for BMPR2, BMPR1a and BMPR1b by SPR and the KD ratio BMPR1a/BMPR1b was calculated.

	KD BMPR2[pM]	KD BMPR1a [pM]	KD BMPR1b [pM]	KD_{BMPR1a} / KD_{BMPR1b}
BMP2	104000	119	72	1.7
GDF5	26500	2080	42	50
M1673	23000	12400	110	113
W417F	15000	85900	115	747
W417R	Could not be measured	Could not be measured	273	Not determined

In addition to the affinity measurements, the ability of BMP2, GDF5 and GDF5 mutants to bind to their BMP receptors and trigger their dimerization was tested in two dimerization assays. The cells used co-express BMPR2 together with BMPR1a or BMPR1b and were stimulated with different concentrations of BMP2, GDF5 and GDF5 mutants. In these cells, receptor dimerization upon ligand binding results in a luminescent signal.

In each dimerization assay, a dose response curve was performed and the half maximal effective concentration (EC50) was calculated for each compound. Each dose-response curve was done twice. The smaller the EC50 value, the greater is the potency of the compound for receptor dimerization. All compounds increased the dimerization of BMPR1a with BMPR2 in a dose-dependent manner. M1673

and BMP2 behave similarly in both experiments with EC50s of 17.61 and 25.34 ng/ml for M1673 and 19.48 and 16.08 ng/ml for BMP2. GDF5 was less potent with an EC50 of 74.32 ng/ml in the first experiment and 73.38 ng/ml in the second experiment, followed by W417F with an EC50 of 155.7 ng/ml in the first experiment and 207.40 ng/ml in the second experiment. The weakest potency was observed for W417R with EC50s of 1048 and 1434 ng/ml (Figure 32). This results in a ranking for the BMPR1a/BMPR2 receptor dimerization potency of BMP2=M1673>GDF5>W417F>W417R. Interestingly, W417R for which no affinity could be measured with BMPR2 and BMPR1a by SPR, was able to stimulate dimerization of BMPR2 and BMPR1a at high concentrations. It indicates that W417R is still able to interact with BMPR1a and BMPR2. The BMPR1b/BMPR2 dimerization assay showed also a dose-dependent receptor dimerization for all analyzed compounds. M1673 was the most potent molecule with an EC50 value of 6.33 ng/ml obtained in the first experiment and 17.82 ng/ml in the second experiment, followed by BMP2, GDF5, W417F and W417R which all behaved similarly: BMP2 obtained an EC50 of 41.68 and 64.35 ng/ml, GDF5 of 54.32 and 91.11 ng/ml, W417F of 50.21 and 126.7 and W417R of 78.88 and 81.47 ng/ml (Figure 32). This results in a ranking for the BMPR1b/BMPR2 receptor dimerization potency of M1673>BMP2=GDF5=W417F=W417R.

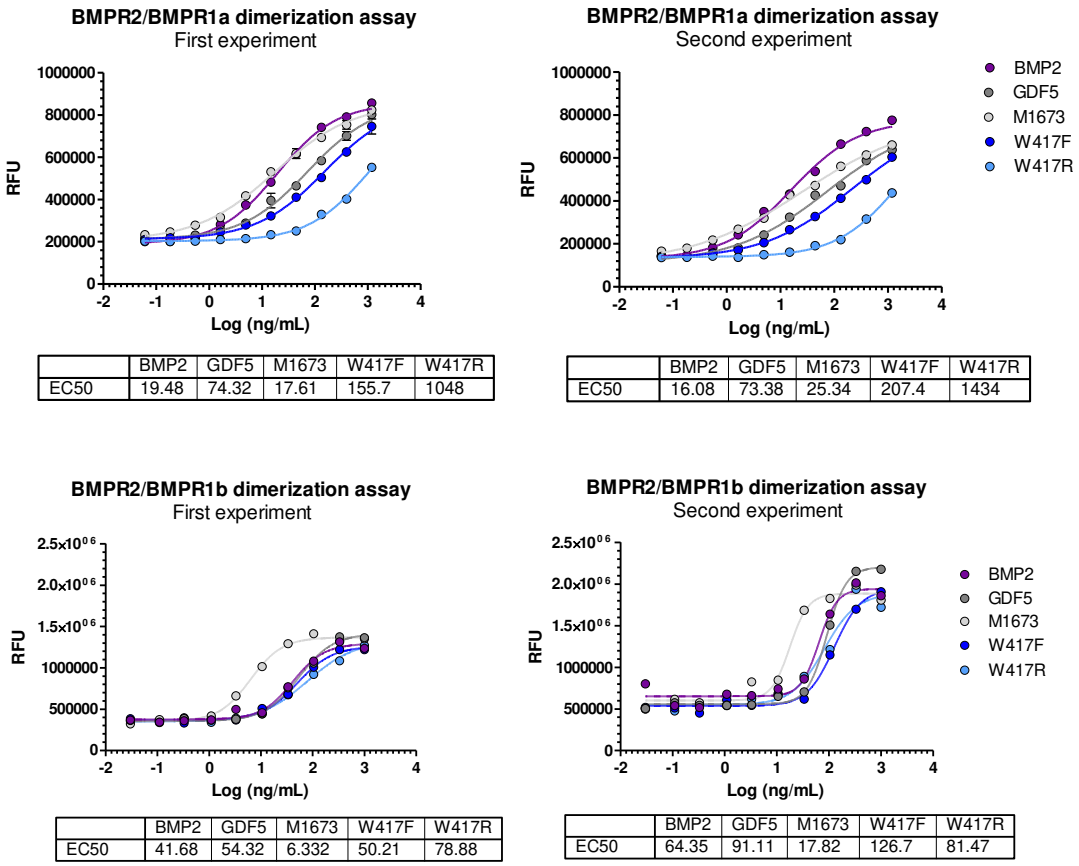

	BMP2	GDF5	M1673	W417F	W417R
EC50	19.48	74.32	17.61	155.7	1048

	BMP2	GDF5	M1673	W417F	W417R
EC50	16.08	73.38	25.34	207.4	1434

	BMP2	GDF5	M1673	W417F	W417R
EC50	41.68	54.32	6.332	50.21	78.88

	BMP2	GDF5	M1673	W417F	W417R
EC50	64.35	91.11	17.82	126.7	81.47

Figure 32 **Ability of BMP2, GDF5 and GDF5 mutants to bind to their receptors and activate dimerization of type 1 and type 2 BMPRs in a cell assay.** BMP2, GDF5 and GDF5 mutants were tested in the BMPR1a/BMPR2 and BMPR1b/BMPR2 dimerization assays. The cells which co-express BMPR2 together with BMPR1a or BMPR1b, were stimulated with different concentrations of the compounds and the developed chemiluminescence signal was analyzed. EC50 values were calculated and reported directly on the graphs. Experiments were repeated twice. RFU = relative fluorescence unit.

In both cell assays, the potencies obtained result to a ranking that is different than the ranking obtained for the affinities for BMPR1a and BMPR1b by SPR. This discrepancy can be due to the difference between the assay systems.

The average of each EC50 from the two experiments and the ratio $EC50_{BMPR1a/BMPR2}/EC50_{BMPR1b/BMPR2}$ (referred as EC50 ratio later in the text) were calculated (Table 8). A higher ratio indicates a higher ability to dimerize BMPR2 with BMPR1b than with BMPR1a. With an EC50 ratio of 0.3, BMP2 was the only compound with a ratio lower than one indicating a higher ability to dimerize BMPR2 with BMPR1a than BMPR1b. GDF5 had a ratio of 1 indicating the comparable ability to dimerize BMPR1a and BMPR1b with BMPR2. Finally, the GDF5 mutants had all ratios higher than 1: M1673 had a ratio of 1.8 followed by W417F with 2 and W417R with 15 indicating that they all have a higher ability to dimerize BMPR2 with BMPR1b than with BMPR1a.

Table 8 **EC50s of BMP2, GDF5 and GDF5 mutants for BMPR1a/BMPR2 and BMPR1b/BMPR2.** The receptor dimerization potency of BMP2, GDF5 and GDF5 mutants were analyzed for BMPR2 together with BMPR1a or BMPR1b. Each receptor dimerization assay was done twice and the mean values of both experiments were calculated respectively. The ratio $EC50_{BMPR1a/BMPR2}/EC50_{BMPR1b/BMPR2}$ of these mean values was calculated.

	EC50 BMPR1a/BMPR2 [ng/ml]	EC50 BMPR1b/BMPR2 [ng/ml]	$EC50_{BMPR1a/BMPR2}/EC50_{BMPR1b/BMPR2}$
BMP2	16.6	52	0.3
GDF5	73	72	1
M1673	21.5	12	1.8
W417F	177	88	2
W417R	1200	79	15

When comparing the potencies obtained with the various compounds, it can be noticed that there are large differences in the EC50s for BMPR1a/BMPR2, whereas the EC50s for BMPR1b/BMPR2 varied less between the tested compounds (Table 8). These observation is in accordance to the results of the affinity measurements (Table 7).

Despite some discrepancies regarding single KDs and EC50s, the ratio of EC50s resulted in the same ranking than the ratio of KDs with (W417R)>W417F>M1673>GDF5>BMP2. This ranking indicates a higher specificity of the GDF5 mutants to BMPR1b than to BMPR1a followed by GDF5 and BMP2. Therefore, the mutations performed on the GDF5 molecule successfully increased the selectivity towards BMPR1b binding in comparison to GDF5. Based on the initial hypothesis that BMPs with a higher binding selectivity to BMPR1b induce chondrogenesis, while BMPs with a higher binding selectivity to BMPR1a induce hypertrophy and osteogenesis, the GDF5 mutants should exhibit a similar chondrogenic but reduced hypertrophic and osteogenic capacities than GDF5. In this regard W417R should be the GDF5 mutant showing the most reduced hypertrophic and osteogenic properties. On the other hand, BMP2 should exert a strong hypertrophic and osteogenic effect in addition to its chondrogenic effect.

5.3.2 Effect of GDF5 mutants on chondrogenesis and osteogenesis in murine MSCs

The chondrogenic and osteogenic capacities of the GDF5 mutants were analyzed in the murine stem cell line C3H10T1/2 and compared to GDF5 and BMP2. As a first step, the murine stem cell line was tested for the presence of BMPRs at the gene expression and protein level by qRT-PCR and western blot analysis. BMPR1a and BMPR2 showing comparable expression levels while the expression of BMPR1b was significantly lower compared to BMPR1a and BMPR2 (Figure 33 A). At the protein level, both BMPR1a and BMPR1b were detectable in C3H10T1/2 cells. In accordance to the gene expression analysis, the protein level of BMPR1b appeared lower than that of BMPR1a (Figure 33 B).

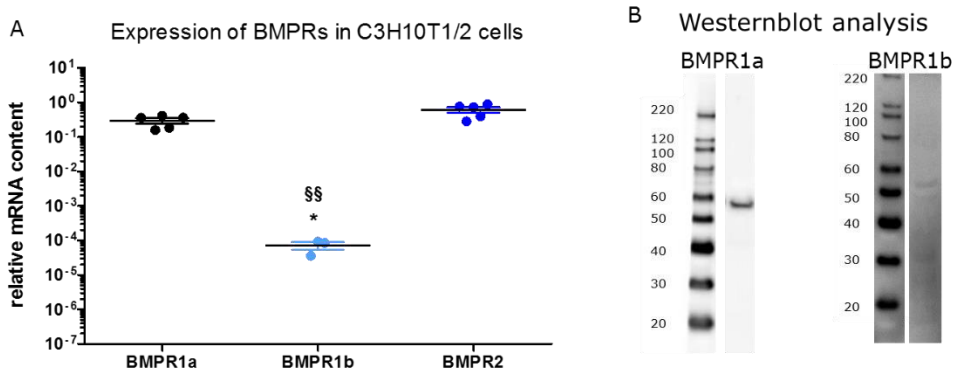

Figure 33 **BMPR analysis in the murine stem cell line C3H10T1/2 at the gene expression and protein level.** The gene expressions of BMPR1a, BMPR1b and BMPR2 were measured in C3H10T1/2 cells (A). In addition, the presence of BMPR1a and BMPR1b in C3H10T1/2 cells was analyzed at the protein level by western blot analysis (B). Stars and section signs indicate significance over BMPR1a or BMPR2 respectively (Dunnett comparison, * means $p<0.05$, whereas §§ means $p<0.01$). Data represent mean ± SEM.

In summary, the presence of the BMPRs responsible for signal transmission of BMPs were confirmed in C3H10T1/2 cells. Next, the GDF5 mutants were tested for their chondrogenic/hypertrophic and osteogenic properties in C3H10T1/2 cells and compared to GDF5 and BMP2.

5.3.2.1 Ability of GDF5 mutants to stimulate chondrogenesis and hypertrophy in murine MSCs

Chondrogenic induction of the murine stem cell line C3H10T1/2 was performed in a pellet culture system with one million cells/pellet. The cells were cultivated in a chondrogenic medium including several essential substances for chondrogenic induction of MSCs (see methods, chapter 4.2.4) and were stimulated with 300 ng/ml BMP2, GDF5 and GDF5 mutants or remained unstimulated over 28 days. On a weekly basis, cell and medium samples were analyzed for several differentiation markers. Type 2 collagen and aggrecan expression are chondrogenic differentiation markers, while type 10 collagen expression and ALP concentration are hypertrophic differentiation markers. In addition, for gene expression analysis cell samples were taken before starting the culture to analyze the initial expression profile of the murine MSCs (defined as day 0).

The stimulation of murine MSCs with BMP2 and GDF5 resulted in an enhanced gene expression of type 2 collagen at 14 and 21 days for GDF5 and at 7 days for BMP2 compared to day 0. Unfortunately, for

GDF5 no RNA could be isolated at day 7 and the gene expression data are missing for this time point. M1673 stimulated the type 2 collagen expression at day 7 and day 14 compared to day 0. Type 2 collagen expression was significantly lesser pronounced with M1673 than with GDF5 at day 14 and day 21. On the contrary to BMP2, GDF5 and M1673, the stimulation of murine MSCs with W417F only led to a slightly enhanced type 2 collagen expression, while no effect was observed on type 2 collagen expression after W417R stimulation compared to day 0 (Figure 34 A). Similarly, the aggrecan expression was enhanced after stimulation with BMP2 and GDF5 for 14, 21 and 28 days compared to the initial expression at day 0. The treatment with M1673 led to a strong upregulation of aggrecan expression at all analyzed time points compared to day 0, but to a significantly lesser extent than observed with GDF5 stimulation. The stimulation with W417F resulted in a significantly reduced aggrecan expression compared to M1673. No effect was observable after W417R stimulation on aggrecan expression compared to day 0 (Figure 34 B).

In summary, GDF5 showed the highest chondrogenic capacity followed by M1673, BMP2 and W417F. BMP2 was ranked after M1673 because of its lower type 2 collagen expression. W417R showed no chondrogenic effect in C3H10T1/2 cells.

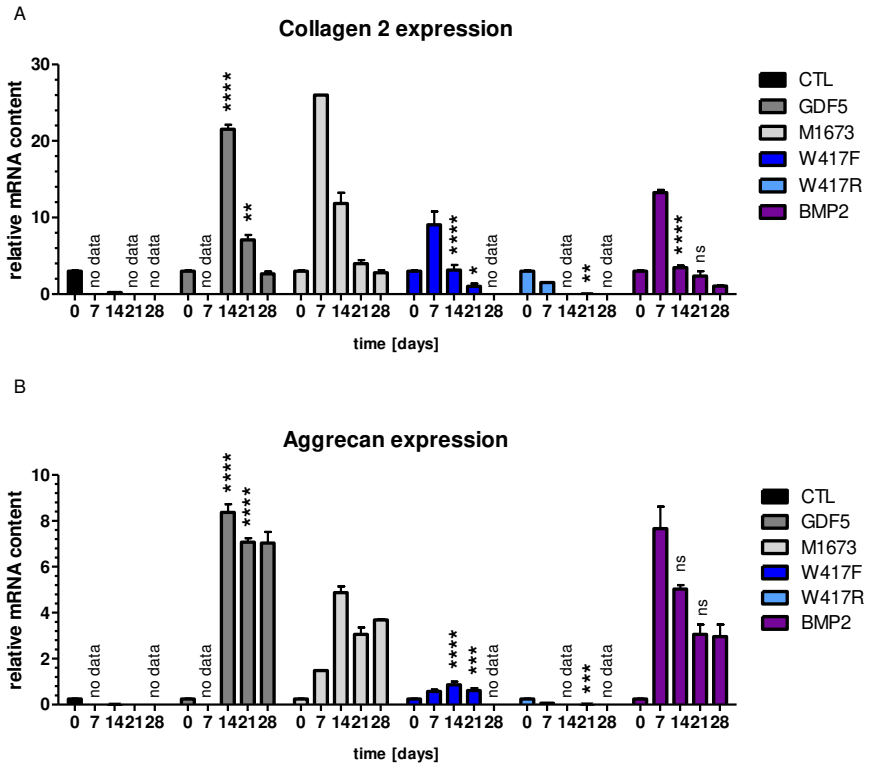

Figure 34 **Analysis of chondrogenic markers in murine MSCs cultured in chondrogenic medium in the absence or presence of BMP2, GDF5 and GDF5 mutants over 28 days.** The murine stem cell line C3H10T1/2 was cultured in a pellet culture system and treated with 300 ng/ml BMP2, GDF5, M1673, W417F, W417R or left untreated (CTL) over 28 days. On a weekly basis, cell samples were analyzed for the type 2 collagen (A) and aggrecan (B) expression. GDF5, W417F and BMP2 were compared to M1673 for days 14 and 21 using a 2-way ANOVA (at days 7 and 28 data are missing and the analysis could not be done). W417R was compared to M1673 at day 21 using a 1-way ANOVA (at day 14 data are missing and analysis could not be done). Stars indicate significance over M1673 with *, **, *** and **** means $p<0.05$, $p<0.01$, $p<0.001$ or $p<0.0001$ respectively. ns= not significant. Data represent mean ± SEM.

While BMP2, GDF5 and M1673 all strongly activated chondrogenesis in murine MSCs, only BMP2 strongly upregulated the expression of the hypertrophic marker type 10 collagen. The expression of type 10 collagen increased after 7 days in the presence of BMP2 compared to day 0 and subsequently decreased with time over 28 days. GDF5 and M1673 also upregulated the type 10 collagen expression, but in a lesser extend in comparison to BMP2. In addition, the expression of type 10 collagen was significantly lower with M1673 compared to GDF5. W417F and W417R showed hardly any type 10 collagen expression (Figure 35 A). Similarly, only the treatment with BMP2 strongly enhanced the ALP concentration in medium in a time-dependent manner over 28 days, but not the treatment with GDF5, M1673, W417F or W417R (Figure 35 B).

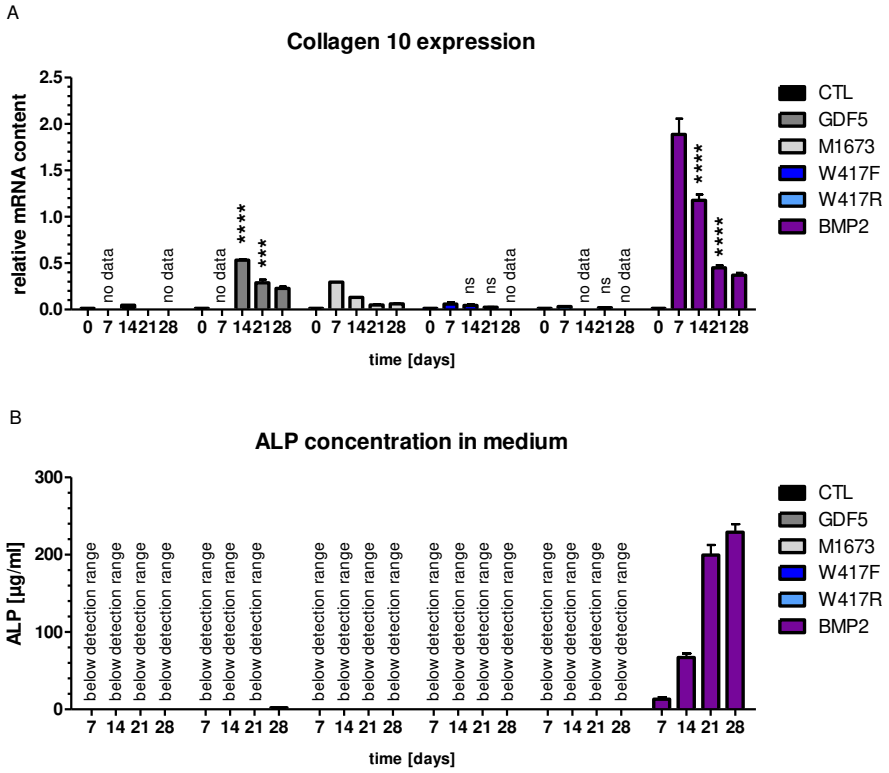

Figure 35 Analysis of hypertrophic markers in murine MSCs cultured in chondrogenic medium in the absence or presence of BMP2, GDF5 and GDF5 mutants over 28 days. The murine stem cell line C3H10T1/2 was cultured in a pellet culture system and treated with 300 ng/ml BMP2, GDF5, M1673, W417F, W417R or left untreated (CTL) over 28 days. On a weekly basis, cell and medium samples were analyzed for the type 10 collagen expression (A) and ALP concentration in medium (B). Regarding gene expression, GDF5, W417F and BMP2 were compared to M1673 for days 14 and 21 using a 2-way ANOVA (at days 7 and 28 data are missing and the analysis could not be done). W417R was compared to M1673 at day 21 using a 1-way ANOVA (at day 14 data are missing and analysis could not be done). Stars indicate significance over M1673 with *** and **** means $p<0.001$ or $p<0.0001$ respectively. ns= not significant. Data represent mean ± SEM.

Taken together, GDF5, M1673 and BMP2 induced chondrogenesis but only BMP2 strongly induced hypertrophy. Both GDF5 and M1673 showed only a weak effect on type 10 collage expression with M1673 showing the smallest stimulation. W417F had a reduced ability to stimulate chondrogenesis in comparison to GDF5 or M1673 and had no effect on hypertrophy. W417R showed no effect at all.

In the light of those results, the initial hypothesis that BMPs, with a higher binding selectivity towards BMPR1b induce chondrogenesis, while BMPs with a higher binding selectivity to BMPR1a promote hypertrophy and osteogenesis had to be refined. BMPR1b signaling alone is not sufficient to stimulate chondrogenesis. Indeed, W417F and W417R, both having a BMPR1b affinity comparable to M1673, but a strongly reduced BMPR1a affinity, showed a diminished or even no chondrogenic capacity. This indicates that BMPR1a activation is necessary for the induction of chondrogenesis. On the other hand, compounds with a higher BMPR1a/BMPR1b ratio seems to prevent hypertrophic differentiation.

To better illustrate this, the ratio of collagen 2/10 (chosen as respective markers for chondrogenesis and hypertrophy) was plotted against the EC50 ratio of BMPR1a/BMPR1b. A lower EC50 ratio corresponds to a lower ratio of collagen 2/10 expression. For instance, BMP2 with a very low EC50 ratio of BMPR1a/BMPR1b showed an increased hypertrophic differentiation but only a moderate chondrogenesis compared to GDF5 and M1673. On the contrary, M1673 with a higher EC50 ratio of BMPR1a/BMPR1b was more chondrogenic than hypertrophic. W417F and W417R with a high EC50 ratio of BMPR1a/BMPR1b but a strongly reduced BMPR1a affinity showed a diminished or even lost its chondrogenic capacity (Figure 36).

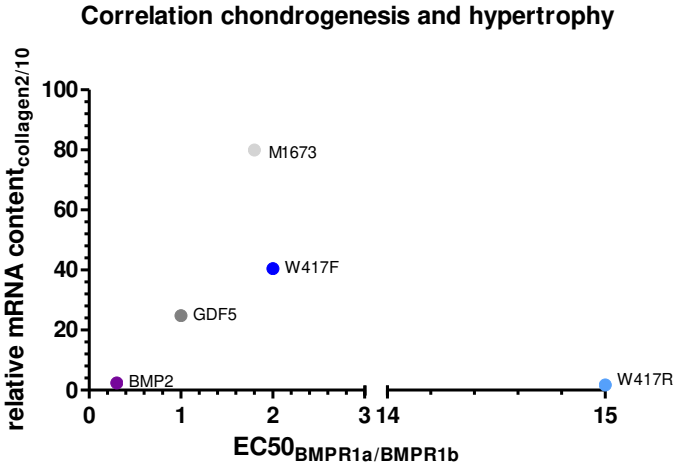

Figure 36 Correlation between the expression ratio of collagen 2/10 and the EC50 ratio of BMPR1a/BMPR1b after treatment with BMP2, GDF5 and GDF5 mutants in murine MSCs cultured for 21 days in chondrogenic medium. The murine stem cell line C3H10T1/2 was cultured as pellets and treated with 300 ng/ml BMP2, GDF5, M1673, W417F and W417R in chondrogenic medium for 21 days. The expression ratio of collagen 2/10 was plotted against the EC50 ratio of BMPR1a/BMPR1b for the respective compounds.

5.3.2.2 Ability of GDF5 mutants to stimulate osteogenesis in murine MSCs

In addition to the chondrogenic and hypertrophic capacities of the GDF5 mutants, their ability to stimulate osteogenesis was compared to GDF5 and BMP2. Osteogenesis of the murine stem cell line C3H10T1/2 was performed in monolayer cultures. After reaching confluence, the cells were cultured and treated with 300 ng/ml BMP2, GDF5 and GDF5 mutants or remained untreated over 28 days. To analyze the osteogenic properties of the compounds, they were cultured in a standard culture medium. On a weekly basis, cell and medium samples were analyzed for the presence of osteogenic markers. The

concentration of ALP was used as an early osteogenic marker, whereas the expression of osteocalcin was used as a late-stage osteogenic marker. In addition, alizarin red staining of the cells was analyzed as a marker for calcium deposition occurring at later stages of osteogenesis. Regarding gene expression analysis, cell samples were also taken before starting the culture to analyze the initial expression profile of the murine MSCs (defined as day 0).

Only the stimulation with BMP2 resulted in an upregulation of ALP concentration in medium at all time points (Figure 37 B). Simultaneously the expression of osteocalcin was enhanced at all time points after stimulation with BMP2 compared to day 0, but not with GDF5, GDF5 mutants or in unstimulated cells (Figure 37 A). In contrast, the alizarin red staining was negative with all compounds at all tested time points (Figure 37 C).

Taken together these results indicate that, as expected, GDF5 and GDF5 mutants showed no osteogenic induction potential in murine MSCs cultivated in the standard culture medium. In contrast, the stimulation with BMP2 resulted in the upregulation of some osteogenic markers. However, a complete osteogenesis was not achieved as no alizarin red staining was detectable.

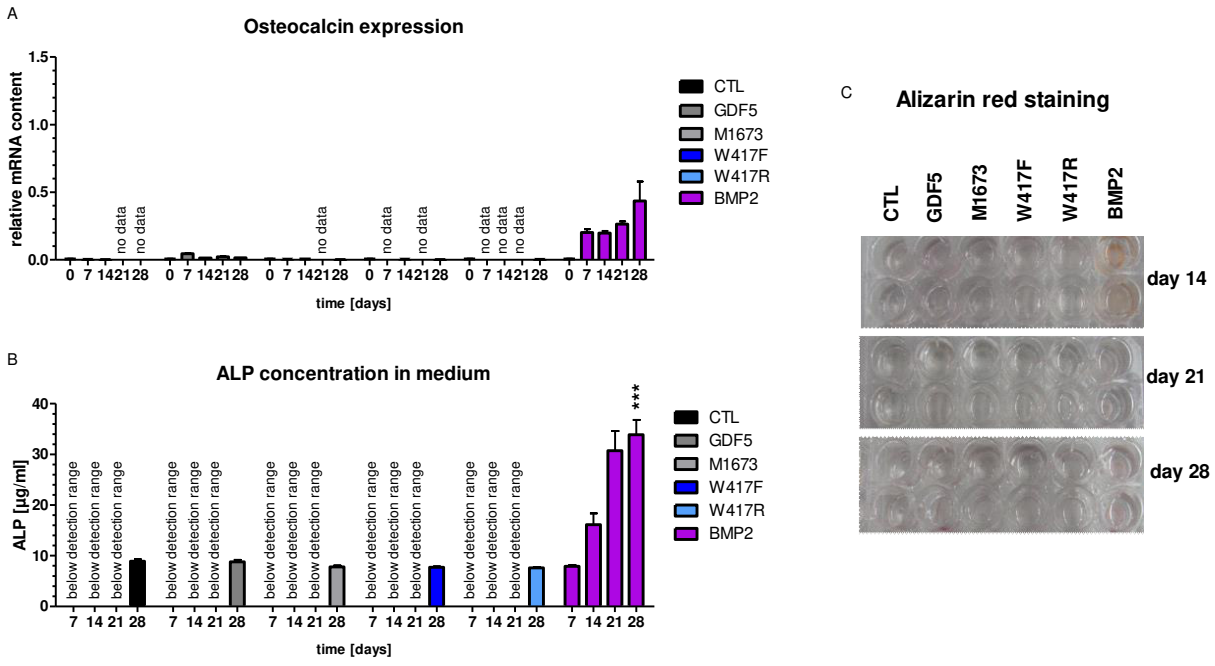

Figure 37 Analysis of osteogenic markers in murine MSCs cultured in standard culture medium in the absence or presence of BMP2, GDF5 and GDF5 mutant over 28 days. The murine stem cell line C3H10T1/2 was cultured until reaching confluence in monolayer and afterwards treated with 300 ng/ml BMP2, GDF5, M1673, W417F, W417R or left untreated (CTL) over 28 days. On a weekly basis, cell and medium samples were analyzed for the osteocalcin expression (A), ALP concentration in medium (B) as well as for alizarin red staining of the cells (C). The osteocalcin expression after stimulation with GDF5, M1673 and W417F was compared to BMP2 for days 14 and 28 using a 2-way ANOVA (at days 7 and 21 data are missing and the analysis could not be done). W417R was compared to BMP2 at day 28 using a 1-way ANOVA (at day 7, 14 and 21 data are missing and analysis could not be done). No significant differences were detectable. Regarding ALP concentration, statistical analysis was performed at day 28 using a 1-way ANOVA. Stars indicate significance of BMP2 over the other compounds with *** means $p<0.001$. Data represent mean ± SEM.

To further analyze the impact of GDF5 mutants compared to GDF5 and BMP2 on osteogenesis in murine MSCs, the cells were cultured as described before, but in an osteogenic medium containing several essential substances for osteogenic induction of MSCs in vitro (see methods, chapter 4.2.3). On a weekly basis, cell and medium samples were analyzed for the presence of osteogenic markers. As in the previous experiment, ALP concentration, osteocalcin expression and alizarin red staining were measured as osteogenic markers. In addition, microscopic images of the cells were recorded. Regarding gene expression analysis, cell samples were also taken before starting the culture to analyze the initial expression profile of the murine MSCs (defined as day 0).

Osteogenesis of murine MSCs was the strongest with BMP2 treatment (Figure 38). The expression of osteocalcin was strongly upregulated after BMP2 treatment compared to day 0 and unstimulated cells. The stimulation with GDF5 resulted in a less pronounced upregulation of osteocalcin expression compared to BMP2 and no effect on osteocalcin expression was detectable with M1673, W417F and W417R (Figure 38 A). The concentration of ALP in medium was only detectable with BMP2, but not with GDF5 or GDF5 mutants (Figure 38 B). In addition, the alizarin red staining was analyzed. An alizarin red staining of murine MSCs cultured in osteogenic medium was not detectable at the beginning of the experiment (day 0) and after 7 days of culture (data not shown). However, an alizarin red staining could be detected after 14 days in presence of BMP2, after 21 days in presence of GDF5 and only after 28 days in the presence of M1673 and W417F (Figure 38 C). The delayed apparition of the alizarin red staining with GDF5 compared to BMP2 and with M1673 and W417F compared to GDF5 indicate a delayed mineralization of the cells. No alizarin red staining could be seen in the presence of W417R and in control cells cultured in osteogenic medium without stimulation (Figure 38 C).

The ranking of the tested compounds for their capacity to induce osteogenesis in murine MSCs is in accordance with their BMPR1a/BMPR1b ratios: BMP2<GDF5<M1673<W417F<W417R. A higher BMPR1a/BMPR1b ratio indicating a higher specificity towards BMPR1b compared to BMPR1a resulted in a reduced osteogenicity of the compounds.

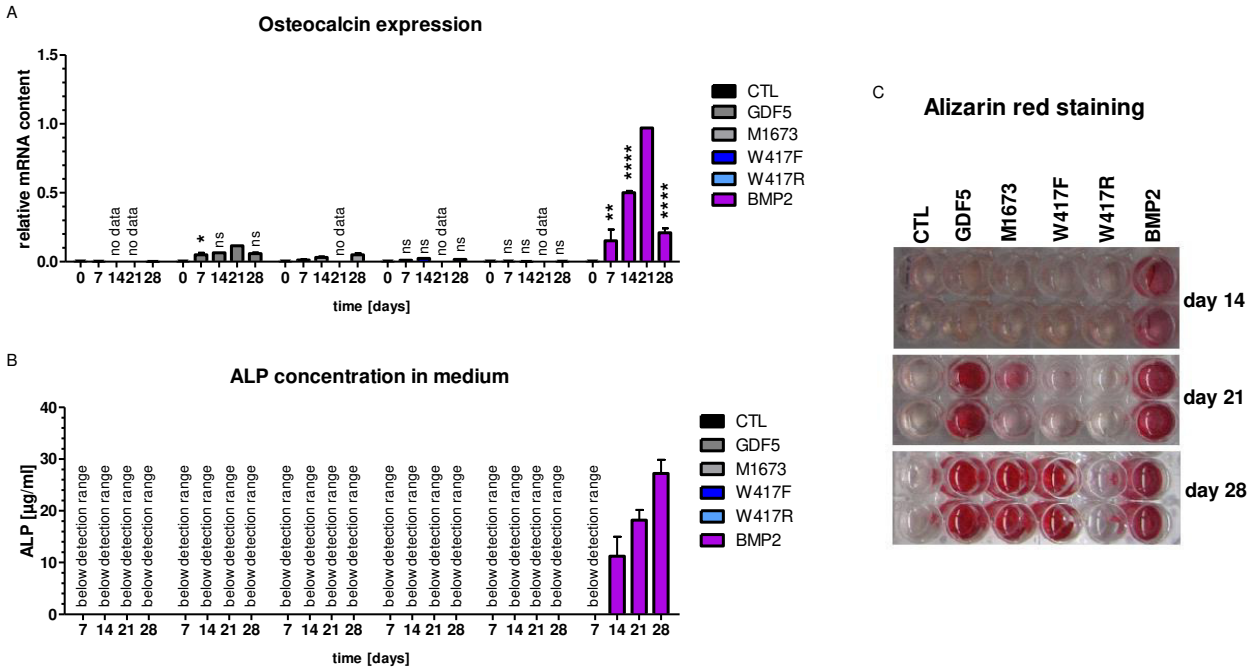

Figure 38 **Analysis of osteogenic markers in murine MSCs cultured in osteogenic medium in the absence or presence of BMP2, GDF5 and GDF5 mutants over 28 days.** The murine stem cell line C3H10T1/2 was cultured until reaching confluence in monolayer and afterwards treated with 300 ng/ml BMP2, GDF5, M1673, W417F, W417R or left untreated (CTL) over 28 days. On a weekly basis, cell and medium samples were analyzed for osteocalcin expression (A) as well as ALP concentration in medium (B) and alizarin red staining of the cells (C). Regarding osteocalcin expression GDF5, W417F, W417R and BMP2 were compared to M1673 for days 7, 14 and 28 using a 2-way ANOVA (at day 21 data are missing and the analysis could not be done). Stars indicate significance over M1673 with *, ** and **** means $p<0.05$, $p<0.01$ or $p<0.0001$ respectively. ns = not significant. Data represent mean ± SEM.

The delayed mineralization of the murine MSCs in presence of GDF5 mutants compared to GDF5 was also observable by looking at the cell morphology. In general, the cells were already over-confluent at day 21 and 28 resulting on the one hand in a changed cell morphology from a fibroblastic to a polygonal cell shape and on the other hand in a cell grew on the top. It was striking that the cells formed black aggregates at day 21 and 28 indicating mineralization of the cells. The mineralization was observable after 21 days of BMP2 treatment and to a lesser extent after 21 days of GDF5 treatment, but not in the presence of M1673, W417F, W417R or in untreated cells at day 21 (Figure 39). After 28 days, a strong mineralization was observable with BMP2 and GDF5 and to a lesser extent in the presence of M1673 and W417F, but not in W417R stimulated cells or in control cells cultured in osteogenic medium without stimulation (Figure 39).

These observations are in accordance with the alizarin red staining and confirmed a delayed mineralization with the GDF5 mutants compared to GDF5 and BMP2. Thus, an earlier mineralization and induced osteogenesis could be confirmed for the compounds having a lower BMPR1a/BMPR1b ratio.

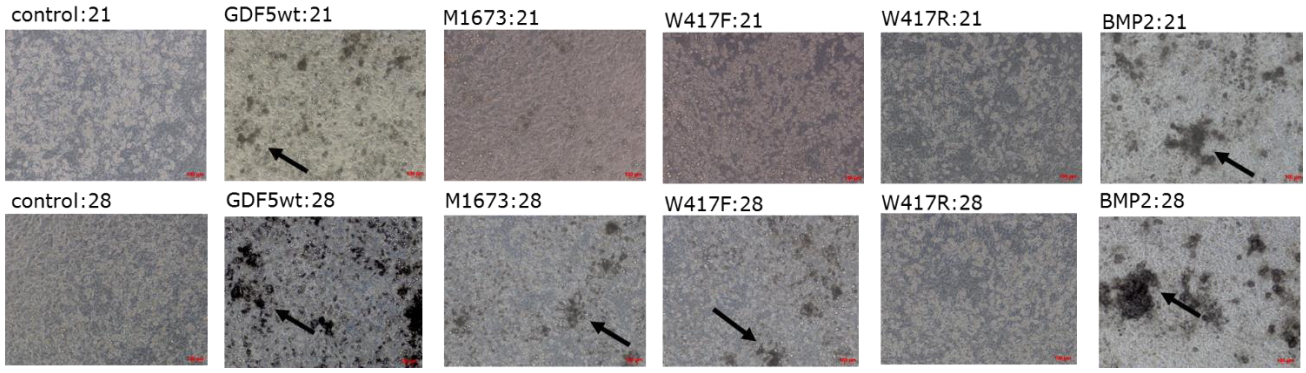

Figure 39 Representative microscopic images of murine MSCs cultured in osteogenic medium in the absence or presence of BMP2, GDF5 and GDF5 mutants for 21 and 28 days. The murine stem cell line C3H10T1/2 was cultured until reaching confluence in monolayer and remained untreated (control) or treated with 300 ng/ml BMP2, GDF5, M1673, W417F, W417R or left untreated (control) over 28 days. After 21 (:21) and 28 (:28) days, microscopic images of the cells were recorded (10X objective, scale bar 100 µm). Clear morphological changes (formation of black aggregates) were marked by arrows indicating mineralization of the cells.

Overall, it was shown that BMP2 exhibits strong osteoinductive properties in murine MSCs even in the absence of osteogenic inductors in the culture medium. Osteogenesis of murine MSCs cultured in osteogenic medium was also the strongest in the presence of BMP2, followed by GDF5, M1673 and W417F. The addition of W417R did not induce osteogenesis in murine MSCs. Therefore, it could be demonstrated that the GDF5 mutants exhibit a lower osteogenicity compared to GDF5 and BMP2.

In combination with the results from the chondrogenic induction in murine MSCs, it was shown that a sufficient binding towards BMPR1a is necessary for both chondrogenesis and osteogenesis. Indeed, W417R which has the lowest affinity for BMPR1a had no effect on both chondrogenic and osteogenic differentiation. Given that the BMPR1a signaling is sufficient, the ratio of BMPR1a/BMPR1b signaling seems to drive chondrogenic and hypertrophic differentiation and not the single binding for BMPR1a or BMPR1b as originally hypothesized. Regarding osteogenesis, a correlation could be also found between the osteogenic stimulation and the BMPR1a/BMPR1b ratio indicating that compounds with a higher BMPR1a/BMPR1b ratio delay osteogenic differentiation.

As a conclusion compounds with a lower BMPR1a/BMPR1b ratio will be more osteogenic, as BMP2, and compounds with a higher BMPR1a/BMPR1b ratio and a sufficient BMPR1a affinity, as M1673, will be more chondrogenic, less hypertrophic and will tend to prevent osteogenesis.

5.3.3 Effect of GDF5 mutants on chondrogenesis and osteogenesis in human MSCs

To confirm the results obtained with the murine mesenchymal stem cell line, chondrogenesis and osteogenesis were also evaluated in human MSCs. As a first step, the expression of BMPRs in human MSC was evaluated at the gene expression and protein level by qRT-PCR and western blot analysis. The BMPR1a and BMPR2 expression levels were comparable, whereas the gene expression of BMPR1b was significantly lower compared to that of BMPR1a and BMPR2 (Figure 40 A). The same was observed at the protein level. BMPR1a and BMPR1b were detectable by western blot analysis, but in accordance to

the gene expression analysis the protein level of BMPR1b appeared lower compared to BMPR1a (Figure 40 B).

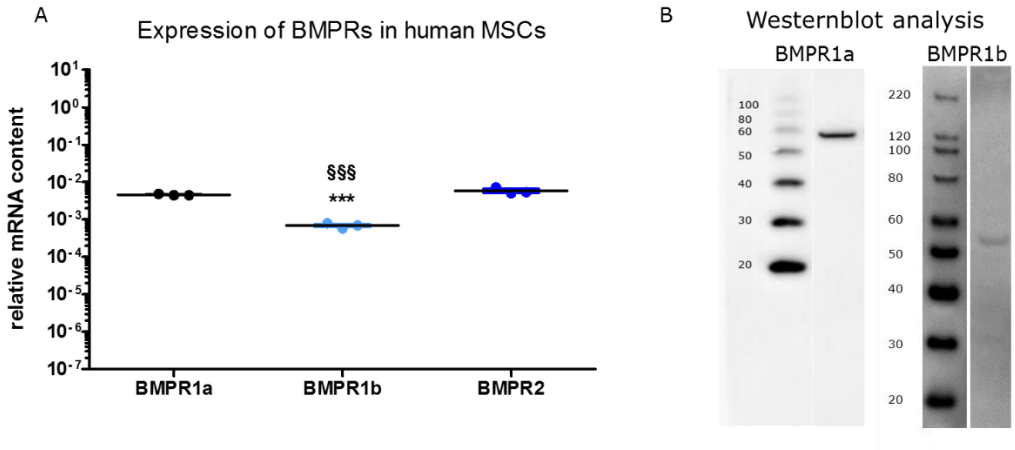

Figure 40 **BMPR analysis in human MSCs at the gene expression and protein level.** The gene expressions of BMPR1a, BMPR1b and BMPR2 were measured in human MSCs (A). In addition, the presence of BMPR1a and BMPR1b in human MSCs was analyzed at the protein level by western blot analysis (B). Stars and section signs indicate significance over BMPR1a or BMPR2 respectively (Dunnett comparison, *** and §§§ means $p<0.001$). Data represent mean ± SEM.

In summary, the presence of the different BMPRs were confirmed in human MSCs. Next, the GDF5 mutants were tested for their chondrogenic/hypertrophic and osteogenic properties in human MSCs and compared to GDF5 and BMP2.

5.3.3.1 Ability of GDF5 mutants to stimulate chondrogenesis and hypertrophy in human MSCs

To induce chondrogenesis, a pellet culture system with one million cells/pellet was used. The cells were cultured in chondrogenic medium and were stimulated with 300 ng/ml BMP2, GDF5 and GDF5 mutants or remained unstimulated over 28 days as described before for the murine MSCs. However, no chondrogenic differentiation of human MSCs was observed (data not shown). To enhance chondrogenesis in human MSCs, the same experiment was repeated, but in the presence of 10 ng/ml TGFβ3. On a weekly basis, cell and medium samples were analyzed for several differentiation markers: Type 2 collagen and aggrecan expression, Safranin O staining and type 2 collagen immunohistochemistry as chondrogenic differentiation markers and type 10 collagen expression, ALP concentration and type 10 collagen immunohistochemistry as hypertrophic differentiation markers.

The expression of type 2 collagen and aggrecan was significantly enhanced in the presence of 10 ng/ml TGFβ3 compared to unstimulated cells in chondrogenic medium. Unfortunately, the combination of 10 ng/ml TGFβ3 with 300 ng/ml GDF5, GDF5 mutants or BMP2 resulted in type 2 collagen expression levels, which were comparable to that detected in the presence of 10 ng/ml TGFβ3 (Figure 41 A). Similarly, the type 2 collagen staining was negative in control cells indicating that these cells did not undergo chondrogenesis while it was positive with TGFβ3 alone or in combination with BMP2, GDF5 or GDF5 mutants but comparable to each other (Figure 41 D). Regarding the expression of aggrecan

significant differences were detected with TGFβ3, GDF5+TGFβ3, M1673+TGFβ3 and W417F+TGFβ3 compared to BMP2+TGFβ3 at day 28 (Figure 41 B). However, the Safranin O staining was similar after the stimulation with TGFβ3 alone or in combination with BMP2, GDF5 or GDF5 mutants (Figure 41 C). Thus, it could be demonstrated that TGFβ3 strongly induced chondrogenesis in human MSCs but no additional induction could be observed with BMP2, GDF5 or the GDF5 mutants under the chosen concentration of TGFβ3. It was hypothesized that the effects of the compounds were shielded by TGFβ3. Consequently, the influence of BMP2, GDF5 and GDF5 mutants on chondrogenesis in human MSCs could not be analyzed.

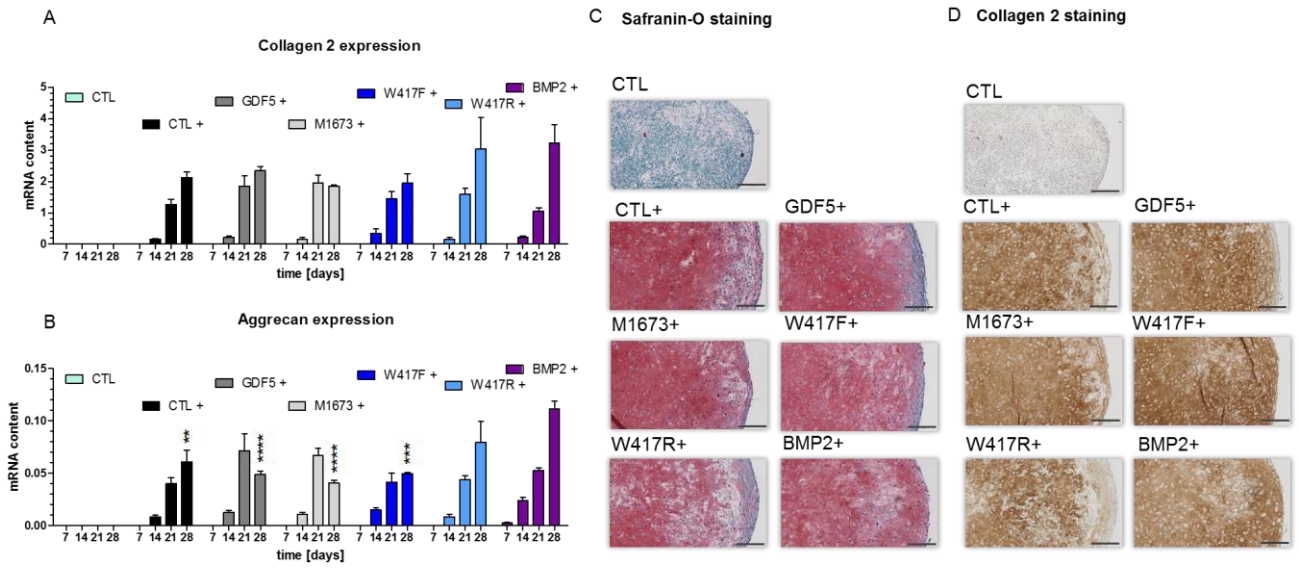

Figure 41 Analysis of chondrogenic markers in human MSCs cultured in chondrogenic medium in the absence or presence of TGFβ3 or in the presence of TGFβ3 with BMP2, GDF5 or GDF5 mutants over 28 days. Human MSCs were cultured in a pellet culture system and treated with 300 ng/ml BMP2, GDF5, M1673, W417F, W417R or left untreated (CTL) over 28 days in the presence of 10 ng/ml TGFβ3 (+). On a weekly basis, cell samples were analyzed for the type 2 collagen (A) and aggrecan (B) expression. In addition, Safranin O staining and type 2 collagen immunohistochemistry of the pellets was performed at day 28 (scale bar = 200 µm). Regarding gene expressions CTL+, GDF5+, M1673+, W417F+, W417R+ and BMP2+ were compared to each other at all days using a 2-way ANOVA. Significances were only detected for aggrecan expression at day 28. Stars indicate significant differences compared to BMP2+ with **, *** and **** means $p<0.01$, $p<0.001$ or $p<0.0001$ respectively. All other comparisons showed no significant differences. Data represent mean ± SEM.

The hypertrophic capacity of BMP2, GDF5 and GDF5 mutants combined with TGFβ3 was analyzed, too. The expression of type 10 collagen was significantly enhanced by adding 10 ng/ml TGFβ3 to the chondrogenic medium compared to unstimulated cells in chondrogenic medium. As observed before for the expression of chondrogenic markers, the type 10 collagen expression was similar for TGFβ3 alone and in combination with BMP2, GDF5 and GDF5 mutants (Figure 42 A). However, the immunohistochemistry showed that the stimulation of human MSCs with BMP2 in combination with TGFβ3 and to a lesser extent with GDF5 in combination with TGFβ3 resulted in a positive type 10 collagen staining at day 28. On the contrary unstimulated cells, cells stimulated with TGFβ3 alone or in combination with GDF5 mutants showed no type 10 collagen staining at day 28 (Figure 42 C). Accordingly, the ALP

concentration in medium was increased more strongly with BMP2 and GDF5 in combination with TGFβ3 than with GDF5 mutants in combination with TGFβ3 or with TGFβ3 alone at day 21 and day 28 (Figure 42 B). These results confirm that a higher BMPR1a/BMPR1b ratio reduces hypertrophy as observed on the murine MSCs.

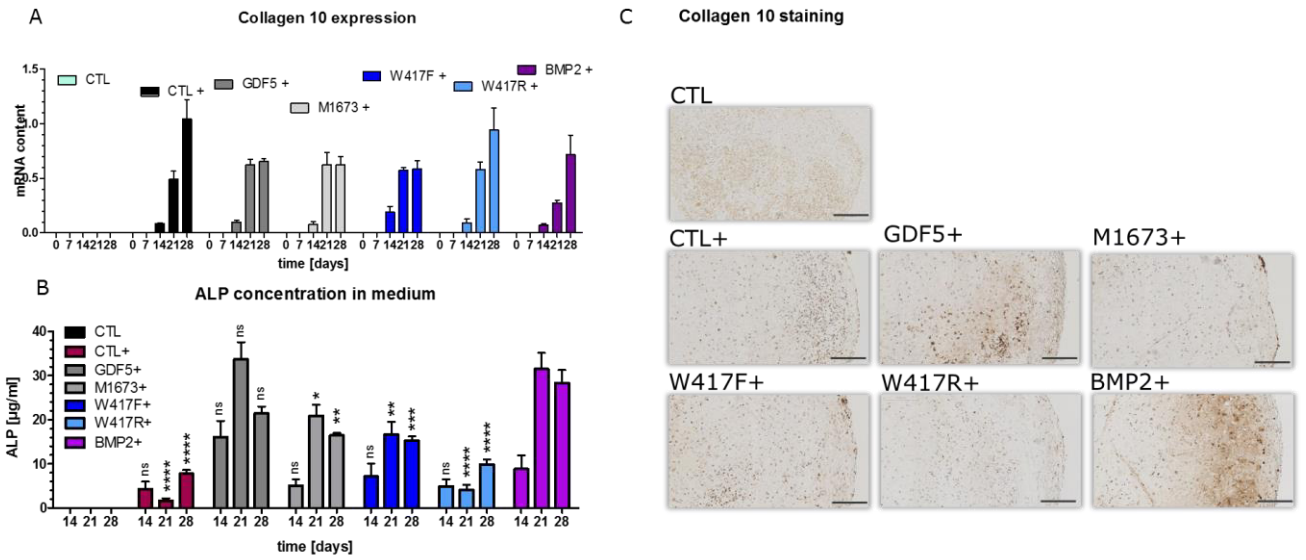

Figure 42 Analysis of hypertrophic markers in human MSCs cultured in chondrogenic medium in the absence or presence of TGFβ3 or in the presence of TGFβ3 with BMP2, GDF5 or GDF5 mutants over 28 days. Human MSCs were cultured in a pellet culture system and treated with 300 ng/ml BMP2, GDF5, M1673, W417F, W417R or left untreated (CTL) over 28 days in the presence of 10 ng/ml TGFβ3 (+). On a weekly basis, cell samples were analyzed for the type 10 collagen expression (A) and medium samples for the ALP concentration (C). In addition, type 10 collagen immunohistochemistry of the pellets was performed at day 28 (scale bar = 200 µm). Regarding type 10 collagen expression no significant differences between the compounds could be detected for any time point using a 2-way ANOVA. Regarding ALP concentration CTL+, GDF5+, M1673+, W417F+ and W417R+ were compared to BMP2+ for all days using a 2-way ANOVA. Stars indicate significant differences with *, **, *** and **** means $p<0.05$, $p<0.01$, $p<0.001$ or $p<0.0001$ respectively. ns = not significant. Data represent mean ± SEM.

Overall, the influence of the GDF5 mutants on chondrogenesis in human MSCs could not be evaluated. Nevertheless, an induction of hypertrophic differentiation was observable with BMP2 and GDF5, but not with M1673, W417F and W417R in combination with TGFβ3 confirming that a higher BMPR1a/BMPR1b ratio prevent hypertrophy in human MSCs.

5.3.3.2 Ability of GDF5 mutants to stimulate osteogenesis in human MSCs

In addition to the chondrogenic and hypertrophic capacities of the GDF5 mutants, their abilities to stimulate osteogenesis in human MSCs were evaluated and compared to GDF5 and BMP2. Osteogenesis of human MSCs was performed in monolayer cultures. After reaching confluence, the cells were cultured in standard cultivation medium and treated with 300 ng/ml BMP2, GDF5 and GDF5 mutants or remained untreated over 28 days as described previously for murine MSCs. On a weekly basis, cell and medium samples were analyzed for the presence of osteogenic markers. The concentration of ALP and the expression of osteopontin were used as early osteogenic markers, whereas the expression of

osteocalcin was used as a late-stage osteogenic marker. In addition, alizarin red staining of the cells was analyzed as a marker for calcium deposition occurring at later stages of osteogenesis.

On the contrary to in the murine MSCs, the expression of early and late osteogenic markers was not enhanced after compound stimulation of human MSCs cultured in standard medium. Neither the expression of osteopontin, nor the expression of osteocalcin was changed by the stimulation with any of the compounds (Figure 43 A+B). Similarly, no ALP concentration (data not shown) and no alizarin red staining was detected at any time (Figure 43 C).

Overall, in human MSCs the addition of osteogenic inductors to the cultivation medium seems to be necessary to induce osteogenesis.

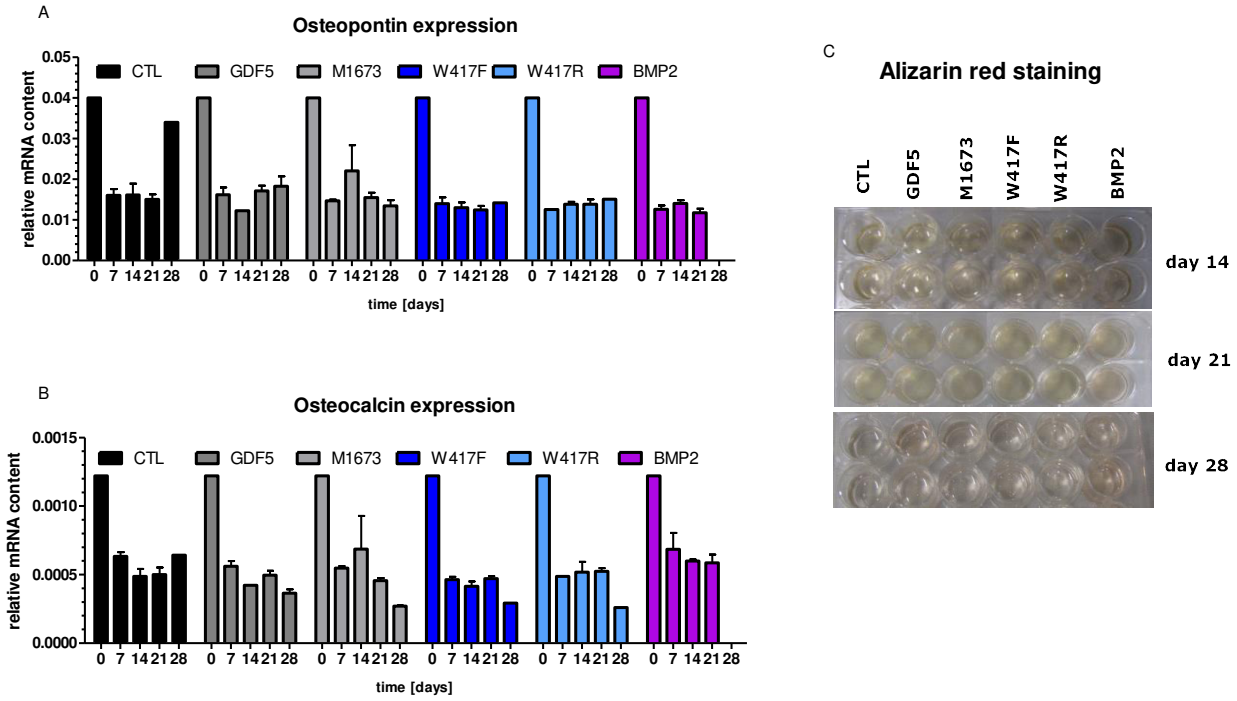

Figure 43 Analysis of osteogenic markers in human MSCs cultured in standard culture medium in the absence or presence of BMP2, GDF5 and GDF5 mutant over 28 days. Human MSCs were cultured until reaching confluence in monolayer and afterwards treated with 300 ng/ml BMP2, GDF5, M1673, W417F, W417R or left untreated (CTL) over 28 days. On a weekly basis, cell samples were analyzed for the osteopontin (A) and osteocalcin (B) expression as well as for alizarin red staining (C). Statistical analysis between the compounds using a 2-way ANOVA indicate no significant differences. Data represent mean ± SEM.

To confirm the influence of GDF5 mutants compared to GDF5 and BMP2 on osteogenesis in human MSCs, the cells were cultured in an osteogenic medium containing several essential substances for osteogenic induction of MSCs in vitro (see methods, chapter 4.2.3). As in the previous experiment, on a weekly basis, cell and medium samples were analyzed for the presence of osteogenic markers.

Osteogenesis of human MSCs cultured in osteogenic medium was the strongest after BMP2 treatment (Figure 44). The expression of osteopontin was strongly upregulated in the presence of BMP2 in comparison to untreated cells, but not with GDF5 and GDF5 mutants (Figure 44 A). Similarly, the

expression of osteocalcin was only upregulated in cells stimulated with BMP2 in comparison to untreated cells, but not with GDF5 and GDF5 mutants (Figure 44 B). In addition, the ALP concentration in medium was only detectable after BMP2, but not after GDF5 and GDF5 mutant stimulation (Figure 44 C). Furthermore, the alizarin red staining became positive after 14 days in presence of BMP2, after 21 days in the presence of GDF5 and after 28 days with M1673 and W417F. No staining could be seen in presence of W417R and in unstimulated cells (Figure 44 D).

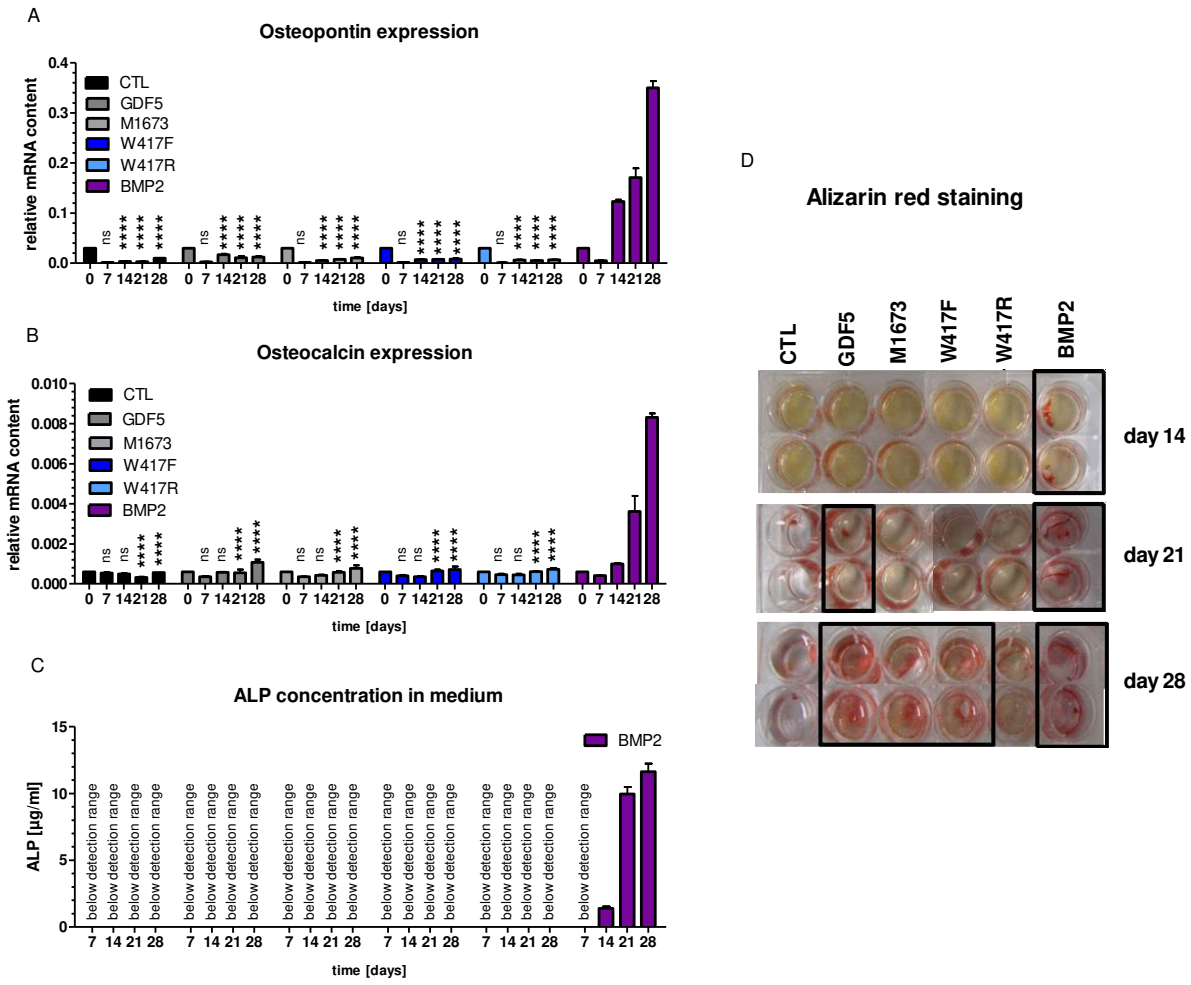

Figure 44 **Analysis of osteogenic markers in human MSCs cultured in osteogenic medium in the absence or presence of BMP2, GDF5 and GDF5 mutants over 28 days.** Human MSCs were cultured until reaching confluence in monolayer and afterwards treated with 300 ng/ml BMP2, GDF5, M1673, W417F, W417R or left untreated (CTL) over 28 days. On a weekly basis, cell and medium samples were analyzed for the osteopontin (A) and osteocalcin (B) expression as well as for alizarin red staining in the cells (D) and ALP concentration in medium (C). Regarding gene expression, CTL+, GDF5+, M1673+, W417F+ and W417R+ were compared to BMP2+ using a 2-way ANOVA. Stars indicate significant differences compared to BMP2+ with **** means p<0.0001. ns = not significant. Data represent mean ± SEM.

To summarize, osteogenesis of human MSCs could only be induced in the presence of osteogenic stimulators within the culture medium and was strongest with BMP2. BMP2 was the only compound, which upregulated all analyzed osteogenic markers. Alizarin red staining of human MSCs showed a delayed mineralization with GDF5, followed by M1673 and W417F compared to BMP2. The delayed

induction of mineralization corresponds with a higher KD or EC50 ratio for BMPR1a/BMPR1b: BMP2<GDF5<M1673<W417F<W417R.
Overall, an evaluation of the GDF5 mutants on chondrogenic induction was not feasible in human MSCs. Nevertheless, it could be confirmed in human MSCs that the GDF5 mutants with a higher KD or EC50 ratio for BMPR1a/BMPR1b exhibit a reduced hypertrophic and osteogenic capacity compared to GDF5 and BMP2.

Taken together the results from the MSC experiments showed that M1673 exhibits the highest chondrogenic capacity among the GDF5 mutants and a lower hypertrophic/osteogenic capacity compared to GDF5. It is hypothesized that M1673 displays an affinity to BMPR1a that enable chondrogenesis of MSCs. Simultaneously, M1673 has a BMPR1a/BMPR1b ratio that is high enough to prevent that MSCs undergo hypertrophy and to reduce osteogenic differentiation of MSCs in comparison to GDF5.

6 Discussion

Currently osteoarthritis (OA) is an incurable disease with only limited and mainly palliative treatment options. Therefore, it exists an unmet medical need for disease modifying OA drugs (DMOADs), which can deliver structural improvements by preventing OA progression or regenerating the damaged cartilage. The growth and differentiation factor 5 (GDF5) is a key regulator for cartilage formation during skeletal development and for its maintenance during adulthood and therefore could be a potentially useful growth factor for cartilage regeneration. Compared to other TGFβ superfamily members like BMP2 or BMP7, the potential of GDF5 has been less investigated in the context of OA. Nevertheless, a few studies were performed to evaluate the therapeutic potential of GDF5. It was shown that GDF5 stimulates ECM production in chondrocytes [1, 4, 135], induces chondrogenesis of mesenchymal stem cells [2, 5, 128] and promotes cartilage repair in an OA rat model [3]. Moreover, there is some evidence for additional anti-catabolic capacities of GDF5 [4]. Finally, single nucleotide polymorphisms (SNPs) within the GDF5 gene leading to a reduced expression of GDF5 was found to be strongly associated with OA in a genome-wide association study [3]. Thus, GDF5 is an interesting target candidate for the regeneration of damaged OA cartilage. However, GDF5 was also shown to have undesirable hypertrophic and osteogenic activities in vitro and in vivo [3, 5]. To design an improved GDF5 with reduced hypertrophic and osteogenic features, different single point mutations in the type 1 receptor binding site of GDF5 were performed previously to this work. For the present work three of these GDF5 mutants (M1673, W417F and W417R) were evaluated for their ability to stimulate cartilage ECM production in chondrocytes and for their chondrogenic and osteogenic potentials in mesenchymal stem cells. Both cell types can produce cartilage and are consequently important target cells of a potential DMOAD.

6.1 Anabolic effect of GDF5 mutants in primary chondrocytes

Among the three GDF5 mutants, M1673 was previously shown to induce strongest the cartilage ECM production in bovine and porcine chondrocytes (see supplementary, S7+8). The present work aimed to confirm this anabolic effect of M1673 in human OA chondrocytes (hOAC).

For this purpose, the anabolic effect of M1673 was investigated in hOAC cultured in monolayer over 7 or 28 days and was compared to that of GDF5. Twelve monolayer cultures were realized with hOAC isolated from twelve different donors. These cultures showed only a weak and inconsistent effect of GDF5 and M1673 on the ECM production. Consequently, the anabolic effect of M1673 previously seen in porcine and bovine chondrocytes could not be confirmed in hOAC with this experimental setting (Table 6 + Figure 12). Contrary to these results, Bobacz and co-workers, showed a stimulatory effect of GDF5 on proteoglycan synthesis in hOAC cultured in monolayer over 7 days [153]. However, in the same study the synthesis of type 2 collagen was not affected by GDF5 indicating that not all ECM production

markers were upregulated by the GDF5 stimulation. This study also differs from the present work as they used a serum-free culture medium [153]. Another previous study by Ratnayake and colleagues is in accordance to the results obtained in the present work. They could not demonstrate a robust anabolic effect of GDF5 on hOAC in a similar monolayer system used in the present work. They showed that the response of hOAC to exogenous GDF5 was detectable, but in a very inconsistent manner among the hOAC from different OA donors, whereas the addition of TGFβ1 led to a reproducible anabolic response in the same cells [154]. The reason for this inconsistency of the GDF5 response could be that the chondrocytes from each OA patient have a different inflammatory status or correspond to various stage of disease progression, and therefore display different phenotypes. In addition, the poor responsiveness of hOAC to GDF5 and M1673 could be explained by the monolayer system itself. In the present work it was shown that the expression of BMPR1a and BMPR1b decreased significantly after culturing the hOAC for 6 days in monolayer compared to freshly isolated chondrocytes (Figure 20+23). Indeed, BMPR1a and BMPR1b are the main receptors for GDF5 and M1673 [113, 115]. This phenomenon might be inherent to the known chondrocyte dedifferentiation occurring in monolayer which is characterized by morphological changes and a shift from type 2 collagen expression to type 1 collagen expression [18, 46]. That phenotype loss was confirmed in hOAC monolayer cultures over 6 days compared to freshly isolated chondrocytes (Figure 18+21).

An approach to overcome chondrocyte dedifferentiation is the culture of hOAC in 3D, which is known to better preserve the chondrocytes phenotype in comparison to monolayer cultures [18]. Consequently, it was hypothesized that culturing hOAC in 3D culture could improve the responsiveness of hOAC to GDF5 and M1673. This hypothesis was tested in two different 3D culture systems. In the first system, hOAC were allowed to aggregate and form cartilage-tissue analogs (CTAs), whereas for the second system hOAC were encapsulated in alginate beads. Both culture models are described to enable the cells to respond to growth factors [155-156]. Unfortunately, no significant effect on GAG accumulation was detectable after GDF5 or M1673 treatment neither in the CTAs nor in alginate beads with hOAC (Figure 13). These results differ from previous results showing a strong anabolic effect of GDF5 and M1673 in porcine and bovine chondrocytes cultured as CTAs (see supplementary, S7+8). However, animal chondrocytes were isolated from young healthy pigs or cows, whereas hOAC were isolated from end-stage OA cartilage of patients who underwent a total joint replacement surgery. These chondrocytes are older, diseased and inflamed. This could lead to an altered BMP receptor expression profile, which in turn could result in a decreased GDF5 response. It was also already described that many cell types become unresponsive to growth factors with age, disease and inflammation [157-158]. For example, it was shown that the responsiveness of human chondrocytes to the growth factors IGF1 and BMP7 declined with the increasing age of the donors from 24 to 81 years [158]. It was also demonstrated that increasing age lead to an enhancement of oxidative stress and lastly to a disruption in signal transmission within

the chondrocytes [158]. In the present work, the only source for human chondrocytes was material from total joint replacement with a donor age of in average 71 years suffering from painful late-stage OA. These cells are probably less responsive to anabolic factors than healthy chondrocytes could be. Consequently, it was hypothesized that culturing the end-stage diseased hOAC in conditions corresponding to the environment of (almost) healthy articular cartilage could improve their condition by making them less diseased and restore their responsiveness to GDF5 and M1673.

One condition of choice to mimic a 'healthier' cartilage environment was the culture of hOAC in hypoxia. Healthy articular cartilage is an avascular tissue, which is supplied with oxygen by diffusion from the synovial fluid resulting in an oxygen gradient within the articular cartilage from 10% in the superficial zone to 1% in the deep zone [31-32]. During OA, the cartilage becomes fibrillated and vascularized resulting in an increased oxygen tension within the OA cartilage [159]. It was hypothesized that lowering the oxygen tension in culture could help hOAC to recover partly a healthy phenotype. That was tested in the present work by the culture of hOAC in monolayer over 7 days or as CTAs over 28 days at a low oxygen tension (1%) and at a standard oxygen tension (21%). However, reducing the oxygen tension to 1% had none or even a negative effect on the GAG concentration of hOAC cultured in monolayer (Figure 14) or as CTAs (Figure 15) compared to the culture at 21% oxygen. Consequently, the culture of hOAC at a low oxygen tension of 1% was not favorable and was not further investigated. In contrast to the present work, it was shown by different research groups that lowering the oxygen tension to 1, 2, or 5% positively influenced the chondrocytes phenotype in 2D or 3D cultures. It enhanced the cartilage ECM production, promoted redifferentiation and even reduced the expression of hypertrophic markers and the production of ECM-degrading enzymes in chondrocytes [33-35]. A reason why hypoxia showed no beneficial effect on hOAC in the present work could be due to the disease status of the cells leading to a different response to hypoxia. It could be possible that the used oxygen tension of 1% was too low for hOAC. hOAC have already a decreased metabolism in comparison to healthy chondrocytes and low oxygen might reduce their metabolic activity even more. In addition, regarding the CTA constructs, the low oxygen tension of 1% may not be able to completely diffuse into the high cell density constructs resulting in an insufficient oxygen tension within the CTAs.

A second way to mimic a 'healthier' cartilage environment and possibly make the hOAC more responsive to GDF5 and M1673 was the culture of hOAC in the presence of heparin additionally to GDF5 or M1673. Indeed, it is well known that heparin can potentiate the activity of some TGFβ superfamily members by prolonging its bioavailability/activity and the presence of a heparin/heparan sulfate binding site was confirmed for the GDF5 molecule [2]. Healthy chondrocytes produce a considerable amount of cartilage ECM, which contains heparan sulfates, whereas OA chondrocytes produce less ECM resulting in a lack of heparan sulfates, which could be possibly the reason for a reduced responsiveness of hOAC to GDF5

or M1673. Additionally anti-inflammatory properties are described for heparin [120], which could improve the hOAC condition. However, in the present work the addition of heparin had no beneficial or even an inhibitory effect on the hOAC responsiveness to GDF5 or M1673 (Figure 17). In contrast, for BMP2 it was shown that the binding of heparin resulted in a prolonged and enhanced biological activity by protecting BMP2 from degradation and by blocking BMP2 antagonists and inhibitory SMADs. This was shown in vitro by using an osteoblastic cell line and was also shown in vivo [120, 160-162]. However, the present work is in accordance to recently published data from Ayerst and colleagues, who demonstrated that the addition of heparin inhibited dose-dependently the GDF5 activity in MSCs [2]. The reason why heparin exerts a negative effect on the activity of GDF5, but not on BMP2 is unclear. It is known that interaction with heparin or heparan sulfate is not necessary for GDF5-receptor binding but prolongs the GDF5 bioavailability/activity. However, a high affinity of heparin for GDF5 may prevent the interactions of GDF5 with its receptors and reduce its effect.

A last tested parameter to mimic a 'healthier' chondrocyte environment was an increased medium osmolarity. Healthy chondrocytes produce an abundant cartilage ECM containing osmotically active proteoglycans responsible for the maintenance of a high negative fixed-charge density and thus for a high osmolarity within healthy articular cartilage, which ranges from 350 to 480 mOsm [43]. During OA progression, the cartilage ECM and thus also the proteoglycans are degraded resulting in a reduction of osmolarity within the OA cartilage down to 270 mOsm at end-stage OA [40]. Consequently, the severity of OA is directly connected to a decrease of osmolarity within articular cartilage. It was suggested that culturing the end-stage hOAC at osmolarities that rather correspond to healthy articular cartilage could improve their condition and possibly restore their responsiveness to GDF5 and M1673. As a first step, it was shown that culturing hOAC for 7 days in monolayer at a medium osmolarity of 380 mOsm -what rather corresponds to osmolarities within healthy articular cartilage- increased significantly the GAG production compared to the culture at the standard medium osmolarity of 340 mOsm -what rather corresponds to osmolarities within OA cartilage (Figure 14). Therefore, it was suggested that increasing the medium osmolarity is beneficial for hOAC. It was then tested if the response to GDF5 and M1673 was increased under these culture condition by comparing two different 3D culture systems. Culturing the hOAC as CTAs over 28 days at an increased medium osmolarity of 380 mOsm did not improve the response of hOAC to GDF5 and M1673 compared to untreated cells (Figure 16 A+B). On the contrary, culturing hOAC in alginate beads at 380 mOsm improved significantly the GAG accumulation after GDF5 or M1673 stimulation compared to untreated cells (Figure 16 C+D). The reason why hOAC were responsive in alginate but not in CTAs is unclear. It is known that chondrocytes are anchorage dependent cells and will die without an appropriate support to adhere to. In 3D culture it was shown that chondrocytes build cell-matrix interactions and bind directly to their surrounding matrix [163]. In alginate, the cells are trapped in the gel and probably rapidly accumulate matrix in their direct vicinity allowing

rapidly cell-matrix interactions. On the contrary, in CTAs matrix molecules can diffuse away and it might take longer for the cells to get surrounded by a matrix they can interact with. Because hOAC produce less cartilage ECM than healthy chondrocytes, this effect might be exacerbated in hOAC, which do not accumulate fast enough sufficient cartilage ECM to allow cell-matrix interactions and cell survival. Indeed, at the end of the CTA culture, the cell content was reduced in comparison to the initial seeding density. As a consequence, it would be possible that the remaining cells in the CTAs are too few to detect differences between GDF5 or M1673 stimulated cells compared to unstimulated cells. In summary, hOAC are responsive to GDF5 and M1673 in alginate culture at a 'healthier' medium osmolarity of 380 mOsm and this condition is therefore the most promising of all tested culture conditions.

However, it was still unclear why hOAC become more responsive under higher osmolarity and whether 380 mOsm is adequate to analyze the effects of GDF5 and M1673 in hOAC. Therefore, the osmolarity effect and its physiological relevance on hOAC was further characterized. For this purpose, monolayer cultures were performed with freshly isolated hOAC. The monolayer cultures were performed over 6 days at the unchanged medium osmolarity of 340 mOsm and at increased medium osmolarities of 380, 420 and 460 mOsm what covers the range of osmolarities reported for healthy cartilage. Afterwards the osmolarity effect was evaluated with hOAC encapsulated in alginate beads.
It was shown that increasing the medium osmolarity reduced the cell concentration of the hOAC in monolayer and in alginate beads in an osmolarity-dependent way, but only significantly at 420 and 460 mOsm compared to 340 mOsm and without falling below the seeding concentration and without a loss in cell viability (Figure 18+21+25). Thus, it could be concluded that the reduced cell concentration at increased osmolarities was not due to cell death but rather due to a reduced proliferation capacity of hOAC. Furthermore, increasing the medium osmolarity had a positive impact on the cartilage ECM molecules production and the phenotype of hOAC cultured in monolayer or encapsulated in alginate beads (Figure 18+21+25). In detail, the GAG production, type 2 collagen and aggrecan expression were enhanced from 380 to 460 mOsm compared to 340 mOsm (Figure 18+21+25). In monolayer cultures a better phenotype maintenance was observed, because the cell dedifferentiation (characterized by an enhanced type 1 collagen and decreased type 2 collagen expression) was prevented by increasing the medium osmolarity from 380 to 460 mOsm compared to 340 mOsm (Figure 18+21). In contrast to the monolayer culture, in alginate culture it could be observed that the chondrocytes phenotype was favored even without modulating the medium osmolarity. Indeed, at the end of the culture the expression of type 1 collagen was lower and the expression of type 2 collagen was higher than in freshly isolated chondrocytes. This effect on type 1 and type 2 collagen expressions were also found to be further enhanced by raising the medium osmolarity from 380 to 460 mOsm (Figure 25). When comparing these results to the literature, most of the findings are in accordance with observations form others. For instance, Windt and co-workers showed that culturing hOAC at an increased medium osmolarity of 480

mOsm reduced the cell proliferation, whereas a moderately elevated medium osmolarity of 380 mOsm did not reduce cell proliferation in comparison to the unchanged medium osmolarity of 280 mOsm. On the contrary to the present work, they also observed a diminished cell viability already after 2 days of hOAC culture at 480 mOsm, but not at 380 or 280 mOsm [37, 46]. However, another study using healthy bovine chondrocytes encapsulated for 6 days in alginate beads demonstrated an unchanged viability after culturing them at enhanced medium osmolarities up to 570 mOsm [37, 39]. Regarding ECM production, it was already demonstrated that type 2 collagen, aggrecan and sox9 expression was enhanced, whereas type 1 collagen expression was decreased after culturing hOAC in monolayer at 380 mOsm compared to 280 mOsm [41, 46]. In addition, the enhanced ECM molecule production at 380 mOsm compared to 280 mOsm was not only observable in unexpanded hOAC, but also in hOAC passaged up to 3 times [46] suggesting that the results of the present work would be also valid for expanded hOAC cultured in monolayer. The same research group showed that the positive influence of an enhanced medium osmolarity was mediated through the tonicity enhancer binding protein (TonEBP) [46]. TonEBP is a key transcription factor, which is known to be activated in response to hyperosmotic stress [45, 48] and mediate the response of chondrocytes to increased osmolarities.

To further characterize the beneficial effect of an enhanced medium osmolarity on hOAC, the production of matrix-degrading enzymes and inflammatory cytokines was analyzed. It could be demonstrated that enhancing the medium osmolarity from 380 to 460 mOsm decreased significantly the MMP13 expression of hOAC cultured in monolayer or alginate beads, whereas the expression of ADAMTS5 was barely influenced (Figure 19+22+26). In addition, the production of MMP3 was shown to be significantly reduced from 380 to 460 mOsm in hOAC monolayer cultures, whereas the production of MMP1 and MMP9 was less or not affected (Figure 21+24). Regarding inflammatory cytokines, the highest production was observed for Il6, followed by TNFα and by Il1β in both, monolayer and alginate bead cultures of hOAC (Figure 19+22+26). Enhancing the medium osmolarity from 380 to 460 decreased significantly and dose-dependently the production of Il6, TNFα and Il1β in monolayer cultures as well as in alginate bead culture of hOAC (Figure 19+22+26). In accordance to the present work, it was already shown that ADAMTS4 and ADAMTS5 expression levels are not affected by an enhanced medium osmolarity in hOAC cultured in monolayer [41]. In contrast to the results of the present work, the same group showed an upregulation of MMP1, 3, 8 and 13 expression levels at 380 mOsm compared to 280 mOsm [41]. These different observations might reside in the difference of the experimental setting; for example, they compared 280 and 380 mOsm while in the present work 340 mOsm was compared with 380, 420 and 460 mOsm. In the present work, the downregulation of MMP13 expression was confirmed with a total of five monolayer experiments with hOAC isolated from five different donors and was also confirmed in a 3D culture system. Therefore, this effect was robustly reproducible. Moreover, it is described that ECM-degrading enzymes like MMP13 are induced by inflammatory cytokines [164] which were also shown to be reduced by increasing the medium osmolarity (Figure 19+22+26). To the best

of our knowledge, the present work is the first analyzing the influence of an enhanced medium osmolarity on the cytokine production of hOAC. Tsuchida and co-workers showed that healthy and OA chondrocytes in culture produce more Il6 than TNFα while Il1β production was the lowest [164]. This order in the cytokine production levels is in accordance to that observed in the present work. Furthermore, it was shown by Tsuchida and co-workers that isolated healthy or OA chondrocytes produce more cytokines than chondrocytes in cartilage [164] indicating that in culture the level of cytokines is artificially elevated. The mechanism is not known but it can be postulated that the dramatic change of the cellular environment upon chondrocyte isolation elicits a stress response resulting in the production of inflammatory cytokines and proteases. It could be further postulated that increasing the culture medium osmolarity makes this environment change less dramatic and reduces this stress response in chondrocytes.

To better understand the increased responsiveness to GDF5 and M1673, the effect of osmolarity on the expression of the BMP receptors was also analyzed. It could be demonstrated that an increased medium osmolarity led in trend to an enhanced expression of BMPR1a, BMPR1b and BMPR2 compared to 340 mOsm (Figure 20+23). Moreover, a connection could be demonstrated between the presence of inflammatory cytokines and the BMP receptors expression (Figure 24) indicating that the reduced cytokine production at higher osmolarities would enable a higher BMPR expression level. However, a direct effect of the osmolarity on BMPR expression could not be excluded. Importantly, these results show that at increased osmolarities, the expression of BMPRs were higher what possibly explain the better responsiveness of the chondrocytes to GDF5 and M1673 in these culture conditions.

In a first instance all these results were obtained by increasing the medium osmolarity with NaCl, which is routinely used for this purpose [37, 46, 48, 165]. The use of NaCl to modulate the medium osmolarity was compared to the use of sucrose with similar outcomes on all analyzed parameters (Figure 18-23). It indicates that the observed effects were not specific effects of sodium or chloride, but rather 'real' osmolarity effects. This is in accordance with a previous study which compared the use of NaCl and sucrose to adjust the medium osmolarity with the conclusion that no significant differences in gene expression patterns were detectable [41].

Overall, an increased osmolarity was found to be an easy way to facilitate investigations with hOAC in vitro and increase their responsiveness to growth factors like GDF5. However, the question of the relevance of such culture conditions remained. The target cells of M1673 are middle-stage OA chondrocytes. Yet, in the present work late-OA chondrocytes which were additionally stressed by cell isolation were used. With an osmolarity of 380 mOsm instead of 340 mOsm the inflammatory status could be reduced to a level that might rather correspond to middle-stage OA chondrocytes in cartilage. To validate this culture system, it was decided to first evaluate the GAG accumulation in chondrocytes from seven different hOAC donors. Culturing the cells in alginate beads at 380 mOsm resulted in an

enhanced and more robust GAG accumulation compared to the culture at 340 mOsm (Figure 29). Consequently, an in vitro model was established, which enable to characterize the anabolic effect of GDF5 and M1673 in hOAC. It consists in an alginate bead culture system combined with a medium osmolarity of 380 mOsm.

Afterwards, the effect of M1673 was evaluated in hOAC cultured in alginate beads at 380 mOsm by analyzing many different cartilage ECM production markers. Because M1673 was already shown to exert the strongest anabolic effect among the GDF5 mutants, only M1673 was investigated in hOAC and compared to GDF5 (see supplementary, S7+8). An anabolic effect of GDF5 as well as M1673 was demonstrated in hOAC. Indeed, an increased GAG accumulation and aggrecan expression in alginate beads indicating proteoglycan synthesis was observed. Furthermore, GDF5 and M1673 also lead to an increased hydroxyproline, pro-peptide of collagen 2 accumulation and type 2 collagen expression in alginate beads indicating an increase of the global collagen synthesis (hydroxyproline) and of type 2 collagen synthesis (Figure 30). In addition, the expression of MMP13 and ADAMTS5 was significantly downregulated after GDF5 and M1673 treatment compared to untreated cells indicating additional anti-catabolic properties of the compounds (Figure 31 A+B). The anabolic and anti-catabolic properties of M1673 were less pronounced than that of GDF5, but they were nevertheless significant over control. Moreover, data of the present work showed some indications for a reduced hypertrophic and dedifferentiation capacity of M1673 compared to GDF5 (Figure 31 C+D). The anabolic effect of GDF5 in 3D culture was previously described by some research groups, but all of them focused on healthy chondrocytes [1, 4, 134-135]. GDF5 was shown to exerts an anabolic effect on proteoglycan synthesis in bovine chondrocytes cultured as pellets for 21 days. The same research group also showed an increased pellet size as well as an enhanced Safranin O staining indicating proteoglycan synthesis after 21 days of GDF5 treatment in human nasal chondrocytes compared to untreated cells. However, no upregulation of type 2 collagen synthesis could be detected after GDF5 treatment neither in bovine nor human nasal chondrocytes compared to untreated cells [1]. Similarly, GDF5 was shown to exhibit anabolic effects on proteoglycan synthesis in healthy, human articular chondrocytes cultured in alginate beads over 9 days [135], in aggregate culture over 7 days [134] or in a pellet culture over 21 days [4]. Again, an anabolic effect of GDF5 on collagen synthesis in healthy, human articular chondrocytes was not detectable [4, 134-135]. The above-mentioned experiments with healthy, human articular chondrocytes in pellet culture showed not only anabolic, but also anti-catabolic and anti-hypertrophic effects of GDF5. In detail, they showed a downregulation of MMP13 and ADAMTS4 expression (catabolic markers) and of the type 10 collagen expression (hypertrophic marker) after GDF5 treatment [4]. An anti-catabolic effect of GDF5 was also observed in the present work. However, the present work led to the suggestion that GDF5 is hypertrophic instead of anti-hypertrophic. The different observations could be due to different experimental settings.

For instance, the present work was performed with osteoarthritic instead of healthy chondrocytes and in medium without chondrogenic inductors.

To the best of our knowledge the present work is the first showing anabolic and anti-catabolic effects of GDF5 and M1673 on diseased hOAC in 3D culture. Additionally, the present work is the first, which showed an anabolic effect of GDF5 not only by enhancing the proteoglycan, but also the type 2 collagen synthesis in chondrocytes. In comparison to GDF5, M1673 showed an equal or slightly reduced anabolic and anti-catabolic effect, but seems to be also less hypertrophic. Based on the results of the present work, it can be concluded that M1673 has the potential to promote cartilage repair and prevent further cartilage degeneration and has therefore the potential to become a DMOAD.

6.2 Differentiation capacities of GDF5 mutants in mesenchymal stem cells

Asides from chondrocytes, mesenchymal stem cells (MSCs) can also produce cartilage. During development, MSCs are able to differentiate into several tissue types including cartilage and bone [32]. Recently various MSC niches within the adult joint including subchondral bone, synovium, infrapatellar fad pad or synovial fluid were discovered [51]. This led to the suggestion that MSCs not only induce the tissue development, but may also contribute to articular cartilage maintenance and repair even during adulthood. Growth factors like members of the TGFβ superfamily regulate embryonic cartilage development and are known to stimulate MSC migration, proliferation and differentiation [110, 166]. For instance, GDF5 was shown to stimulate not only matrix production in chondrocytes, but also to promote chondrogenesis in MSCs and to induce cartilage formation in an OA rat model [1-3]. Therefore, it was hypothesized in the present work that articular application of GDF5 could support the differentiation of the joint resident MSCs into chondrocytes and promote cartilage repair. However, GDF5 was also shown to have some undesired hypertrophic and osteogenic capacities in vitro and in vivo [3, 5] what can lead to osteophytes formation or mineralization and hardening of the cartilage matrix, two unwanted phenomenons. Thus, previously to the present work, different GDF5 mutants were designed by single point mutations in the type 1 receptor binding site of GDF5 to generate improved GDF5 versions with reduced hypertrophic and osteogenic properties. BMPs like GDF5 mediate their signals primarily by binding to the BMP receptors (BMPR), BMPR1a or BMPR1b in combination with BMPR2. Both receptor complexes, BMPR1a with BMPR2 or BMPR1b with BMPR2, are responsible for intracellular signal transmission and influence the fate of MSCs toward chondrogenesis or osteogenesis. However, the distinct roles of BMPR1a and BMPR1b are poorly understood until now and opinions about their different roles are contradictory. From the body of literature, it was hypothesized that BMPs inducing BMPR1a activation, promote osteogenesis and hypertrophy, while BMPs inducing BMPR1b activation, promote chondrogenesis. On this basis, the three GDF5 mutants M1673, W417F, and W417R were selected, all having a reduced BMPR1a affinity and a similar BMPR1b affinity compared to GDF5. It was

hypothesized that these GDF5 mutants have a reduce osteogenic/hypertrophic capacity and a maintained chondrogenic capacity compared to GDF5. To verify this hypothesis, the GDF5 mutants were evaluated for their chondrogenic and osteogenic differentiation potentials in MSCs and compared to those of GDF5. BMP2 was used as a control for osteogenesis and chondrocyte hypertrophy. In addition, it was aimed to better understand the respective roles of BMPR1a and BMPR1b.

As a first step, the binding affinities to BMPR1a, BMPR1b and BMPR2 of all GDF5 mutants as well as GDF5 and BMP2 were confirmed by SPR. In addition, they were characterized regarding their receptor dimerization potential in a cell assay that better represents the complexity of receptor interactions.
BMP2 showed the highest binding affinity to BMPR1a of all tested compounds. For the GDF5 mutants a reduced BMPR1a affinity in comparison to GDF5 was confirmed. M1673 showed a reduced BMPR1a affinity compared to GDF5, which was further reduced for W417F. For W417R no binding to BMPR1a could be detected with the conditions used (Table 7). However, this does not exclude per se that W417R is unable to bind to BMPR1a. Indeed, W417R stimulated the dimerization of BMPR1a with BMPR2 in the in vitro assay (Figure 32+Table 8) indicating that W417R is still able to interact with BMPR1a. In contrast to the large BMPR1a affinity differences (factor 720 between the highest and lowest affinity), the affinities towards BMPR1b vary less among the compounds (factor 6 between the highest and lowest affinity). The ratio KD BMPR1a/KD BMPR1b were calculated and it was 1.7 for BMP2 and increased strongly for GDF5, followed by the GDF5 mutants (Table 7). Other studies also reported a similar affinity of BMP2 for BMPR1b and BMPR1a and a higher affinity of GDF5 for BMPR1b compared to BMPR1a [131, 154].
The compounds were also tested for their receptor dimerization potential in cell assays. The single affinities for BMPR1a or BMPR1b are not always in line with the potencies of the respective compounds to dimerize BMPR2 with BMPR1a or BMPR1b (Table 7+8). This discrepancy can be explained by the differences between the assay systems. The affinity measurements evaluate the binding of the respective BMPs to one single receptor. They do not take in account that the oligomerization of type 1 and type 2 BMP receptors is required for the signal transmission of BMPs. Most of the receptors are present on the cell surface as single receptor subtypes. BMPs bind to one receptor subtype and induce the recruitment of the second receptor subtype resulting in a BMP-induced signal complexes (BISC) [126]. It was shown that BMP2 and GDF5 bind BMP receptor type 1 (BMPR1a or BMPR1b) with a higher affinity than BMP receptor type 2 (BMPR2). The resulting BMP/BMP receptor type 1 complex showed an increased affinity for the BMP receptor type 2 than BMPs alone. In addition, a minor receptor subset of about 10% is present on the cell surface as preformed receptor complexes (PFCs) containing both receptor subtypes. BMPs bind to these PFCs with higher affinities than to the single receptor subtypes [167]. In this regard, the affinity measurements represent only the first binding step of BMPs to one receptor subtype and does not capture the complexity of the receptors/ligand interactions. On the contrary, the in vitro dimerization

assays probably take in account the multiple possibilities for the formation of the receptors/ligand complexes and consequently better represent the complexity of receptor interactions.
Despite the discrepancies regarding single affinities and dimerization potencies, the ratio of the potencies obtained in the BMPR1a/BMPR2 and BMPR1b/BMPR2 assay showed the same ranking as the ratios obtained for the binding affinities (Table 7+8). In summary, it was evaluated that all GDF5 mutants were able to bind to their receptors and initiate receptor dimerization. The performed mutations within the GDF5 molecule successfully decreased the binding selectivity towards BMPR1a and shifted it towards BMPR1b. Thus, according to the initial hypothesis, W417R having the lowest BMPR1a affinity of all tested compounds and a BMPR1b binding selectivity similar to GDF5 should show the most reduced osteogenic/hypertrophic properties and still exhibit a similar chondrogenic potential compared to GDF5.

To verify this hypothesis, the GDF5 mutants, GDF5 and BMP2 were tested for their chondrogenic and osteogenic potential in the murine stem cell line C3H10T1/2, which was established from mouse embryos in 1973 [168]. The advantages of the stem cell line over primary MSCs is that the C3H10T1/2 cell line represents a homogenous cell population, which do not undergo spontaneous differentiation under standard culture conditions. Consequently, the addition of exogenous factors like BMPs are necessary to induce differentiation of C3H10T1/2 cells [169-170]. These cells were shown to have comparable osteogenic and chondrogenic differentiation potentials to that of primary murine bone-marrow derived MSCs [170] and are consequently a valid tool to study differentiation processes. Nevertheless, human bone-marrow-derived MSCs were used to confirm the results obtained with C3H10T1/2 cells.

Firstly, it was shown that all BMPRs including BMPR1a, BMPR1b and BMPR2 are present in C3H10T1/2 cells with BMPR1b showing the lowest level of expression compared to BMPR1a and BMPR2 (Figure 33). In contrast, previous studies could not show any expression of BMPR1b in C3H10T1/2 cells with the conclusion that these cells do not express BMPR1b [130, 171-172]. However, on the contrary to the present work the authors used a RT-PCR method that is not quantitative and has a lower sensitivity in comparison to quantitative RT-PCR. This could explain why they could not detect BMPR1b expression. The lower expression of BMPR1b compared to BMPR1a and BMPR2 was also shown for human MSCs (Figure 40) and it is also described by literature [128, 154].

Chondrogenesis of C3H10T1/2 cells was performed in a pellet culture over 28 days in chondrogenic medium. The stimulation with GDF5, M1673 and BMP2 induced chondrogenesis, while only BMP2 strongly induced hypertrophy in murine MSCs. GDF5 showed a less pronounced hypertrophic capacity compared to BMP2, which was even more reduced with M1673. W417F induced chondrogenesis only moderately compared to BMP2, GDF5 and M1673 and showed no effect on hypertrophy. W417R showed

neither a chondrogenic nor a hypertrophic induction potential (Figure 34+35). Chondrocytes terminal differentiation or hypertrophy results in mineralization of the ECM and hardening of the cartilage [2] what is an unwanted effect. Consequently, the therapeutic potential of a potential DMOAD depends not only on its chondrogenic, but also on a low or an absence of hypertrophic differentiation potential. The chondrogenic and hypertrophic capacity of BMP2 in the murine stem cell line C3H10T1/2 was demonstrated several times [130, 169, 173-174] , whereas GDF5 was less intensively studied in these cells. To the best of our knowledge only Kaps and co-workers demonstrated a lower hypertrophic induction but also a lower chondrogenic induction potential of GDF5 compared to BMP2 in C3H10T1/2 cells [130].

Additionally, it was aimed to better understand the respective roles of BMPR1a and BMPR1b in these differentiation processes. Our initial hypothesis postulated that BMPs, with a higher binding selectivity towards BMPR1b induce chondrogenesis, while BMPs with a higher binding selectivity to BMPR1a promote hypertrophy/osteogenesis. In the light of the chondrogenesis and hypertrophy results obtained in the C3H10T1/2 cells, this hypothesis had to be refined. The chondrogenic induction potential rather seems to depend on the binding selectivity of the compounds towards BMPR1a. Compounds with a strongly reduced BMPR1a affinity, like W417F and W417R, showed a reduced or even an absence of chondrogenic capacity in murine MSCs. Thus, a sufficient BMPR1a binding of the compounds seems to be necessary to induce chondrogenesis in murine MSCs. Furthermore, a higher BMPR1a affinity of the compounds, like BMP2 and GDF5, promoted hypertrophic differentiation of murine MSCs. By looking at the EC50 values, M1673 with its greater potency for BMPR1a/BMPR2 dimerization compared to GDF5 should show a higher hypertrophic capacity than GDF5. On the contrary, it showed a lower hypertrophic capacity compared to GDF5. As M1673 had simultaneously the highest EC50 value for BMPR1b/BMPR2 this led to the suggestion that BMPR1b might also play an important role in hypertrophic differentiation possibly by preventing it. Thus, it seems that it is not the single binding selectivity towards BMPR1a or BMPR1b, but rather the ratio between BMPR1a and BMPR1b which determine the cell fate. The literature concerning the distinct roles of BMPR1a and BMPR1b during chondrogenesis and hypertrophy is controversial. Several previous studies are in accordance with the observation of the present work, that BMPR1a is necessary for chondrogenesis [113, 129-130]. Moreover, some studies showed, in accordance to the results obtained in the present work, that BMPR1a also mediates hypertrophy and that BMPR1b rather prevent hypertrophy [112, 124, 131]. Kaps and co-workers concluded that BMPR1a initiate chondrogenesis, whereas the role for BMPR1b remained unclear [130]. In contrast two other studies demonstrated that BMPR1b mediates the chondrogenic properties of GDF5 [175] and that BMPR1b is crucial for chondrogenesis of MSCs [176].

In summary, BMP2 with a very low BMPR1a/BMPR1b ratio has a strong hypertrophic, but only a moderate chondrogenic capacity compared to GDF5 and M1673. Provided that a sufficient BMPR1a binding is given, a higher BMPR1a/BMPR1b ratio of the GDF5 mutants seems to prevent hypertrophic

and enhance chondrogenic differentiation. It could be demonstrated in the present work, that the compound combining the best chondrogenic and anti-hypertrophic induction potential is the GDF5 mutant M1673 having a BMPR1a affinity high enough for stimulating chondrogenesis and a BMPR1a/BMPR1b ratio high enough to already prevent hypertrophic induction (Figure 36).

It was then evaluated if these results could be confirmed in human mesenchymal stem cells (human MSCs). Unfortunately, the chondrogenic capacity of the various compounds could not be analyzed in human MSCs. As a first step, the same experimental layout used for murine MSCs was applied. Indeed, in the murine stem cell line chondrogenesis was induced by the tested compounds in absence of TGFβ and it was consequently decided to use similar culture conditions with the human MSC. However, in absence of TGFβ, no chondrogenesis could observed with human MSCs, even not in the presence of BMP2, GDF5 or the GDF5 mutants (data not shown). TGFβ1/3 are well-known chondrogenic stimulators, which are routinely used to induce chondrogenesis in human MSCs [2]. TGFβ3 was also described to have a higher chondrogenic capacity compared to TGFβ1 [177]. Consequently, a second chondrogenesis experiment was then performed with human MSCs in presence of TGFβ3. Chondrogenesis of hMSCs was shown to be enhanced by stimulation with TGFβ3, but no effect of the compounds could be detected anymore (Figure 41). It can be suggested that TGFβ3 covered the effect of the tested compounds. In contrast, several previous studies demonstrated that the usage of TGFβ1/3 enhanced chondrogenesis of human MSCs but GDF5 could exert an additional effect [2, 5, 134, 178]. This additional chondrogenic effect of GDF5 over TGFβ was mainly demonstrated at the gene expression level [2, 5, 134, 178]. One research group showed additionally an enhanced Safranin O staining after treatment with GDF5+TGFβ3 compared to TGFβ3 alone. However, they could not confirm an enhanced staining of type 2 collagen by immunohistochemistry [5]. Similarly, another research group demonstrated an enhanced gene expression of type 2 collagen and aggrecan after GDF5+TGFβ1 stimulation compared to solely TGFβ1, but detected a comparable type 2 collagen and Safranin O staining [134]. To optimize the system used in the present work to induce chondrogenesis, it could be beneficial to use a lower TGFβ3 concentration or higher concentrations of BMP2, GDF5 and GDF5 mutants to prevent that TGFβ3 shields the effect of the tested compounds. However, other working groups demonstrated an additional effect of GDF5 over TGFβ by using the same [2, 178] or even lower GDF5 concentrations [5, 128, 134] and the same TGFβ concentration than the concentration used in the present work [2, 5, 128, 134, 178]. However, the experimental setting used in the present work might be slightly different and it remains a possibility that adapting the concentrations of the tested compounds and TGFβ3 could enable to evaluate the chondrogenic effects of the GDF5 mutants. Another optimization strategy to enhance chondrogenesis in human MSCs could be the culture of the cells in a scaffold-free transwell culture system. This system enables the cells to form shallow flat cartilage discs on a porous membrane, which allows an uniform nutrient supply to all cells. In addition, this system was shown to be more efficient for inducing

chondrogenesis of human MSCs than the routinely used pellet culture system [179]. It was shown by Ratnayake and colleagues that the stimulation of the cartilage discs with a combination of GDF5 and TGFβ3 resulted in an increased chondrogenesis already after 7 days of culture compared to unstimulated cells [128]. Unfortunately, they did not compare the effect of GDF5+TGFβ3 to the effect of TGFβ3 alone. Nevertheless, it would be possible that this system could enable chondrogenesis of human MSCs after GDF5 stimulation, even in the absence of TGFβ3.

Despite the fact that an effect of the tested compounds on chondrogenesis could not be confirmed in human MSCs, the hypertrophic capacities of BMP2, GDF5 and GDF5 mutants were evaluated in combination with TGFβ3 in the same system. A reduced hypertrophic induction potential for the GDF5 mutants compared to GDF5 and BMP2 was observed: Indeed, GDF5 and BMP2 showed the strongest ALP activity. In addition, the type 10 collagen staining was positive only in presence of BMP2 or GDF5 (Figure 42). Regarding type 10 collagen in human MSCs, all culture conditions containing TGFβ3 showed the same gene expression profile (Figure 42) while only the cells treated with TGFβ3 together with BMP2 or GDF5 showed a positive immunostaining. The reason for this is unclear. Although, the mRNA level can give a suggestion that the protein is produced, it is known that sometimes mRNA levels and their corresponding protein levels are only weakly correlated [180-182] due to post transcriptional regulations [182-183]. Overall, a reduced hypertrophic induction potential for the GDF5 mutants having a higher binding selectivity towards BMPR1b compared to BMPR1a could be confirmed in human MSCs (Figure 42). Regarding the hypertrophic differentiation in human MSCs in presence of GDF5, our results are in accordance with the literature. Coleman and co-workers for example reported an increased ALP and type 10 collagen production (analyzed by western blot) in presence of GDF5 + TGFβ3 in comparison to TGFβ3 alone. Similarly, Murphy and colleagues showed an increased type 10 collagen expression with GDF5+TGFβ1 and BMP2+TGFβ1 in comparison to TGFβ1 alone but no positive staining for type 10 collagen. However, they used an aggregate culture over 7 days only [134] which might be too short to observe any type 10 collagen accumulation.

To further characterize the therapeutic potential of the GDF5 mutants, their osteogenic capacities were analyzed and compared to GDF5 and BMP2. Osteogenesis of the murine stem cell line C3H10T1/2 was performed in monolayer cultures. The cells were treated with the GDF5 mutants, GDF5 or BMP2 over 28 days in a standard culture medium. Osteocalcin expression and ALP activity were upregulated only in the presence of BMP2, but not in the presence of GDF5 and GDF5 mutants for up to 28 days. An alizarin red staining indicating matrix mineralization was not detectable with any of the tested compounds over 28 days (Figure 37). To enhance osteogenesis of C3H10T1/2 cells, an osteogenic medium was used which contains the typical supplements dexamethasone, ascorbate-2-phosphate and β-glycerolphosphate. These supplements are well-known for imitating the actions of several substances

which are present in vivo and supporting osteogenic differentiation of MSCs [184]. ALP activity of the C3H10T1/2 cells was only detectable in the presence of BMP2, but not in the presence of GDF5 or GDF5 mutants. The expression of osteocalcin was the strongest in the presence of BMP2, less pronounced with GDF5 and not detectable with the GDF5 mutants. In addition, matrix mineralization of C3H10T1/2 cells appeared in the presence of BMP2 at day 14, followed by GDF5 at day 21 and the GDF5 mutants M1673 and W417F at day 28. No matrix mineralization was observed in the presence of W417R and in unstimulated cells cultured in osteogenic medium (Figure 38). These results indicate that BMP2 is more osteogenic than GDF5 and confirmed a reduced osteogenicity of the GDF5 mutants compared to GDF5. The reduced osteogenicity corresponds with a higher BMPR1a/BMPR1b ratio of the compounds. In accordance to these results, Date and co-workers demonstrated an enhanced osteocalcin expression and ALP activity after cultivation of the murine stem cell line in a standard culture medium containing BMP2 [173]. The osteogenic effect of BMP2 was also confirmed by two other research groups. Both demonstrated that GDF5 did not influence the osteocalcin expression and ALP activity of the murine stem cell line cultured in standard culture medium [185-186]. Lastly and in accordance to the data of the present work, Kaps and colleagues demonstrated a reduced osteogenicity of GDF5 compared to BMP2 in C3H10T1/2 cells cultured in osteogenic medium. They showed a less pronounced ALP staining and osteocalcin expression in the presence of GDF5 compared to BMP2 [130]. Others also demonstrated that BMP2 is more osteogenic than GDF5 in C3H10T1/2 cells [185, 187].

These new findings were confirmed in human mesenchymal stem cells. Osteogenesis of the human MSCs was performed in monolayer cultures. The cells were treated with GDF5 mutants, GDF5 or BMP2 over 28 days in a standard culture medium. In contrast to the murine stem cell line, neither the ALP activity, nor the osteopontin or osteocalcin expression was enhanced, not even with BMP2. In accordance to the murine results, an alizarin staining was not detected with any compound over 28 days (Figure 43). Next, the human MSCs were cultured as described above, but in osteogenic medium. The ALP activity as well as the expression of osteopontin and osteocalcin was upregulated in the presence of BMP2, but not in the presence of GDF5 or the GDF5 mutants for up to 28 days. In addition, the earliest alizarin red staining was observed in the presence of BMP2 at day 14, followed by GDF5 at day 21, followed by M1673 and W417F at day 28. No alizarin red staining was detectable in the presence of W417R and in unstimulated cells cultured in osteogenic medium (Figure 44). These results confirmed that BMP2 is more osteogenic than GDF5 and that GDF5 is more osteogenic than the GDF5 mutants. It was also observed that the reduced osteogenicity of the GDF5 mutants compared to GDF5 and BMP2 corresponds to a higher BMPR1a/BMPR1b ratio. In contrast to the results of the presented work, Kleinschmidt and co-workers detected an alizarin red staining and an ALP activity in human MSCs already by culturing them in osteogenic medium for 21 days, in absence of BMP stimulation [188]. They showed that the stimulation with BMP2 or GDF5 did not result in a significantly higher osteogenic differentiation in addition of the

induction observed with osteogenic medium alone [188]. An explanation could be that in comparison to the present work a 10-fold higher concentration of dexamethasone was used, which is known to be necessary to stimulate osteogenesis in in vitro cultures of human MSCs [184]. This elevated dexamethasone concentration might have shielded the effect of GDF5 and BMP2. In accordance to the results of the present work, Marupanthorn and colleagues demonstrated an enhanced osteogenic differentiation of human MSCs after stimulation with BMP2 compared to that in osteogenic medium alone [189]. The effects of GDF5 and BMP2 were hardly compared in human MSCs. To the best of our knowledge, only Kwon and colleagues compared their effects. However, they showed an enhanced osteogenic differentiation with GDF5 compared to BMP2 stimulation [190].

In summary, M1673 was the GDF5 mutant with the strongest chondrogenic induction potential. Chondrogenesis was lower with M1673 compared to GDF5, but M1673 showed advantages over GDF5. Indeed, M1673 showed a reduced hypertrophic and osteogenic capacity compared to GDF5.
Regarding the role of BMPR1a and BMPR1b in osteogenesis and chondrogenesis, it was shown that the ability of BMPs to stimulate cartilage or bone formation is not regulated by their single binding for BMPR1a or BMPR1b per se, but rather by their BMPR1a/BMPR1b ratio. Provided that a sufficient BMPR1a binding is given, compounds having a higher BMPR1a/BMPR1b ratio showed stronger chondrogenic and reduced hypertrophic and osteogenic capacities. As the results from the present work showed a critical role of BMPR1a not only for osteogenesis, but also for chondrogenesis, BMPR1a and BMPR1b could have respective supporting functions rather than controlling distinct pathways. Additional indications for this suggestion is given by the fact that BMPR1a and BMPR1b transmit their signals by activation of the same downstream pathways. It would be possible that BMPR1a promote differentiation processes including chondrogenesis, hypertrophy and osteogenesis, whereas BMPR1b would initiate fine-tuning mechanisms to control these differentiation processes.

6.3 M1673 as a possible DMOAD candidate

M1673 was shown to stimulate the ECM production of mature chondrocytes including bovine, porcine and human OA chondrocytes. In addition, M1673 strongly activated mesenchymal stem cells to differentiate into chondrocytes and simultaneously prevented them to undergo hypertrophic differentiation. In addition, osteogenesis of mesenchymal stem cells was delayed with M1673 compared to GDF5.

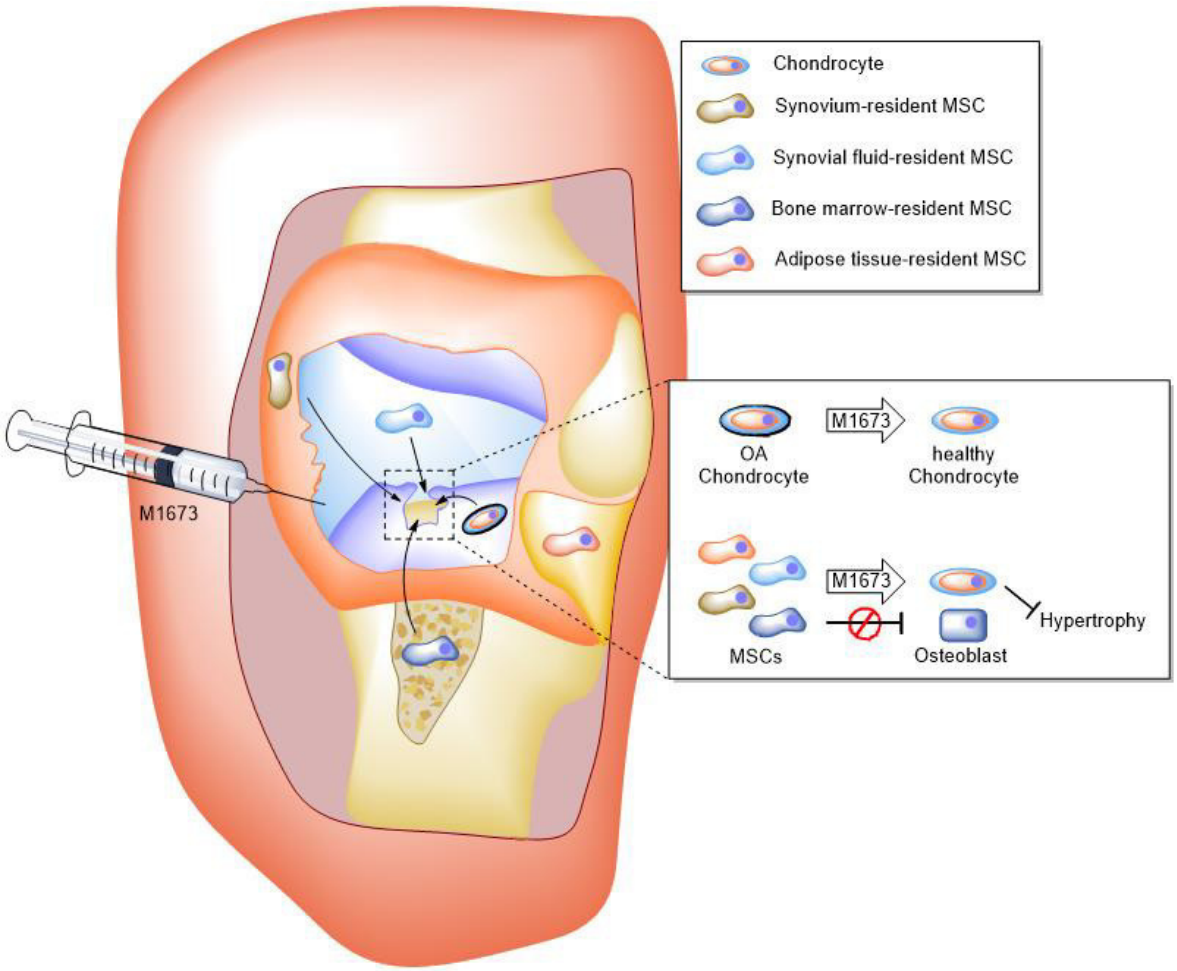

Figure 45 **An intra-articular injection of M1673 might have a therapeutic potential as a possible DMOAD.** The intra-articular application of M1673 could regenerate damaged OA cartilage. M1673 has a positive impact on OA chondrocytes and probably activates mesenchymal stem cells from several joint niches to differentiate into chondrocytes, but without inducing them to undergo hypertrophic or osteogenic differentiation. MSCs = mesenchymal stem cells; OA chondrocyte = osteoarthritic chondrocyte having only low extracellular matrix molecules and produce high levels of proinflammatory cytokines and proteases; healthy chondrocyte = produce extracellular matrix molecules and only low levels of proinflammatory cytokines and proteases.

Taken together, M1673 was evaluated in the present work to be the GDF5 mutant with the greatest therapeutic potential to induce regeneration of OA cartilage and could therefore considered as a possible DMOAD candidate. From the results of the present work, it can be suggested that the intra-articular injection of M1673 could have two positive aspects. First, it will stimulate the OA chondrocytes within the cartilage to produce ECM resulting in a regeneration of the damaged cartilage. Second, it will activate MSCs from several joint niches to migrate to the damaged cartilage and will induce their chondrogenesis which will contribute to the regeneration of the OA cartilage. This regenerated cartilage will be hyaline cartilage as M1673 prevents hypertrophy of MSCs and consequently mineralization and hardening of the regenerated cartilage. Moreover, M1673 will prevent osteogenesis of the MSCs suggesting that there would be no unwanted osteophyte formation in vivo in contrary to what was previously demonstrated for GDF5 [3].

7 Future perspectives

The aim of the work presented herein was to evaluate the therapeutic potential of three GDF5 mutants M1673, W417F and W417R in vitro and to compare them to GDF5. The results of this work demonstrated that M1673 has a greater therapeutic potential as a DMOAD than the two other GDF5 mutants but also than GDF5 itself. Indeed, M1673 has similar anabolic and chondrogenic properties but a reduced hypertrophy and osteogenicity compared to GDF5 and therefore might have a higher potential for cartilage regeneration.

For future investigations, it would be interesting to further investigate the mode of action of M1673. Two signal pathways are described for BMPs, the SMAD-dependent pathway and the non-SMAD pathway through MAPKs [110]. Both pathways are probably necessary for inducing chondrogenesis or osteogenesis. However, most of the literature concerning downstream pathways of BMPs focus on the SMAD-dependent pathway, whereas the non-SMAD pathway remains not fully understood. A crosstalk between the SMAD-dependent and the non-SMAD pathways also probably exists. Moreover, the distinct mode of receptor oligomerization seems to determine which of the both pathways are activated. The binding of BMPs to preformed receptor complexes (PFC) induces the SMAD-dependent pathway. In contrast, the formation of a BMP induced receptor complex (BISC) activates mainly the MAPK pathway, but is also able to activate the SMAD-dependent pathway [126, 167].

Both, GDF5 and BMP2, are described to activate the phosphorylation of SMAD1/5/8 [131, 154, 157]. A 10-fold higher concentration of GDF5 was needed to induce a SMAD phosphorylation level, which was comparable to that induced by BMP2. Furthermore, GDF5 and BMP2 are described to activate the phosphorylation of the MAPKs, p38 [191-192] and ERK [192-193] at similar levels [131, 191]. The MAPKs, p38 and ERK, modulate the SMAD-dependent pathway probably by mediating the proteasomal degradation of SMAD1/5/8 [126, 194-195]. The MAPK JNK was shown to be neither phosphorylated by GDF5 nor by BMP2 [191].

During the present work, the investigation of the activation of signaling pathways by GDF5, GDF5 mutants and BMP2 was already started. The goal was to evaluate whether the compounds with different BMPR1a/BMPR1b binding profiles activate differently the SMAD or the MAPK pathways and what is the role of these two signaling pathways in chondrogenesis or osteogenesis. Human chondrocytes would have been the material of choice for this study but because of the high donor variability and the lack of responsiveness of the hOAC in monolayer, this option was excluded. Another possibility would have been to differentiate MSCs into cartilage and bone cells and subsequently analyze signaling pathway activations. However, there is also a high donor variability and it is difficult to determine a time point for these analyses - it would be possible that several time points are necessary. Finally, it was decided to use a human chondrogenic and a human osteogenic cell line.

It was first tested which cell lines show an expression of all BMP receptors, especially of the weakly expressed BMPR1b. On this basis, the osteoblast-like cell line Saos-2 and the chondrocyte cell line HCS2/8 were selected for signaling pathway analyses. The osteoblast-like cell line Saos-2 was derived from an osteosarcoma, it is known to react to anabolic factors and to preserve a typical osteoblastic phenotype closely related to that of primary human osteoblasts [196-197]. However, this osteoblast-like cell line has to be stimulated with an osteogenic medium containing ascorbic acid and β-glycerolphosphate to induce terminal differentiation and mineralization of the cells [198-199]. Unfortunately, the assay validation was not successful and the focus was subsequently placed on the chondrogenic cell line. The HCS2/8 cell line was derived from a human chondrosarcoma, it was shown to react to anabolic factors and it is known to preserve a chondrocyte phenotype closely related to that of primary human chondrocytes [200-201]. During the present work, it was shown that HCS2/8 cells are responsive to GDF5, GDF5 mutants and BMP2. The expected signaling pathways (SMAD1/5/8, p38 and ERK) were activated, while JNK was not activated by the compounds. However, a robust and reproducible differential activation by the different compounds was only detectable for the SMAD1/5/8 activation. A stronger phosphorylation of SMAD1/5/8 was detectable for the compounds having a higher BMPR1a affinity (data not shown). That observation is in accordance with a previous study by Klammert and colleagues [131]. For future investigations, it would be interesting to demonstrate robust different activation patterns of the tested compounds for p38 and ERK and also to analyze the downstream pathways in a suitable osteogenic cell line. That could enable to better understand the different roles of BMPR1a and BMPR1b on downstream activation and the role of these pathways in chondrogenesis and osteogenesis.

On the other hand, the present work focused on in vitro assays to evaluate the therapeutic potential of the GDF5 mutants compared to GDF5. It is a crucial question whether M1673 will also show promising results in vivo.

Before analyzing the efficacy of M1673 on the disease by using an OA animal model, an ectopic mouse model would offer a possibility to confirm the in vitro data of the present work regarding mutant selection. An ectopic mouse model offers advantageous over an OA animal model by being faster and outcomes are easier to measure. In addition, fewer animals are needed and a larger number of compounds can be analyzed compared to an OA animal model. That could enable to show the superiority of M1673 over the other GDF5 mutants and GDF5 also in vivo with the aim to start an OA animal model only with one compound – M1673.

Commonly used are immune-deficient mice like SCID mice, which permit a xenogene implantation of human derived cells or tissues [202-203]. For the above-mentioned purpose, two different cell types could be used for subcutaneous implantation in the dorsum of SCID mice. Firstly, human OA chondrocytes (hOAC) could be implanted to confirm that the treatment with M1673 led to a better phenotype maintenance of hyaline cartilage compared to the treatment with GDF5. Secondly, human mesenchymal

stem cells (human MSCs) could be implanted to confirm in addition that M1673 is less osteogenic compared to GDF5. Both approaches are suitable to compare the chondrogenic potential of M1673 with the other GDF5 mutants and GDF5.

In more details, hOAC as well as human MSCs could be pre-inducted with the compounds in in vitro pellet cultures for two to six weeks, followed by a subcutaneous implantation time for four to eight weeks. For human MSCs, it is described that this kind of model rather lead to a calcification of the implants than to maintain a stable cartilage structure [204] allowing to investigate the osteogenic potential of the compounds. One option to reach a stable ectopic chondrogenesis of human MSCs was described to be a longer in vitro pre-differentiation of 12 weeks, which allows a nearly complete pronounced chondrogenic differentiation stage in vivo [205]. The pre-induction with the compounds in vitro results in the production of extracellular cartilage matrix, which varies between the different compound stimulations. Thus, the in vitro pre-induction method allows to analyze what happens with the pre-formed pellets in vivo.

An alternative could be to analyze the effects of the compounds directly in vivo without previous in vitro pre-induction. Therefore, both cell types should be polymerized in a fibrin/thrombin mixture, which is supplemented with the compounds respectively to ensure a permanent compound supply after implantation. Moreover, it would be possible to encapsulate these constructs in alginate, which imitate the chondrogenic environment and was shown to enhance chondrogenesis in vivo compared to non-encapsulated pellets [202]. In addition, the encapsulation prevents inter alia the degradation of the compounds by immune cells of the mice [202]. Indeed, SCID mice are deficient for B- and T-lymphocytes, but they still contain macrophages, granulocytes and NK-cells.

The explanted constructs should be analyzed for chondrogenic markers like Safranin O staining or type 2 collagen immunohistochemistry as well as for hypertrophic and osteogenic markers like alizarin red staining or immunohistochemistry of type 1 and 10 collagens.

Based on that it would be possible to demonstrate the beneficial effects of M1673 over the other GDF5 mutants as well as over GDF5 also in vivo. Moreover, the above described approaches using human MSCs could be also interesting for cartilage tissue engineering analyses for example for the treatment of cartilage injuries.

OA animal models are indispensable to provide proof of concept data before starting human clinical trials [206]. They should be used to analyze the efficacy of M1673 on osteoarthritis. OA animal models can be divided into spontaneous and induced ones. Spontaneous models display the slow development of OA closely related to the human situation, but they require a long time and are expensive. Induced OA models rather mimicking the post-traumatic OA development, can be performed chemically or surgically and are much shorter compared to spontaneous models [207]. Chemically induced OA models are performed by intra-articular application of a toxin or inflammatory compound into the joint and are

primary used to evaluate the symptomatic effect of drugs [207]. In contrast, surgically induced OA models are performed by a surgery leading to joint destabilization/changes and enable to analyze structural and symptomatic effects of drugs.

As a first step, the efficacy of M1673 could be evaluated in small animals like mice, rats, rabbits or guinea pigs. Recently it was demonstrated by Parrish and colleagues that the intra-articular application of GDF5 reversed OA progression and stimulated cartilage repair in a surgically induced OA rat model using medial meniscus transection [3]. Based on this, it would be recommended to use the same rat model to evaluate the therapeutic potential of M1673 on OA in vivo. After the therapeutic effect of M1673 has been demonstrated in small animals, larger animal OA models using dogs, sheep's, goats or horses should be performed. This could confirm the efficacy of M1673 in animals having joints, which are closer related to human joints and thus better mimic the human scenario [206-207] and to set up better predictions of the drug dosing in humans.

Before starting clinical trials, it would be interesting to propose a strategy to classify patient subgroups, which could potentially show a higher benefit from a potential M1673 treatment. That classification could for example be performed based on the patient's genotype. GDF5 was shown to be a susceptibility gene for OA. Single nucleotide polymorphisms (SNPs), rs143383 and rs143384, were identified within the promoter sequence of the human GDF5 gene. Both SNPs lead to a C/T transition substitution. The risk allele thymine was shown to reduce the expression of GDF5 within the whole joint [208], which in turn is associated with a 1.3- to 1.8-fold higher risk for developing OA [136]. It can be suggested that hOAC from donors bearing the thymine allele will have a reduced GDF5 expression and could show a higher response to the application of exogenous GDF5 or M1673. It would be interesting to correlate the SNPs of hOAC isolated from different patients with their responsiveness to GDF5 and M1673 in vitro. If a positive correlation is seen, it could be proposed to perform a similar analysis in the clinical setting to possibly identify high responders. For the present work, hOAC from ten donors were analyzed for their SNPs and correlated to their responsiveness to GDF5 and M1673. Unfortunately, the weak and inconsistent response to the compounds in monolayer culture did not enable to establish a correlation. Moreover, ten different hOAC cultured in alginate beads were also analyzed for their SNPs, but a better responsiveness to GDF5 or M1673 of hOAC having the risk allele thymine was not observable (data not shown). However, these correlation experiments in vitro should be performed with a much larger sample size to reach a sufficient statistical power.

8 References

[1] B. Appel, J. Baumer, D. Eyrich, H. Sarhan, S. Toso, C. Englert, D. Skodacek, S. Ratzinger, S. Grässel, A. Goepferich, T. Blunk, Synergistic effects of growth and differentiation factor-5 (GDF-5) and insulin on expanded chondrocytes in a 3-D environment, *Osteoarthritis and Cartilage* **2009**, *17*, 1503-1512.

[2] B. I. Ayerst, R. A. A. Smith, V. Nurcombe, A. J. Day, C. L. R. Merry, S. M. Cool, Growth Differentiation Factor 5-Mediated Enhancement of Chondrocyte Phenotype Is Inhibited by Heparin: Implications for the Use of Heparin in the Clinic and in Tissue Engineering Applications, *Tissue Engineering. Part A* **2017**, *23*, 275-292.

[3] W. R. Parrish, B. A. Byers, D. Su, J. Geesin, U. Herzberg, S. Wadsworth, A. Bendele, B. Story, Intra-articular therapy with recombinant human GDF5 arrests disease progression and stimulates cartilage repair in the rat medial meniscus transection (MMT) model of osteoarthritis, *Osteoarthritis Cartilage* **2017**, *25*, 554-560.

[4] L. Enochson, J. Stenberg, M. Brittberg, A. Lindahl, GDF5 reduces MMP13 expression in human chondrocytes via DKK1 mediated canonical Wnt signaling inhibition, *Osteoarthritis Cartilage* **2014**, *22*, 566-577.

[5] C. M. Coleman, E. E. Vaughan, D. C. Browe, E. Mooney, L. Howard, F. Barry, Growth differentiation factor-5 enhances in vitro mesenchymal stromal cell chondrogenesis and hypertrophy, *Stem cells and development* **2013**, *22*, 1968-1976.

[6] M. Ondrésik, F. R. Azevedo Maia, A. da Silva Morais, A. C. Gertrudes, A. H. Dias Bacelar, C. Correia, C. Gonçalves, H. Radhouani, R. Amandi Sousa, J. M. Oliveira, R. L. Reis, Management of knee osteoarthritis. Current status and future trends, *Biotechnology and Bioengineering* **2017**, *114*, 717-739.

[7] D. Felson, J. Niu, B. Sack, P. Aliabadi, C. McCullough, M. C. Nevitt, Progression of osteoarthritis as a state of inertia, *Ann Rheum Dis* **2013**, *72*, 924-929.

[8] J. R. Kirwan, C. J. Elson, Is the progression of osteoarthritis phasic? Evidence and implications, *The Journal of rheumatology* **2000**, *27*, 834-836.

[9] G. S. Man, G. Mologhianu, Osteoarthritis pathogenesis – a complex process that involves the entire joint, *Journal of Medicine and Life* **2014**, *7*, 37-41.

[10] R. Plotnikoff, N. Karunamuni, E. Lytvyak, C. Penfold, D. Schopflocher, I. Imayama, S. T. Johnson, K. Raine, Osteoarthritis prevalence and modifiable factors: a population study, *BMC Public Health* **2015**, *15*, 1195.

[11] I. J. Wallace, S. Worthington, D. T. Felson, R. D. Jurmain, K. T. Wren, H. Maijanen, R. J. Woods, D. E. Lieberman, Knee osteoarthritis has doubled in prevalence since the mid-20th century, *Proceedings of the National Academy of Sciences of the United States of America* **2017**, *114*, 9332-9336.

[12] G. Musumeci, F. C. Aiello, M. A. Szychlinska, M. Di Rosa, P. Castrogiovanni, A. Mobasheri, Osteoarthritis in the XXIst Century: Risk Factors and Behaviours that Influence Disease Onset and Progression, *International Journal of Molecular Sciences* **2015**, *16*, 6093-6112.

[13] E. R. Vina, D. Ran, E. L. Ashbeck, C. Ratzlaff, C. K. Kwoh, Race, sex, and risk factors in radiographic worsening of knee osteoarthritis, *Seminars in Arthritis and Rheumatism* **2017**.

[14] D. Chen, J. Shen, W. Zhao, T. Wang, L. Han, J. L. Hamilton, H.-J. Im, Osteoarthritis: toward a comprehensive understanding of pathological mechanism, *Bone Research* **2017**, *5*, 16044.

[15] D. J. Hunter, L. Sharma, T. Skaife, Alignment and osteoarthritis of the knee, *The Journal of bone and joint surgery. American volume* **2009**, *91 Suppl 1*, 85-89.

[16] W. Zhang, H. Ouyang, C. R. Dass, J. Xu, Current research on pharmacologic and regenerative therapies for osteoarthritis, *Bone Research* **2016**, *4*, 15040.

[17] A. Mobasheri, M. Batt, An update on the pathophysiology of osteoarthritis, *Annals of physical and rehabilitation medicine* **2016**, *59*, 333-339.
[18] S. Camarero-Espinosa, B. Rothen-Rutishauser, E. J. Foster, C. Weder, Articular cartilage: from formation to tissue engineering, *Biomaterials science* **2016**, *4*, 734-767.
[19] A. J. Sophia Fox, A. Bedi, S. A. Rodeo, The Basic Science of Articular Cartilage: Structure, Composition, and Function, *Sports Health* **2009**, *1*, 461-468.
[20] Y. Wang, L. Wei, L. Zeng, D. He, X. Wei, Nutrition and degeneration of articular cartilage, *Knee Surgery, Sports Traumatology, Arthroscopy* **2013**, *21*, 1751-1762.
[21] Y. Luo, D. Sinkeviciute, Y. He, M. Karsdal, Y. Henrotin, A. Mobasheri, P. Önnerfjord, A. Bay-Jensen, The minor collagens in articular cartilage, *Protein & Cell* **2017**, *8*, 560-572.
[22] M. L. Tiku, B. Madhan, Preserving the longevity of long-lived type II collagen and its implication for cartilage therapeutics, *Ageing Research Reviews* **2016**, *28*, 62-71.
[23] B. Yue, Biology of the Extracellular Matrix: An Overview, *Journal of glaucoma* **2014**, S20-S23.
[24] M. Rahmati, G. Nalesso, A. Mobasheri, M. Mozafari, Aging and osteoarthritis: Central role of the extracellular matrix, *Ageing Research Reviews* **2017**, *40*, 20-30.
[25] A. Aspberg, The Different Roles of Aggrecan Interaction Domains, *Journal of Histochemistry and Cytochemistry* **2012**, *60*, 987-996.
[26] S. A. Flowers, A. Zieba, J. Örnros, C. Jin, O. Rolfson, L. I. Björkman, T. Eisler, S. Kalamajski, M. Kamali-Moghaddam, N. G. Karlsson, Lubricin binds cartilage proteins, cartilage oligomeric matrix protein, fibronectin and collagen II at the cartilage surface, *Scientific Reports* **2017**, *7*, 13149.
[27] P. J. Roughley, Articular cartilage and changes in arthritis: Noncollagenous proteins and proteoglycans in the extracellular matrix of cartilage, *Arthritis Research* **2001**, *3*, 342-347.
[28] R. E. Wilusz, J. Sanchez-Adams, F. Guilak, The Structure and Function of the Pericellular Matrix of Articular Cartilage, *Matrix biology : journal of the International Society for Matrix Biology* **2014**, *0*, 25-32.
[29] M. L. Tiku, H. E. Sabaawy, Cartilage regeneration for treatment of osteoarthritis: a paradigm for nonsurgical intervention, *Therapeutic Advances in Musculoskeletal Disease* **2015**, *7*, 76-87.
[30] B. Bakker, G. B. Eijkel, R. M. A. Heeren, M. Karperien, J. N. Post, B. Cillero-Pastor, Oxygen-Dependent Lipid Profiles of Three-Dimensional Cultured Human Chondrocytes Revealed by MALDI-MSI, *Analytical chemistry* **2017**, *89*, 9438-9444.
[31] J. Fernandez-Torres, Y. Zamudio-Cuevas, G. A. Martinez-Nava, A. G. Lopez-Reyes, Hypoxia-Inducible Factors (HIFs) in the articular cartilage: a systematic review, *European review for medical and pharmacological sciences* **2017**, *21*, 2800-2810.
[32] T. Gómez-Leduc, M. Desancé, M. Hervieu, F. Legendre, D. Ollitrault, C. de Vienne, M. Herlicoviez, P. Galéra, M. Demoor, Hypoxia Is a Critical Parameter for Chondrogenic Differentiation of Human Umbilical Cord Blood Mesenchymal Stem Cells in Type I/III Collagen Sponges, *International Journal of Molecular Sciences* **2017**, *18*, 1933.
[33] E. Duval, S. Leclercq, J. M. Elissalde, M. Demoor, P. Galera, K. Boumediene, Hypoxia-inducible factor 1alpha inhibits the fibroblast-like markers type I and type III collagen during hypoxia-induced chondrocyte redifferentiation: hypoxia not only induces type II collagen and aggrecan, but it also inhibits type I and type III collagen in the hypoxia-inducible factor 1alpha-dependent redifferentiation of chondrocytes, *Arthritis and rheumatism* **2009**, *60*, 3038-3048.
[34] J. E. Lafont, S. Talma, C. L. Murphy, Hypoxia-inducible factor 2alpha is essential for hypoxic induction of the human articular chondrocyte phenotype, *Arthritis and rheumatism* **2007**, *56*, 3297-3306.

[35] B. D. Markway, H. Cho, B. Johnstone, Hypoxia promotes redifferentiation and suppresses markers of hypertrophy and degeneration in both healthy and osteoarthritic chondrocytes, *Arthritis research & therapy* **2013**, *15*, R92.
[36] A. C. Hall, E. R. Horwitz, R. J. Wilkins, The cellular physiology of articular cartilage, *Experimental physiology* **1996**, *81*, 535-545.
[37] K. Negoro, S. Kobayashi, K. Takeno, K. Uchida, H. Baba, Effect of osmolarity on glycosaminoglycan production and cell metabolism of articular chondrocyte under three-dimensional culture system, *Clinical and experimental rheumatology* **2008**, *26*, 534-541.
[38] P. G. Bush, A. C. Hall, Passive osmotic properties of in situ human articular chondrocytes within non-degenerate and degenerate cartilage, *Journal of cellular physiology* **2005**, *204*, 309-319.
[39] S. Kobayashi, in *Regenerative Medicine and Tissue Engineering*, InTech, Rijeka, **2013**, p. Ch. 22.
[40] M. Huttu, S. Turunen, V. Sokolinski, V. Tiitu, M. Lammi, R. K. Korhonen, Effects of medium and temperature on cellular responses in the superficial zone of hypo-osmotically challenged articular cartilage, *Journal of functional biomaterials* **2012**, *3*, 544-555.
[41] A. E. van der Windt, E. Haak, N. Kops, J. A. Verhaar, H. Weinans, H. Jahr, Inhibiting calcineurin activity under physiologic tonicity elevates anabolic but suppresses catabolic chondrocyte markers, *Arthritis and rheumatism* **2012**, *64*, 1929-1939.
[42] S. S. Ozturk, B. O. Palsson, Effect of medium osmolarity on hybridoma growth, metabolism, and antibody production, *Biotechnology and Bioengineering* **1991**, *37*, 989-993.
[43] A. Karim, A. C. Hall, Hyperosmolarity normalises serum-induced changes to chondrocyte properties in a model of cartilage injury, *European cells & materials* **2016**, *31*, 205-220.
[44] D. Le, M. A. Hofbauer, C. A. Towle, Differential effects of hyperosmotic challenge on interleukin-1-activated pathways in bovine articular cartilage, *Archives of biochemistry and biophysics* **2006**, *445*, 1-8.
[45] Z. I. Johnson, I. M. Shapiro, M. V. Risbud, Extracellular osmolarity regulates matrix homeostasis in the intervertebral disc and articular cartilage: evolving role of TonEBP, *Matrix Biol* **2014**, *40*, 10-16.
[46] A. E. van der Windt, E. Haak, R. H. Das, N. Kops, T. J. Welting, M. M. Caron, N. P. van Til, J. A. Verhaar, H. Weinans, H. Jahr, Physiological tonicity improves human chondrogenic marker expression through nuclear factor of activated T-cells 5 in vitro, *Arthritis research & therapy* **2010**, *12*, R100.
[47] H. Jahr, C. Matta, A. Mobasheri, Physicochemical and biomechanical stimuli in cell-based articular cartilage repair, *Current rheumatology reports* **2015**, *17*, 22.
[48] M. M. Caron, A. E. van der Windt, P. J. Emans, L. W. van Rhijn, H. Jahr, T. J. Welting, Osmolarity determines the in vitro chondrogenic differentiation capacity of progenitor cells via nuclear factor of activated T-cells 5, *Bone* **2013**, *53*, 94-102.
[49] B. Poulet, Models to define the stages of articular cartilage degradation in osteoarthritis development, *International Journal of Experimental Pathology* **2017**, *98*, 120-126.
[50] G. Herrero-Beaumont, J. A. Roman-Blas, O. Bruyère, C. Cooper, J. Kanis, S. Maggi, R. Rizzoli, J.-Y. Reginster, Clinical settings in knee osteoarthritis: Pathophysiology guides treatment, *Maturitas* **2017**, *96*, 54-57.
[51] D. McGonagle, T. G. Baboolal, E. Jones, Native joint-resident mesenchymal stem cells for cartilage repair in osteoarthritis, *Nature reviews. Rheumatology* **2017**, *13*, 719-730.
[52] S. Amar, L. Smith, G. B. Fields, Matrix metalloproteinase collagenolysis in health and disease, *Biochimica et Biophysica Acta (BBA) - Molecular Cell Research* **2017**, *1864*, 1940-1951.
[53] L. Troeberg, H. Nagase, Proteases involved in cartilage matrix degradation in osteoarthritis, *Biochimica et biophysica acta* **2012**, *1824*, 133-145.

[54] H. J. Kosasih, K. Last, F. M. Rogerson, S. B. Golub, S. J. Gauci, V. C. Russo, H. Stanton, R. Wilson, S. R. Lamande, P. Holden, A. J. Fosang, A Disintegrin and Metalloproteinase with Thrombospondin Motifs-5 (ADAMTS-5) Forms Catalytically Active Oligomers, *The Journal of Biological Chemistry* **2016**, *291*, 3197-3208.
[55] R. Kelwick, I. Desanlis, G. N. Wheeler, D. R. Edwards, The ADAMTS (A Disintegrin and Metalloproteinase with Thrombospondin motifs) family, *Genome Biology* **2015**, *16*, 113.
[56] C. Y. Yang, A. Chanalaris, L. Troeberg, ADAMTS and ADAM metalloproteinases in osteoarthritis - looking beyond the 'usual suspects', *Osteoarthritis Cartilage* **2017**, *25*, 1000-1009.
[57] H. Li, D. Wang, Y. Yuan, J. Min, New insights on the MMP-13 regulatory network in the pathogenesis of early osteoarthritis, *Arthritis research & therapy* **2017**, *19*, 248.
[58] P. Lu, K. Takai, V. M. Weaver, Z. Werb, Extracellular matrix degradation and remodeling in development and disease, *Cold Spring Harbor perspectives in biology* **2011**, *3*.
[59] B. J. Rose, D. L. Kooyman, A Tale of Two Joints: The Role of Matrix Metalloproteases in Cartilage Biology, *Disease Markers* **2016**, *2016*, 4895050.
[60] J.-F. Budzik, J. Ding, L. Norberciak, T. Pascart, H. Toumi, S. Verclytte, R. Coursier, Perfusion of subchondral bone marrow in knee osteoarthritis: A dynamic contrast-enhanced magnetic resonance imaging preliminary study, *European Journal of Radiology* **2017**, *88*, 129-134.
[61] J. Geurts, A. Patel, M. T. Hirschmann, G. I. Pagenstert, M. Muller-Gerbl, V. Valderrabano, T. Hugle, Elevated marrow inflammatory cells and osteoclasts in subchondral osteosclerosis in human knee osteoarthritis, *Journal of orthopaedic research : official publication of the Orthopaedic Research Society* **2016**, *34*, 262-269.
[62] A. Mathiessen, P. G. Conaghan, Synovitis in osteoarthritis: current understanding with therapeutic implications, *Arthritis research & therapy* **2017**, *19*, 18.
[63] T. Ushiyama, T. Chano, K. Inoue, Y. Matsusue, Cytokine production in the infrapatellar fat pad: another source of cytokines in knee synovial fluids, *Annals of the Rheumatic Diseases* **2003**, *62*, 108-112.
[64] Z. Ge, Y. Hu, B. C. Heng, Z. Yang, H. Ouyang, E. H. Lee, T. Cao, Osteoarthritis and therapy, *Arthritis and rheumatism* **2006**, *55*, 493-500.
[65] M. Rahmati, A. Mobasheri, M. Mozafari, Inflammatory mediators in osteoarthritis: A critical review of the state-of-the-art, current prospects, and future challenges, *Bone* **2016**, *85*, 81-90.
[66] T. Mabey, S. Honsawek, Cytokines as biochemical markers for knee osteoarthritis, *World Journal of Orthopedics* **2015**, *6*, 95-105.
[67] J. Sokolove, C. M. Lepus, Role of inflammation in the pathogenesis of osteoarthritis: latest findings and interpretations, *Therapeutic Advances in Musculoskeletal Disease* **2013**, *5*, 77-94.
[68] S. Grässel, A. Aszódi, *Cartilage: Volume 2: Pathophysiology*, Springer International Publishing, **2017**.
[69] F. Eymard, X. Chevalier, Inflammation of the infrapatellar fat pad, *Joint Bone Spine* **2016**, *83*, 389-393.
[70] O.-M. Aho, M. Finnilä, J. Thevenot, S. Saarakkala, P. Lehenkari, Subchondral bone histology and grading in osteoarthritis, *PLoS ONE* **2017**, *12*, e0173726.
[71] P. Das Neves Borges, T. L. Vincent, M. Marenzana, Automated assessment of bone changes in cross-sectional micro-CT studies of murine experimental osteoarthritis, *PLoS ONE* **2017**, *12*, e0174294.
[72] C.-J. Wang, J.-H. Cheng, W.-Y. Chou, S.-L. Hsu, J.-H. Chen, C.-Y. Huang, Changes of articular cartilage and subchondral bone after extracorporeal shockwave therapy in osteoarthritis of the knee, *International Journal of Medical Sciences* **2017**, *14*, 213-223.

[73] C. Liu, C. Liu, X. Ren, L. Si, H. Shen, Q. Wang, W. Yao, Quantitative evaluation of subchondral bone microarchitecture in knee osteoarthritis using 3T MRI, *BMC Musculoskeletal Disorders* **2017**, *18*, 496.
[74] S. Zheng, D. J. Hunter, J. Xu, C. Ding, Monoclonal antibodies for the treatment of osteoarthritis, *Expert Opinion on Biological Therapy* **2016**, *16*, 1529-1540.
[75] E. Utzeri, P. Usai, Role of non-steroidal anti-inflammatory drugs on intestinal permeability and nonalcoholic fatty liver disease, *World Journal of Gastroenterology* **2017**, *23*, 3954-3963.
[76] Z. Varga, S. r. a. Sabzwari, V. Vargova, Cardiovascular Risk of Nonsteroidal Anti-Inflammatory Drugs: An Under-Recognized Public Health Issue, *Cureus* **2017**, *9*, e1144.
[77] M. B. Goldring, F. Berenbaum, Emerging targets in osteoarthritis therapy, *Current Opinion in Pharmacology* **2015**, *22*, 51-63.
[78] S. Bisicchia, C. Tudisco, Hyaluronic acid vs corticosteroids in symptomatic knee osteoarthritis: a mini-review of the literature, *Clinical cases in mineral and bone metabolism : the official journal of the Italian Society of Osteoporosis, Mineral Metabolism, and Skeletal Diseases* **2017**, *14*, 182-185.
[79] P. Wehling, C. Evans, J. Wehling, W. Maixner, Effectiveness of intra-articular therapies in osteoarthritis: a literature review, *Therapeutic Advances in Musculoskeletal Disease* **2017**, *9*, 183-196.
[80] S. E. Gwilym, T. C. Pollard, A. J. Carr, Understanding pain in osteoarthritis, *The Journal of bone and joint surgery. British volume* **2008**, *90*, 280-287.
[81] H. S. Vasiliadis, K. Tsikopoulos, Glucosamine and chondroitin for the treatment of osteoarthritis, *World Journal of Orthopedics* **2017**, *8*, 1-11.
[82] S. Harrison-Munoz, V. Rojas-Briones, S. Irarrazaval, Is glucosamine effective for osteoarthritis?, *Medwave* **2017**, *17*, e6867.
[83] D. J. Hunter, D. T. Felson, Osteoarthritis, *BMJ : British Medical Journal* **2006**, *332*, 639-642.
[84] A. Gigout, H. Guehring, D. Froemel, A. Meurer, C. Ladel, D. Reker, A. C. Bay-Jensen, M. A. Karsdal, S. Lindemann, Sprifermin (rhFGF18) enables proliferation of chondrocytes producing a hyaline cartilage matrix, *Osteoarthritis Cartilage* **2017**, *25*, 1858-1867.
[85] A. Barr, p. conaghan, *Disease-modifying osteoarthritis drugs (DMOADs): what are they and what can we expect from them?, Vol. 35*, **2013**.
[86] M. A. Karsdal, M. Michaelis, C. Ladel, A. S. Siebuhr, A. R. Bihlet, J. R. Andersen, H. Guehring, C. Christiansen, A. C. Bay-Jensen, V. B. Kraus, Disease-modifying treatments for osteoarthritis (DMOADs) of the knee and hip: lessons learned from failures and opportunities for the future, *Osteoarthritis and Cartilage* **2016**, *24*, 2013-2021.
[87] P. Qvist, A.-C. Bay-Jensen, C. Christiansen, E. B. Dam, P. Pastoureau, M. A. Karsdal, The disease modifying osteoarthritis drug (DMOAD): Is it in the horizon?, *Pharmacological Research* **2008**, *58*, 1-7.
[88] B. M. Conaghan PG, Kingsbury SR, Brett A, Guillard G, Jansson Å, Wadell C, Bethell R, Oehd J, Miv-711, a Novel Cathepsin K Inhibitor Demonstrates Evidence of Osteoarthritis Structure Modification: Results from a 6 Month Randomized Double-Blind Placebo-Controlled Phase IIA Trial, *Arthritis Rheumatol* **2017**, *69 (suppl 10)*.
[89] D. S. van der Aar E, Fagard L, De Smet M, Amantini D, Larsson S, Struglics A, Lohmander LS, Vanhoutte F, Desrivot J, Favorable Human Safety, Pharmacokinetics and Pharmacodynamics of the Adamts-5 Inhibitor GLPG1972, a Potential New Treatment in Osteoarthritis, *Arthritis Rheumatol.* **2017**, *69 (suppl 10)*.

[90] B. H. Fleischmann R, Blanco FJ, Schnitzer TJ, Peterfy C, Chen S, Wang L, Conaghan PG, Berenbaum F, Pelletier JP, Martel-Pelletier J, Vaeterlein O, Liu W, Levy G, Zhang L, Medema JK, Levesque MC, Safety and Efficacy of ABT-981, an Anti–Interleukin-1α/β Dual Variable Domain (DVD) Immunoglobulin, in Subjects with Knee Osteoarthritis: Results from the Randomized, Double-Blind, Placebo-Controlled, Parallel-Group Phase 2 Trial, *Arthritis Rheumatol.* **2017**, *69 (suppl 10)*.

[91] M. Kloppenburg, C. Peterfy, I. Haugen, F. Kroon, S. Chen, L. Wang, W. Liu, G. Levy, R. Fleischmann, F. Berenbaum, D. v. d. Heijde, J. Medema, M. Levesque, OP0168 A phase 2a, placebo-controlled, randomized study of ABT-981, an anti-interleukin-1ALPHA and -1BETA dual variable domain immunoglobulin, to treat erosive hand osteoarthritis (EHOA), *Annals of the Rheumatic Diseases* **2017**, *76*, 122-122.

[92] S. X. Wang, S. B. Abramson, M. Attur, M. A. Karsdal, R. A. Preston, C. J. Lozada, M. P. Kosloski, F. Hong, P. Jiang, M. J. Saltarelli, B. A. Hendrickson, J. K. Medema, Safety, tolerability, and pharmacodynamics of an anti-interleukin-1α/β dual variable domain immunoglobulin in patients with osteoarthritis of the knee: a randomized phase 1 study, *Osteoarthritis and Cartilage* **2017**, *25*, 1952-1961.

[93] V. Deshmukh, H. Hu, C. Barroga, C. Bossard, S. Kc, L. Dellamary, J. Stewart, K. Chiu, M. Ibanez, M. Pedraza, T. Seo, L. Do, S. Cho, J. Cahiwat, B. Tam, J. R. S. Tambiah, J. Hood, N. E. Lane, Y. Yazici, A small-molecule inhibitor of the Wnt pathway (SM04690) as a potential disease modifying agent for the treatment of osteoarthritis of the knee, *Osteoarthritis and Cartilage* **2018**, *26*, 18-27.

[94] S. Onuora, Wnt inhibitor shows potential as a DMOAD, *Nature Reviews Rheumatology* **2017**, *13*, 634.

[95] M. T. Yazici Y, Gibofsky A, Lane NE, Clauw DJ, Armas E, Skrepnik N, Swearingen CJ, DiFrancesco A, Tambiah J, Hochberg M, Results from a 52 Week Randomized, Double-Blind, Placebo-Controlled, Phase 2 Study of a Novel, Intra-Articular, Wnt Pathway Inhibitor (SM04690) for the Treatment of Knee Osteoarthritis *Arthritis Rheumatol.* **2017**, *69 (suppl 10)*.

[96] D. J. Hunter, Pharmacologic therapy for osteoarthritis--the era of disease modification, *Nature reviews. Rheumatology* **2011**, *7*, 13-22.

[97] B. Sridharan, B. Sharma, M. S. Detamore, A Road Map to Commercialization of Cartilage Therapy in the United States of America, *Tissue Engineering. Part B, Reviews* **2016**, *22*, 15-33.

[98] L. N. McGuire D, Segal N, Metyas S, Barthel HR, Miller M, Rosen D, Kumagai Y, Significant, Sustained Improvement in Knee Function after Intra-Articular TPX-100: A Double-Blind, Randomized, Multi-Center, Placebo-Controlled Phase 2 Trial, *Arthritis Rheumatol.* **2017**, *69 (suppl 10)*.

[99] M. S. Dhillon, S. Patel, R. John, PRP in OA knee – update, current confusions and future options, *SICOT-J* **2017**, *3*, 27.

[100] E. Knop, L. E. d. Paula, R. Fuller, Platelet-rich plasma for osteoarthritis treatment, *Revista Brasileira de Reumatologia (English Edition)* **2016**, *56*, 152-164.

[101] J. Cho, T. Kim, J. Shin, S. Kang, B. Lee, *A phase III clinical results of INVOSSA™(TissueGene C): A clues for the potential disease modifying OA drug, Vol. 19*, **2017**.

[102] D. P. Tonge, M. J. Pearson, S. W. Jones, The hallmarks of osteoarthritis and the potential to develop personalised disease-modifying pharmacological therapeutics, *Osteoarthritis and Cartilage* **2014**, *22*, 609-621.

[103] D. J. Hunter, M. C. Pike, B. L. Jonas, E. Kissin, J. Krop, T. McAlindon, Phase 1 safety and tolerability study of BMP-7 in symptomatic knee osteoarthritis, *BMC Musculoskelet Disord* **2010**, *11*, 232.

[104] N. Muurahainen, Cartilage repair and the sprifermin story: mechanisms, preclinical and clinical study results, and lessons learned, *Osteoarthritis and Cartilage* **2016**, *24*, S4.

[105] G. A. Hochberg MC, Guehring H, Aydemir A, Wax S, Fleuranceau-Morel P, Bihlet AR, Byrjalsen I, Andersen JR, Eckstein F, Efficacy and Safety of Intra-Articular Sprifermin in Symptomatic Radiographic Knee Osteoarthritis: Results of the 2-Year Primary Analysis from a 5-Year Randomised, Placebo-Controlled, Phase II Study *Arthritis Rheumatol.* **2017**, *69 (suppl 10)*.
[106] M. R. Urist, Bone: formation by autoinduction, *Science (New York, N.Y.)* **1965**, *150*, 893-899.
[107] T. Katagiri, T. Watabe, Bone Morphogenetic Proteins, *Cold Spring Harbor perspectives in biology* **2016**, *8*.
[108] L. Grgurevic, M. Pecina, S. Vukicevic, Marshall R. Urist and the discovery of bone morphogenetic proteins, *International Orthopaedics* **2017**, *41*, 1065-1069.
[109] J. M. Wozney, V. Rosen, A. J. Celeste, L. M. Mitsock, M. J. Whitters, R. W. Kriz, R. M. Hewick, E. A. Wang, Novel regulators of bone formation: molecular clones and activities, *Science (New York, N.Y.)* **1988**, *242*, 1528-1534.
[110] R. N. Wang, J. Green, Z. Wang, Y. Deng, M. Qiao, M. Peabody, Q. Zhang, J. Ye, Z. Yan, S. Denduluri, O. Idowu, M. Li, C. Shen, A. Hu, R. C. Haydon, R. Kang, J. Mok, M. J. Lee, H. L. Luu, L. L. Shi, Bone Morphogenetic Protein (BMP) signaling in development and human diseases, *Genes Dis* **2014**, *1*, 87-105.
[111] M. Beederman, J. D. Lamplot, G. Nan, J. Wang, X. Liu, L. Yin, R. Li, W. Shui, H. Zhang, S. H. Kim, W. Zhang, J. Zhang, Y. Kong, S. Denduluri, M. R. Rogers, A. Pratt, R. C. Haydon, H. H. Luu, J. Angeles, L. L. Shi, T.-C. He, BMP signaling in mesenchymal stem cell differentiation and bone formation, *Journal of biomedical science and engineering* **2013**, *6*, 32-52.
[112] Y. Jing, J. Jing, L. Ye, X. Liu, S. E. Harris, R. J. Hinton, J. Q. Feng, Chondrogenesis and osteogenesis are one continuous developmental and lineage defined biological process, *Scientific Reports* **2017**, *7*, 10020.
[113] B. S. Yoon, D. A. Ovchinnikov, I. Yoshii, Y. Mishina, R. R. Behringer, K. M. Lyons, Bmpr1a and Bmpr1b have overlapping functions and are essential for chondrogenesis in vivo, *Proc Natl Acad Sci U S A* **2005**, *102*, 5062-5067.
[114] I. H. A. Ali, D. P. Brazil, Bone morphogenetic proteins and their antagonists: current and emerging clinical uses, *British Journal of Pharmacology* **2014**, *171*, 3620-3632.
[115] S. Lin, K. K. H. Svoboda, J. Q. Feng, X. Jiang, The biological function of type I receptors of bone morphogenetic protein in bone, *Bone Research* **2016**, *4*, 16005.
[116] A. Hari Reddi, D. Haudenschild, *BMP Family*, **2000**.
[117] G. Sanchez-Duffhues, C. Hiepen, P. Knaus, P. Ten Dijke, Bone morphogenetic protein signaling in bone homeostasis, *Bone* **2015**, *80*, 43-59.
[118] M. S. Rahman, N. Akhtar, H. M. Jamil, R. S. Banik, S. M. Asaduzzaman, TGF-β/BMP signaling and other molecular events: regulation of osteoblastogenesis and bone formation, *Bone Research* **2015**, *3*, 15005.
[119] S. M. Rao, G. M. Ugale, S. B. Warad, Bone Morphogenetic Proteins: Periodontal Regeneration, *North American Journal of Medical Sciences* **2013**, *5*, 161-168.
[120] N. S. Gandhi, R. L. Mancera, Prediction of heparin binding sites in bone morphogenetic proteins (BMPs), *Biochim Biophys Acta* **2012**, *1824*, 1374-1381.
[121] S. Vukicevic, K. T. Sampath, *Bone Morphogenetic Proteins: Systems Biology Regulators*, Springer International Publishing, **2017**.
[122] A. Guzman, M. Z. Femiak, J. H. Boergermann, S. Paschkowsky, P. A. Kreuzaler, P. Fratzl, G. S. Harms, P. Knaus, SMAD versus Non-SMAD Signaling Is Determined by Lateral Mobility of Bone Morphogenetic Protein (BMP) Receptors, *The Journal of Biological Chemistry* **2012**, *287*, 39492-39504.

[123] A. R. Sharma, S. Jagga, S.-S. Lee, J.-S. Nam, Interplay between Cartilage and Subchondral Bone Contributing to Pathogenesis of Osteoarthritis, *International Journal of Molecular Sciences* **2013**, *14*, 19805-19830.
[124] T. Onishi, Y. Ishidou, T. Nagamine, K. Yone, T. Imamura, M. Kato, T. K. Sampath, P. ten Dijke, T. Sakou, Distinct and overlapping patterns of localization of bone morphogenetic protein (BMP) family members and a BMP type II receptor during fracture healing in rats, *Bone* **1998**, *22*, 605-612.
[125] A. Benn, C. Hiepen, M. Osterland, C. Schutte, A. Zwijsen, P. Knaus, Role of bone morphogenetic proteins in sprouting angiogenesis: differential BMP receptor-dependent signaling pathways balance stalk vs. tip cell competence, *FASEB journal : official publication of the Federation of American Societies for Experimental Biology* **2017**, *31*, 4720-4733.
[126] J. B. Maxhimer, J. P. Bradley, J. C. Lee, Signaling pathways in osteogenesis and osteoclastogenesis: Lessons from cranial sutures and applications to regenerative medicine, *Genes & Diseases* **2015**, *2*, 57-68.
[127] H. Zou, R. Wieser, J. Massague, L. Niswander, Distinct roles of type I bone morphogenetic protein receptors in the formation and differentiation of cartilage, *Genes & development* **1997**, *11*, 2191-2203.
[128] M. Ratnayake, M. Tselepi, R. Bloxham, F. Ploger, L. N. Reynard, J. Loughlin, A consistent and potentially exploitable response during chondrogenesis of mesenchymal stem cells from osteoarthritis patients to the protein encoded by the susceptibility gene GDF5, *PLoS One* **2017**, *12*, e0176523.
[129] J. Jing, Y. Ren, Z. Zong, C. Liu, N. Kamiya, Y. Mishina, Y. Liu, X. Zhou, J. Q. Feng, BMP receptor 1A determines the cell fate of the postnatal growth plate, *International journal of biological sciences* **2013**, *9*, 895-906.
[130] C. Kaps, A. Hoffmann, Y. Zilberman, G. Pelled, T. Haupl, M. Sittinger, G. Burmester, D. Gazit, G. Gross, Distinct roles of BMP receptors Type IA and IB in osteo-/chondrogenic differentiation in mesenchymal progenitors (C3H10T1/2), *BioFactors (Oxford, England)* **2004**, *20*, 71-84.
[131] U. Klammert, T. D. Mueller, T. V. Hellmann, K. K. Wuerzler, A. Kotzsch, A. Schliermann, W. Schmitz, A. C. Kuebler, W. Sebald, J. Nickel, GDF-5 can act as a context-dependent BMP-2 antagonist, *BMC biology* **2015**, *13*, 77.
[132] S. Zoricic, I. Maric, D. Bobinac, S. Vukicevic, Expression of bone morphogenetic proteins and cartilage-derived morphogenetic proteins during osteophyte formation in humans, *Journal of Anatomy* **2003**, *202*, 269-277.
[133] A. Kotzsch, J. Nickel, A. Seher, W. Sebald, T. D. Müller, Crystal structure analysis reveals a spring-loaded latch as molecular mechanism for GDF-5–type I receptor specificity, *The EMBO Journal* **2009**, *28*, 937-947.
[134] M. K. Murphy, D. J. Huey, J. C. Hu, K. A. Athanasiou, TGF-beta1, GDF-5, and BMP-2 stimulation induces chondrogenesis in expanded human articular chondrocytes and marrow-derived stromal cells, *Stem cells (Dayton, Ohio)* **2015**, *33*, 762-773.
[135] S. Chubinskaya, D. Segalite, D. Pikovsky, A. A. Hakimiyan, D. C. Rueger, Effects induced by BMPS in cultures of human articular chondrocytes: Comparative studies, *Growth Factors* **2008**, *26*, 275-283.
[136] T. D. Capellini, H. Chen, J. Cao, A. C. Doxey, A. M. Kiapour, M. Schoor, D. M. Kingsley, Ancient selection for derived alleles at a GDF5 enhancer influencing human growth and osteoarthritis risk, *Nature genetics* **2017**, *49*, 1202-1210.
[137] A. W. Dodd, C. M. Syddall, J. Loughlin, A rare variant in the osteoarthritis-associated locus GDF5 is functional and reveals a site that can be manipulated to modulate GDF5 expression, *European Journal of Human Genetics* **2013**, *21*, 517-521.

[138] H. Schreuder, A. Liesum, J. Pohl, M. Kruse, M. Koyama, Crystal structure of recombinant human growth and differentiation factor 5: Evidence for interaction of the type I and type II receptor-binding sites, *Biochemical and biophysical research communications* **2005**, *329*, 1076-1086.
[139] A. M. Khalil, H. Dotimas, J. Kahn, J. E. Lamerdin, D. B. Hayes, P. Gupta, M. Franti, Differential Binding Activity of TGFβ Family Proteins to Select TGFβ Receptors, *Journal of Pharmacology and Experimental Therapeutics* **2016**, *358*, 423-430.
[140] R. Seethala, L. Zhang, *Handbook of Drug Screening, Second Edition*, CRC Press, **2016**.
[141] V. Kamat, A. Rafique, Extending the throughput of Biacore 4000 biosensor to accelerate kinetic analysis of antibody-antigen interaction, *Analytical biochemistry* **2017**, *530*, 75-86.
[142] H. H. Nguyen, J. Park, S. Kang, M. Kim, Surface Plasmon Resonance: A Versatile Technique for Biosensor Applications, *Sensors (Basel, Switzerland)* **2015**, *15*, 10481-10510.
[143] D.-P. Tang, R. Yuan, Y.-Q. Chai, Novel immunoassay for carcinoembryonic antigen based on protein A-conjugated immunosensor chip by surface plasmon resonance and cyclic voltammetry, *Bioprocess and Biosystems Engineering* **2006**, *28*, 315-321.
[144] R. W. Farndale, C. A. Sayers, A. J. Barrett, A direct spectrophotometric microassay for sulfated glycosaminoglycans in cartilage cultures, *Connective tissue research* **1982**, *9*, 247-248.
[145] D. Pfander, B. Swoboda, T. Kirsch, Expression of early and late differentiation markers (proliferating cell nuclear antigen, syndecan-3, annexin VI, and alkaline phosphatase) by human osteoarthritic chondrocytes, *The American journal of pathology* **2001**, *159*, 1777-1783.
[146] J. A. Rees, S. Y. Ali, Ultrastructural localisation of alkaline phosphatase activity in osteoarthritic human articular cartilage, *Annals of the Rheumatic Diseases* **1988**, *47*, 747-753.
[147] N. S. Gudmann, J. Wang, S. Hoielt, P. Chen, A. S. Siebuhr, Y. He, T. G. Christiansen, M. A. Karsdal, A. C. Bay-Jensen, Cartilage Turnover Reflected by Metabolic Processing of Type II Collagen: A Novel Marker of Anabolic Function in Chondrocytes, *International Journal of Molecular Sciences* **2014**, *15*, 18789-18803.
[148] G. Panicker, I. Rajbhandari, B. M. Gurbaxani, T. D. Querec, E. R. Unger, Development and evaluation of multiplexed immunoassay for detection of antibodies to HPV vaccine types, *Journal of immunological methods* **2015**, *417*, 107-114.
[149] E. Arikawa, Y. Sun, J. Wang, Q. Zhou, B. Ning, S. L. Dial, L. Guo, J. Yang, Cross-platform comparison of SYBR(®)Green real-time PCR with TaqMan PCR, microarrays and other gene expression measurement technologies evaluated in the MicroArray Quality Control (MAQC) study, *BMC Genomics* **2008**, *9*, 328-328.
[150] T. B. Morrison, J. J. Weis, C. T. Wittwer, Quantification of low-copy transcripts by continuous SYBR Green I monitoring during amplification, *BioTechniques* **1998**, *24*, 954-958, 960, 962.
[151] E. Barbau-Piednoir, N. Botteldoorn, M. Yde, J. Mahillon, N. H. Roosens, Development and validation of qualitative SYBR®Green Real-Time PCR for detection and discrimination of Listeria spp. and Listeria monocytogenes, *Applied Microbiology and Biotechnology* **2013**, *97*, 4021-4037.
[152] K. J. Livak, T. D. Schmittgen, Analysis of relative gene expression data using real-time quantitative PCR and the 2(-Delta Delta C(T)) Method, *Methods (San Diego, Calif.)* **2001**, *25*, 402-408.
[153] K. Bobacz, R. Gruber, A. Soleiman, W. B. Graninger, F. P. Luyten, L. Erlacher, Cartilage-derived morphogenetic protein-1 and -2 are endogenously expressed in healthy and osteoarthritic human articular chondrocytes and stimulate matrix synthesis, *Osteoarthritis Cartilage* **2002**, *10*, 394-401.
[154] M. Ratnayake, F. Plöger, M. Santibanez-Koref, J. Loughlin, Human Chondrocytes Respond Discordantly to the Protein Encoded by the Osteoarthritis Susceptibility Gene GDF5, *PLOS ONE* **2014**, *9*, e86590.

[155] F. De Ceuninck, C. Lesur, P. Pastoureau, A. Caliez, M. Sabatini, Culture of chondrocytes in alginate beads, *Methods in molecular medicine* **2004**, *100*, 15-22.
[156] B. Mohanraj, A. J. Farran, R. L. Mauck, G. R. Dodge, Time-dependent functional maturation of scaffold-free cartilage tissue analogs, *Journal of biomechanics* **2014**, *47*, 2137-2142.
[157] K. S. Vanderman, R. F. Loeser, S. Chubinskaya, A. Anderson, C. M. Ferguson, Reduced Response of Human Meniscal Cells to Osteogenic Protein 1 during Osteoarthritis and Pro-inflammatory Stimulation, *Osteoarthritis and cartilage / OARS, Osteoarthritis Research Society* **2016**, *24*, 1036-1046.
[158] R. F. Loeser, U. Gandhi, D. L. Long, W. Yin, S. Chubinskaya, Aging and oxidative stress reduce the response of human articular chondrocytes to insulin-like growth factor 1 and osteogenic protein 1, *Arthritis Rheumatol* **2014**, *66*, 2201-2209.
[159] S. Ströbel, M. Loparic, D. Wendt, A. D. Schenk, C. Candrian, R. L. P. Lindberg, F. Moldovan, A. Barbero, I. Martin, Anabolic and catabolic responses of human articular chondrocytes to varying oxygen percentages, *Arthritis research & therapy* **2010**, *12*, R34.
[160] S. Kanzaki, W. Ariyoshi, T. Takahashi, T. Okinaga, T. Kaneuji, S. Mitsugi, K. Nakashima, T. Tsujisawa, T. Nishihara, Dual effects of heparin on BMP-2-induced osteogenic activity in MC3T3-E1 cells, *Pharmacological reports : PR* **2011**, *63*, 1222-1230.
[161] T. Takada, T. Katagiri, M. Ifuku, N. Morimura, M. Kobayashi, K. Hasegawa, A. Ogamo, R. Kamijo, Sulfated polysaccharides enhance the biological activities of bone morphogenetic proteins, *J Biol Chem* **2003**, *278*, 43229-43235.
[162] B. Zhao, T. Katagiri, H. Toyoda, T. Takada, T. Yanai, T. Fukuda, U. I. Chung, T. Koike, K. Takaoka, R. Kamijo, Heparin potentiates the in vivo ectopic bone formation induced by bone morphogenetic protein-2, *J Biol Chem* **2006**, *281*, 23246-23253.
[163] A. Gigout, M. Jolicoeur, M. Nelea, N. Raynal, R. Farndale, M. D. Buschmann, Chondrocyte aggregation in suspension culture is GFOGER-GPP- and beta1 integrin-dependent, *J Biol Chem* **2008**, *283*, 31522-31530.
[164] A. I. Tsuchida, M. Beekhuizen, M. C. 't Hart, T. R. D. J. Radstake, W. J. A. Dhert, D. B. F. Saris, G. J. V. M. van Osch, L. B. Creemers, Cytokine profiles in the joint depend on pathology, but are different between synovial fluid, cartilage tissue and cultured chondrocytes, *Arthritis research & therapy* **2014**, *16*, 441.
[165] K. L. Bertram, R. J. Krawetz, Osmolarity regulates chondrogenic differentiation potential of synovial fluid derived mesenchymal progenitor cells, *Biochemical and biophysical research communications* **2012**, *422*, 455-461.
[166] C. Baugé, K. Boumédiene, Use of Adult Stem Cells for Cartilage Tissue Engineering: Current Status and Future Developments, *Stem Cells International* **2015**, *2015*, 438026.
[167] K. Heinecke, A. Seher, W. Schmitz, T. D. Mueller, W. Sebald, J. Nickel, Receptor oligomerization and beyond: a case study in bone morphogenetic proteins, *BMC biology* **2009**, *7*, 59.
[168] C. A. Reznikoff, D. W. Brankow, C. Heidelberger, Establishment and characterization of a cloned line of C3H mouse embryo cells sensitive to postconfluence inhibition of division, *Cancer research* **1973**, *33*, 3231-3238.
[169] R. Takacs, C. Matta, C. Somogyi, T. Juhasz, R. Zakany, Comparative analysis of osteogenic/chondrogenic differentiation potential in primary limb bud-derived and C3H10T1/2 cell line-based mouse micromass cultures, *Int J Mol Sci* **2013**, *14*, 16141-16167.
[170] L. Zhao, G. Li, K. M. Chan, Y. Wang, P. F. Tang, Comparison of multipotent differentiation potentials of murine primary bone marrow stromal cells and mesenchymal stem cell line C3H10T1/2, *Calcified tissue international* **2009**, *84*, 56-64.

[171] H. Huang, T.-J. Song, X. Li, L. Hu, Q. He, M. Liu, M. D. Lane, Q.-Q. Tang, BMP signaling pathway is required for commitment of C3H10T1/2 pluripotent stem cells to the adipocyte lineage, *Proceedings of the National Academy of Sciences* **2009**, *106*, 12670-12675.
[172] S. S. Wang, H. Y. Huang, S. Z. Chen, X. Li, W. T. Zhang, Q. Q. Tang, Gdf6 induces commitment of pluripotent mesenchymal C3H10T1/2 cells to the adipocyte lineage, *The FEBS journal* **2013**, *280*, 2644-2651.
[173] T. Date, Y. Doiguchi, M. Nobuta, H. Shindo, Bone morphogenetic protein-2 induces differentiation of multipotent C3H10T1/2 cells into osteoblasts, chondrocytes, and adipocytes in vivo and in vitro, *Journal of orthopaedic science : official journal of the Japanese Orthopaedic Association* **2004**, *9*, 503-508.
[174] A. E. Denker, A. R. Haas, S. B. Nicoll, R. S. Tuan, Chondrogenic differentiation of murine C3H10T1/2 multipotential mesenchymal cells: I. Stimulation by bone morphogenetic protein-2 in high-density micromass cultures, *Differentiation; research in biological diversity* **1999**, *64*, 67-76.
[175] L. Erlacher, J. McCartney, E. Piek, P. ten Dijke, M. Yanagishita, H. Oppermann, F. P. Luyten, Cartilage-derived morphogenetic proteins and osteogenic protein-1 differentially regulate osteogenesis, *Journal of bone and mineral research : the official journal of the American Society for Bone and Mineral Research* **1998**, *13*, 383-392.
[176] Y. Kawakami, T. Ishikawa, M. Shimabara, N. Tanda, M. Enomoto-Iwamoto, M. Iwamoto, T. Kuwana, A. Ueki, S. Noji, T. Nohno, BMP signaling during bone pattern determination in the developing limb, *Development (Cambridge, England)* **1996**, *122*, 3557-3566.
[177] M. B. Mueller, M. Fischer, J. Zellner, A. Berner, T. Dienstknecht, L. Prantl, R. Kujat, M. Nerlich, R. S. Tuan, P. Angele, Hypertrophy in mesenchymal stem cell chondrogenesis: effect of TGF-beta isoforms and chondrogenic conditioning, *Cells, tissues, organs* **2010**, *192*, 158-166.
[178] X. Bai, Z. Xiao, Y. Pan, J. Hu, J. Pohl, J. Wen, L. Li, Cartilage-derived morphogenetic protein-1 promotes the differentiation of mesenchymal stem cells into chondrocytes, *Biochemical and biophysical research communications* **2004**, *325*, 453-460.
[179] A. D. Murdoch, L. M. Grady, M. P. Ablett, T. Katopodi, R. S. Meadows, T. E. Hardingham, Chondrogenic differentiation of human bone marrow stem cells in transwell cultures: generation of scaffold-free cartilage, *Stem cells (Dayton, Ohio)* **2007**, *25*, 2786-2796.
[180] Y. Liu, A. Beyer, R. Aebersold, On the Dependency of Cellular Protein Levels on mRNA Abundance, *Cell* **2016**, *165*, 535-550.
[181] T. Maier, M. Güell, L. Serrano, Correlation of mRNA and protein in complex biological samples, *FEBS letters* **2009**, *583*, 3966-3973.
[182] F. Edfors, F. Danielsson, B. M. Hallström, L. Käll, E. Lundberg, F. Pontén, B. Forsström, M. Uhlén, Gene-specific correlation of RNA and protein levels in human cells and tissues, *Molecular Systems Biology* **2016**, *12*, 883.
[183] C. Vogel, E. M. Marcotte, Insights into the regulation of protein abundance from proteomic and transcriptomic analyses, *Nature reviews. Genetics* **2012**, *13*, 227-232.
[184] K. Kaveh, R. Ibrahim, M. Zuki Abu B, T. Azmi Ibrah, *Mesenchymal Stem Cells, Osteogenic Lineage and Bone Tissue Engineering: A Review, Vol. 10*, **2011**.
[185] H. Cheng, W. Jiang, F. M. Phillips, R. C. Haydon, Y. Peng, L. Zhou, H. H. Luu, N. An, B. Breyer, P. Vanichakarn, J. P. Szatkowski, J. Y. Park, T. C. He, Osteogenic activity of the fourteen types of human bone morphogenetic proteins (BMPs), *The Journal of bone and joint surgery. American volume* **2003**, *85-a*, 1544-1552.

[186] H. H. Luu, W. X. Song, X. Luo, D. Manning, J. Luo, Z. L. Deng, K. A. Sharff, A. G. Montag, R. C. Haydon, T. C. He, Distinct roles of bone morphogenetic proteins in osteogenic differentiation of mesenchymal stem cells, *Journal of orthopaedic research : official publication of the Orthopaedic Research Society* **2007**, *25*, 665-677.

[187] Q. Kang, W. X. Song, Q. Luo, N. Tang, J. Luo, X. Luo, J. Chen, Y. Bi, B. C. He, J. K. Park, W. Jiang, Y. Tang, J. Huang, Y. Su, G. H. Zhu, Y. He, H. Yin, Z. Hu, Y. Wang, L. Chen, G. W. Zuo, X. Pan, J. Shen, T. Vokes, R. R. Reid, R. C. Haydon, H. H. Luu, T. C. He, A comprehensive analysis of the dual roles of BMPs in regulating adipogenic and osteogenic differentiation of mesenchymal progenitor cells, *Stem cells and development* **2009**, *18*, 545-559.

[188] K. Kleinschmidt, F. Ploeger, J. Nickel, J. Glockenmeier, P. Kunz, W. Richter, Enhanced reconstruction of long bone architecture by a growth factor mutant combining positive features of GDF-5 and BMP-2, *Biomaterials* **2013**, *34*, 5926-5936.

[189] K. Marupanthorn, C. Tantrawatpan, P. Kheolamai, D. Tantikanlayaporn, S. Manochantr, Bone morphogenetic protein-2 enhances the osteogenic differentiation capacity of mesenchymal stromal cells derived from human bone marrow and umbilical cord, *International Journal of Molecular Medicine* **2017**, *39*, 654-662.

[190] Y. Sam Kwon, J. Joon Yoo, H. J. Chun, H. Joong Kim, *Comparison Study for Effects of BMP-2 and GDF-5 on Osteogenic Differentiation of Rat Bone Marrow-Derived Mesenchymal Stem Cells, Vol. 6*, **2009**.

[191] K. Nakamura, T. Shirai, S. Morishita, S. Uchida, K. Saeki-Miura, F. Makishima, p38 mitogen-activated protein kinase functionally contributes to chondrogenesis induced by growth/differentiation factor-5 in ATDC5 cells, *Experimental cell research* **1999**, *250*, 351-363.

[192] G. Yosimichi, T. Nakanishi, T. Nishida, T. Hattori, T. Takano-Yamamoto, M. Takigawa, CTGF/Hcs24 induces chondrocyte differentiation through a p38 mitogen-activated protein kinase (p38MAPK), and proliferation through a p44/42 MAPK/extracellular-signal regulated kinase (ERK), *European journal of biochemistry* **2001**, *268*, 6058-6065.

[193] C. Thouverey, J. Caverzasio, Focus on the p38 MAPK signaling pathway in bone development and maintenance, *BoneKEy Reports* **2015**, *4*, 711.

[194] J. Cai, E. Pardali, G. Sanchez-Duffhues, P. ten Dijke, BMP signaling in vascular diseases, *FEBS letters* **2012**, *586*, 1993-2002.

[195] K. N. Retting, B. Song, B. S. Yoon, K. M. Lyons, BMP canonical Smad signaling through Smad1 and Smad5 is required for endochondral bone formation, *Development (Cambridge, England)* **2009**, *136*, 1093-1104.

[196] E. Hay, J. Lemonnier, O. Fromigue, H. Guenou, P. J. Marie, Bone morphogenetic protein receptor IB signaling mediates apoptosis independently of differentiation in osteoblastic cells, *J Biol Chem* **2004**, *279*, 1650-1658.

[197] J. Liskova, O. Babchenko, M. Varga, A. Kromka, D. Hadraba, Z. Svindrych, Z. Burdikova, L. Bacakova, Osteogenic cell differentiation on H-terminated and O-terminated nanocrystalline diamond films, *International Journal of Nanomedicine* **2015**, *10*, 869-884.

[198] A. Cmoch, P. Podszywalow-Bartnicka, M. Palczewska, K. Piwocka, P. Groves, S. Pikula, Stimulators of Mineralization Limit the Invasive Phenotype of Human Osteosarcoma Cells by a Mechanism Involving Impaired Invadopodia Formation, *PLoS ONE* **2014**, *9*, e109938.

[199] X. Yin, Z. Chen, Z. Liu, C. Song, Tissue transglutaminase (TG2) activity regulates osteoblast differentiation and mineralization in the SAOS-2 cell line, *Brazilian journal of medical and biological research = Revista brasileira de pesquisas medicas e biologicas* **2012**, *45*, 693-700.

[200] J. Saas, K. Lindauer, B. Bau, M. Takigawa, T. Aigner, Molecular phenotyping of HCS-2/8 cells as an in vitro model of human chondrocytes, *Osteoarthritis Cartilage* **2004**, *12*, 924-934.

[201] M. Takigawa, K. Tajima, H. O. Pan, M. Enomoto, A. Kinoshita, F. Suzuki, Y. Takano, Y. Mori, Establishment of a clonal human chondrosarcoma cell line with cartilage phenotypes, *Cancer research* **1989**, *49*, 3996-4002.
[202] D. Lichtenberg, Universität Leipzig (Leipzig), **2013**.
[203] M. A. Scott, B. Levi, A. Askarinam, A. Nguyen, T. Rackohn, K. Ting, C. Soo, A. W. James, Brief Review of Models of Ectopic Bone Formation, *Stem cells and development* **2012**, *21*, 655-667.
[204] K. Pelttari, A. Winter, E. Steck, K. Goetzke, T. Hennig, B. G. Ochs, T. Aigner, W. Richter, Premature induction of hypertrophy during in vitro chondrogenesis of human mesenchymal stem cells correlates with calcification and vascular invasion after ectopic transplantation in SCID mice, *Arthritis and rheumatism* **2006**, *54*, 3254-3266.
[205] K. Liu, G. D. Zhou, W. Liu, W. J. Zhang, L. Cui, X. Liu, T. Y. Liu, Y. Cao, The dependence of in vivo stable ectopic chondrogenesis by human mesenchymal stem cells on chondrogenic differentiation in vitro, *Biomaterials* **2008**, *29*, 2183-2192.
[206] C. R. Chu, M. Szczodry, S. Bruno, Animal models for cartilage regeneration and repair, *Tissue Eng Part B Rev* **2010**, *16*, 105-115.
[207] E. L. Kuyinu, G. Narayanan, L. S. Nair, C. T. Laurencin, Animal models of osteoarthritis: classification, update, and measurement of outcomes, *Journal of orthopaedic surgery and research* **2016**, *11*, 19.
[208] L. N. Reynard, C. Bui, C. M. Syddall, J. Loughlin, CpG methylation regulates allelic expression of GDF5 by modulating binding of SP1 and SP3 repressor proteins to the osteoarthritis susceptibility SNP rs143383, *Human genetics* **2014**, *133*, 1059-1073.
[209] M. Dominici, K. Le Blanc, I. Mueller, I. Slaper-Cortenbach, F. Marini, D. Krause, R. Deans, A. Keating, D. Prockop, E. Horwitz, Minimal criteria for defining multipotent mesenchymal stromal cells. The International Society for Cellular Therapy position statement, *Cytotherapy* **2006**, *8*, 315-317.
[210] P. A. Sotiropoulou, S. A. Perez, M. Salagianni, C. N. Baxevanis, M. Papamichail, Characterization of the optimal culture conditions for clinical scale production of human mesenchymal stem cells, *Stem cells (Dayton, Ohio)* **2006**, *24*, 462-471.

9 Appendix

9.1 Supporting information

S 1 **Fresh unprocessed human bone marrow from Lonza.** Certificate of analysis, processing until cryoconservation and human MSC characterization via FACS analysis.

Certificate of analysis:

Lonza Walkersville Inc.
8830 Biggs Ford Road
Walkersville, MD 21793 8415
Tel (301) 898 7025
Fax (301) 845 4024

Lonza

Printed on, 02-Aug-2012 16:45 Page 1 / 1

CERTIFICATE OF ANALYSIS

Product Code:	1M-125	**Lot Number:**	0000313406
Product:	Human Bone Marrow, Fresh 25 ml	**Manufacture Date:**	02-Aug-2012

TEST (Method)	SPECIFICATIONS Min.	Max.	Results
Age	***	***	21
Sex	***	***	MALE
Race	***	***	AFRICAN AMERICAN
HIV	***	***	Negative
Hepatitis B	***	***	NEGATIVE
Hepatitis C	***	***	NEGATIVE
Cell Count (cells/ml)	***	***	27.0E6

This lot has been isolated from human tissue obtained under "informed consent". Details concerning the use of our cell and media products can be downloaded from our website at www.lonza.com.

Processing of human bone marrow:

The fresh unprocessed human bone marrow was divided in two tubes and each fraction was mixed with 50 mL PBS and centrifuged. The pellet was thoroughly resuspended in 20 mL of red cell lysis buffer (Sigma, Cat.N°87157), let on ice 3 min and centrifuged. This step was repeated 2 additional times. The two cell pellets were then combined and washed two times with PBS, the cells were counted and inoculated at $10x10^6$ cells/cm^2 in DMEM-hg supplemented with 10% FBS, 2 mM Glutamine, 8 ng/mL bFGF on gelatin-coated tissue culture flasks. When 60-80% confluency was achieved, cells were harvested with TrypLE express (Gibco, Cat. N°126403) and passaged until passage 2. Passage 2 was realized in a gelatin-coated 10-tray cell factory system with 1500 cells/cm^2 and 2 l of the same medium. Cells were then frozen at 5 million cells/ml in Cryostor (Stem Cell Technologies Cat. N°07930), and kept in liquid nitrogen until use.

Charaterization of human MSCs:

Additionally, the colleagues from MilliPoreSigma characterized the cells harvested from passage 2 by FACS analysis. Cells were resuspended at 50 000 cells/mL in DMEM + 2% (W/v) BSA and incubated with the respective antibodies 20 min in the dark. Cells were then washed once in PBS and analyzed with a Guava flow cytometer. According to the International Society for Cell Therapy [209], the following markers were investigated: CD105 (Abcam, Cat.N°53318), CD90 (Millipore, Cat.N°FCMAB211F), CD73 (Abcam, Cat. N°106697), CD11b (Millipore, Cat.N°FCMAB178P), CD79a (Millipore, Cat.N° FCMAB208P), CD14 (Millipore, Cat. N°FCMAB181F), CD45 (Millipore FCMAB118P), CD34 (Millipore Cat.N°CBL555F), CD19 (Millipore, Cat.N°FCMAB184F) and HLA-DR (Millipore, Cat.N°FCMAB184F). The MSCs were CD105+, CD90+, CD73+, CD11b-, CD79a-, CD14-, CD45-, CD34- , CD19 -and HLA-DR+, the latter being due to the expansion in presence of bFGF [210].

S 2 **ECM production and phenotype analysis of hOAC in monolayer cultures at different osmolarities adjusted with NaCl.** After a total cultivation time of 6 days at 340, 380, 420 and 460 mOsm, the cell concentration and cell viability as well as the GAG production (µg/million cells) were determined. Additionally, the type 1 collagen, type 2 collagen and aggrecan expressions were measured after 6 days of cultivation. For each donor and each readout, the mean value of two to six replicates was calculated. The results represent the x-fold increase of the mean values over control cells cultured at 340 mOsm.

	GAG production			Cell concentration			Cell viability		
	380 mOsm	420 mOsm	460 mOsm	380 mOsm	420 mOsm	460 mOsm	380 mOsm	420 mOsm	460 mOsm
Donor 1	1.07	2.18	2.47	1.10	0.71	0.65	1.03	0.98	1.01
Donor 2	1.19	1.81	2.01	0.89	0.80	0.85	1.02	1.04	1.04
Donor 3	1.23	1.50	1.87	0.91	0.86	0.77	1.00	1.00	0.99
Donor 4	1.67	2.52	2.77	0.92	0.75	0.70	1.00	0.96	0.98
Donor 5	1.23	1.31	1.44	0.74	0.55	0.48	1.00	0.94	0.95

	Collagen 1 expression			Collagen 2 expression			Aggrecan expression		
	380 mOsm	420 mOsm	460 mOsm	380 mOsm	420 mOsm	460 mOsm	380 mOsm	420 mOsm	460 mOsm
Donor 1	0.94	1.38	0.92	1.62	3.37	4.59	1.59	3.91	7.12
Donor 2	0.82	0.60	0.48	1.71	2.22	2.78	1.52	1.69	3.47
Donor 3	0.77	0.71	0.65	1.26	1.08	4.38	3.95	4.09	29.19
Donor 4	0.86	0.93	0.45	2.19	3.10	2.64	1.52	2.80	4.46
Donor 5	0.86	0.54	0.37	3.49	4.81	5.91	3.76	4.25	8.96

S 3 **Proteases and cytokines production of hOAC in monolayer cultures at different osmolarities adjusted with NaCl** After a total cultivation time of 6 days at 340, 380, 420 and 460 mOsm, the MMP13 and ADAMTS5 expressions as well as the production of Il1β, TNFα and Il6 (pg/million cells) were determined. For each donor and each readout, the mean value of two to six replicates was calculated. The results represent the x-fold increase of the mean values over control cells cultured at 340 mOsm.

	MMP13 expression			ADAMTS5 expression		
	380 mOsm	420 mOsm	460 mOsm	380 mOsm	420 mOsm	460 mOsm
Donor 1	0.73	0.46	0.50	0.88	0.70	0.69
Donor 2	0.95	0.96	0.77	0.89	0.97	0.83
Donor 3	0.59	0.58	0.30	0.84	0.78	0.55
Donor 4	0.70	0.51	0.43	0.94	1.06	0.81
Donor 5	1.06	0.58	0.29	1.01	0.69	0.50

	Il1β production			TNFα production			Il6 production		
	380 mOsm	420 mOsm	460 mOsm	380 mOsm	420 mOsm	460 mOsm	380 mOsm	420 mOsm	460 mOsm
Donor 1	0.82	0.81	0.56	0.79	0.72	0.48	0.79	0.72	0.48
Donor 2	1.25	1.57	1.41	1.19	1.47	1.35	1.19	1.47	1.35
Donor 3	0.99	0.48	0.23	0.95	0.60	0.41	0.95	0.60	0.41
Donor 4	0.97	0.95	0.63	1.07	1.05	0.74	0.79	0.79	0.76
Donor 5	0.89	0.87	0.33	0.94	0.94	0.46	0.74	0.68	0.47

S 4 **BMPR expression analysis of hOAC in monolayer culture at different osmolarities adjusted with sucrose.** After a total cultivation time of 6 days at 340, 380, 420 and 460 mOsm, BMPR1a, BMPR1b and BMPR2 expressions were determined. For each donor and each readout, the mean value of two to three replicates was calculated. The results represent the fold increase of the mean values over control cells cultured at 340 mOsm.

	BMPR1a expression			BMPR1b expression			BMPR2 expression		
	380 mOsm	420 mOsm	460 mOsm	380 mOsm	420 mOsm	460 mOsm	380 mOsm	420 mOsm	460 mOsm
Donor 1	1.17	1.30	1.26	0.95	0.81	2.96	1.16	1.37	1.91
Donor 2	1.08	1.62	1.54	1.08	1.18	2.21	1.07	1.35	1.32
Donor 3	1.36	1.56	2.87	1.52	1.76	2.48	1.03	1.18	2.92
Donor 4	0.92	1.16	1.66	1.36	1.81	2.33	1.16	1.32	1.41
Donor 5	1.16	1.18	1.25				1.03	0.99	1.01

S 5 **Expression of BMP receptors in hOAC cultured in monolayer after stimulation with TNFα, Il1β or Il6.** hOAC were cultured in monolayer and stimulated with 10 ng/ml TNFα, Il1β and 100 ng/ml Il6 for 2 days. Afterwards cell samples were analyzed for the expression of BMPR1a, BMPR1b and BMPR2. For each donor and each readout, the mean value of three replicates was calculated. The results represent the x-fold difference of the mean values over unstimulated cells. Red highlighted values and arrows indicate a significant increase or decrease compared to control.

BMPR1a			
	Il1β	TNFα	Il6
Donor 1	1.39	0.64	0.15
Donor 2	0.72	0.03	0.09
Donor 3	0.92	0.27	0.08
Donor 4	2.75	0.81	0.18
	↑↑	↓↓↓	↓↓↓
BMPR1b			
	Il1β	TNFα	Il6
Donor 1	1.43	0.02	0.01
Donor 2	1.91	0.03	0.02
Donor 3	0.91	0.02	0.004
Donor 4	5.31	0.21	0.03
	↑↑↑	↓↓↓	↓↓↓
BMPR2			
	Il1β	TNFα	Il6
Donor 1	1.97	0.66	0.14
Donor 2	3.78	1.03	0.03
Donor 3	1.02	0.32	0.07
Donor 4	3.29	1.36	0.18
	↑↑↑	↓↑	↓↓↓

S 6 **Anabolic effect of GDF5 and GDF5 mutants on ECM synthesis in porcine chondrocytes.** Porcine chondrocytes were cultured as CTAs over 28 days and treated with 300 ng/ml GDF5, M1673, W417F and W417R or remained untreated (CTL). At the end of the culture the proteoglycan production was analyzed by measuring the glycosaminoglycan (GAG) concentration (A) and the expression of aggrecan (B) per CTA. The collagen production was analyzed by measuring hydroxyproline (HPro) accumulation (C) and the gene expression of type 2 collagen (D) in the CTAs. Stars indicate significance compared to unstimulated cells (Dunnett comparison, p<0.05). Safranin O staining indicating proteoglycan content was performed at the end of the culture with 28-day old CTAs (E).

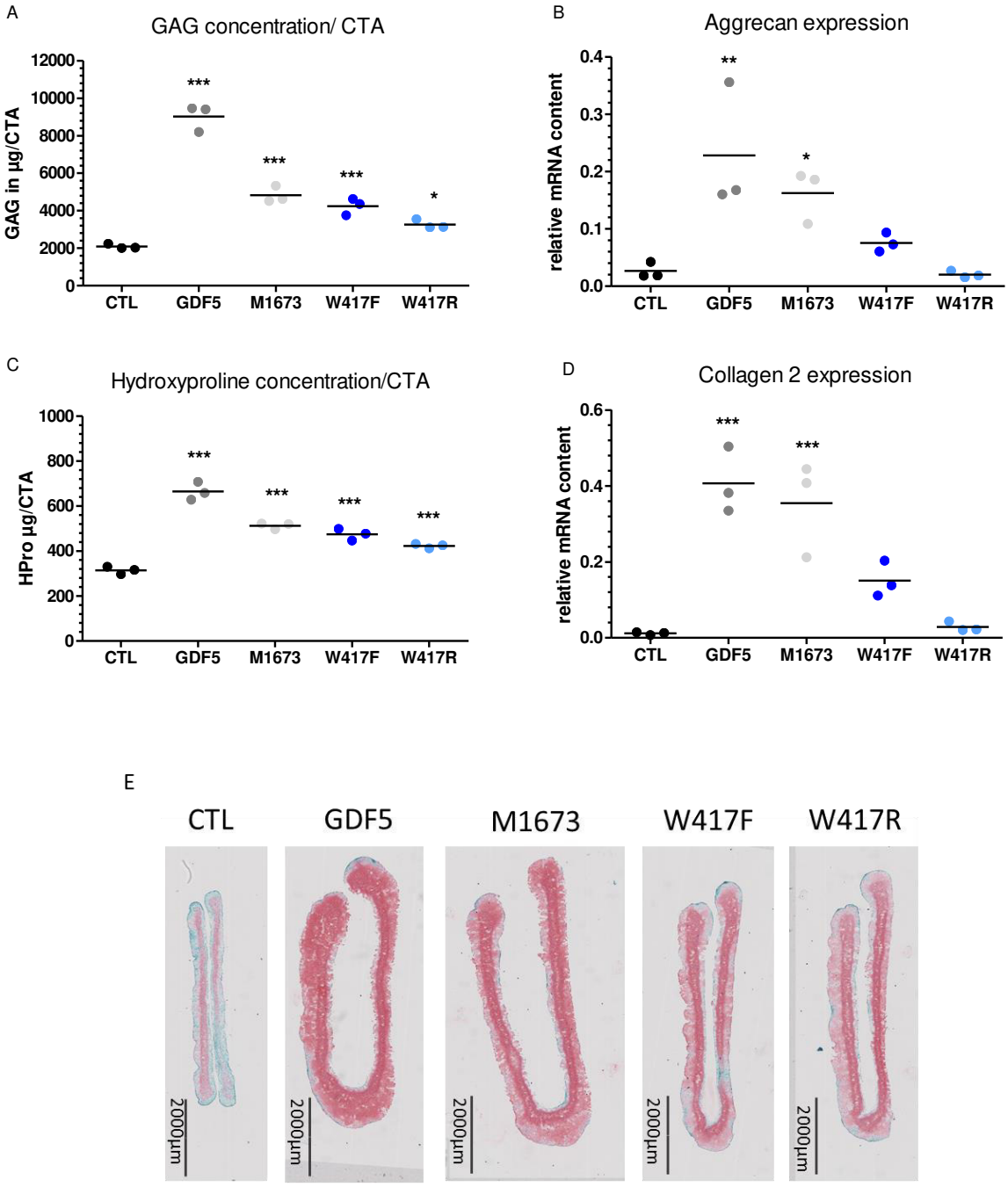

S 7 **Anabolic effect of GDF5 and GDF5 mutants on ECM synthesis in bovine chondrocytes.** Bovine chondrocytes were cultured as CTAs over 28 days and treated with 300 ng/ml GDF5, M1673, W417F and W417R or remained untreated (CTL). At the end of the culture the proteoglycan production was analyzed by measuring the glycosaminoglycan (GAG) accumulation (A) and the expression of aggrecan (B) per CTA. The collagen production was analyzed by measuring hydroxyproline (HPro) accumulation (C) and the gene expression of type 2 collagen (D) in the CTAs. Stars indicate significance compared to unstimulated cells (Dunnett comparison, $p<0.05$). Safranin O staining indicating proteoglycan content was performed at the end of the culture with 28-day old CTAs (E).

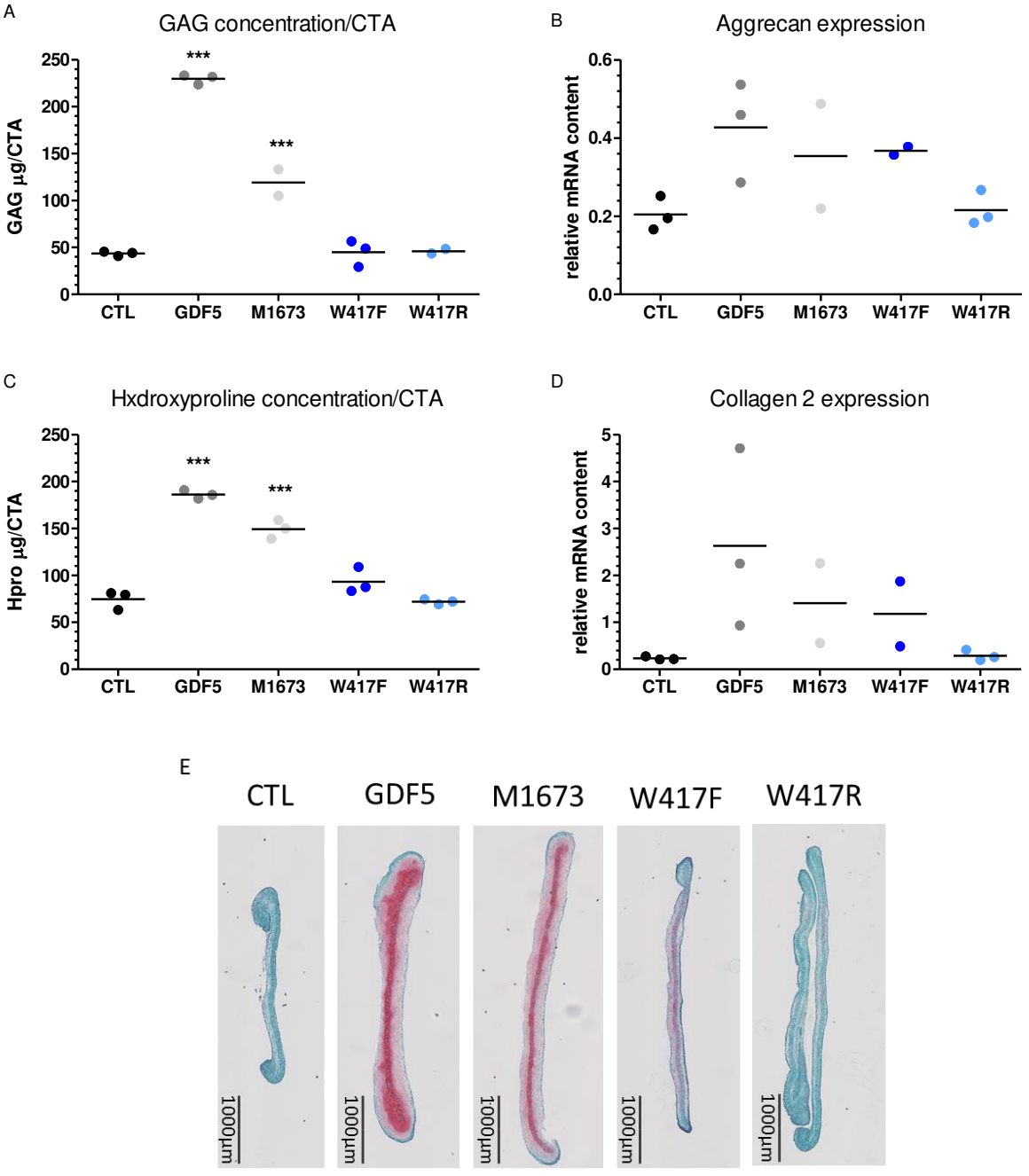

S 8 **Anabolic effect of GDF5 and M1673 on proteoglycan synthesis in hOAC at 380 mOsm.** hOAC were encapsulated in alginate beads and treated over 14 days with 300 ng/ml GDF5 or M1673 or remained untreated. At the end of the culture the glycosaminoglycan (GAG) accumulation in the beads and the expression of aggrecan were measured. For each donor and each readout, the mean value of eight (GAG concentration) or three (Aggrecan expression) replicates was calculated. The results represent the x-fold increase of the mean values over untreated cells at 380 mOsm.

	GAG concentration in beads		Aggrecan expression	
	Fold increase at 380		*Fold increase at 380*	
	GDF5	M1673	GDF5	M1673
Donor 1	1.71	1.41	3.96	2.64
Donor 2	2.23	2.20	4.37	2.27
Donor 3	2.72	2.10	2.11	1.29
Donor 4	2.25	1.70	5.11	2.89
Donor 5	1.98	1.49	3.65	2.74
Donor 6	2.07	1.83	2.50	1.26
Donor 7	1.59	1.37	1.49	1.51
Donor 8	1.83	1.62		
Donor 9	1.93	1.59		
Donor 10	3.76	1.98		
Donor 11	2.46	1.92		
Donor 12	3.84	2.15		
Donor 13	2.04	1.71		
Donor 14	1.90	1.64		
Donor 15	2.50	1.81		

S 9 **Anabolic effect of GDF5 and M1673 on collagen synthesis in hOAC at 380 mOsm.** hOAC were encapsulated in alginate beads and treated over 14 days with 300 ng/ml GDF5 or M1673 or remained untreated. At the end of the culture the expression of type 2 collagen as well as the hydroxyproline (HPro) and pro-peptide of collagen 2 (ProC2) accumulation in the beads were measured. For each donor and each readout, the mean value of six (HPro concentration) or three (Collagen 2 expression, ProC2 concentration) replicates was calculated. The results represent the x- fold increase of the mean values over untreated cells at 380 mOsm.

	Collagen 2 expression		HPro concentration in beads		ProC2 concentration in beads	
	Fold increase at 380		*Fold increase at 380*		*Fold increase at 380*	
	GDF5	M1673	GDF5	M1673	GDF5	M1673
Donor 1	13.31	6.33	1.22	1.17	3.17	1.72
Donor 2	9.82	4.72	1.05	0.98	1.17	1.05
Donor 3	5.38	4.62	1.38	1.19	2.08	1.88
Donor 4	9.15	5.21				
Donor 5	2.99	3.09				
Donor 6	5.67	2.98				
Donor 7	2.54	2.57				

S 10 **Anti-catabolic effect of GDF5 and M1673 on MMP13 expression in hOAC at 380 mOsm.** hOAC were encapsulated in alginate beads and treated over 14 days with 300 ng/ml GDF5 or M1673 or remained untreated. At the end of the culture the expression of MMP13 was determined. For each donor, the mean value of three replicates was calculated. The results represent the x- fold increase of the mean values over untreated cells at 380 mOsm.

	MMP13 expression	
	Fold increase at 380	
	GDF5	M1673
Donor 1	0.31	0.82
Donor 2	0.28	0.48
Donor 3	0.12	0.24
Donor 4	0.05	0.15
Donor 5	0.33	0.82
Donor 6	0.28	0.52

9.2 *Curriculum vitae*

Personal data

Name	Tanja Mang
Date of birth	September, 26th 1989
Place of birth	Bergisch-Gladbach, Germany
Private address	Rheinstrasse 55, 64683 Einhausen, Germany

Education

01/2015 – now	Doctorate in biochemistry, Merck KGaA and Technical University Darmstadt in Prof. Dr. Kolmar´s group, Darmstadt, Germany
10/2012 – 12/2014	Technical University Darmstadt, Germany, Master of Science in Technical Biology Specialization: biochemistry and cell culture Master thesis: 'Assessment of protease activity in preclinical assays related to osteoarthritis research' Supervisor: Dr. Hans Gühring, Translational Osteoarthritis, Merck KGaA, Darmstadt, Germany
10/2009 – 09/2012	University of Applied Science, Darmstadt, Germany, Bachelor of Science in Biotechnology Area of studies: Molecular biology, Microbiology, Biochemistry, Enzyme technology, Inorganic chemistry, Organic chemistry, Instrument-based analytics, Cell culture technology, Biochemical engineering, Bioassay & design of experiments Bachelor thesis: 'Detection of specific cellular proteins to characterize human cell culture models for preclinical, pharmacodynamic investigations' Supervisor: Dr. Harry F. Abts, Biopharmacy Dermatology, Merz Pharmaceuticals GmbH, Frankfurt/Main, Germany
09/2000 – 06/2009	Goethe-Gymnasium, Bensheim, Germany Qualification level: Allgemeine Hochschulreife

Working experience

10/2013 – 01/2014	‘Site-specific modification of human C4b-binding protein (hC4Bp)’ Supervisor: Dr. Harald Kolmar, Department of chemistry and biochemistry, Technical University Darmstadt, Germany
03/2012 – 05/2012	‘Establishment of a cellular protein analysis from in vitro cultured malignant and non-malignant epithelial cells’ Supervisor: Dr. Harry F. Abts, Biopharmacy Dermatology, Merz Pharmaceuticals GmbH, Frankfurt/Main, Germany
08/2011 – 09/2011	‘Establishment of an auto-inductive medium to produce bacterial histone deacetylase' Supervisor: Dr. Meyer-Almes, Department biochemistry, University of Applied Science Darmstadt, Germany

9.3 Data dissemination

Publications derived from this work

T. Mang, K. Kleinschmidt-Doerr, F. Ploeger, A. Schoenemann, S. Lindemann, A. Gigout, A GDF5 mutant induces chondrogenesis in mesenchymal stem cells similarly to GDF5 wildtype but shows a decreased osteogenic potential, *Osteoarthritis and Cartilage* **2018**, *26*, S77.

T. Mang, K. Kleinschmidt-Doerr, F. Ploeger, S. Lindemann, A. Gigout, M1673 (GDF5 mutant) increases matrix production in primary porcine and human osteoarthritic chondrocytes, *Osteoarthritis and Cartilage* **2018**, *26*, S82.

T. Mang, C. Arras, S. Lindemann, A. Gigout, A strong correlation - influence of medium osmolarity on "chondrocyte health", *Osteoarthritis and Cartilage* **2017**, *25*, S154-S155.

Contributions to conferences

T. Mang, K. Kleinschmidt-Doerr, F. Ploeger, A. Schoenemann, S. Lindemann, A. Gigout, A GDF5 mutant induces chondrogenesis in mesenchymal stem cells similarly to GDF5 wildtype but shows a decreased osteogenic potential, *OARSI World Congress 2018,* ACC Conference Center, Liverpool, UK, April 26th – 29th **2018**, poster presentation + additionally selected to be part of the OARSI´s Breakfast Poster Tour

T. Mang, K. Kleinschmidt-Doerr, F. Ploeger, S. Lindemann, A. Gigout, M1673 (GDF5 mutant) increases matrix production in primary porcine and human osteoarthritic chondrocytes, *OARSI World Congress 2018,* ACC Conference Center, Liverpool, UK, April 26th – 29th **2018**, poster presentation

T. Mang, C. Arras, S. Lindemann, A. Gigout, A strong correlation - influence of medium osmolarity on "chondrocyte health", *OARSI World Congress 2017,* Ceasar´s Palace, Las Vegas, USA, April 27th - 30th **2017**, poster presentation

T. Mang, F. Plöger, K. Kleinschmidt-Dörr, S. Lindemann, A. Gigout, Chondrogenic and osteogenic differentiation of murine stem cells is triggered by the affinity ratio of BMPRIA and IB, *11th International BMP conference,* Martin Conference Center at Harvard Medical School, Boston, USA, October 26th -30th **2016**, poster presentation

9.4 Affirmations

Tanja Mang
Rheinstrasse 55
64683 Einhausen

Erklärung

Ich erkläre hiermit, dass ich meine Dissertation selbstständig und nur mit den angegebenen Hilfsmitteln angefertigt und noch keinen Promotionsversuch unternommen habe.

Mang, Tanja

Tanja Mang
Rheinstrasse 55
64683 Einhausen

Erklärung der Übereinstimmung

Ich erkläre hiermit, dass die elektronische Version der Doktorarbeit mit der schriftlichen Version übereinstimmt. Die elektronische Version liegt dem Prüfungssekretariat vor.

Mang, Tanja